

THE "UNIVERSAL POLYMER BACKBONE" CONCEPT

A Dissertation
Presented to
The Academic Faculty

By

Joel Matthew Pollino

In Partial Fulfillment
Of the Requirements For the Degree
Doctor of Philosophy in the
School of Chemistry and Biochemistry

Georgia Institute of Technology

October, 2004

Copyright © Joel Matthew Pollino 2004

THE "UNIVERSAL POLYMER BACKBONE" CONCEPT

Approved by:

Dr. Marcus Weck, Advisor
(Chemistry & Biochemistry)

Dr. Uwe H. F. Bunz
(Chemistry & Biochemistry)

Dr. David M. Collard
(Chemistry & Biochemistry)

Dr. Christopher W. Jones
(Chemical Engineering)

Dr. Charles L. Liotta
(Chemistry & Biochemistry)

November, 5th 2004

Our observation of Nature must be diligent, our reflection profound, and our experiments exact.

Denis Diderot

To My Wife Amy and My Son Tyler

ACKNOWLEDGEMENT

The work described in this dissertation would not have been possible without the strong scientific, educational, and financial support of my research advisor, Professor Marcus Weck. I am greatly indebted to Marcus for affording me the opportunity to help initiate his group. I am especially fortunate that Marcus allowed me tremendous flexibility in my work schedule and the freedom to pursue my own initiatives, both of which created an ideal and productive working environment and fostered my maturation into an independent thinker and researcher. Furthermore, Marcus' role in developing my writing and presentation skills was paramount. His strong work ethic and passion for science were not only inspiring, but also contagious. I am truly fortunate to have been mentored by such a wonderful person.

I would also like to thank the members of my thesis committee- Professors Uwe Bunz, David Collard, Chris Jones, and Charles Liotta for always taking time to assist me with my scientific endeavors. Their insights, instrumental assistance, and words of encouragement have profoundly impacted the success of my project. I especially thank Chris Jones for all of his insightful comments and encouraging words during group meetings. I am grateful to Uwe for his daily enthusiasm, useful discussions, and interest in my projects.

Two undergraduate mentors, Professors Jennifer Gillies and Karen Quaal were fundamental to my success in graduate school. I thank Dr. Gillies for giving me an appreciation for physical chemistry and for affording me the opportunity to do summer research. I am indebted to Dr. Quaal for inspiring me to pursue graduate studies in

polymer and organic chemistry. I will always value my time at Siena College. I would also like to thank William Towne, my high school chemistry teacher, who first ignited my passion for chemistry.

Some of my fondest memories of the lab took place in the evenings working alongside our German postdoc, Dr. Ludger Paul Stubbs (“Homie”). I owe virtually all of my capabilities in the lab to “Homie” who early on became a pivotal force in my success. I thank Paul, a remarkable individual and a good friend, for teaching me what to do and what not to do in lab. His work ethic and strong synthetic skills made me want to follow in his footsteps. I will never forget our late nights, in depth discussions of Southern culture, and mutual taste for good “bier” and dogs.

Shortly after starting my studies, I encountered Dr. Robert Kriegel, a very knowledgeable individual who helped me greatly with preparing for candidacy requirements. He always gave me abundant information about anything and everything, and who helped make group meetings very stimulating and interesting.

The graduate students who assisted me throughout my studies are Joe Carlise, Matija Crne, Warren Gerhardt, Mary Nell Higley, William Sommer, and Kamlesh Nair. I especially thank Warren for sharing his awesome “action hero” adventures with me. You really are a “little bastard”, but that’s why we like you. You are the hardest working person I know. I am grateful to Joe for always being a great person to talk to and for all of his enthusiasm towards science and useful conversations about parenting and relationships. Mary Nell deserves much praise for successfully taking on the CTA project. William (“Frenchie”) was always a good friend in lab and shared many ACS

meetings with me. He is a gifted researcher. I also thank my undergraduate assistant, Erik Hollembeak for all of his efforts with the CTA project.

I am grateful for having the opportunity to meet and work with my successor on the UPB project, Kamlesh Nair. I am especially indebted to Kamlesh for taking the TGA and DSC measurements for the crosslinked UPB paper. As a first year student, Kamlesh's passion for science and desire to publish was remarkable. Kamlesh is a very talented researcher. I look forward to reading many high impact papers from him.

Aside from those mentioned above, two postdocs who joined the group close to my departure are Dr. Michael Holbach and Xian-Yong Wang. Both are astounding scientists that I am glad to have known. I especially thank Michael who helped me with my practice talk for Dupont and for discussions on how to write this thesis. He is an exceptional role model. Also, I thank James Wilson, my friend from the Bunz group, for always being around at night to provide that emergency can of ether and for his discussions about science. I wish him luck at Stanford. Other group members who supported me throughout my Ph.D. include: Caroline Burd, Tosin Ige, Alpay Kimyonok, and Poorva Tayal. I must also thank Amy Meyers for her hard work at keeping the chemical inventory up to date.

Of paramount importance to my success in life, as well as in school, is my family. My parents, Joe and Linda, taught me early in life the importance of hard work and dedication. They also supported me financially throughout my undergraduate studies. To be blessed with such a loving and supportive upbringing, I am truly grateful. I also thank my brother Josh for being a great friend that has always supported me in life. My grandparents have always believed in me and given me the desire to make them proud. I

am enormously thankful for the strong relationship I had with my grandfather at a young age. He was instrumental in my success in life as he taught me how to make things with my hands. As a skilled woodworker, he exposed me to the process of crafting and building. I am still saddened by his early departure from us.

Last but certainly not least; I would like to thank my wife and life's love, Amy. She has been exceptionally supportive over the last five years. Without her patience and tolerance for my late night hours, I would have never made it through graduate school. I am grateful to her for giving me the second love of my life, Tyler. Her hard work and dedication to making our family run has been astonishing. I am especially indebted to her for taking on many of the parenting responsibilities during this last and most difficult phase of the Ph.D. process. Amy, I love you!

TABLE OF CONTENTS

ACKNOWLEDGEMENT	v
TABLE OF CONTENTS	ix
LIST OF TABLES	xiii
LIST OF FIGURES	xiv
LIST OF SCHEMES	xx
LIST OF ABBREVIATIONS	xxii
SUMMARY	xxvi

CHAPTER 1. SELF-ASSEMBLY IN POLYMER SCIENCE

1.1	Abstract	1
1.2	Introduction	1
1.3	Definition of Self-Assembly	2
1.4	Non-Covalent Bonds	4
1.5	Self-Assembled Polymers	8
1.6	Side-Chain Functionalized Polymers Based on a Single Recognition Motif	14
1.6.1	The Earliest Examples: Self-Assembled Side-Chain Liquid Crystalline Polymers	15
1.6.2	Nature Inspired Systems: Advancements in the Preparation and Functionalization of Hydrogen Bonding Side-Chain Polymers	21
	Controlled Routes to Nature Inspired Systems	21
	Template-Directed Polymerizations	24
	“Plug and Play” Polymer Functionalization	26
1.6.3	Side-Chain Metal Containing Polymers (SCMPs): Engineered Metal-Ligand Interactions, Functionalization Strategies, and Applications	33
1.7	Self-Assembled Polymers Based on Multiple Recognition Motifs	38
1.8	Conclusion	42
1.9	References	45

CHAPTER 2. THE “UNIVERSAL POLYMER BACKBONE” CONCEPT

2.1	Abstract.....	50
2.2	State of the Art Materials Synthesis: The “Covalent” Conundrum	50
2.3	Nature’s Design Lessons.....	54
2.4	The UPB Concept: Beyond Covalent Polymer Functionalization.....	57
2.5	Challenges, Design Elements, and Perspective	60
2.6	References.....	63

CHAPTER 3. SYNTHESIS AND SELF-ASSEMBLY OF POLYMERS BEARING PALLADATED SCS PINCER COMPLEXES

3.1	Abstract.....	65
3.2	Introduction.....	65
3.2.1	Pincer Ligands.....	67
3.2.2	Ring-Opening Metathesis Polymerization	71
3.2.3	Monomer Design.....	73
3.3	Monomer and Polymer Synthesis	74
3.4	Synthesis of Nitrile and Pyridine Anchored Mesogenic Units	76
3.5	Polymer Functionalization	78
3.6	Characterization of Self-Assembly	79
3.7	Conclusion	84
3.8	Experimental.....	85
3.9	References.....	100

CHAPTER 4. OPTIMIZATION OF NORBORNENE MONOMERS POSSESSING TERMINAL RECOGNITION ELEMENTS

4.1	Abstract.....	103
4.2	Introduction.....	103
4.3	Monomer Synthesis	106
4.4	Polymerization Studies	108
4.5	Copolymerization Studies.....	112
4.6	Conclusion	114
4.7	Experimental.....	114

4.8	References.....	122
CHAPTER 5. MULTI-STEP AND ONE-STEP “UNIVERSAL POLYMER BACKBONE” FUNCTIONALIZATION		
5.1	Abstract.....	124
5.2	Introduction.....	124
5.3	UPB Synthesis and Characterization	126
5.4	Non-Covalent Functionalization of UPBs	128
5.5	Thermal Characterization Studies.....	134
5.6	Conclusion	136
5.7	Experimental.....	137
5.8	References.....	145
CHAPTER 6. APPLICATIONS OF THE UPB CONCEPT: CROSS LINKED MATERIALS		
6.1	Abstract.....	146
6.2	Introduction.....	146
6.3	Research Design.....	149
6.4	Monomer and Terpolymer (UPB) Synthesis	151
6.5	Directed Self-Assembly: Non-Covalent Crosslinking.....	154
6.6	One-Step Orthogonal Self-assembly: Crosslinking and Small Molecule Functionalization	164
6.7	Conclusion	168
6.8	Experimental.....	168
6.9	References.....	179
CHAPTER 7. THE UPB CONCEPT: TODAY’S SYSTEM AND POTENTIAL APPLICATIONS OF TOMORROW		
7.1	Abstract.....	182
7.2	The Current Status of the UPB Concept: Summary and Perspective	182
7.3	Future Development of UPB Methodologies	185
	7.3.1 UPBs Based on One Type of Recognition Unit.....	186

7.3.2	Metal Connected Di-Block UPBs	188
7.3.3	Grafted UPBs	190
7.3.4	Main-chain UPBs	192
7.4	Potential Applications	194
7.4.1	Photorefractive Polymers	195
7.4.2	Drug Delivery Devices	198
7.4.3	Sensor Technologies	199
7.4.4	Thermoplastic Elastomers	201
7.4.5	UPB Assisted Formation of Nano-Devices via Hierarchical Self-Assembly	202
7.5	References	204

APPENDIX A. TANDEM CATALYSIS AND SELF-ASSEMBLY

A.1	Abstract	207
A.2	Introduction	207
A.3	Design, Prerequisites, and Objectives	209
A.3	Catalytic Properties of Polymer Supported SCS Pincer Ligands	211
A.4	Self-Assembly of a Mesogenic Component Onto the Polymer Backbone	213
A.5	One-Pot Tandem Catalysis and Self-Assembly	215
A.6	Conclusion	216
A.8	References	218

LIST OF TABLES

Table 1.1	Non-covalent interactions ordered according to bond strength. ⁴	5
Table 2.1	Comparison of covalent and non-covalent synthesis.....	54
Table 3.1	Comparison of ¹ H NMR chemical shifts of the 1:1 mixture (polymer 21 and mesogen 26 or 27) and the pyridine functionalized polymers 31 and 32 respectively.....	81
Table 3.2	Comparison of ¹ H NMR chemical shifts of the 1:1 mixture (polymer 21 and mesogens 24 or 28) and the self-assembled nitrile-based polymers 29 and 30	83
Table 3.3	Thermal characterization data.....	84
Table 4.1	Representative data for polymers initiated by 4.	108
Table 4.2	First order rate constants determined for <i>exo</i> and 80:20 <i>endo/exo</i> 11 and 12	109
Table 5.1	UPB characterization data.....	128
Table 5.2	Thermal data for functionalized copolymers.....	135
Table 5.3	Thermal data: concentration dependence of the complimentary hydrogen bonding unit.....	136
Table 6.1	UPB characterization data.....	153
Table 6.2	Thermal characterization data for crosslinked UPBs.....	164
Table A.1	Heck reaction data using 1 as a precatalyst.	212

LIST OF FIGURES

Figure 1.1	Multiple hydrogen bonded complexes possessing different arrangements of acceptor and donor units. A) ADA-DAD, B) ADD-DAA, and C) AAA-DDD.	7
Figure 1.2	Cartoon schematic that depicts the differences between A) main-chain self-assembled polymers and B) side-chain self-assembled polymers.....	9
Figure 1.3	Select homonuclear self-assembled polymers. A) Meijer's homonuclear main-chain self-assembled polymers, and B) Coates' homonuclear side-chain self-assembled copolymers. ³⁴ In both cases self-dimerizing ureidopyrimidinone recognition elements are employed.....	10
Figure 1.4	Heteronuclear main-chain self-assembled polymers A) The AABB structure formed from two symmetrically bisfunctionalized monomer units, B) The ABAB configuration resulting from the use of a single asymmetrically end-functionalized monomer unit, and C) An example of Lehn's liquid crystalline heteronuclear main-chain self-assembled polymers.	12
Figure 1.5	Side-chain heteronuclear polymers. A) Those formed by self-functionalization strategies, and B) those formed using modular functionalization.	14
Figure 1.6	Schematic illustration of the structural components used to fabricate simple LCs, SCLCPs, and self-assembled SCLCPs from rod-shaped mesogens.....	16
Figure 1.7	Molecular components used to prepare the first examples of self-assembled SCLCPs.	16
Figure 1.8	Schematic illustration depicting a variety of structurally configured hydrogen bonded self-assembled SCLCPs. A) Side-chain anchored mesogens, B) side-chain extended mesogens or mesogen formation, C) main-chain anchored mesogens, and D) crosslinked side-chain anchored mesogens.....	18
Figure 1.9	Poly(nucleoside)-based polymers containing uridine (10) and adenosine (11) recognition motifs synthesized via ATRP.....	22
Figure 1.10	ROMP monomers and polymers possessing recognition elements capable of forming multiple hydrogen bonds.	23

Figure 1.11	Sleiman’s AB block copolymers made via ROMP.....	24
Figure 1.12	Template directed polymerization.	25
Figure 1.13	Schematic depicting functionalization of a “plug and play” scaffold. Modification approaches: A) monofunctionalization, B) step-wise multifunctionalization, and C) one-step multifunctionalization.	27
Figure 1.14	Non-covalent attachment of stilbazole electron donor and acceptor mesogen components via multifunctionalization strategies.	28
Figure 1.15	Self-Assembled complexes formed via intermolecular hydrogen bonding of a) flavin 22 and diaminotriazine random copolymer 20 and b) 22 and diaminopyridine random copolymer 21	29
Figure 1.16	Intermolecular complexation of thymine functionalized random copolymer 23 and diaminopyridine-polyhedral oligomeric silsesquioxane (POSS) entities.	30
Figure 1.17	A) Block co-poly(styrene)s containing triazine and diaminopyridine recognition motifs non-covalently attached to gold nanoparticles and B) crosslinked with bisthymine, respectively.	31
Figure 1.18	Poly(4-vinylpyridine)-pentadecylphenol and poly(styrene)-block-poly(4-vinylpyridine) pentadecylphenol surfactant complexes used by Ikkala and coworkers.	32
Figure 1.19	Cartoon showing the differences between classes of side-chain metal containing polymers. A) The ligand is bound to the backbone, and B) The metal complex is attached to the backbone.	35
Figure 1.20	Cartoon representations of the different categories of side-chain polymers possessing multiple recognition motifs.....	39
Figure 1.21	Complexes formed as a result of hydrogen bonding and proton transfer non-covalent forces, both are joined at each repeat unit of poly(4-vinylpyridine).	40
Figure 1.22	Multicomb polymeric assemblies formed via simultaneous employment of metal coordination and ionic-interactions.	40
Figure 1.23	ABC block copolymers containing diacetamidopyridine and dicarboxyimide hydrogen bonding recognition units that are complementary to one another.....	41

Figure 2.1	Structure property relationships for photorefractive polymers and polymeric OLEDs. A) Photorefractive polymers can be formed from random copolymers possessing a NLO chromophore, a charge transport agent, and a charge generator, B) polymeric OLEDs arise when block copolymers are made containing a hole transport layer, an electroluminescent layer, and an electron transport layer.	51
Figure 2.2	Materials synthesis and optimization using traditional covalent methods, which are serial in nature.....	52
Figure 2.3	One of Nature’s marvels, the structure of DNA.	55
Figure 2.4	Cartoon depicting the UPB concept. A single UPB can “parent” a multitude of functionalized copolymers via orthogonal one-step self-assembly of recognition counterparts.	58
Figure 2.5	Cartoon depicting the iterative optimization of a polymeric device via the UPB concept.....	59
Figure 3.1	Synthesis of side-chain functionalized polymers via metal coordination.	66
Figure 3.2	Structural attributes of pincer ligands and pincer metallacycles.	67
Figure 3.3	Self-assembled palladium SCS pincer complexes in supramolecular science.	70
Figure 3.4	Chauvin’s mechanism for the olefin metathesis reaction.	72
Figure 3.5	Mechanism for ROMP.....	72
Figure 3.6	Grubbs’ ruthenium alkylidene olefin metathesis catalysts.	73
Figure 3.7	The structural components of monomer design.....	74
Figure 3.8	Non-spaced nitrile functionalized mesogen 28	78
Figure 3.9	The aromatic and olefin region of the ¹ H NMR spectra depicting the metal coordination of mesogen 27 onto 21 (φ = CD ₂ Cl ₂). A) Mesogen 27 , B) polymer 21 . C) a 1:1 mixture of 27 and 21 , and D) the 1:1 mixture after addition of 1 equiv. of AgBF _{4(aq)} (polymer 31).	80

Figure 3.10	The aromatic and olefin region of the ^1H NMR spectra depicting the metal coordination of mesogen 14 onto 11 ($\phi = \text{CD}_2\text{Cl}_2$). A) Mesogen 14 , B) polymer 11 , C) a 1:1 mixture of 14 and 11 , and D) the 1:1 mixture after addition of 1 equiv. of $\text{AgBF}_4(\text{aq})$ (polymer 20).	82
Figure 4.1	Monomers used in ROMP to introduce functionality at the side-chain (1-3) and commercially available ruthenium olefin metathesis initiators (4-5).	104
Figure 4.2	Plot of conversion (%) as a function of time (sec) for the polymerization of 80:20 <i>endo/exo</i> - 11 (—●—), 80:20 <i>endo/exo</i> - 12 (—○—), <i>exo</i> - 11 (—■—), and <i>exo</i> - 12 (—□—).	109
Figure 4.3	Plot of M_n versus monomer-to-catalyst ratios for polymers 13 (—■—, eluant = THF) and 14 (—○—, eluant = CH_2Cl_2).	111
Figure 4.4	I) GPC traces of polymers prepared using monomer 12 . II) GPC traces of polymers prepared using monomer 11 . A) (—) Polymer after complete conversion ($[\text{M}]:[\text{I}] = 20:1$, M_w (11) = 8.1×10^3 , M_n (11) = 7.2×10^3 , PDI (11) = 1.13; M_w (12) = 6.3×10^4 , M_n (12) = 4.9×10^4 , PDI (12) = 1.29). B) (—) Same polymer after standing for 0.5 h followed by polymerization of 200 equiv ($[\text{M}_2]:[\text{M}_1] = 200:1$, $[\text{M}]:[\text{I}] = 20:1$, M_w (11) = 1.0×10^5 , M_n (11) = 7.1×10^4 , PDI (11) = 1.41; M_w (12) = 4.5×10^5 , M_n (12) = 3.4×10^5 , PDI (12) = 1.32) of additional monomer.	111
Figure 5.1	A cartoon depicting the formation of complex copolymers using stepwise and one-step, non-covalent multi-functionalization strategies.	125
Figure 5.2	The aromatic region of the ^1H NMR spectra depicting the stepwise functionalization (metal coordination followed by hydrogen bonding) of 5a . A) Pyridine (* = α -pyridyl protons), B) copolymer 5a (+ = amide protons), C) copolymer following directed metal coordination (5b), D) <i>N</i> -butylthymine (“ = imide proton), and E) fully functionalized copolymer 5d	131
Figure 5.3	The aromatic region of the ^1H NMR spectra depicting the stepwise functionalization (hydrogen bonding followed by metal coordination) of 5a . A) <i>N</i> -butylthymine (“ = imide proton), B) copolymer 5a (+ = amide protons), C) copolymer following directed hydrogen bonding (5c), D) Pyridine (* = α -pyridyl protons), and E) fully functionalized copolymer 5d	132

Figure 5.4	The aromatic region of the ^1H NMR spectra depicting the one-step multi-functionalization of 5a . A) Pyridine (* = α -pyridyl protons) B) <i>N</i> -butylthymine (“ = imide proton) C) copolymer 5a (+ = amide protons), and D) fully functionalized copolymer 5d	133
Figure 6.1	A cartoon depicting multi-step self-assembly via metal coordination based crosslinking and polymer functionalization via hydrogen bonding.	147
Figure 6.2	Recognition motifs for self-assembly and crosslinking studies: a) metal coordination, b) hydrogen bonding.....	150
Figure 6.3	Plot of relative viscosity as a function of solution concentration for metal crosslinked copolymers with varying concentrations (11a = 1.5%, 11b = 2.5%, 11c = 5.0%) of recognition units in the backbone.	156
Figure 6.4	Plot of relative viscosity as a function of solution concentration indicating large differences in solution viscosity between metal crosslinked (11b) and non-crosslinked copolymers (5b and 5b-Cl).	158
Figure 6.5	Plot of relative viscosity as a function of added mole equivalents of metal crosslinker 10 and the same polymer solution following titration with PPh_3	159
Figure 6.6	Plot of relative viscosity as a function of added mole equivalents of hydrogen bonding crosslinkers 12a , 12b , and 14	163
Figure 6.7	The aromatic region of the ^1H NMR spectra showing one-step multi-functionalization of 5c with hydrogen bonding crosslinker 12b and pyridine. A) Pyridine (* = α -pyridyl protons), B) Crosslinker 12b (“ = imide proton), C) Terpolymer 5c (+ = amide protons); and D) Crosslinked and functionalized copolymer 17	167
Figure 7.1	Proposed UPB structures based on a single type of interaction: A) multisite functionalization of metal coordination UPBs, and B) multisite self-assembly onto hydrogen bonding UPBs.....	187
Figure 7.2	Di-block UPB synthesis using metal-centered trpy-Ru-trpy bridges.....	189
Figure 7.3	Multicomponent polymer brushes based on the UPB concept. A) alternating grid structures formed using perfectly alternating UPB copolymers. B) perfectly alternating layers formed from pincer homopolymer grafting.	191

Figure 7.4	Main-chain self-assembled polymers. A) Meijer's famous telechelic ureidopyrimidinone main-chain self-assembled polymer, B) proposed statistical UPBs formed from monomer mixtures, and C) proposed perfectly alternating UPBs derived from a single self-assembling monomer unit.	193
Figure 7.5	A random three-component UPB amenable to one-step orthogonal functionalization and tethered functional groups that constitute the components required for photorefractivity.	197
Figure 7.6	A proposed multi-stage drug delivery vessel that could be prepared from biocompatible UPBs.....	199
Figure 7.7	One example of UPBs applied to sensor technology. A) a fluorescent UPB containing binding units for polyvalent toxins, B) a "universal" field-test kit that could potentially detect the presence of large numbers of biological threats.	200
Figure 7.8	UPB crosslinking methods that could potentially result in interesting "elastomers contained within elastomers" type materials. A) a UPB crosslinked with bifunctional crosslinkers, and B) tri- and tetra- heterofunctionalized crosslinkers.	201
Figure 7.9	Schematic showing the rapid formation of hierarchical architectures and nano-scale devices, which may be possible via implementation of the UPB concept.	203
Figure A.1	Cartoon depicting a one-pot tandem catalysis and self-assembly sequence.....	209
Figure A.2	Structure of polymer 1 , a supported Heck catalyst precursor and polymeric scaffold for self-assembly.....	210
Figure A.3	The aromatic and olefin region of the ¹ H NMR spectra depicting the metal coordination of stilbene 4d onto 1 (*CD ₂ Cl ₂). A) Stilbene 4d . B) Polymer 1 . C) A 1:1 mixture of 4d and 1 . D) The 1:1 mixture after addition of 1 equiv. of AgBF _{4(aq)}	212
Figure A.4	The aromatic and olefin region of the ¹ H NMR spectra depicting the tandem catalysis/self-assembly sequence ("DMF-d ₇ , *CD ₂ Cl ₂). A) 1:1 mixture of 2 and 3 . B) Polymer 1 . C) A 1:1:1 mixture of 1 , 2 , and 3d . D) The 1:1 mixture of 4d and 1 following catalytic Heck coupling. E) The 1:1 mixture following the addition of 1 equiv. of AgBF _{4(aq)}	216

LIST OF SCHEMES

Scheme 1.1	A post-functionalization route to polymeric scaffolds.....	19
Scheme 1.2	Hierarchical self-organization of side-chain self-assembled polymers.....	33
Scheme 1.3	Functionalization of terpyridine polyligands via self-assembly.....	36
Scheme 3.1	Dechlorination of Pd-Cl PCP pincer complexes.....	68
Scheme 3.2	Ligand displacement reactions.....	69
Scheme 3.3	Synthesis of <i>para</i> -hydroxy SCS pincer ligand.....	75
Scheme 3.4	Monomer synthesis and ROMP.....	76
Scheme 3.5	Synthesis of spaced nitrile and pyridine based mesogens.....	77
Scheme 3.6	Synthesis of non-spaced pyridine functionalized mesogen.....	78
Scheme 3.7	Synthesis of side-chain functionalized polymers via metal coordination.....	79
Scheme 4.1	Synthesis and ROMP of isomerically pure <i>exo</i> -norbornene monomers.....	107
Scheme 4.2	Synthesis of AB block copolymers containing both diaminopyridine and Pd ^{II} pincer receptor units.....	113
Scheme 5.1	UPB synthesis.....	127
Scheme 5.2	Non-covalent UPB functionalization strategies.....	129
Scheme 6.1	Cyanuric acid functionalized monomer synthesis.....	151
Scheme 6.2	Synthesis of random terpolymer 5	152
Scheme 6.3	Synthesis of random terpolymer 9	153
Scheme 6.4	Directed crosslinking via metal coordination.....	155
Scheme 6.5	Polymer activation at the metal center.....	157
Scheme 6.6	Directed crosslinking via triple hydrogen bonded diaminopyridine-thymine interactions.....	161

Scheme 6.7	Directed crosslinking via cyanuric wedges (ADA-ADA arrays) that bind to isophthalamide receptors (DAD-DAD arrays).....	162
Scheme 6.8	One-step orthogonal self-assembly with metal coordination based crosslinking and hydrogen bonding small molecule functionalization.	165
Scheme 6.9	One-step orthogonal self-assembly with hydrogen bonding based crosslinking and metal coordination small molecule functionalization.	166
Scheme A.1	The Heck reaction. ⁵¹	211
Scheme A.2	Tandem catalysis and self-assembly.....	214

LIST OF ABBREVIATIONS

Å	angstrom
A	acceptor (in hydrogen bonding)
ATRP	atom transfer radical polymerization
¹³ C NMR	carbon magnetic resonance
°C	degrees centigrade
CG	charge generator
cm ⁻¹	wavenumber
CTA	charge transport agent
δ	chemical shift
D	donor (in hydrogen bonding)
DAP	diaminopyridine
DCC	dicyclohexyl carbodiimide
DCM	dichloromethane
DMAP	4-dimethylamino pyridine
DMF	<i>N,N</i> -dimethylformamide
DMSO	dimethyl sulfoxide
DNA	deoxyribonucleic acid
DSC	differential scanning calorimetry
EI	electron ionization
EL	electroluminescence
ETL	electron transport layer
FAB	fast atom bombardment

FT-IR	Fourier transform infrared
g	gram
GPC	gel permeation chromatography
h	hour
$^1\text{H NMR}$	proton nuclear magnetic resonance
HRMS	high-resolution mass spectroscopy
HTL	hole transport layer
Hz	hertz
IR	infrared
J	coupling constant
Kcal	kilocalorie
k_i	rate constant for initiation
k_p	rate constant for propagation
L	liter
LC	liquid crystal
μL	microliter
M	molar
M^+	molecular ion
M^{-1}	inverse molar
m/z	mass-to-charge ratio
mg	milligram
MHz	megahertz
min	minute

mL	milliliter
mmol	milimole
M_n	number-average molecular weight
mol	mole
MsCl	methanesulfonyl chloride
M_w	weight-average molecular weight
NBT	<i>N</i> -butylthymine
NCN	nitrogen-carbon-nitrogen
NLO	nonlinear optical
NMNBT	<i>N</i> -methyl <i>N</i> -butylthymine
NMR	nuclear magnetic resonance
OLED	organic light emitting diode
^{31}P NMR	phosphorus magnetic resonance
PCP	phosphorus-carbon-phosphorus
PDI	polydispersity index
POSS	polyhedral oligomeric silsesquioxane
ppm	parts per million
r.t.	room temperature
ROMP	ring-opening metathesis polymerization
SCFP	side-chain functionalized polymers
SCLCP	side-chain liquid crystalline polymers
SCMP	side-chain metal containing polymers
SCS	sulfur-carbon-sulfur

sec	second
SHG	second harmonic generation
TBAF	tetrabutyl ammonium fluoride
TBDMSCl	<i>tert</i> -butyl dimethyl silyl chloride
T _{dec}	decomposition onset temperature
T _g	glass transition temperature
TGA	thermogravimetric analysis
THF	tetrahydrofuran
TOF	turnover frequency
TON	turnover number
trpy	terpyridine
UPB	universal polymer backbone
UV-VIS	ultraviolet-visible

SUMMARY

This thesis begins with a brief analysis of the synthetic methodologies utilized in polymer science. A conclusion is drawn inferring that upper limits in molecular design are inevitable, which arise as a direct consequence of the predominance of covalent strategies in the field. To address these concerns, the “universal polymer backbone” (UPB) concept has been hypothesized.

A UPB has been defined as any copolymer, side-chain functionalized with multiple recognition elements that are individually capable of forming strong, directional, and reversible non-covalent bonds. Non-covalent functionalization of these scaffolds can lead to the formation of a multitude of new polymer structures, each stemming from a single parent or “universal polymer backbone”.

To prepare such a UPB, isomerically pure *exo*-norbornene esters containing either a Pd^{II} SCS pincer complex or a diaminopyridine residue were synthesized, polymerized, and copolymerized via ROMP. All polymerizations were living under mild reaction conditions. Kinetic studies showed that the k_p values are highly dependent upon the isomeric purity but completely independent of the terminal recognition units. Non-covalent functionalization of these copolymers was accomplished via 1) *directed self-assembly*, 2) *multi-step self-assembly*, and 3) *one-step orthogonal self-assembly*. This system shows complete specificity of each recognition motif for its complementary unit with no observable changes in the association constant upon functionalization.

To explore potential applications of this UPB concept, random terpolymers possessing high concentrations of pendant alkyl chains and small amounts of recognition units were synthesized. Non-covalent crosslinking using a directed functionalization

strategy resulted in dramatic increases in solution viscosities for metal crosslinked polymers with only minor changes in viscosity for hydrogen bonding motifs. The crosslinked materials were further functionalized via self-assembly by employing the second recognition motif, which gave rise to functionalized materials with tailored crosslinks. This non-covalent crosslinking/functionalization strategy could allow for rapid and tunable materials synthesis by overcoming many difficulties inherent to the preparation of covalently crosslinked polymers.

Finally, the current status of the UPB concept is reviewed and methodological extensions of the concept are suggested. Evaluation of how UPBs may be used to optimize materials and their potential use in fabricating unique electro-optical materials, sensors, and drug delivery vesicles are explored.

CHAPTER 1.

SELF-ASSEMBLY IN POLYMER SCIENCE

1.1 Abstract

In this chapter, self-assembly and supramolecular science are defined and placed in the context of polymer science, with distinction made between main-chain and side-chain self-assembled polymers. The design principles, non-covalent functionalization strategies, and historical evolution of the field of side-chain self-assembled polymers are critically reviewed. Emphasis is placed on metal coordination and hydrogen bonding recognition elements. Moreover, side-chain self-assembled polymers possessing single recognition motifs and copolymers possessing multiple recognition elements are appropriately categorized.

1.2 Introduction

From before Linus Pauling's groundbreaking work on the hydrogen bond in the 1930's¹ to Jean Marie Lehn's "Chemistry beyond the molecule" that led to the term "supramolecular chemistry", the nature of non-covalent bonds has fascinated chemists for over a century.² In particular, the last thirty years have been exceptionally fruitful for scientists from a variety of disciplines who have made enormous advances in exploiting the non-covalent bond to construct sophisticated architectures.²⁻¹¹ As macromolecular structures and functional materials have continued to evolve with higher degrees of

complexity and function, traditional covalent-based synthetic strategies have become increasingly difficult to employ. Accordingly, many scientists have begun to replace traditional polymer synthesis with self-assembly in order to overcome a variety of synthetic hurdles and to exploit the dynamic nature of the non-covalent bond.^{3,5,11-13} Tremendous growth and elegant advances in polymer science have taken place as supramolecular science, self-assembly, and polymer chemistry continue to converge. This chapter explores the fundamental concepts of self-assembly and places strong emphasis on the design principles and functionalization strategies employed in the field of self-assembled side-chain functionalized polymers (SCFPs) by highlighting the advancements that have given rise to the sophisticated non-covalent functionalization methods employed today.

1.3 Definition of Self-Assembly

The term self-assembly has become ubiquitously incorporated into today's scientific repertoire as a direct consequence of the field's current popularity and growth. However, the definition of self-assembly has increasingly become an issue of debate, which arises mainly due to the large number of scientific disciplines perusing concepts that wholly or partially embody the original concepts of supramolecular science.⁴ Thus, the meaning of self-assembly is often times loosely adapted to fulfill a criterion set forth by a specific research goal or, in some cases, the pursuits of entire fields. Although highly debated, several definitions have evolved into today's literature; each somewhat unlike the other, yet all simultaneously encompass the importance of the non-covalent bond. These variations can be evidence of nothing more than a healthy growth of the field to incorporate increasingly broader ranges of concepts and situations.

One of the most frequently cited definitions comes from Lehn, who formally describes self-assembly² as “...*the spontaneous association of either a few or many components, resulting in the generation of either discrete oligomolecular supermolecules or of extended polymolecular assemblies.*” In this definition, emphasis is placed on the process of forming complexes via association of components with less importance placed upon the nature of the “higher ordered”¹⁴ structures that arise from host-guest molecular association. On the other hand, Lindsey draws a distinction between *strict* self-assembly and other classes of self-assembly. He defines, *strict* self-assembly¹⁴ as “...*the spontaneous formation of higher-ordered structures. The product is contained within the subunits or precursor molecules, and neither additional factors nor energy input are required for assembly to occur.*” He then goes on to define other categorized levels of self-assembly placed in a biological context that include: i) *self-assembly with post modification*, where covalent linkages are formed following a self-assembly step in order to irreversibly join an assembled structure, ii) *self-assembly with intermittent processing*, where a series of host-guest complex formations, each of which is subsequently exposed to a secondary step that induces irreversibility into the system, resulting in a well-defined superstructure, and iii) *directed self-assembly*, where a template or scaffold is employed to organize the self-assembling components, but does not become a part of the overall supramolecular structure.¹⁴ Similarly, Whitesides defines self-assembly¹⁵ as “...*the spontaneous association of molecules under equilibrium conditions into stable, structurally well-defined aggregates joined by non-covalent bonds.*” In both Lindsey’s and Whitesides’ definitions, a strong emphasis is placed on the superstructure or supramolecular entity formed from the self-assembling event. Others contend that the

formation of even the simplest non-covalent host-guest complexes be deemed self-assembly.^{2,4,16-18} The latter modifications to the definition generally exclude the formation higher-ordered structures. Those who follow this definition argue that the formation of the non-covalently adjoined entity is unto itself a higher ordered structure when compared to individual components from which it was formed.

In this thesis, self-assembly is defined as the spontaneous formation of well-designed host-guest complexes, including the complexation of ligands to metals, each of which may not necessarily result in the formation of highly ordered supramolecular architectures. The definition of self-assembly presented herein focuses not upon the growth of large molecular assemblies, but rather exploits the non-covalent bond to spontaneously join or serve as an intermolecular “tether” that forms as a consequence of a host-guest complexation event to yield stable, well-defined, intermolecular pairs in solution and in the solid state.

1.4 Non-Covalent Bonds

Non-covalent bonds can be thought of as the building blocks or “molecular legos” that are used to construct all host-guest linkages used in self-assembly. While in general non-covalent interactions are classified by the nature of the interaction, special attention must be given to the categorical strength or bond energies of a non-covalent pair when selecting an interaction for use in self-assembly. According to Steed and Atwood, the strongest non-covalent bonds, ion-ion interactions, arise from cation-to-anion bonding and possess bond energies comparable in strength to covalent bonds (24-85 Kcal/mol); whereas Van der Waals forces, formed by polarization of electron clouds located in the proximity of an adjacent nuclei can be considered the weakest, with bond energies of less

than 1 Kcal/mol.⁴ Table 1.1 outlines a variety of non-covalent interactions and their respective bond strengths. Due to their high dependence on external influences such as pressure, solvent, and temperature, most non-covalent forces do not fall into a single strength category; however, generalizations can be drawn.^{2,4} For example, single π - π ¹⁹, cation- π ²⁰, or van-der-Waals interactions^{2,4} and some hydrogen bonds^{2,21-23} may be classified as being weak while metal coordination complexes^{2,4,24} (highly dependant on the ligand system and the metal used) and ion-ion interactions^{2,4,25} are usually considered strong.

Table 1.1 Non-covalent interactions ordered according to bond strength.⁴

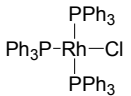
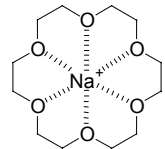
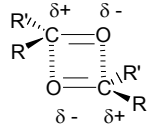
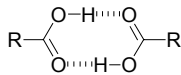
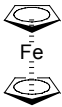

Non-Covalent Bond	Strength (Kcal/mol)	Example
Ion-Ion Interactions	24-85	NaCl
Metal Coordination	12-60	 Wilkinson's Catalyst
Ion-Dipole Interactions	12-50	
Dipole-Dipole Interactions	1-12	
Hydrogen Bonding	1-30	

Table 1.1 (CONT.)

Cation- π Interactions	1-20	
π - π Stacking	0-12	<div style="display: flex; justify-content: space-around; align-items: center;"> <div style="text-align: center;">  <p>Face-to-Face</p> </div> <div style="text-align: center;">  <p>Edge-to-Face</p> </div> </div>
Van der Waals Forces	<1	Noble Gases, Inclusion Complexes

The strength of a single hydrogen bond is generally weak, highly dependent upon the electronic nature of the donor and acceptor, and is greatly influenced by solvent polarity.²¹⁻²³ However, synthetic hydrogen bonding recognition elements have recently emerged that combine multiple hydrogen bonds in a variety of configurations in order to amass strength, stability, and selectivity.^{2,5,23} Recognition motifs that incorporate more than one hydrogen bonding unit rely primarily on electrostatic factors where the arrangement and number of neighboring donor and acceptor units plays an important role in dictating the strength of complexation.^{5,23,26,27} Figure 1.1 illustrates how the location of multiple hydrogen bonding donor (D) and acceptor (A) moieties relative to one another impacts the strength of the resulting complex. Many multiple hydrogen bonded complexes found in Nature possess ADA-DAD arrangements (**1** and **2**) which give rise to association constants around 10^2 M^{-1} to 10^3 M^{-1} , whereas synthetic complexes such as **5** and **6** possess an AAA-DDD arrangement that gives rise to much larger K_a values ($>10^5 \text{ M}^{-1}$).⁵ This phenomenon is easily explained by differences in repulsive and attractive

secondary interactions between adjacent motifs.^{5,26,27} If the diagonally opposite sides experience net electrostatic repulsion, then the final complex is less stable. If the diagonally opposite sides experience net electrostatic attractive forces, then the final complex is stabilized. In Figure 1.1-A the ADA-DAD complex possesses the largest number of net repulsive forces and is therefore the least stable, whereas in Figure 1.1-C the AAA-DDD motif possesses the maximum amount of secondary attractive electrostatic forces is therefore the most stable.

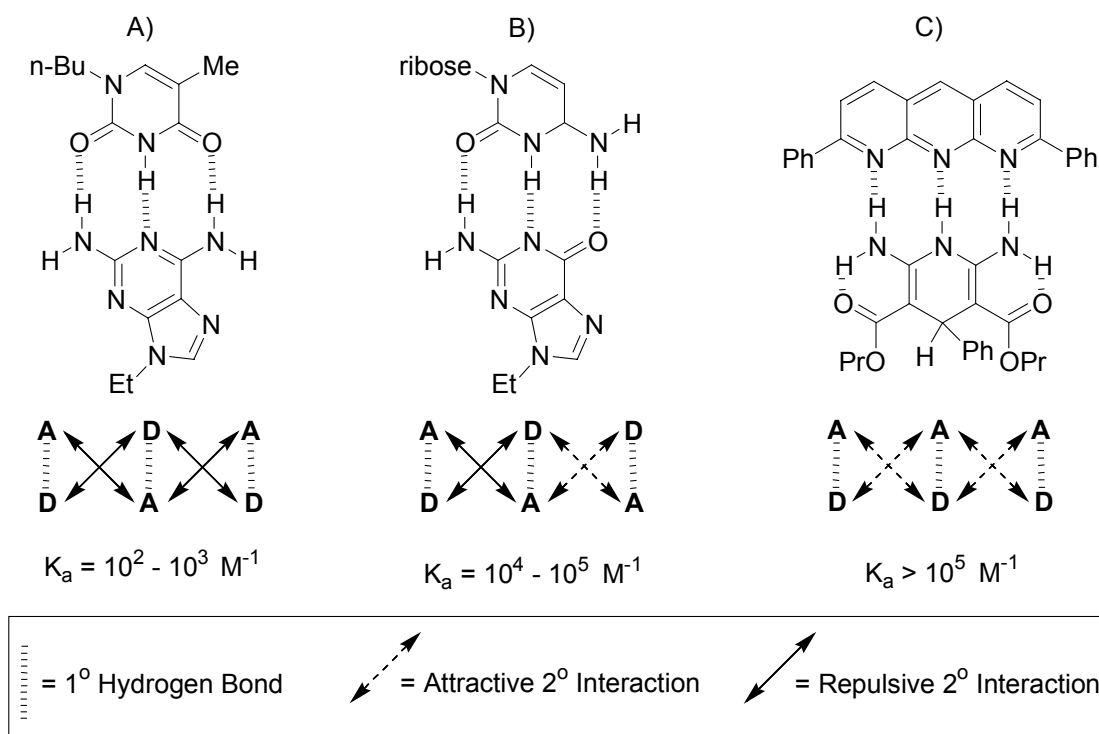


Figure 1.1 Multiple hydrogen bonded complexes possessing different arrangements of acceptor and donor units. A) ADA-DAD, B) ADD-DAA, and C) AAA-DDD.

Coordination motifs are generally thought of as strong interactions.^{2,4,24} Tailoring their strength is largely dictated by crystal field theory.²⁸ Several electronic factors govern metal coordination strength, including the degree of orbital overlap between the metal and the ligand as well as the location of the ligand along the spectrochemical series.²⁸ Furthermore, the presence or absence of non-electronic factors such as chelate effects and steric effects greatly influence the stability of a coordination sphere.²⁸ All of the above factors contribute to the large number of coordination motifs that can be employed as recognition elements.

Today, a large variety of recognition elements are available for the supramolecular chemist to choose from, each possessing a variety of bond strengths and varying physical properties, however, the appropriate selection is highly dependent upon the desired application. For example, supramolecular polymeric materials for electro-optical applications must be stable for thousands of working hours, requiring strong and stable non-covalent bonds. While a system designed for drug delivery might necessitate the use of weaker bonds to facilitate ease of drug release. Regardless of the situation, choice of recognition element is not an easy one and can be further complicated by other parameters such as solubility or biological compliance.

1.5 Self-Assembled Polymers

Self-assembled polymers are formed when the covalent linkages utilized in traditional polymer chemistry, including bonds that connect monomer units together and those that attach side-chain functional groups to polymer backbones, are substituted with highly directional and sufficiently strong non-covalent host-guest pairs.^{3,5,12,13,24} Replacement of covalent bonds with non-covalent linkages provide unique and highly functional

polymeric structures that contain the chief features of most self-assembled entities such as reversibility, self-healing character, and susceptibility to external stimuli, but also, in many cases, maintain the strength and physical properties of covalently constructed polymers. This concept stems from direct observation of natural polymers where the complexity and molecular function found in biomaterials can be directly credited to Nature's efficient use of non-covalent bonds to form the most eloquent materials including DNA and proteins.^{14,29}

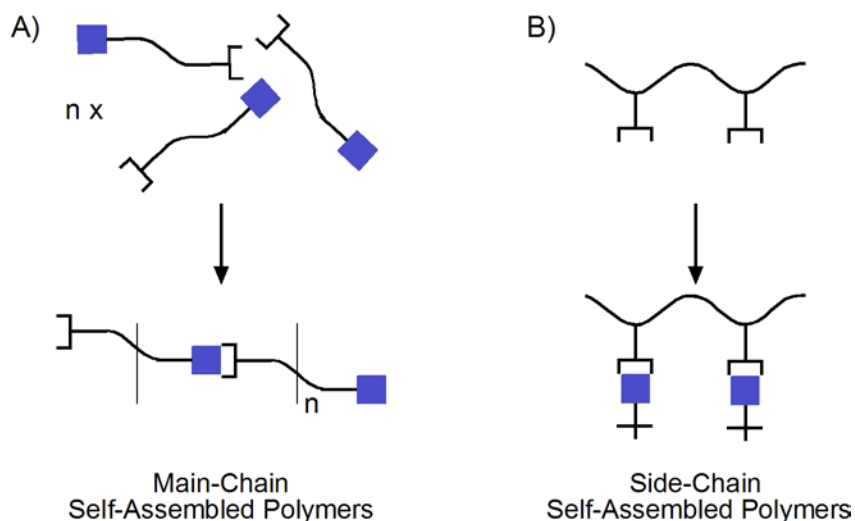


Figure 1.2 Cartoon schematic that depicts the differences between A) main-chain self-assembled polymers and B) side-chain self-assembled polymers.

In recent years, self-assembly has become an important sub-field of polymer science, arising as a consequence of major advances in the fields of molecular recognition and small molecule self-assembly. Self-assembled polymers are typically divided into two major categories: main-chain and side-chain (Figure 1.2).^{5,12,13} Main-chain supramolecular polymers can be described as polymeric systems that are held together by

directional non-covalent interactions in the polymer backbone or main-chain. In contrast, side-chain supramolecular polymers are based on a covalently linked polymer backbone that contains molecular recognition units on its side-chain and can be functionalized via self-assembly.

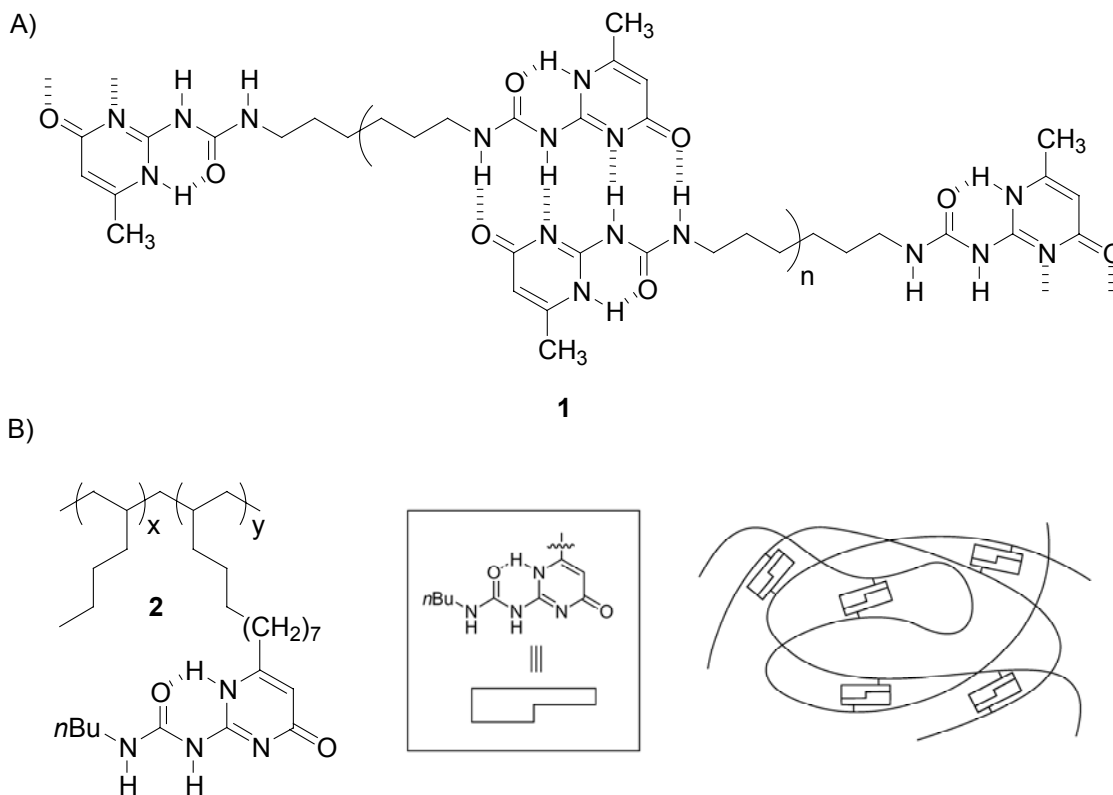


Figure 1.3 Select homonuclear self-assembled polymers. A) Meijer's homonuclear main-chain self-assembled polymers, and B) Coates' homonuclear side-chain self-assembled copolymers.³⁴ In both cases self-dimerizing ureidopyrimidinone recognition elements are employed.

Both main-chain and side-chain self-assembled polymers can be subcategorized as homonuclear or heteronuclear according to the nature of the recognition motif employed.⁵ In homonuclear self-assembly, polymers are synthesized or functionalized using recognition elements that possess a strong propensity to dimerize. In contrast, heteronuclear self-assembled polymers utilize complimentary recognition pairs with strong association constants and inherently low dimerization constants.

Homonuclear main-chain polymerizations almost always employ a single monomer unit bisfunctionalized with self-dimerizing recognition units and therefore give rise to AA homopolymers.⁵ Meijer and coworkers have provided one of the earliest examples of homonuclear main-chain self-assembled polymers (Figure 1.3-A).³⁰⁻³³ Here, the tethering of two ureidopyrimidinone units together ($K_{\text{dim}} > 10^6 \text{ M}^{-1}$) using a central C-6 alkyl chain results in the formation of linear homopolymers (**1**). The rheological behavior of these assemblies mimics that of linear polymers and possesses thermal reversibility, a unique feature of hydrogen bonded supramolecular polymers.³³

In comparison, homonuclear side-chain self-assembly often results in thermally reversible crosslinked polymers and globular structures.³⁴ These structures form when self-dimerizing recognition elements are implemented onto the side-chain of covalent polymer backbones. In 2001, Coates and coworkers reported an excellent example of homonuclear side-chain polymers where α -hexene can be copolymerized with a small amount of ureidopyrimidinone-functionalized α -olefin monomer (Figure 1.3-B).³⁴ The resulting random copolymers, (**2**), give rise to interesting, non-covalently crosslinked materials possessing thermoplastic elastomeric properties.

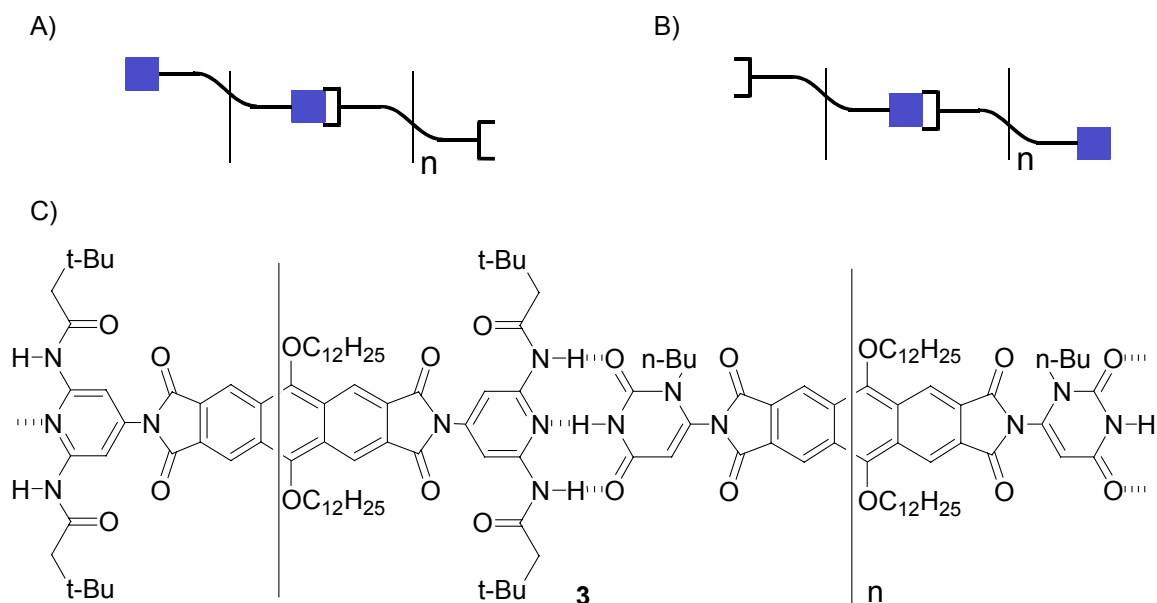


Figure 1.4 Heteronuclear main-chain self-assembled polymers A) The AAB structure formed from two symmetrically bisfunctionalized monomer units, B) The ABAB configuration resulting from the use of a single asymmetrically end-functionalized monomer unit, and C) An example of Lehn's liquid crystalline heteronuclear main-chain self-assembled polymers.

Unlike homonuclear self-assembled polymers, whose recognition elements rely upon self-dimerizing species, heteronuclear main-chain self-assembled polymers arise when multiple monomer units, each end-functionalized with complimentary recognition unit elements capable of strong and directional self-assembly, are employed.^{5,35-39} As shown in Figure 1.4, these systems allow for AAB or ABAB copolymers to be accessed depending upon the monomer(s) symmetry. If two symmetrically bisfunctionalized monomers are employed (Figure 1.4-A), then AAB self-assembled copolymers are formed³⁶⁻³⁹, whereas ABAB configurations can be accessed using single asymmetrically end-functionalized monomer units (Figure 1.4-B).³⁵ Lehn and coworkers published some of the early and most elegant examples of heteronuclear main-chain self-assembly in the

early 1990's.³⁶⁻³⁹ By simple 1:1 mixing of two symmetrically functionalized dialkyloxyanthrocene rigid rods, each possessing either a diaminopyridine residue or a uracil recognition element, lyotropic liquid crystalline self-assembled main-chain copolymers (**3**) could be formed (Figure 1.4-C).³⁸ This study nicely illustrates the complexity, functionality, and sheer elegance of applying the principles of self-assembly to main-chain polymer science.

In comparison, side-chain heteronuclear polymers incorporate complimentary recognition units located along the side-chains of a covalent polymer backbone. These systems allow for either self-functionalization or modular functionalization depending upon number of and location of the complimentary pair(s). If both complimentary units are tethered to a covalent backbone, then self-functionalization or intramolecular folding is likely to occur (Figure 1.5-A).⁴⁰ However, if a single complimentary unit is placed along the backbone and subsequent self-assembly of a small molecule containing the recognition counterpart occurs, then modular functionalization or intermolecular functionalization takes place (Figure 1.5-B).^{16-18,41-62} In Nature, the formation of hierarchical peptide architectures such as α -helices or β -sheets are based on self-functionalization while the replication of DNA is based on a modular functionalization strategy.^{14,29}

Compared to main-chain self-assembled polymers, side-chain self-assembled polymers have not yet attracted as much interest despite their importance for a variety of applications including drug delivery and electro-optical materials. Only a limited number of literature reports use self-assembly as a side-chain functionalization tool.^{16-18,41-59} One of the major objectives of this thesis is to further develop this important area of polymer

science and to introduce completely new ways to multifunctionalize side-chain copolymers via self-assembly. To place these objectives in context, the remainder of this chapter focuses upon the evolution of heteronuclear side-chain self-assembled polymers.

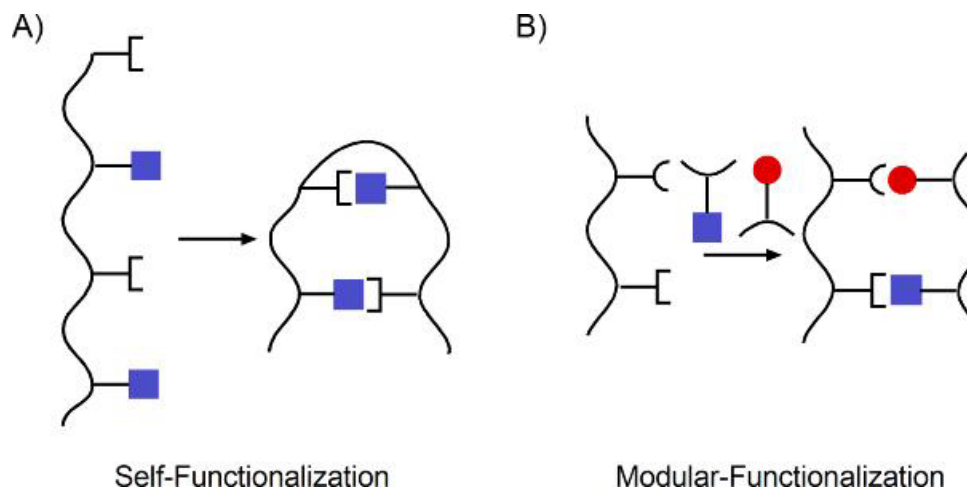


Figure 1.5 Side-chain heteronuclear polymers. A) Those formed by self-functionalization strategies, and B) those formed using modular functionalization.

1.6 Side-Chain Functionalized Polymers Based on a Single Recognition Motif

Side-chain self-assembled polymers are largely based on a single recognition motif.^{16-18,41-59} Non-covalent grafting of molecular components to the side-chain of polymer backbones has been accomplished using a variety of non-covalent interactions. The most ubiquitous examples employ simple hydrogen bonds,^{16,17,41-47,51-59,63-67} with fewer examples that extend this methodology to ionic interactions, π - π stacking, or metal coordination.^{18,48-50} The earliest reported cases use a single non-covalent bond to attach a mesogen that is able to phase segregate to yield higher ordered architectures such as liquid crystalline phases.^{41-43,45-49} Many examples mimic Nature's ability to cooperatively

bind a complementary recognition unit, citing the potential of these systems to mimic or interfere with biological systems.^{59,63-67} Other examples employ non-covalent crosslinkers and hydrophobic or hydrophilic interactions to give rise to various micellar structures.^{43,50,51} Regardless of the motivation, each of these systems relies on two types of design principles: i) those that are specific to the intended application, and ii) those that can be generalized to all supramolecular side-chain functionalized polymers (SCFPs).

1.6.1 The Earliest Examples: Self-Assembled Side-Chain Liquid Crystalline Polymers

Non-covalent side-chain functionalization strategies were first reported for the synthesis of liquid crystalline materials.^{46,48} Liquid crystals (LCs) possess orientational or weak positional ordering that give rise to materials possessing important orientational characteristics of crystals but with flow behavior similar to liquids. Polymeric liquid crystals employ a variety of self-organizational processes to achieve long-range order. Conventional side-chain liquid crystalline polymers (SCLCPs) are typically prepared via covalent tethering of mesogenic entities, structurally similar to low molecular weight LCs mesogens, with long, flexible aliphatic chains.⁶⁸ This spacer group, situated between the polymer backbone and the mesogen, decouples the motion of the polymer from the side-chain giving flexibility to the molecular orientation of the mesogenic components.⁶⁹ In the field of self-assembled SCLCPs, the principles described above for SCLCPs are generally followed, however covalent attachment of the mesogen is replaced with non-covalent bonds (Figure 1.6).

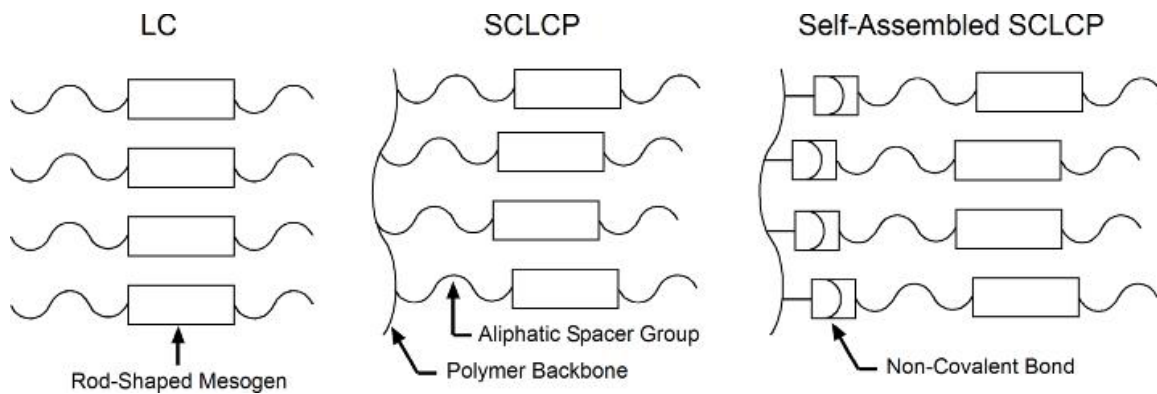


Figure 1.6 Schematic illustration of the structural components used to fabricate simple LCs, SCLCPs, and self-assembled SCLCPs from rod-shaped mesogens.

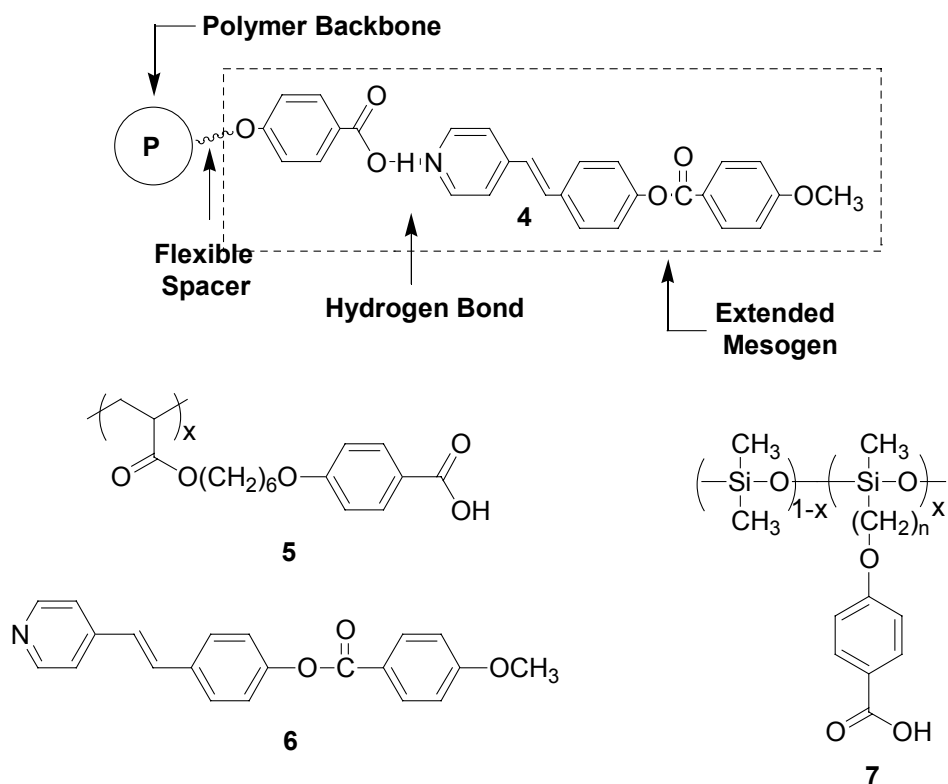


Figure 1.7 Molecular components used to prepare the first examples of self-assembled SCLCPs.

Kato and Fréchet were the first to explore the non-covalent attachment of traditional liquid crystalline components to a variety of polymer backbones.⁴⁶ In 1989, they disclosed their report describing binary mixtures of **5** and **6** to form thermotropic self-assembled SCLCPs via simple single pyridine-benzoic acid hydrogen bonded complexes (**4**) (Figure 1.7).^{42,46} Here, each component independently shows liquid crystalline behavior. However, when 1:1 mixtures of **5** and **6** or **7** and **6** are prepared, nematic mesophases with higher transition temperatures than those of the individual components are observed. This mesophase stabilization is attributed to the formation of extended mesogenic units involving the hydrogen bonded complex **4** shown in Figure 1.7.

While Kato and Fréchet's novel class of liquid crystalline polymers was based on a single weak non-covalent bond, this report held much significance not only for the field of self-assembled SCLCPs, but also established fundamental design strategies for the preparation of supramolecular SCFPs in general. Following their original report, much effort was directed toward examining self-assembled SCLCPs engineered with a variety of structural configurations.^{41-49,55} In particular, examples followed that included: i) the employment of anchored hydrogen bonding complexes for the attachment of mesogenic components (Figure 1.8-A),^{43,45} ii) the self-assembly of two entities that individually show no liquid crystalline behavior alone, but give rise to mesogenic hydrogen bonded entities upon association (Figure 1.8-B),^{41,47} iii) the main-chain insertion of hydrogen bonding units that can subsequently bind complementary hydrogen bonding units that are tethered to a mesogenic component (Figure 1.8-C),⁴⁴ and iv) the formation of liquid crystalline networks via the crosslinking of two polymer strands using bisfunctionalized hydrogen bonding mesogenic entities (Figure 1.8-D).^{43,55}

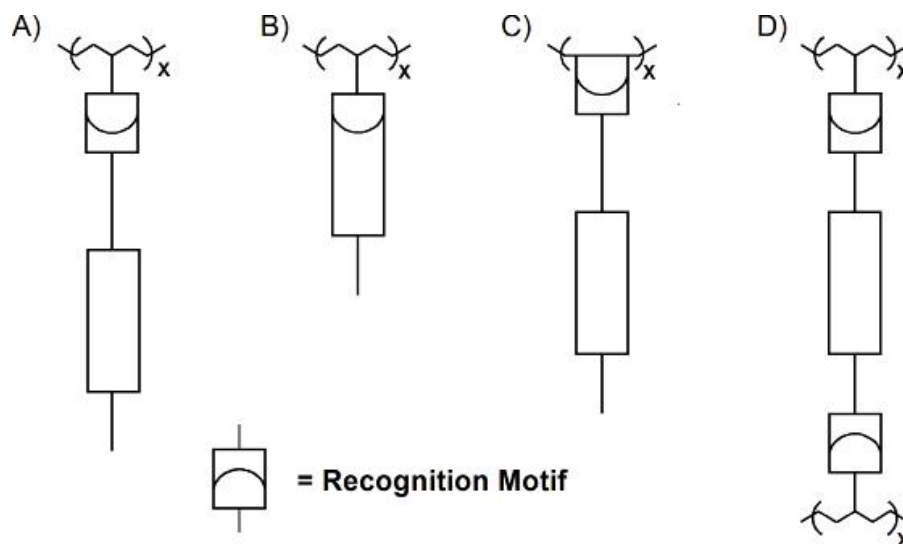
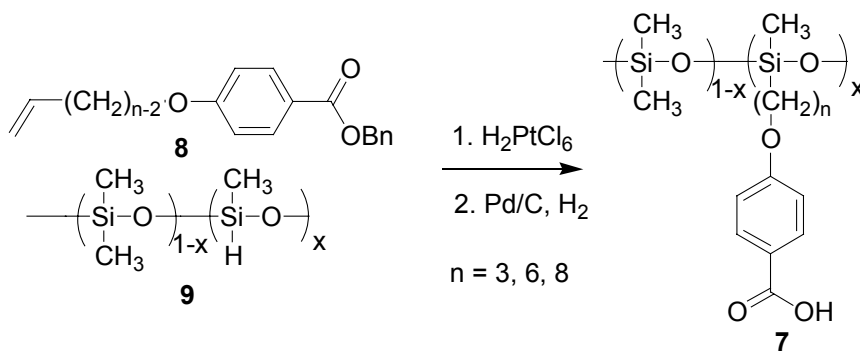


Figure 1.8 Schematic illustration depicting a variety of structurally configured hydrogen bonded self-assembled SCLCPs. A) Side-chain anchored mesogens, B) side-chain extended mesogens or mesogen formation, C) main-chain anchored mesogens, and D) crosslinked side-chain anchored mesogens.

Perhaps, the most challenging aspects of synthesizing self-assembled SCLCPs is the incorporation of the recognition motif into the monomer and the formation of the polymeric scaffold. The synthesis of polymers possessing recognition units must take into consideration a variety of factors including: i) the type of polymer backbone, ii) the physical and mechanical properties of the backbone, iii) the method used to incorporate the recognition motif, and iv) the polymerization technique to be employed. This concept can be best illustrated by analyzing the benzoic acid functionalized self-assembled SCLCPs first explored by Kato and Fréchet (Figure 1.7).^{42,46} First, a decision to utilize a backbone amenable to the intended application was made, which was based largely upon the desired physical properties of the resultant polymers and the ease of synthesis. Thus, poly(acrylate)s and poly(siloxane)s were chosen. Secondly, a decision to either incorporate the benzoic acid moiety in the original monomer design or in a post-

polymerization functionalization strategy required a detailed understanding of the polymerization technique. For example, poly(acrylate) **5** was obtained via free radical polymerization of 4-[(5-acryloylhexyl)oxy] benzoic acid.⁴⁶ In this example, the polymerization strategy is tolerant to the benzoic acid moiety and the synthetic challenges lie in the preparation of the monomer.

Scheme 1.1 A post-functionalization route to polymeric scaffolds.



Although pre-functionalization may seem like a more elegant strategy, many polymerization techniques are often unavailable due to functional group incompatibilities. For example, **7** required modification of a prefabricated polymer backbone because poly(siloxane)s, prepared via condensation reactions, are functional group intolerant of carboxylic acids. Here, the benzoic acid moiety is introduced into the side-chain after the polymerization using a hydrosilylation reaction with benzyl protected alkene **8** and commercially available poly(methylhydro-siloxane-co-dimethylsiloxane) **9** (Scheme 1.1).⁴² A second reaction, hydrogenolysis of the benzyl-protecting group, is required to yield the final polymer **7**. In this example, the synthesis of the polymeric scaffold is complicated by two post-polymerization reactions: i) functionalization of the

prefabricated polymer and ii) deprotection. Although successful, this strategy adds the stringent requirement that all reactions have to proceed in near quantitative yields. Otherwise, incomplete reactions can lead to poorly defined systems limiting the utilization of self-assembled SCLCPs in functional devices.

These early examples of liquid crystalline SCFPs are based on very weak non-covalent interactions that contain either one or two hydrogen bonds. While these interactions allow for dynamic bonding between the mesogens and the polymer backbones, the final self-assembled polymer's properties are limited due to the inherent weakness of the hydrogen bonds. To overcome this hurdle, other non-covalent recognition motifs, such as ionic interactions and metal coordination, have been investigated following the basic design principles described above for hydrogen bonding based systems.^{48,49}

Self-assembled SCLCPs are the earliest and most widely studied class of supramolecular side-chain functionalized polymers. These studies have clearly established a variety of design principles for supramolecular SCFPs in general and have demonstrated that the concept of non-covalent side-chain functionalization can be employed for the formation of this important class of materials. In recent years, literature reports have presented a variety of ways to optimize the strength of the non-covalent interactions, the polymer backbone, as well as the liquid crystalline properties.⁶⁸ At this time, no devices based on supramolecular side-chain functionalized liquid crystalline polymers have been reported, a drawback that should be addressed in the near future.

1.6.2 Nature Inspired Systems: Advancements in the Preparation and Functionalization of Hydrogen Bonding Side-Chain Polymers

The best-known example of side-chain functionalization via self-assembly is DNA. The structure of DNA is rather simple, composed of only four complementary base pairs and a sugar phosphate backbone, yet it is arguably one of the most complex and dynamic functional biomaterials.^{14,29,70} It is well accepted that the diversity and intricacy of DNA is achieved primarily via Nature's efficient use of components capable of undergoing non-covalent interactions including hydrogen bonding.^{14,29} Decades after Watson and Crick reported the structure of DNA,⁷¹ many research programs continue to take design lessons from Nature, dedicated toward the preparation of side-chain polymers capable of imitating the complexity and functionality of DNA.^{59,63-67} These reports generally explore the synthesis of hydrogen bonding polymers citing the high potential such systems hold for the preparation of advanced dynamic, reversible, and self-healing materials.

Controlled Routes to Nature Inspired Systems

Fundamental to the exploration and exploitation of the remarkable structure-property relationships inherent to biopolymers is the synthesis of structures that closely resemble those found in Nature. Research efforts towards this goal have been hampered by the fact that most polymerization methods produce polymers with broad molecular weight distributions. In fact, most examples of bio-inspired polymers that incorporate recognition units^{16-18,41-43,45-49,51-58,60-62} are synthesized either by using conventional free-radical polymerization techniques or via statistical attachment to poorly defined polymer backbones. These methods provide limited models of the monodisperse biopolymers found in Nature. Accordingly, much attention has recently been focused on the

preparation of polymers⁶³⁻⁶⁷ with low polydispersity via controlled polymerization methods using ATRP⁷² and ROMP.⁷³

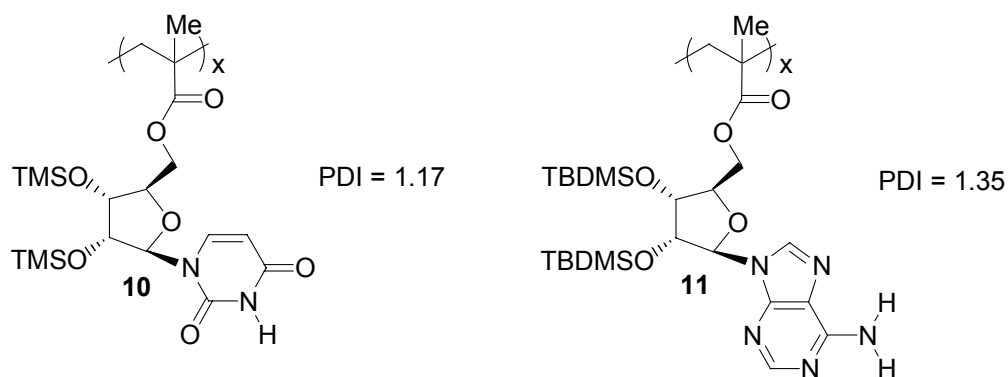


Figure 1.9 Poly(nucleoside)-based polymers containing uridine (**10**) and adenosine (**11**) recognition motifs synthesized via ATRP.

In one account, Marsh and coworkers showed that ATRP could be employed to synthesize well-defined poly(nucleoside)-based polymers containing uridine and adenosine recognition motifs.⁶⁶ In this example, polymers **10** and **11** were synthesized with predictable molecular weights and low polydispersities (1.17-1.35). Additionally, these studies showed that ATRP is inert to many of the functional groups found in natural systems (Figure 1.9). Although successful, this method is susceptible to oxidation and requires inert atmospheric conditions, thereby limiting the approach.

A more robust polymerization method for preparing polymers with controlled architectures and low polydispersity is ROMP.⁷³ Gibson and coworkers were first to report that thymine functionalized norbornenes could be polymerized via ROMP in a controlled manner (PDI=1.07).⁶⁵ However, extension of this methodology to a variety of other nucleic-acid base containing monomers was hampered by low reactivity.⁶⁴ Weck

and Stubbs explored a variety of possible solutions to circumvent the poor polymerization of sluggish triazine based hydrogen bonding monomers (**12**).⁶⁷ One strategy, fundamental to monomer design, was removal of the carbonyl moiety from the norbornene unit (**12**) in order to destroy any steric or electronic factors that may be retarding polymerization. Indeed, this minor modification resulted in a largely accelerated propagation but unveiled a second difficulty; that of poor polymer solubility and precipitation due to strong self-association of recognition units during polymerization. To circumvent this problem a clever protecting group approach was implemented.⁶⁷ Pretreatment of **13** with *N*-butylthymine yielded complex **15** in 100% yield with no evidence of precipitation. Although this novel strategy removed both the difficulty of the low reactivity and the problem of precipitation for densely functionalized hydrogen norbornene monomers, the polymerizations remained uncontrolled. (Figure 1.10)

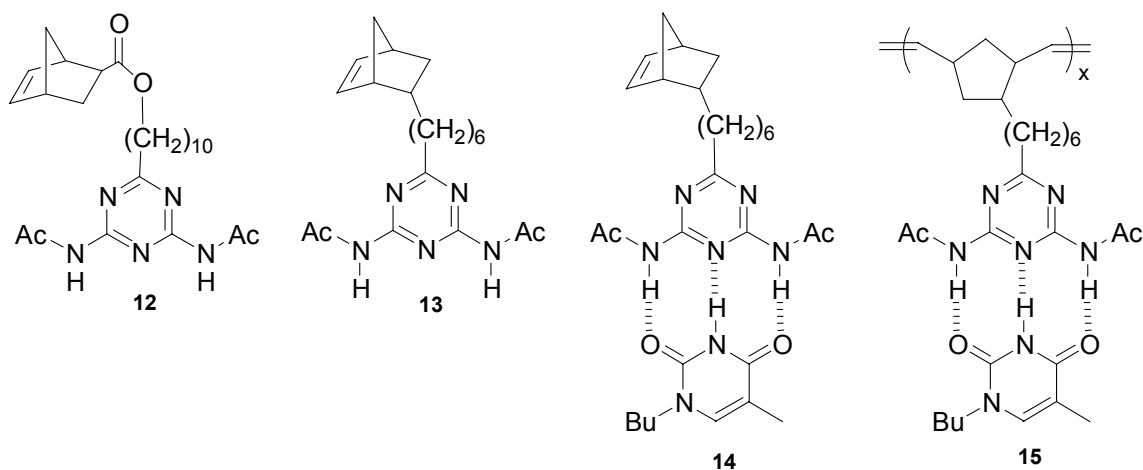


Figure 1.10 ROMP monomers and polymers possessing recognition elements capable of forming multiple hydrogen bonds.

Sleiman and coworkers reported attempts to extend this methodology to the preparation of AB block copolymers (**16**) by sequential addition of adenine-functionalized norbornene:succinimide complexes to fully propagated, but non-terminated *N*-butyl functionalized poly(norbornene)s.⁶³ However, this route led to poorly defined copolymers due to drastically faster rates of propagation compared to initiation. Under these kinetic circumstances, unreacted catalyst is inevitably present upon addition of the co-monomer.⁷³ Consequently, block formation must also compete with homopolymer formation upon addition of the second monomer, yielding this approach rather unsuccessful.

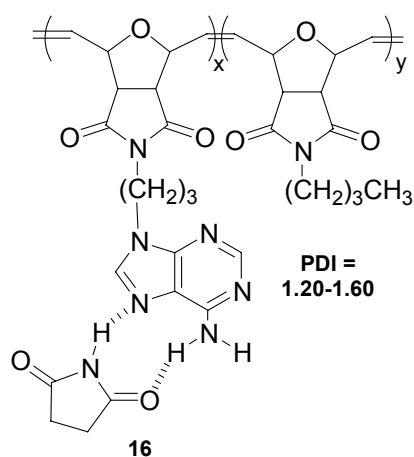


Figure 1.11 Sleiman's AB block copolymers made via ROMP.

Template-Directed Polymerizations

Template-directed polymerizations offer a unique alternative to the above strategies for the preparation of well-defined polymeric architectures.⁵⁹ Here, a prefabricated template structure selectively binds to functional monomers. Subsequent polymerization

yields a daughter polymer with structural features identical to the template with the exception that the resulting polymer possesses the complementary recognition units. Finally, the binary polymer assembly is precipitated and the two recognition units are separated.

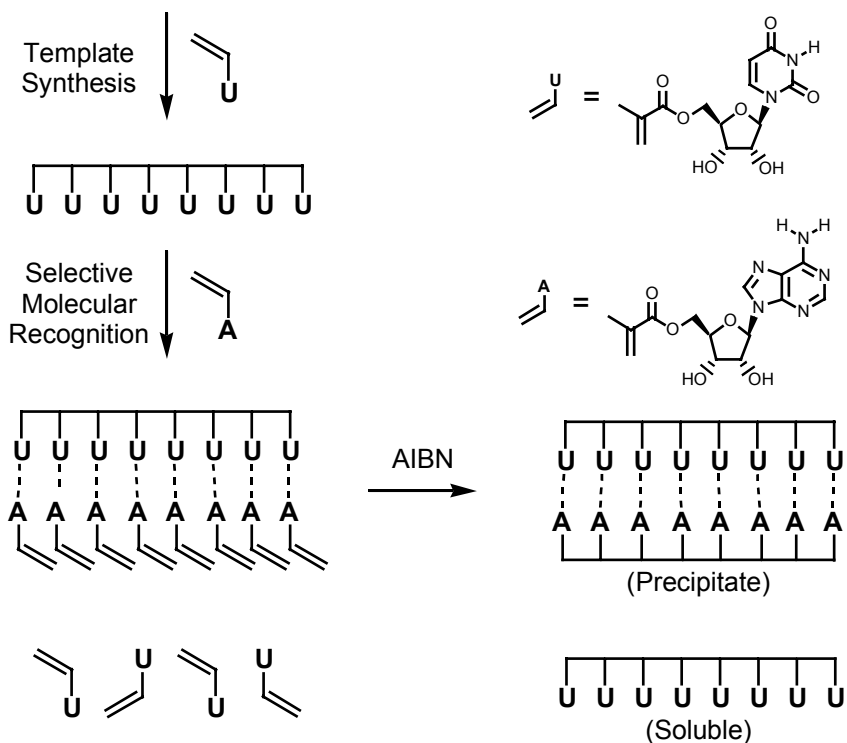


Figure 1.12 Template directed polymerization.

Marsh and coworkers reported an example of this procedure (Figure 1.12).⁵⁹ A hydrogen bonding template was prepared via free radical polymerization of uridine containing monomers. Subsequently, a mixture of adenine and uridine nucleosides was added to the template. Selective binding of the adenine nucleosides followed by exposure to free radical initiator (AIBN) resulted in the formation of a poly(5'acryloyluridine)-

poly(5'-acryloadenosine) complex, which could be selectively precipitated. Separation of the binary complex was achieved and characterization indicated that the template process takes place with high fidelity of transcription from parent to daughter polymer.

Although the template method suggests an elegant route to highly regular and potentially monodisperse polymer structures, it suffers from several potential limitations. First, the structure of the final polymer is completely dependent upon the architecture of the parent polymer and is therefore limited to advanced polymerization strategies. Second, the separation procedures are not always quantitative and often extensive, leaving complementary residues in the samples. Third, weak non-covalent interactions are often unable to translate the parent polymeric scaffold quantitatively due to low association constants leading to imperfect self-assembly. Regardless of these limitations, this method shows outstanding promise as a way to make monodisperse polymers that cannot be synthesized using other methods.

“Plug and Play” Polymer Functionalization

Although the preparation of well-defined polymeric structures is often difficult, functionalization via self-assembly provides efficient routes, unmatched in their simplicity, to a variety of complex materials. Self-assembly allows for easy modification of the polymer structure, giving access to a multitude of functionalized polymers stemming from a single backbone. Rotello has appropriately labeled this important class of molecular scaffolds “plug and play” polymers for their ease of functionalization.¹⁷ The dynamic nature of the non-covalent bond allows for control of intermolecular complexation in these systems via external factors such as solvent polarity and temperature. Figure 1.13 depicts two potential ways one may functionalize

homopolymers containing a single side-chain recognition motif. First, monofunctionalization can take place by mixing the scaffold with a functional entity anchored to the complementary unit. Second, multifunctionalization may be carried out by the addition of mixtures of one or more anchored entities to the complementary unit resulting in uncontrolled random multifunctionalization. This route has exceptional potential for the rapid optimization of novel materials based on compositional blends of functional components.

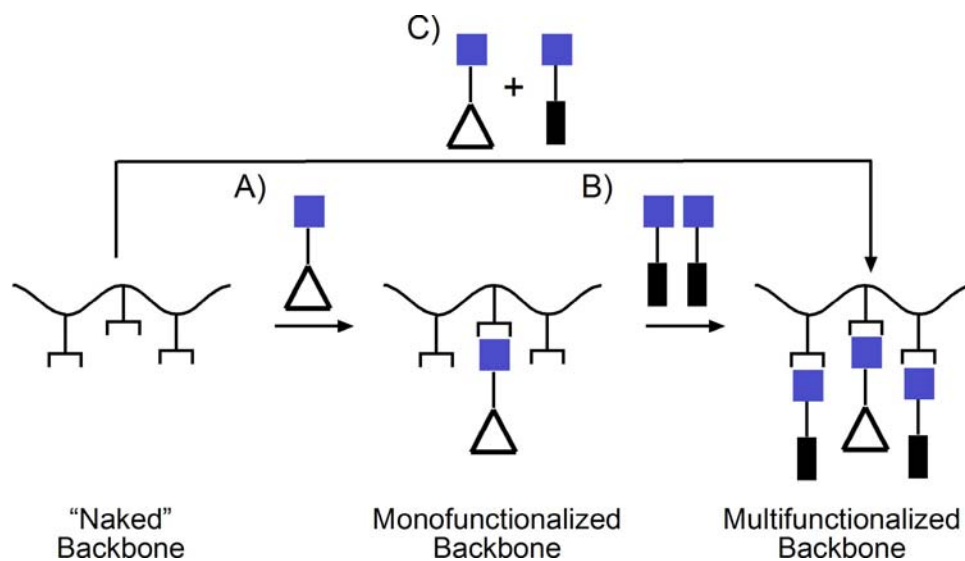


Figure 1.13 Schematic depicting functionalization of a “plug and play” scaffold. Modification approaches: A) monofunctionalization, B) step-wise multifunctionalization, and C) one-step multifunctionalization.

Kato was first to report single recognition motif multifunctionalization for the preparation of SCLCPs using a blend of mesogenic components.^{55,56} Poly(acrylate)s possessing pendant benzoic acid moieties (**17**) were added to binary mixtures of stilbazoles containing either electron donor (-OCH₃) or electron acceptor (-CN, -NO₂)

end groups (**18** and **19**) resulting in the formation of self-assembled multifunctionalized side-chain polymers (Figure 1.14).

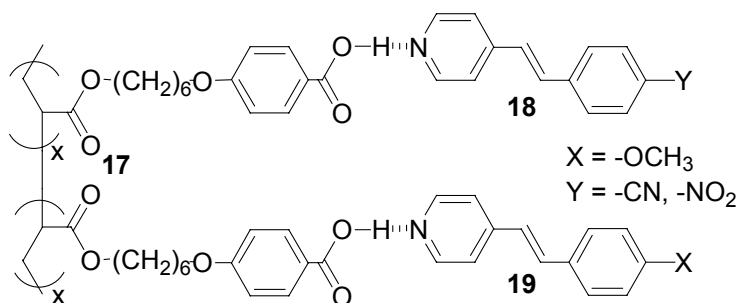


Figure 1.14 Non-covalent attachment of stilbazole electron donor and acceptor mesogen components via multifunctionalization strategies.

Rotello and coworkers later provided the vast majority of reports demonstrating the versatility of single recognition monofunctionalization in polymer science.^{16,17,51-54} This group's early accounts describe the design of poly(styrene)-based random copolymer systems, post-functionalized with donor-acceptor-donor hydrogen bonding units.¹⁷ In particular they studied the self-assembly of flavin (**22**) onto polymeric scaffolds (Figure 1.15). Moreover, they showed that the efficiency of molecular association is directly related to the propensity of the pendant hydrogen bonding unit to undergo intermolecular self-assembly. Polymers containing self-dimerizing triazine units (**20**) were less effective in binding **22** ($K_a=36 \text{ M}^{-1}$) than closely related polymeric scaffolds based on diaminopyridine motifs (**21**) ($K_a=220 \text{ M}^{-1}$) because of the intramolecular association of triazines.¹⁷

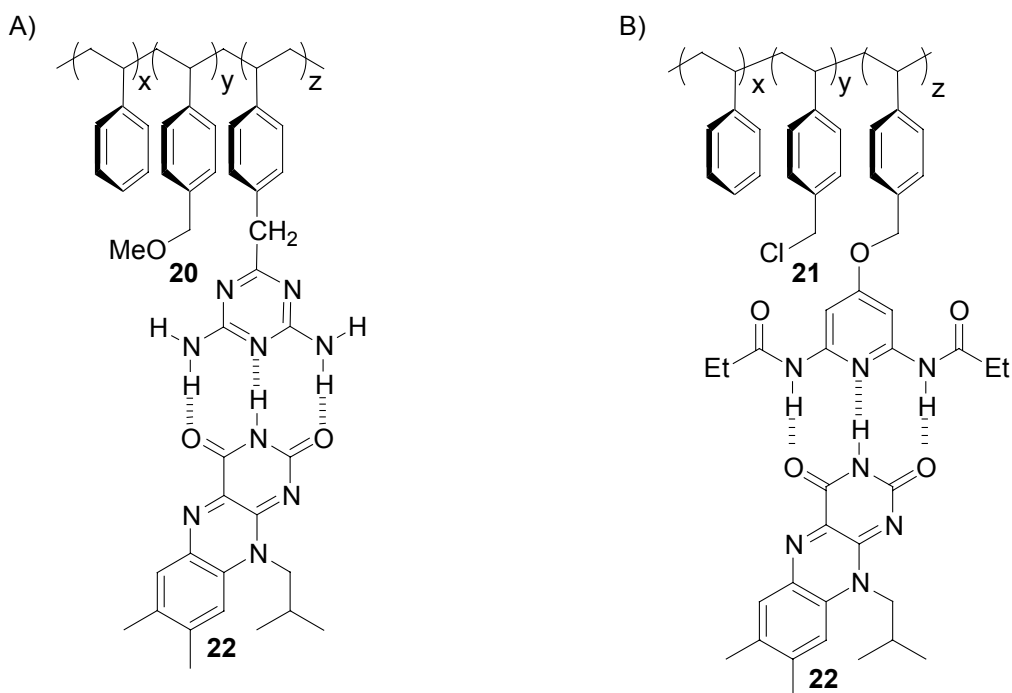


Figure 1.15 Self-Assembled complexes formed via intermolecular hydrogen bonding of a) flavin **22** and diaminotriazine random copolymer **20** and b) **22** and diaminopyridine random copolymer **21**.

Rotello later reported an application of this methodology to the synthesis of hybrid materials.¹⁶ Here, polyhedral oligomeric silsesquioxane (POSS), a common inorganic additive in many nanocomposite materials, was tethered to a diaminopyridine (DAP)-based hydrogen bonding motif (**24**). Non-covalent functionalization of random copoly(styrene)s bearing thymine recognition units (**23**) was accomplished via simple mixing of POSS-DAP in chloroform followed by slow evaporation of the solvent. The coupling of hydrogen bonding directed self-assembly and POSS-POSS crystallization afforded the desired POSS/copolymer nanocomposite material rapidly and efficiently (Figure 1.16).

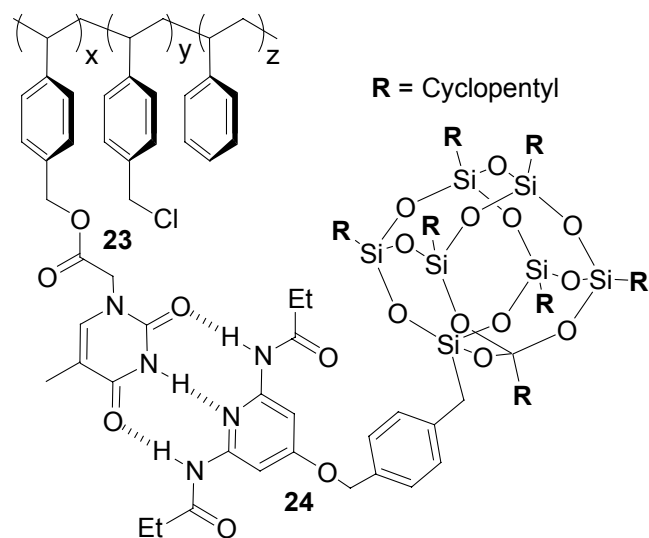


Figure 1.16 Intermolecular complexation of thymine functionalized random copolymer **23** and diaminopyridine-polyhedral oligomeric silsesquioxane (POSS) entities.

In another example, Rotello and coworkers used self-assembly to control multi-scale ordering of spherical aggregates (Figure 1.17-A).⁵⁴ Gold nanoparticles possessing thymine residues (**26**) were self-assembled onto block co-poly(styrene)s functionalized with the triazine moiety (**25**) via hydrogen bonding. These systems were called “bricks and mortar” polymer-mediated self-assemblies.⁵² The use of diblock copolymers gave rise to microphase separation of the copolymer and the nanoparticles, allowing for control of the spherical aggregate size by simple modification of the polystyrene block bearing the triazine residue.

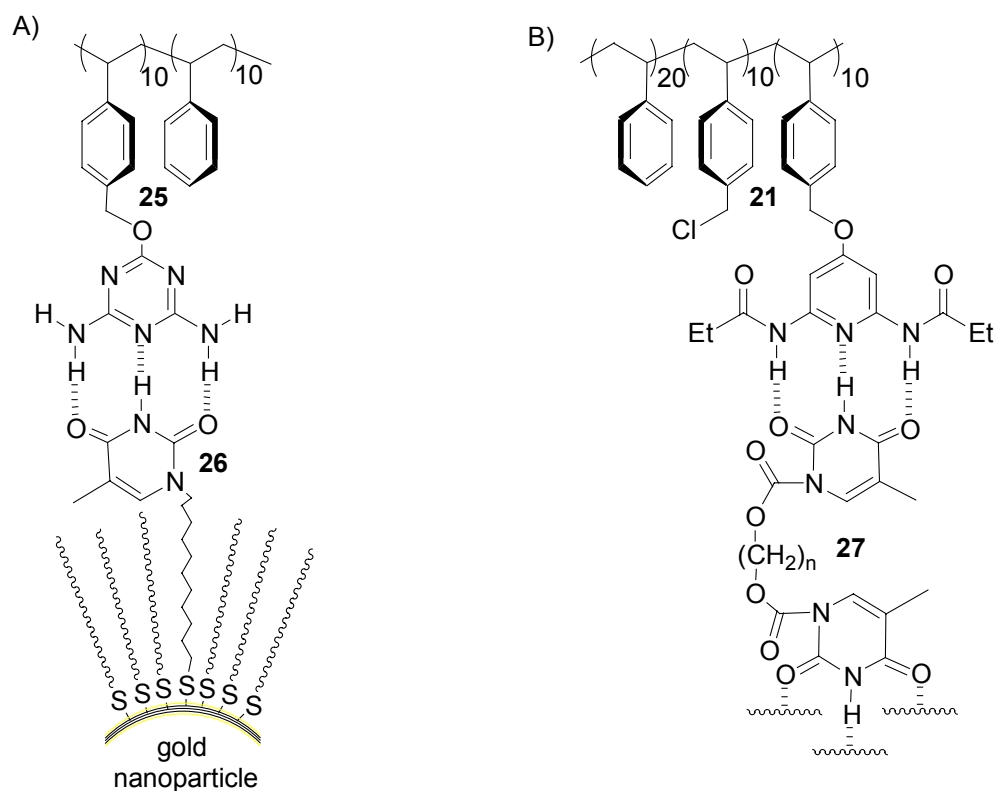


Figure 1.17 A) Block co-poly(styrene)s containing triazine and diaminopyridine recognition motifs non-covalently attached to gold nanoparticles and B) crosslinked with bisthymine, respectively.

Building upon earlier examples from the same group that describe the formation of recognition-induced polymersomes via polymer-polymer hydrogen bonding,^{74,75} a report in 2003, investigates the formation of micron-sized aggregates via non-covalent crosslinking of diaminopyridine functionalized copolymers **21** using bisthymine crosslinker **27** (Figure 1.17-B).⁵¹ Microsphere formation was thermally reversible with full destruction of the hydrogen bonds at 50 °C and subsequent reconstruction upon cooling to room temperature. In fact, the particle dispersities could be tailored through this simple annealing process demonstrating the ability of dynamic and reversible non-covalent systems to undergo self-optimization.

Ikkala and coworkers reported an excellent account of applying side-chain self-assembly to materials design.⁵⁸ Here, hydrogen bonded complexes composed of a 1:1 mixture of poly(4-vinylpyridine) and a non-mesogenic 3-pentadecylphenol surfactant (**28**) were prepared, giving rise to lamellar secondary structures (Scheme 1.2-A). Simple modifications of the surfactant to polymer ratios resulted in partial complexation and an observed increase in the long period.

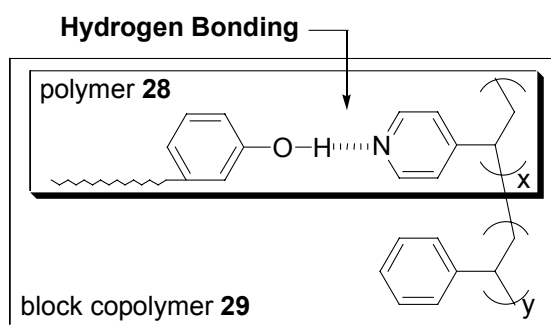
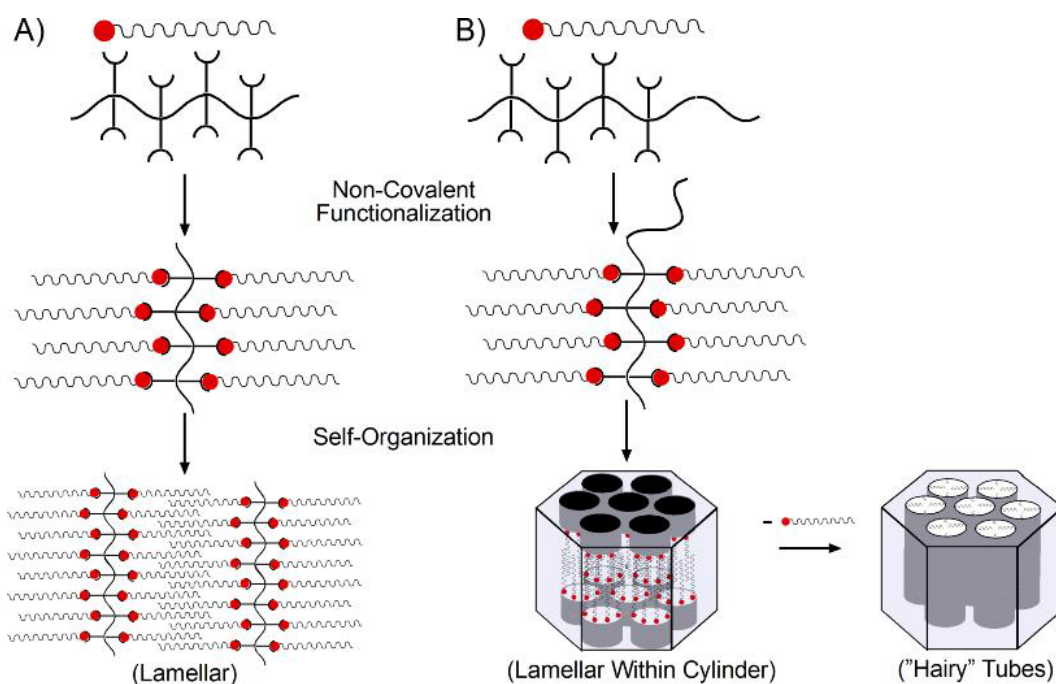


Figure 1.18 Poly(4-vinylpyridine)-pentadecylphenol and poly(styrene)-block-poly(4-vinylpyridine) pentadecylphenol surfactant complexes used by Ikkala and coworkers.

By applying the same design principles to poly(styrene)-block-poly(4-vinylpyridine) block copolymers (**29**) of appropriate block lengths, a lamellar substructure within a cylindrical mesomorphic architecture could be formed (Scheme 1.2-B).⁵⁷ The cylinders formed via self-organization of hydrogen bonded pentadecyl phenol were “emptied” by washing away hydrogen bonded surfactants exploiting the reversible nature of the non-covalent bond. Following the facile removal of the surfactant, the cylindrical structures remain in the rigid glassy polystyrene matrix. Since the pyridine-containing portion of the block copolymer is intact following surfactant removal, the inner walls of the cylinder

can be described as “hairy tubes” or a mesoporous material containing hollow cylinders with polymer brushes lining the inner walls.

Scheme 1.2 Hierarchical self-organization of side-chain self-assembled polymers.



A) Systems stemming from the association between poly(4-vinylpyridine) and pentadecyl phenol and B) structures arising from the association between poly(styrene)-block-poly(4-vinylpyridine) and pentadecyl phenol.

1.6.3 Side-Chain Metal Containing Polymers (SCMPs): Engineered Metal-Ligand Interactions, Functionalization Strategies, and Applications

Side-chain metal containing polymers (SCMPs) belong to a unique sub-field of polymer science mainly concerned with the fabrication of novel catalytic and electro-optical materials. Here, the physical properties of both the inorganic and polymer components exist simultaneously, giving rise to a variety of hybrid materials exhibiting

metal-specific properties such as conductivity and magnetism while maintaining the benefit of solubility and processability inherent to the polymer backbone. Furthermore, SCMPs have been exploited as recyclable, homo- and heterogeneous transition metal supported catalysts and have been suggested for numerous other applications including wastewater treatment additives, metal-scavengers, liquid crystals, and NLO materials.²⁴

Although many examples of side-chain metal coordinated polymers exist, only a handful are designed to serve as recognition motifs for side-chain functionalization.^{50,76,77} These polymers represent a new class of metallo- “plug and play” materials that are similar in concept to the hydrogen bonding systems described earlier, yet differ greatly because of the high bond strength of the interaction as well as the unique physical properties of transition metal complexes. In this section, the important design principles, functionalization strategies, applications, and limitations of non-covalent side-chain functionalization using metal coordination will be reviewed, outlined, and discussed.

SCMPs can potentially fall into two classes according to the position of the metal complex with respect to the polymer backbone. In the first class, the metal is covalently tethered to the assembling building block, whereas the complementary component, a pendant ligand, is located along the side-chain of the polymer backbone (Figure 1.19-A). These scaffolds are sometimes referred to as polymeric ligands.²⁴ The second class is based on a polymer-metal complex that is grafted onto the polymer side-chains and the desired functionalization step takes place via the coordination of a ligand based anchoring unit. In both cases, the resultant polymers may possess identical structures and the choice of the synthetic strategy is dependant on the ease of the synthetic method (Figure 1.19-B).

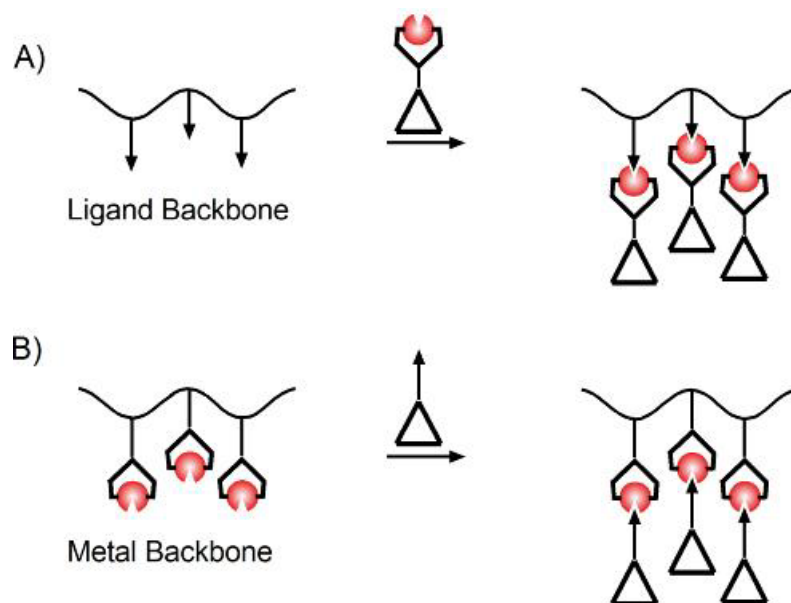
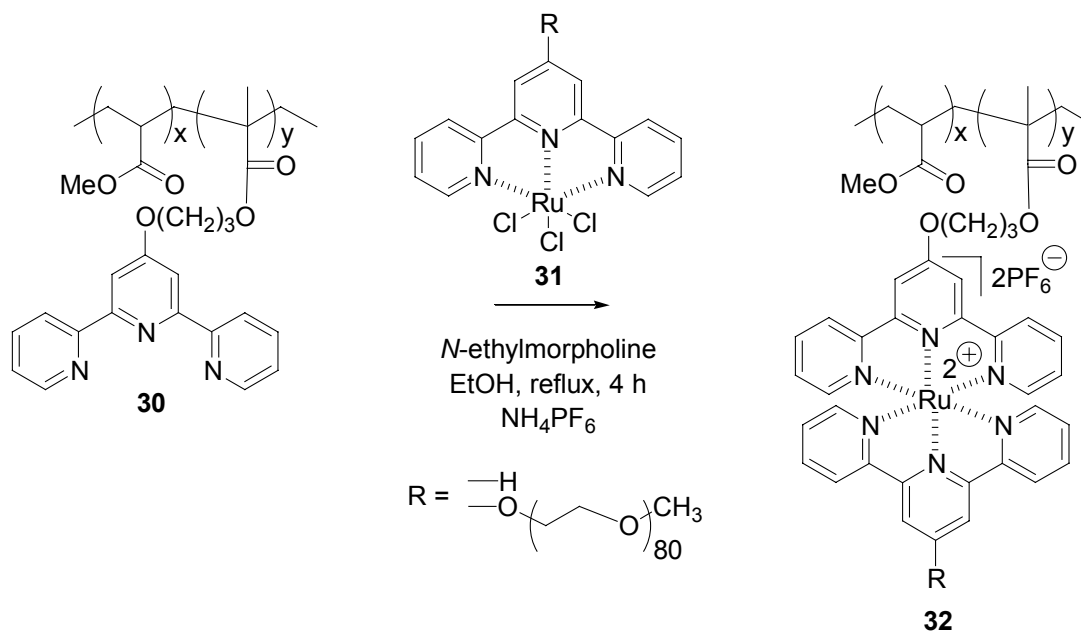


Figure 1.19 Cartoon showing the differences between classes of side-chain metal containing polymers. A) The ligand is bound to the backbone, and B) The metal complex is attached to the backbone.

The design of “plug and play” systems based on metal coordination requires careful attention when choosing between a polymeric ligand scaffold and a metal-containing backbone. Polymeric ligand-based scaffolds are generally easier to synthesize but less economical because of the required extensive synthesis of the metal-recognition motifs for each self-assembling component. Furthermore, the polymerization strategies available for these systems are numerous and usually straightforward. In contrast, the incorporation of a metal-complex into the polymer backbone is more economical due to the ease of preparing an assortment of ligand anchored functional components, but is limited to a small number of polymerization methods as a result of metal group intolerance of most polymerization techniques. Consequently, there are currently limited accounts of this category in the literature.⁷⁸

Scheme 1.3 Functionalization of terpyridine polyligands via self-assembly.



On the other hand, several articles explore the incorporation of pendant side-chain ligands moieties for self-assembly.^{50,76-78} Schubert, has reported a variety of examples of thermally robust side-chain polymeric ligands. In one account, terpyridine modified methacrylates were copolymerized with methyl methacrylate using free radical polymerization methods (30).⁵⁰ Subsequent functionalization using terpyridine-ruthenium (III) trichlorides (31) could be accomplished (Scheme 1.3). Although these systems achieve the primary objective of functionalizing a polymer backbone using metal-to-ligand interactions, it should be noted that the extensive reaction times and elevated temperatures required for what the authors consider “self-assembly” contradict the spontaneous character inherent to most self-assembled entities. Nonetheless, applying this strategy using heteroleptic bisterpyridine ruthenium (II) poly(ethyleneglycol) complexes has resulted in the successful formation of aqueous micellar structures.⁵⁰

In general, the employment of metal coordination units as recognition motifs gives rise to limitations not seen for hydrogen bonds. First, the self-assembly step usually results in charge formation at each repeat unit often limiting solubility in organic solvents. However, in future systems, this problem can be overcome by the attachment of solubilizing groups such as alkyl spacers situated between the polymer and the recognition unit or by adding multiple alkyl chains to the ligand sphere of the metal complex. However, these alterations will further complicate the use of such systems by increasing synthetic time. Second, the high strength of these non-covalent complexes is inferior to the dynamic nature of the hydrogen bond. Here, reversibility usually has to take place chemically via ligand displacement reactions. Only limited accounts of thermal reversibility exist. Schubert and coworkers showed that thermal bleaching could be observed for iron-terpyridine complexes.⁷⁹ However, this is an exception rather than the rule since transition metal complexes usually decompose prior to showing reversibility.²⁴ Another limitation of metal coordination based supramolecular polymer systems is the potential for complication during the characterization. Paramagnetic metal species cannot be easily analyzed via NMR and GPC of SCMPs often fails due to aggregate formation of charges or shear-induced rupture of the metal complexes.^{78,80} Despite these limitations, the field of SCMPs offers many opportunities to optimize organic/metal hybrid material properties as a result of the strong non-covalent bonds involved. As this area of self-assembled SCFPs continues to mature, exciting applications and novel solutions to these problems will inevitably emerge.

1.7 Self-Assembled Polymers Based on Multiple Recognition Motifs

The synthesis of supramolecular polymers is primarily motivated by simplicity, ease of synthesis, and direct resemblance to biological materials design. Even though biological systems employ a wide variety of non-covalent interactions such as hydrogen bonding, metal coordination, and hydrophobic interactions in an orthogonal fashion to introduce function, diversity, and complexity, today's state of the art self-assembled SCFPs do not. Almost all known synthetic supramolecular polymers are based solely upon a single recognition motif (usually hydrogen bonding). As materials science and polymer synthesis continue to evolve, a movement toward polymer structures with increasing architectural complexity will be required. This evolution of the field will most certainly encompass the use of multiple recognition elements in an attempt to match the elegance inherent to biological materials and to meet the technological needs of tomorrow.

At present, all examples of supramolecular SCFPs found in the literature based on more than one recognition motif fall into two major categories: i) systems where multifunctionalization using two or more non-covalent interactions join at a single anchoring site embedded along a polymer backbone (Figure 1.20-A),⁶⁰⁻⁶² and ii) systems with polymer backbones that contain two or more sets of recognition motifs, each one complementing the other, allowing for self-functionalization or intramolecular folding to take place (Figure 1.20-B).⁴⁰ A third category may also be envisaged where two or more discrete recognition motifs are located along a polymer backbone that can bind their respective complementary recognition units selectively and intermolecularly, allowing for modular functionalization strategies (Figure 1.20-C). Currently, no reports of such a system exists.

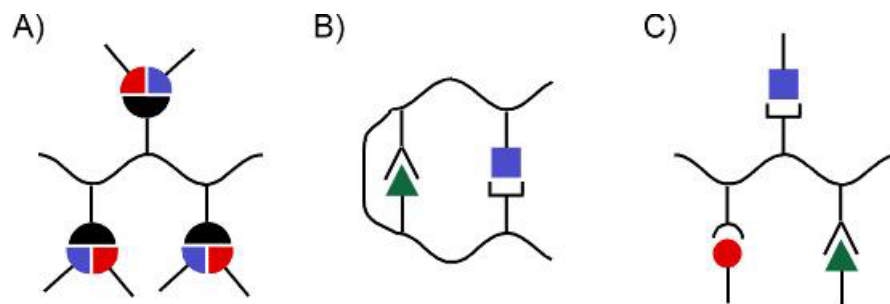


Figure 1.20 Cartoon representations of the different categories of side-chain polymers possessing multiple recognition motifs.

The first category of multi-functionalized SCFPs, where more than one type of non-covalent bond is joined at a single anchoring site thereby allowing for multi-functionalization at each repeat unit, can be nicely illustrated by examining the recent work of Ikkala and coworkers.⁶⁰⁻⁶² This group's first report on the matter describes the functionalization of poly(4-vinylpyridine) via proton transfer using methane sulfonic acid.⁶⁰ Subsequent mixing of the polymeric salt in the presence of pentadecyl phenol lead to hydrogen bond formation between the phenolic hydroxyl group and the sulfonate group of methane sulfonic acid to provide polymers **33** and **34** (Figure 1.21). Microphase-separated diblock copolymer **34** further self-organizes to form structures-in-structures similar to those noted earlier (Scheme 1.2) whose hierarchical phase transitions could be controlled systematically leading to temperature-dependent transitions in electrical conductivity.

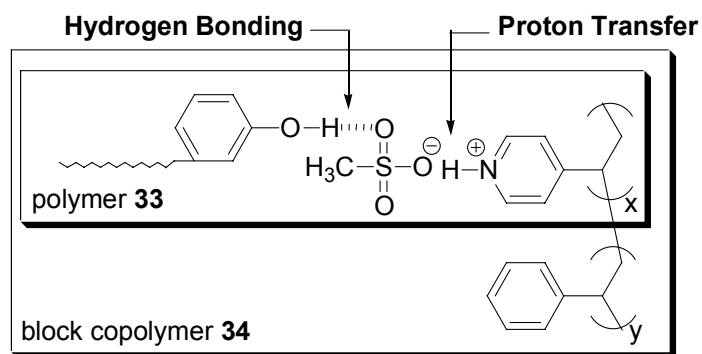


Figure 1.21 Complexes formed as a result of hydrogen bonding and proton transfer non-covalent forces, both are joined at each repeat unit of poly(4-vinylpyridine).

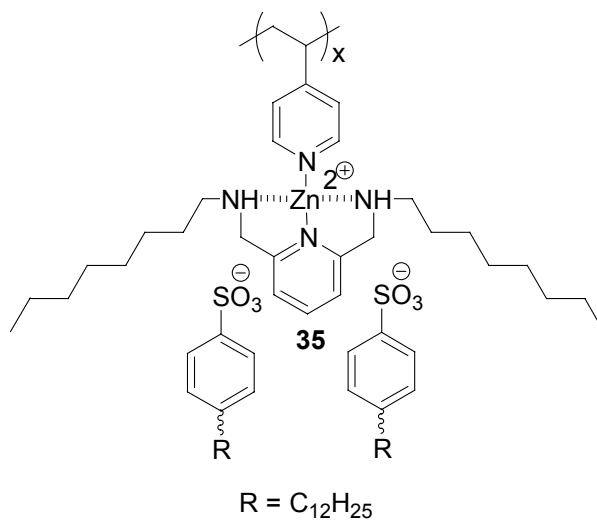


Figure 1.22 Multicomb polymeric assemblies formed via simultaneous employment of metal coordination and ionic-interactions.

In a later report, Ikkala extended the above methodology by combining metal coordination and ionic interactions to functionalize polymers.⁶¹ Zinc was coordinated to poly(4-vinylpyridine) containing dodecylbenzenesulfonate counter ions (**35**). The resulting supramolecular structure gave rise to a synthetically facile preparation method for multicomponent polymeric assemblies (Figure 1.22).

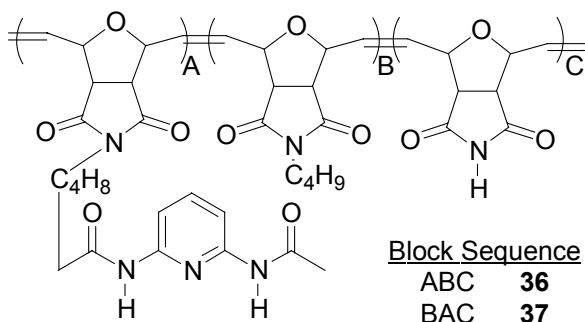


Figure 1.23 ABC block copolymers containing diacetamidopyridine and dicarboxyimide hydrogen bonding recognition units that are complementary to one another.

In late 2003, Sleiman and coworkers reported the only known synthetic example of polymer self-functionalization or intramolecular folding using multiple interactions;⁴⁰ a class of multifunctionalized polymers that can be copiously found in nature.^{14,29,70} In an attempt to mimic the ability of natural systems to fold into complex secondary and tertiary structures, self-complementary ABC triblock copolymers containing various block sequences of diacetamidopyridine, dicarboxyimide, and alkyl residues were prepared (Figure 1.23).⁴⁰ These copolymers showed sequence dependent morphological changes in organic solvents, which suggest that intramolecular folding of the complementary dicarboxyimide and diacetamidopyridine units could be taking place via

hydrogen bonding. However, these results do not exclude the possibility that intermolecular association of the complimentary units is taking place as well.

The concept of multiple interactions along a polymer backbone is theoretically simple. However, the design, preparation, and functionalization of systems containing more than one recognition motif can be quite complex. The difficulty in making and successfully functionalizing side-chain polymers based on multiple examples is corroborated by the fact that the examples shown above constitute the only three known literature occurrences where multiple interactions have been employed. The coexistence of a large number of stringent design criteria, including i) polymerization strategies that allow for defined copolymer formation, ii) sufficiently strong self-assembly motifs, iii) selective binding of each recognition motif for its partner in the presence of potentially competitive interactions, and iv) full solubility of resultant polymers that can be complicated by either the formation of ionic species or the polarity of many recognition motifs is mainly responsible for the low occurrence of self-assembled polymers based on multiple recognition motifs.

1.8 Conclusion

In the last decades, polymer science and self-assembly have converged to formulate an ever expanding field that concerns itself with building complicated polymeric entities from the bottom up. As a direct consequence of the field's diversity, many definitions of self-assembly have emerged that partially or fully embody the process of non-covalent bond formation as a central component. A large number of recognition units are currently available for use in self-assembly, the selection of which is often made according to the desired strength and application. Categorically, self-assembly in polymer science can be

broken down into two major areas: i) main-chain self-assembled polymers, and ii) side-chain self-assembled polymers. While the latter remains in its infancy, the former has become a mature area of polymer science.

Thanks to the pioneering liquid crystal work of Kato and Fréchet, the fundamental principles of hydrogen bonding based SCFPs have been established and are well understood. Synthetic routes to SCFPs often rely upon polymer post-functionalization strategies, which give rise to poorly defined polymer structures. Several attempts to apply controlled polymerization methods to the preparation of SCFPs containing nature-derived hydrogen bonding motifs have proven successful, but are limited in scope. Further expansion of hydrogen bonded SCFPs has led to a “plug and play” mentality in polymer synthesis. Rotello and Ikkala have made several important advancements toward materials applications for SCFPs based on a single interaction with examples of nanocomposites, spherical aggregates of gold nanoparticles, reversible microspheres, and mesomorphic materials.

Despite these accomplishments for hydrogen bonding based SCFPs, only limited accounts engineered of metallo- “plug and play” polymers are known. This may be attributed to inherent limitations of metal coordination systems, such as poor solubility and difficulty in characterization that arise from charge clustering and paramagnetism respectively. Regardless of these restrictions, the important properties of metal based SCFPs, such as conductivity and magnetism, makes them highly desirable candidates for future studies.

Only few reports can be found in the literature which describe the use of multiple weak interactions to functionalize polymers even though there is tremendous potential for

these systems to overcome some of the drawbacks of covalent copolymer synthesis including reagent incompatibility and lengthy synthesis. The coexistence of a large number of stringent design criteria such as recognition unit compatibility, solubility, selectivity is mainly responsible for the low occurrence of self-assembled polymers based on multiple recognition motifs. This thesis aims to take on these difficulties and establish orthogonal multifunctionalization methodologies as a synthetic tool for polymer science. In doing so, the synthetic hurdles of ill-defined SCFPs, as well as the limited scope of metallo-“plug and play” polymers, will be overcome.

1.9 References

- (1) Pauling, L. *The Nature of the Chemical Bond and the Structure of Molecules and Crystals*; Cornell University Press: Ithaca, NY, 1939.
- (2) Lehn, J.-M. *Supramolecular Chemistry*; Wiley-VCH: Weinheim, 1995.
- (3) Ciferri, A. *Supramolecular Polymers*; Dekker: New York, NY, 2000.
- (4) Steed, J. W.; Atwood, J. L. *Supramolecular Chemistry*; John Wiley & Sons, Ltd: Chichester, West Sussex, 2000.
- (5) Brunsveld, L.; Folmer, B. J. B.; Meijer, E. W.; Sijbesma, R. P. *Chem. Rev.* **2001**, *101*, 4071.
- (6) Lehn, J.-M. *Pure Appl. Chem.* **1994**, *66*, 1961.
- (7) Lehn, J.-M. *Angew. Chem. Int. Ed.* **1988**, *27*, 89.
- (8) Reinhoudt, D. N.; Crego-Calama, M. *Science* **2002**, *295*, 2403.
- (9) Lehn, J.-M. *Science* **2002**, *295*, 2400.
- (10) Hollingsworth, M. D. *Science* **2002**, *295*, 2410.
- (11) Ikkala, O.; ten Brinke, G. *Science* **2002**, *295*, 2407.
- (12) Ciferri, A. *Macromol. Rapid Commun.* **2002**, *23*, 511.
- (13) Lehn, J.-M. *Polym. Int.* **2002**, *51*, 825.
- (14) Lindsey, J. S. *New J. Chem* **1991**, *15*, 153.
- (15) Whitesides, G. M.; Mathias, J. P.; Seto, C. T. *Science* **1991**, *254*, 1312.
- (16) Carroll, J. B.; Waddon, A. J.; Nakade, H.; Rotello, V. M. *Macromolecules* **2003**, *36*, 6289.
- (17) Ilhan, F.; Gray, M.; Rotello, V. M. *Macromolecules* **2001**, *34*, 2597.
- (18) Schubert, U. S.; Eschbaumer, S. C. *Angew. Chem. Int. Ed.* **2002**, *41*, 2892.
- (19) Hunter, C. A.; Sanders, J. K. M. *J. Am. Chem. Soc.* **1990**, *112*, 5525.
- (20) Ma, J. C.; Dougherty, D. *Chem. Rev.* **1997**, *97*, 1303.

- (21) Cooke, G.; Rotello, V. M. *Chem. Soc. Rev.* **2002**, *31*, 274.
- (22) Jeffery, G. A. *An Introduction to Hydrogen Bonding*; Oxford University Press: Oxford, 1997.
- (23) Prins, L. J.; Reinhoudt, D. N.; Timmerman, P. *Angew. Chem. Int. Ed.* **2001**, *40*, 2382.
- (24) Kaliyappan, T.; Kannan, P. *Prog. Polym. Sci.* **2000**, *25*, 343.
- (25) Alamgir Hossain, M.; Schneider, H.-J. *Chem. Eur. J.* **1999**, *5*, 1284.
- (26) Jorgenson, W. L.; Pranata, J. *J. Am. Chem. Soc.* **1990**, *112*, 2008.
- (27) Pranata, J.; Wierschke, S. G.; Jorgenson, W. L. *J. Am. Chem. Soc.* **1991**, *113*, 2810.
- (28) Cotton, F. A.; Wilkinson, G.; Murillo, C. A.; Bochmann, M. *Advanced Inorganic Chemistry*; 6th ed.; John Wiley Sons, Inc.: New York, NY, 1999.
- (29) Philp, D.; Stoddart, J. F. *Angew. Chem., Int. Ed. Eng.* **1996**, *35*, 1154.
- (30) Folmer, B. J. B.; Sijbesma, R. P.; Versteegen, R. M.; van der Rijt, J. A. J.; Meijer, E. W. *Adv. Mater.* **2000**, *12*, 874.
- (31) Folmer, B. J. B.; Cavini, E.; Sijbesma, R. P.; Meijer, E. W. *Chem. Commun.* **1998**, 1847.
- (32) Folmer, B. J. B.; Sijbesma, R. P.; Meijer, E. W. *Polym. Mater. Sci. Eng.* **1999**, *217*, 39.
- (33) Sijbesma, R. P.; Beijer, F. H.; Brunsveld, L.; Folmer, B. J. B.; Hirschberg, J. H. K. K.; Lange, R. F. M.; Lowe, J. K. L.; Meijer, E. W. *Science* **1997**, *278*, 1601.
- (34) Rieth, L. R.; Eaton, R. F.; Coates, G. W. *Angew. Chem. Int. Ed.* **2001**, *40*, 2153.
- (35) Hofmeier, H.; El-ghayoury, A.; Schenning, A. P. H. J.; Schubert, U. S. *Chem. Commun.* **2004**, 318.
- (36) Fouquey, C.; Lehn, J.-M.; Levelut, A.-M. *Adv. Mater.* **1990**, *2*, 254.
- (37) Lehn, J.-M. *Makromol. Chem. Macromol. Symp.* **1993**, *69*, 1.
- (38) Kotera, M.; Lehn, J.-M.; Vigneron, J.-P. *J. Chem. Soc. Chem. Commun.* **1994**, 197.

- (39) Kotera, M.; Lehn, J.-M.; Vigneron, J.-P. *Tetrahedron* **1995**, *51*, 1953.
- (40) Bazzi, H. S.; Bouffard, J.; Sleiman, H. F. *Macromolecules* **2003**, *36*, 7899.
- (41) Malik, S.; Dhal, P. K.; Mashelkar, R. A. *Macromolecules* **1995**, *28*, 2159.
- (42) Kumar, U.; Kato, T.; Fréchet, J. M. J. *J. Am. Chem. Soc.* **1992**, *114*, 6630.
- (43) Kawakami, T.; Kato, T. *Macromolecules* **1998**, *31*, 4475.
- (44) Kato, T.; Ihata, O.; Ujiie, S.; Tokita, M.; Watanabe, J. *Macromolecules* **1998**, *31*, 3551.
- (45) Brandys, F. A.; Bazuin, C. G. *Chem. Mater.* **1996**, *8*, 83.
- (46) Kato, T.; Fréchet, J. M. J. *Macromolecules* **1989**, *22*, 3818.
- (47) Kato, T.; Nakano, M.; Moteki, T.; Uryu, T.; Ujiie, S. *Macromolecules* **1995**, *28*, 8875.
- (48) Ujiie, S.; Iimura, K. *Macromolecules* **1992**, *25*, 3174.
- (49) Bazuin, C. G.; Tork, A. *Macromolecules* **1995**, *28*, 8877.
- (50) Gohy, J.-F.; Hofmeier, H.; Alexeev, A.; Schubert, U. S. *Macromol. Chem. Phys.* **2003**, *204*, 1524.
- (51) Thibault, R. J.; Hotchkiss, P. J.; Gray, M.; Rotello, V. M. *J. Am. Chem. Soc.* **2003**, *125*, 11249.
- (52) Boal, A. K.; Ilhan, F.; DeRouchey, J. E.; Thurn-Albrecht, T.; Russell, T. P.; Rotello, V. M. *Nature* **2000**, *404*, 746.
- (53) Drechsler, U.; Thibault, R. J.; Rotello, V. M. *Macromolecules* **2002**, *35*, 9621.
- (54) Frankamp, B. L.; Uzun, O.; Ilhan, F.; Boal, A. K.; Rotello, V. M. *J. Am. Chem. Soc.* **2002**, *124*, 892.
- (55) Kato, T.; Kihara, H.; Kumar, U.; Uryu, T.; Fréchet, J. M. J. *Angew. Chem. Int. Ed. Engl.* **1994**, *33*, 1644.
- (56) Kato, T.; Kihara, H.; Ujiie, S.; Uryu, T.; Fréchet, J. M. J. *Macromolecules* **1996**, *29*, 8734.

- (57) Mäki-Ontto, R.; de Moel, K.; de Odorico, W.; Ruokolainen, J.; Stamm, M.; ten Brinke, G.; Ikkala, O. *Adv. Mater.* **2001**, *13*, 117.
- (58) Ruokolainen, J.; Brinke, G. T.; Ikkala, O.; Torkkeli, M.; Serimaa, R. *Macromolecules* **1996**, *29*, 3409.
- (59) Khan, A.; Haddleton, D. M.; Hannon, M. J.; Kukulj, D.; Marsh, A. *Macromolecules* **1999**, *32*, 6560.
- (60) Ruokolainen, J.; Mäkinen, R.; Torkkeli, M.; Mäkelä, T.; Serimaa, R.; ten Brinke, G. *Science* **1998**, 280.
- (61) Valkama, S.; Lehtonen, O.; Lappalainen, K.; Kosonen, H.; Castro, P.; Repo, T.; Torkkeli, M.; Serimaa, R.; ten Brinke, G.; Ikkala, O. *Macromol. Rapid. Commun.* **2003**, *24*, 556.
- (62) van Ekenstein, G. A.; Polushkin, E.; Nijland, H.; Ikkala, O.; ten Brinke, G. *Macromolecules* **2003**, *36*, 3684.
- (63) Bazzi, H. S.; Sleiman, H. F. *Macromolecules* **2002**, *35*, 9617.
- (64) Davies, R. G.; Gibson, V. C.; Hursthouse, M. B.; Light, M. E.; Marshall, E. L.; North, M.; Robson, D. A.; Thompson, I.; White, A. J. P.; Williams, D. J.; Williams, P. J. *J. Chem. Soc., Perkin Trans. 1* **2001**, 3365.
- (65) Gibson, V. C.; Marshall, E. L.; North, M.; Robson, D. A.; Williams, D. J. *Chem. Commun.* **1997**, 1095.
- (66) Marsh, A.; Khan, A.; Haddleton, D. M.; Hannon, M. J. *Macromolecules* **1999**, *32*, 8725.
- (67) Stubbs, L. P.; Weck, M. *Chem. Eur. J.* **2003**, *9*, 992.
- (68) Kato, T.; Mizoshita, N.; Kanie, K. *Macromol. Rapid Commun.* **2001**, *22*, 797.
- (69) Portugall, M.; Ringsdorf, H.; Wendorff, J. H. *Makromol. Chem.* **1978**, *179*, 273.
- (70) Lehninger, A. L.; Cox, M. M.; Nelson, D. L. *Principles of Biochemistry*; 4th ed.; W. H. Freeman Company: New York, NY, 2004.
- (71) Watson, J. D.; Crick, F. H. C. *Nature* **1953**, *171*, 738.
- (72) Matyjaszewski, K.; Xia, J. *Chem. Rev.* **2001**, *101*, 2921.
- (73) Fürstner, A. *Angew. Chem. Int. Ed.* **2000**, *39*, 3012.

- (74) Ilhan, F.; Galow, T. H.; Clavier, G.; Rotello, V. M. *J. Am. Chem. Soc.* **2000**, *122*, 5895.
- (75) Deans, R.; Ilhan, F.; Rotello, V. M. *Macromolecules* **1999**, *32*, 4956.
- (76) Calzia, K. J.; Tew, G. N. *Macromolecules* **2002**, *35*, 6090.
- (77) Schubert, U. S.; Hofmeier, H. *Polym. Mat. Sci. & Eng.* **2002**, *87*, 209.
- (78) Carlise, J. R.; Weck, M. J. *Poly. Science A, Poly. Chem.* **2004**, *42*, 2973.
- (79) Gohy, J.-F.; Lohmeijer, B. G. G.; Schubert, U. S. *Chem. Eur. J.* **2003**, *9*, 3472.
- (80) Meier, M. A. R.; Lohmeijer, B. G. G.; Schubert, U. S. *Macromol. Rapid Commun.* **2003**, *24*, 852.

CHAPTER 2.

THE “UNIVERSAL POLYMER BACKBONE” CONCEPT

2.1 Abstract

This chapter commences with a detailed analysis of the synthetic methodologies commonly used in materials science today. A conclusion is drawn inferring that upper limits in molecular design are inevitable, arising as a direct consequence of the predominance of covalent strategies in the field. To address these concerns, Nature’s non-covalent routes to complex biomaterials are explored and essential design principles are extracted. Accordingly, a new concept in polymer science, the “Universal Polymer Backbone” (UPB) concept, which applies Nature’s design elements to circumvent these limitations, is introduced. The UPB concept is thoroughly explored within the context of materials science and device optimization. Moreover, fundamental design features and challenges prerequisite to its development and implementation are addressed.

2.2 State of the Art Materials Synthesis: The “Covalent” Conundrum

Modern synthetic routes to polymeric materials with desirable properties for applications ranging from electronics to biomaterials are based upon covalent bond construction. Today, both industry and academia are strongly interested in organic based functional materials such as photorefractive polymers¹⁻⁴ for data storage in three

dimensions and flexible polymeric organic light emitting diodes (OLEDs)⁵⁻¹² for thin display technologies (Figure 2.1).

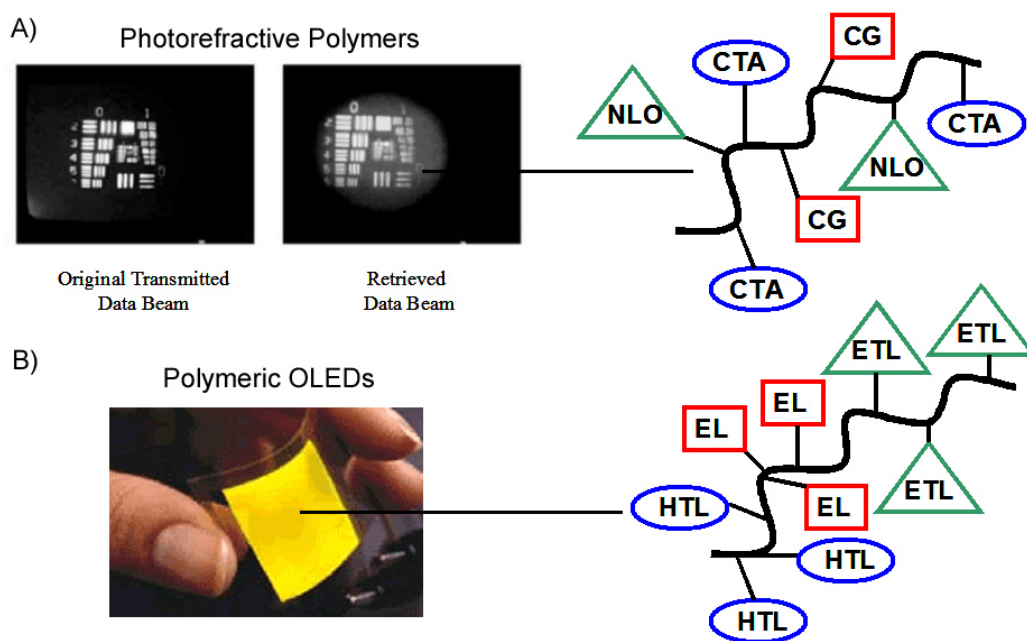


Figure 2.1 Structure property relationships for photorefractive polymers and polymeric OLEDs. A) Photorefractive polymers can be formed from random copolymers possessing a NLO chromophore, a charge transport agent, and a charge generator, B) polymeric OLEDs arise when block copolymers are made containing a hole transport layer, an electroluminescent layer, and an electron transport layer.

In both cases, these materials can be derived from a fusion of essential functional side-chain or main-chain components commonly referred to as mesogens.^{1,2,4-6,10} For example, photorefractive materials have been synthesized as random side-chain copolymers possessing a non-linear optical (NLO) chromophore, a charge transport agent, and a charge generator (Figure 2.1-A).¹ Polymeric OLEDs can be synthesized as block copolymers with three essential side-chain tethered mesogens including a hole

transport layer, an electroluminescent layer, and an electron transport layer (Figure 2.1-B).⁶

Unfortunately, inefficient routes to these elaborate polymers plague the field, which is often a direct consequence of a “covalent mentality” in materials science.¹³⁻¹⁹ To illustrate the problem, one can consider, for example, the classical methods used to prepare and optimize a photorefractive polymer using covalent methods.^{1,3} This process usually follows a three step serial pathway where: i) several monomers are prepared, ii) a polymerization method, tolerant of all monomer structures is employed, and iii) the photophysical properties of the material are evaluated (Figure 2.2). Optimization usually leads back to monomer synthesis and the entire process must be repeated until the desired physical properties are finally tuned.

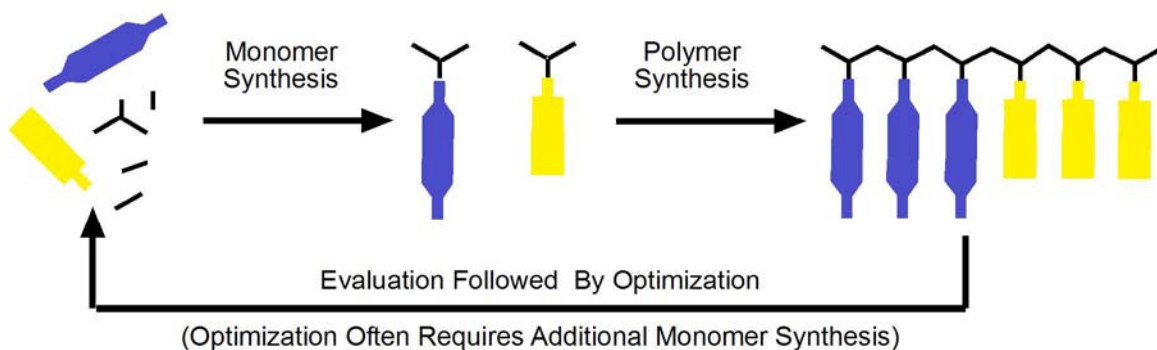


Figure 2.2 Materials synthesis and optimization using traditional covalent methods, which are serial in nature.

These long, cumbersome protocols for preparing advanced materials inevitably suffer from numerous time consuming, tedious reactions that are often low yielding and require multiple reagents. Furthermore, the polymerization of intricate monomer structures can

be troublesome due to functional group intolerant polymerization reactions, which often leads to poorly defined polymers whose structures vary greatly from batch to batch. As the molecular components of future technologies become even more elaborate and economic factors retard their deployment, an upper limit to the design and synthesis of densely functionalized materials and devices based on covalent methods is inevitable.

Ironically, most practical problems that threaten future growth of the field arise from factors that have thus far taken the field to where it is today. In principle, these difficulties stem from two fundamental flaws: i) the inherent complexity of the monomer structures themselves, and ii) the serial, covalent synthetic strategies used to prepare such materials. To eliminate long and extensive synthesis, thereby facilitating future progress in materials science, Nature, leading by example, suggests self-assembly to be used to fabricate advanced materials.¹⁸⁻²² Direct replacement of traditional covalent bonds with non-covalent linkages would provide alternative routes to structurally elaborate materials that are otherwise difficult or impossible to prepare using traditional covalent functionalization methods. In fact, applying non-covalent synthetic strategies to materials device fabrication offers solutions that easily circumvent nearly all problems that impede upon the vitality of the field.

Table 2.1 compares the advantages of replacing covalent synthesis with rationally designed and engineered materials based on self-assembly.^{18,19,23-25} Compared to covalent synthesis, self-assembled polymeric architectures may have superior features when matched up against their covalently bound polymeric counterparts. Advantages include increased flexibility in tailoring the functionality of the polymer (the synthesis of smaller components is generally more facile and more cost effective than that of large

molecules), and the inherent reversibility of non-covalent interactions. Moreover, molecular self-assembly allows for a simple and spontaneous formation of complex structures, such as two- and three-dimensional networks, and one-dimensional polymers.^{13-16,24} In broad perspective, one could envision translating features of molecular, covalent polymer chemistry to the supramolecular level, such as the formation of functionalized copolymers including the random and block copolymer structures described earlier for photorefractive polymers and polymeric OLEDs respectively.

Table 2.1 Comparison of covalent and non-covalent synthesis.

	Covalent Chemistry	Self-Assembly
Information	Must add appropriate reagents to accomplish transformations	All information is contained in the assembling parts
Reversibility	Non-reversible	Reversible
Economy	Multiple reagents and low yields Time consuming synthetic steps	Building block design essential Results in complex molecules
Error Checking	Incomplete reactions Unfavorable side reactions	Deformed building blocks not included in the final structure Self healing

2.3 Nature's Design Lessons

Nature's ability to quickly and efficiently create elaborate and highly functional biomaterials lies primarily upon its unique fabrication methods.¹⁸⁻²² Unlike most modern synthetic strategies, which rely primarily upon covalent bond formation, Nature employs non-covalent methodologies to achieve high degrees of complexity and functionality. DNA²⁰⁻²² and protein structures²¹ are prime examples of Nature's strategy. The structure

of DNA is composed of only 4 complementary base pairs and a sugar phosphate backbone,^{21,22} yet it is arguably one of the most complex and dynamic biomaterials (Figure 2.3).^{18,20}

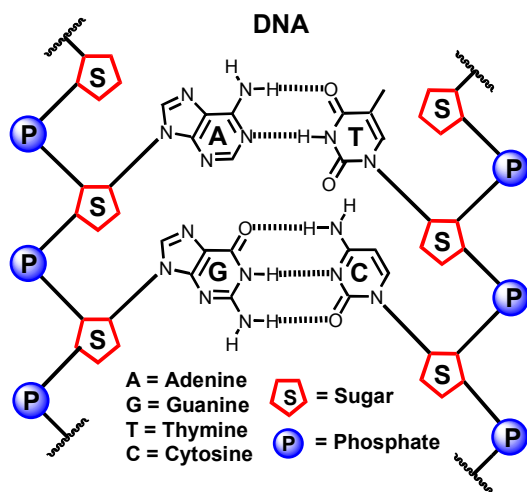


Figure 2.3 One of Nature’s marvels, the structure of DNA.

It is well accepted that the diversity and intricacy of DNA is achieved primarily via Nature’s efficient use of components capable of undergoing self-assembly.^{18,20,21} Similarly, protein structures built from only 20 amino acids can perform an immense range of complex biological functions from hormone regulation to energy production for cellular activities.²¹ Apparently, the complexity found in Nature is not predicated on the use of a large number of building blocks, but is rather dependent upon the preprogrammed and non-covalent character of a select few building blocks. Nature’s use of self-assembly imparts unique properties including reversibility, selectivity, and self-healing character into the materials it forges. Furthermore, Nature almost never makes use of a single or serial recognition element, but rather employs a wide array of non-

covalent interactions (including hydrogen bonding, metal coordination, Coulombic interactions, and hydrophobic interactions), all of which operate orthogonal to and in symphony with one another to create vast libraries of functional biological materials.^{18,19,21} In short, Nature's unique design principles give rise to ponderously elaborate and dynamically functional devices that are thus far unmatched in function and complexity when compared to the synthetic materials and devices of today.

As reviewed in Chapter 1, Nature has inspired many facets of research aimed at duplicating its complexity. Many researchers who focus upon self-assembly in polymer science have stuck to simple and relatively easy to synthesize Natural analogs, all of which rely upon the use of a single non-covalent pair.²⁶⁻³⁴ Although these accounts have taken Nature's lead to combine self-assembly and polymer science, they have largely ignored the concept of using multiple recognition elements in an orthogonal fashion. In this thesis, an orthogonal or parallel self-assembly approach to polymer functionalization is addressed. Aptly named the UPB concept, the methodology presented herein employs Nature's design motifs to create densely multi-functionalized random and block copolymers using simple one-step and multi-step orthogonal self-assembly processes. Unlike its predecessors, the UPB concept is particularly useful from an application standpoint in that it offers the ability to rapidly fabricate and tune the properties of complex materials such as electro-optical,¹⁻¹² biomolecular,^{18-20,35} or drug delivery devices^{35,36} that are otherwise difficult or impossible to prepare using traditional covalent functionalization methods.

2.4 The UPB Concept: Beyond Covalent Polymer Functionalization

A UPB can be defined as any copolymer, side-chain functionalized with multiple recognition elements that are individually capable of forming strong, directional, and reversible non-covalent bonds. Furthermore, each recognition unit operates independent of and in the presence of one another. Non-covalent functionalization of these scaffolds leads to the formation of a multitude of new polymer structures, each stemming from a single parent or “Universal Polymer Backbone”. As the name suggests, a single UPB could be used to prepare polymeric materials for a wide variety of applications. For example, simple modification of the side-chain elements from liquid crystalline mesogens³⁷ to photorefractive elements^{1,3} would allow for two entirely unique classes of materials to be created from a single parent backbone (Figure 2.4) Furthermore, all fundamental and preprogrammed attributes of the polymer backbone such as chain length, rigidity, and polydispersity could be inevitably translated to all materials prepared from the same UPB.

Multifunctionalization of UPBs via orthogonal self-assembly could provide novel pathways to complex polymer architectures that, in principle, will be far superior to the covalent functionalization routes used today. Unlike covalent synthetic strategies, which are serial in nature, the UPB concept employs parallel self-assembly processes that allow for simple and spontaneous formation of complex structures. Since UPB functionalization is based on self-assembly, it is inherently reversible and self-healing which allows for facile and precise tuning of the side-chains by outside stimuli such as solvent polarity and temperature. These fundamental attributes not only make the UPB concept a potentially powerful synthetic tool, but also introduce new strategies to rapidly optimize functional materials.

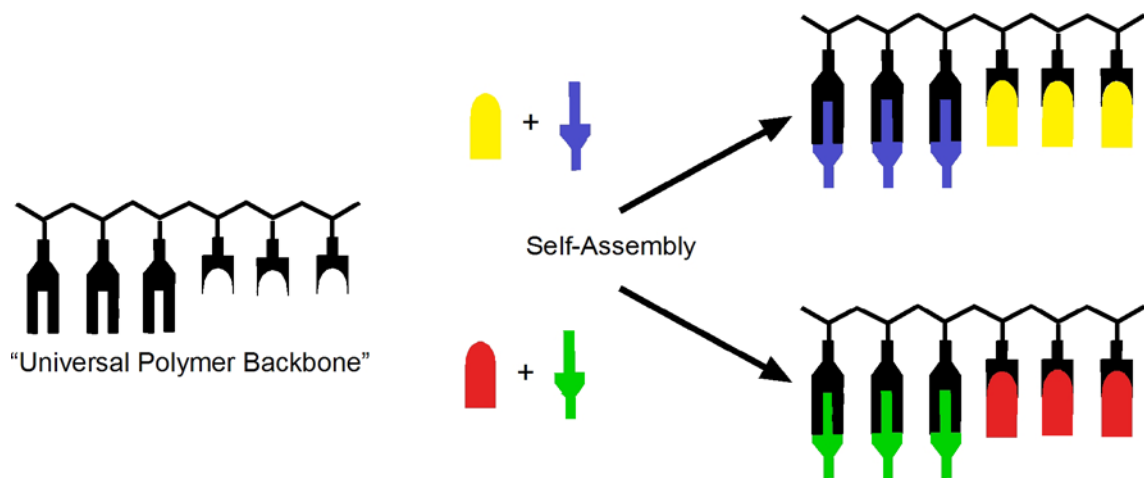


Figure 2.4 Cartoon depicting the UPB concept. A single UPB can “parent” a multitude of functionalized copolymers via orthogonal one-step self-assembly of recognition counterparts.

One approach to optimizing materials using the UPB concept is depicted in Figure 2.5. Here, an iterative optimization strategy may be possible via exploitation of the reversible nature of the non-covalent bond. As depicted, functionalized materials possessing multiple side-chain mesogens (blue and yellow) could be deconstructed by applying external stimuli to selectively remove a single mesogen (yellow). This step would result in the formation of a singly functionalized UPB (blue only) possessing open binding sites that could be subsequently functionalized with a different mesogenic component (red). The newly fabricated copolymer (blue and red) could then be examined for desired physical properties. If the physical characterization of the new copolymer is unsuccessful, the entire process could be carried out an infinite number of times with a variety of configurations until a copolymer structure possessing desirable physical properties is identified.

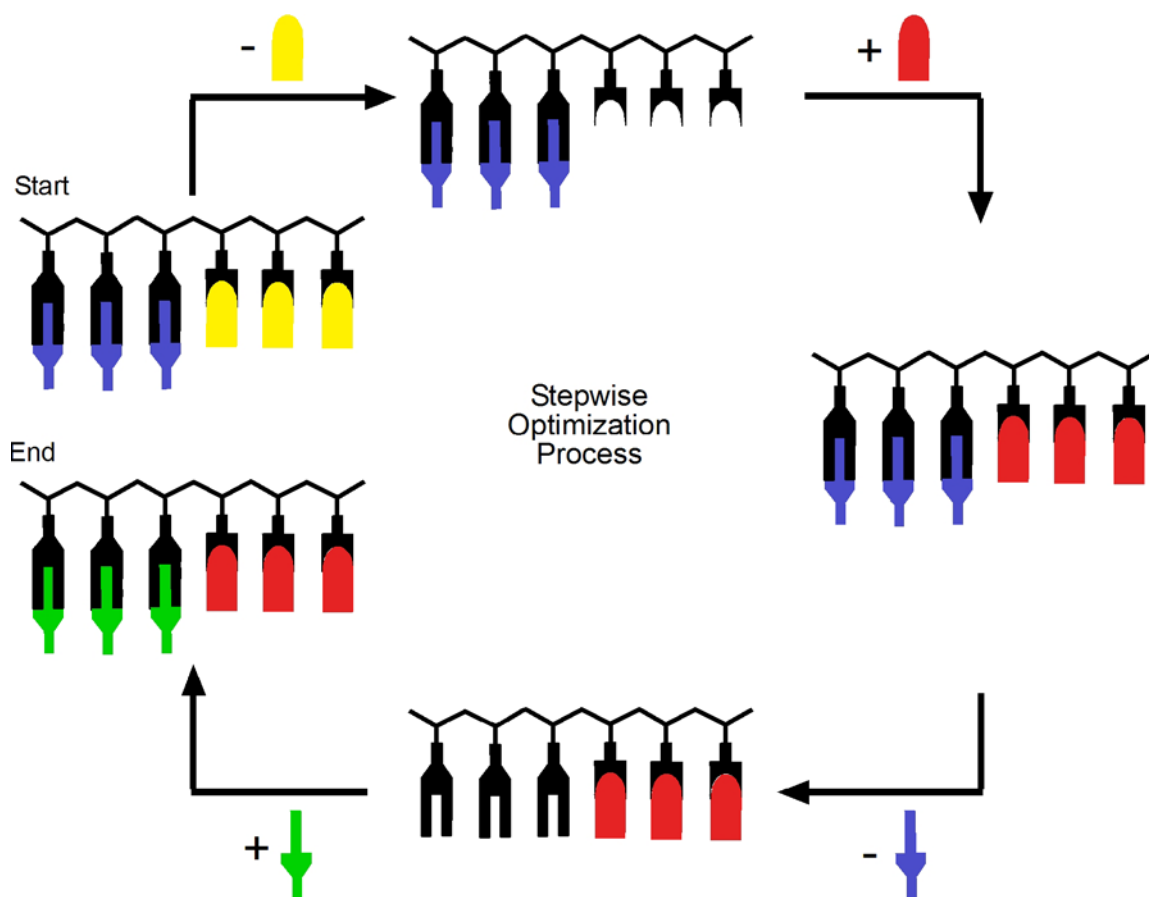


Figure 2.5 Cartoon depicting the iterative optimization of a polymeric device via the UPB concept.

Additionally, the UPB concept could be easily employed to optimize copolymer structures for materials applications by exploiting the facile nature of the functionalization step. One-step multifunctionalization, a parallel synthetic approach, has the potential to allow for combinatorial techniques to be applied to polymer science. One could imagine a scenario where vast libraries of copolymers arising from simple mixtures of different UPBs and functional mesogens are prepared instantly. Under these circumstances, the time required to bring advanced materials to market would no longer

be directly dependent upon synthetic limitations, but rather would be measured by how quickly the libraries could be analyzed for lead copolymer architectures.

Clearly, the utility of the UPB concept offers profound alternatives to the problems associated with covalent strategies in materials science. However, the above-mentioned capabilities will require the design, synthesis, and implementation of a UPB system that possesses rather extraordinary control and manipulation over both the covalent and non-covalent bond. From a research standpoint, the fabrication and realization of the UPB concept may be even more challenging, complex, and time consuming than simple employment of traditional covalent routes to materials. However, once perfected, the UPB concept offers a tremendous payoff in terms of its the capabilities and ease in manufacturing materials.

2.5 Challenges, Design Elements, and Perspective

The major goal of this thesis is to develop and implement the UPB concept. However, duplicating Nature's complexity, even on a very basic level, will require mastery of both the covalent and non-covalent bond that goes well beyond the methods of non-covalent polymer functionalization known today. Thus, several subordinate objectives/design criteria essential to the realization of UPB concept must be addressed throughout the course of its development.

Specifically, these important areas include:

- The design, synthesis, and evaluation of variety of molecular recognition motifs.

Perhaps this will be the most important area of focus since the recognition units themselves must meet several stringent design criterion including: i) rapid and quantitative self-assembly behavior, ii) the ability to operate independent of and

in the presence of one another, iii) strong affinity toward its partner with little or no self-association, and iv) the ability to decouple quickly and efficiently upon application of external stimuli such as solvent, pressure or temperature.

- Development of anchoring units with the universal functionalization of copolymers in mind. Here, the anchoring group may or may not be a structural feature of the mesogenic component itself. By definition, it should meet virtually all design criteria established above for the recognition motifs. However, it should be designed with ease derivatization in mind in order to streamline the preparation of anchored mesogens.
- Basic monomer preparation and homo-polymerization. Here, both the design of the monomer and implementation of a particular polymerization method must meet the following requirements: i) the final polymers must be highly soluble, ii) the recognition unit must not interfere with either the polymerization process nor should the polymer backbone interfere with the self-assembly, and iii) the final polymers must be well-defined and easily tailored to a variety of molecular weights and various compositions.
- Homopolymer functionalization and characterization. Here, essential tools capable of measuring the presence and strength of a recognition event must be developed. The properties of functionalized polymers and non-functionalized homopolymers must be directly compared to investigate the influence of self-assembly on polymer structure, thermal behavior, and solubility.

Once addressed, the above-mentioned challenges, objectives, and design criteria will allow for realization of the final goal: one-step orthogonal multi-functionalization of

copolymers via self-assembly. Every consideration described above must be taken into account when designing and executing the UPB concept. None of these issues are independent from each other, and all must work in combination with one another. Detailed studies of natural systems offer some assistance in pursuit of these goals by suggesting important trends and tendencies and giving insight into the daunting task of combining these objectives.¹⁸⁻²² However, the ponderous complexity of natural systems is largely a consequence of billions of years of evolution.²¹

The remainder of this thesis focuses upon the experimental steps taken during the development, realization, and fine-tuning of the UPB concept. The major strides made during the maturation and advancement of this concept follow four major landmark achievements: i) the design and synthesis of homopolymers containing strong directional recognition motifs and their self-assembly behavior (Chapter 3), ii) the optimization of polymerization conditions and monomer structures to obtain fully “living” systems where surgical precision over the architecture of the final polymers and copolymer structures is possible (Chapter 4), iii) the synthesis of first generation UPBs and subsequent multi-site functionalization where both interactions are instantaneous, quantitative, and selective (Chapter 5), and iv) applications of the UPB concept, including the fabrication of well-controlled crosslinked materials (Chapter 6), and detailed discussions centered on the non-covalent fabrication of other materials including photorefractives, polymeric liquid crystals, drug delivery devices, biosensor technologies, and nonporous materials (Chapter 7).

2.6 References

- (1) Bratcher, M. J.; DeClue, M. S.; Grunnet-Jepsen, A.; Wright, D.; Smith, B. R.; Moerner, W. E.; Siegel, J. S. *J. Am. Chem. Soc.* **1998**, *120*, 9680.
- (2) Chen, Y.; He, Y.; Wang, F.; Chen, H.; Gong, Q. *Polymer* **2001**, *42*, 1101.
- (3) Moerner, W. E.; Silence, S. M. *Chem. Rev.* **1994**, *94*, 127.
- (4) Yu, L.; Chan, W. K.; Peng, Z.; Gharavi, A. *Acc. Chem. Res.* **1996**, *29*, 13.
- (5) Burroughes, J. H.; Bradley, D. D. C.; Brown, A. R.; Marks, R. N.; Mackay, K.; Friend, R. H.; Burns, P. L.; Holmes, A. B. *Nature* **1990**, *347*, 539.
- (6) Danielson, E.; Golden, J. H.; McFarland, E. W.; Reaves, C. M.; Weinberg, W. H.; Wu, X. D. *Nature* **1997**, *389*.
- (7) Halls, J. J. M.; Walsh, C. A.; Greenham, N. C.; Marseglia, E. A.; Friend, R. H.; Moratti, S. C.; Holmes, A. B. *Nature* **1995**, *376*, 498.
- (8) Leclerc, M. *Adv. Mater.* **1999**, *11*, 1491.
- (9) Davidov, D.; Neumann, R. *Acta Polym.* **1998**, *49*, 642.
- (10) Friend, R. H.; Gymer, A. B.; Holmes, J. H.; Burroughes, J. H.; Marks, R. N.; Taliani, C.; Bradley, D. D. C.; Dos Santos, D. A.; Brédas, J. L. *Nature* **1999**, *397*, 121.
- (11) Sheats, J. R.; Antoniadis, H.; Hueschen, M.; Leonard, W.; Miller, J.; Moon, R.; Roitman, D.; Stocking, A. *Science* **1996**, *273*, 884.
- (12) Sheats, J. R. *Science* **1997**, *277*, 191.
- (13) Lehn, J.-M. *Pure Appl. Chem.* **1994**, *66*, 1961.
- (14) Lehn, J.-M. *Polym. Int.* **2002**, *51*, 825.
- (15) Brunsveld, L.; Folmer, B. J. B.; Meijer, E. W.; Sijbesma, R. P. *Chem. Rev.* **2001**, *101*, 4071.
- (16) Hollingsworth, M. D. *Science* **2002**, *295*, 2410.
- (17) Ikkala, O.; ten Brinke, G. *Science* **2002**, *295*, 2407.
- (18) Lindsey, J. S. *New J. Chem* **1991**, *15*, 153.

- (19) Philp, D.; Stoddart, J. F. *Angew. Chem. Int., Ed. Eng.* **1996**, *35*, 1154.
- (20) Kool, E. T.; Morales, J. C.; Guckian, K. M. *Angew. Chem. Int. Ed.* **2000**, *39*, 990.
- (21) Lehninger, A. L.; Cox, M. M.; Nelson, D. L. *Principles of Biochemistry*; 4th ed.; W. H. Freeman Company: New York, NY, 2004.
- (22) Watson, J. D.; Crick, F. H. C. *Nature* **1953**, *171*, 738.
- (23) Whitesides, G. M.; Mathias, J. P.; Seto, C. T. *Science* **1991**, *254*, 1312.
- (24) Lehn, J.-M. *Supramolecular Chemistry*; Wiley-VCH: Weinheim, 1995.
- (25) Steed, J. W.; Atwood, J. L. *Supramolecular Chemistry*; John Wiley & Sons, Ltd: Chichester, West Sussex, 2000.
- (26) Kawakami, T.; Kato, T. *Macromolecules* **1998**, *31*, 4475.
- (27) Bazzi, H. S.; Sleiman, H. F. *Macromolecules* **2002**, *35*, 9617.
- (28) Davies, R. G.; Gibson, V. C.; Hursthouse, M. B.; Light, M. E.; Marshall, E. L.; North, M.; Robson, D. A.; Thompson, I.; White, A. J. P.; Williams, D. J.; Williams, P. J. *J. Chem. Soc., Perkin Trans. 1* **2001**, 3365.
- (29) Gibson, V. C.; Marshall, E. L.; North, M.; Robson, D. A.; Williams, D. J. *Chem. Commun.* **1997**, 1095.
- (30) Khan, A.; Haddleton, D. M.; Hannon, M. J.; Kukulj, D.; Marsh, A. *Macromolecules* **1999**, *32*, 6560.
- (31) Marsh, A.; Khan, A.; Haddleton, D. M.; Hannon, M. J. *Macromolecules* **1999**, *32*, 8725.
- (32) Stubbs, L. P.; Weck, M. *Chem. Eur. J.* **2003**, *9*, 992.
- (33) Bazzi, H. S.; Bouffard, J.; Sleiman, H. F. *Macromolecules* **2003**, *36*, 7899.
- (34) Ilhan, F.; Gray, M.; Rotello, V. M. *Macromolecules* **2001**, *34*, 2597.
- (35) Langer, R. *Acc. Chem. Res.* **2000**, *33*, 94.
- (36) Langer, R. *Science* **1990**, *249*, 1527.
- (37) Kato, T. *Science* **2002**, *295*, 2414.

CHAPTER 3.

SYNTHESIS AND SELF-ASSEMBLY OF POLYMERS BEARING PALLADATED SCS PINCER COMPLEXES

3.1 Abstract

In this chapter, poly(norbornene)s bearing palladated SCS pincer complexes at each repeat unit have been synthesized using ring-opening metathesis polymerization (ROMP). Small mesogenic molecules possessing nitrile or pyridine-based anchoring units are instantaneously and quantitatively coordinated to the palladium center in one simple self-assembly step which gives rise to a densely functionalized polymer. These results suggest that the coordination of mesogenic small molecules onto the polymer scaffold can provide a simple and efficient route to a variety of materials.

3.2 Introduction

The aim of the research described herein¹ is to develop non-covalent routes to side-chain self-assembled homopolymers that incorporate design elements and characterization techniques that will enable the larger goal of realizing the UPB concept. Several stringent prerequisite design elements must be built into all homopolymers prepared for future use as UPBs. These requirements include: i) the use of a highly directional self-assembly motif that can accommodate a large number of recognition units for easy backbone functionalization, ii) the development of facile synthetic routes to

monomer structures containing the desired recognition motif, ii) the design and synthesis of anchoring groups, covalently attached to functional mesogenic components that are complementary to the monomer, iii) the implementation of a controlled polymerization technique that will eventually enable the formation of copolymers, and iv) the development of sound characterization techniques to probe the nature of the non-covalent linkages.

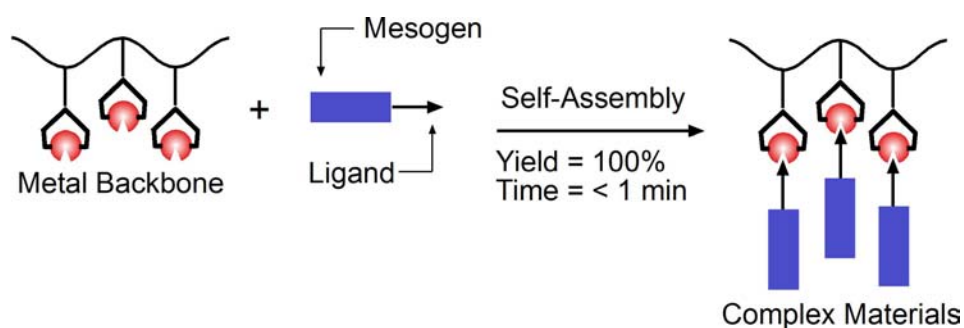


Figure 3.1 Synthesis of side-chain functionalized polymers via metal coordination.

Early on, it was anticipated that a self-assembly motif based upon metal coordination offers distinct advantages when compared to other recognition units.²⁻⁶ First, the introduction of metal ions could give access to important physical properties such as magnetism and conductivity. Second, the strength of coordination bonds is easily tailored. Third, the selection of the metal ion and, therefore, the selection of the coordination geometry, will provide excellent flexibility in materials design. In particular, the properties of metallated pincer ligands as recognition motifs were chosen (Figure 3.1).

3.2.1 Pincer Ligands

The tridentate ligand systems used throughout this thesis are called “pincer ligands”, which are named for their chelating shape.^{7,8} These ligands, first reported in the late 1970s⁹ possess the general formula $[2,6-(ECH_2)_2C_6H_3]^-$ (ECE) where E is a neutral two-electron donor such as phosphorus, sulfur, or nitrogen. The ligands are commonly abbreviated NCN, PCP, and SCS depending upon the donor atoms employed. Transition metals can be inserted into the aromatic C-H σ -bond situated between donor atoms, giving rise to a meridional coordination mode where two metallacycles share the M-C bond, providing enhanced stability to the complex. Metallation is commonly achieved using d^8 –metal centers (platinum group metals), which results in the formation of a square planar geometry (Figure 3.2).

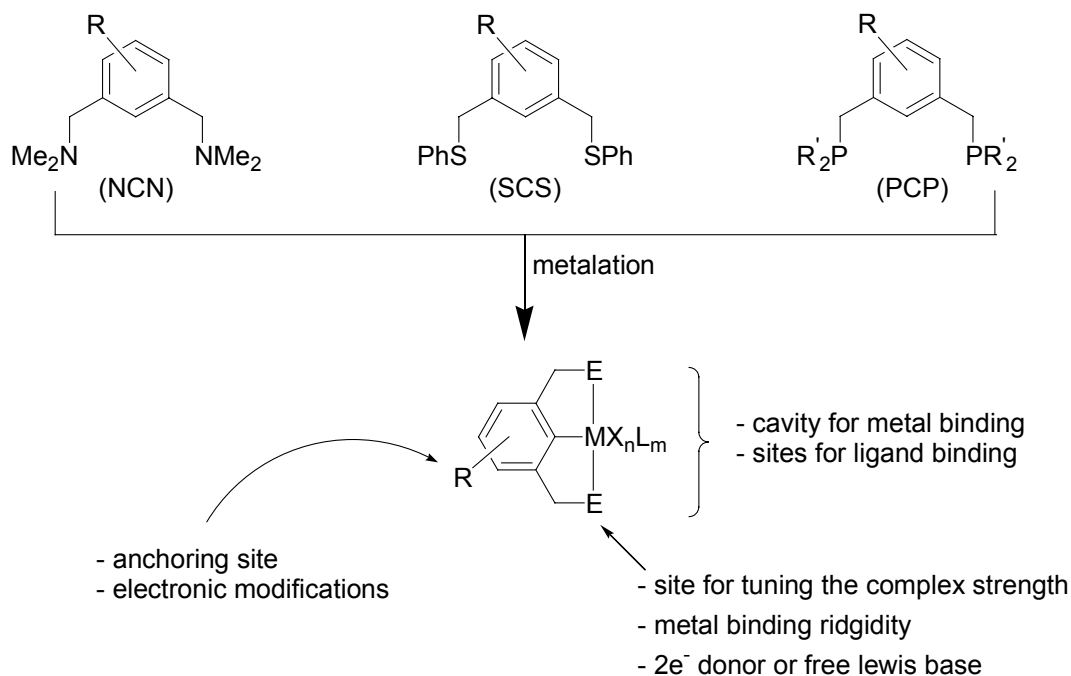
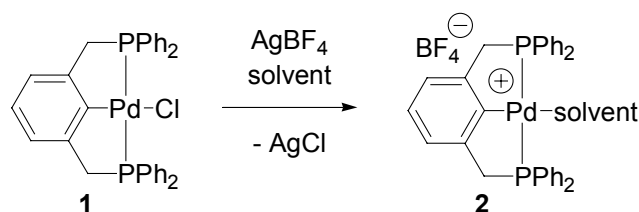


Figure 3.2 Structural attributes of pincer ligands and pincer metallacycles.

The construction of cyclometallated pincer ligand complexes is highly dependent upon the type and strength of the donor atoms (ECE).^{7,8} Therefore, only specific metals may be employed with certain donor-carbon-donor configurations. In general, nitrogen atoms (NCN pincer) are neutral,⁸ sulfur atoms (SCS pincer) are weakly activating,¹⁰ and phosphorous (PCP pincer) are highly activating.^{9,11} Consequently, only cyclopalladations are known for the SCS ligand system.^{7,10,12-20} Whereas, PCP pincer ligands readily accommodate a variety of transition metals including Ni(II), Ir(III), Pt(II), and Pd(II).^{7,9,11} Furthermore, substituents located in the *para*-position electronically influence the metal center and therefore affect the complex strength and redox properties of the transition metal.⁷

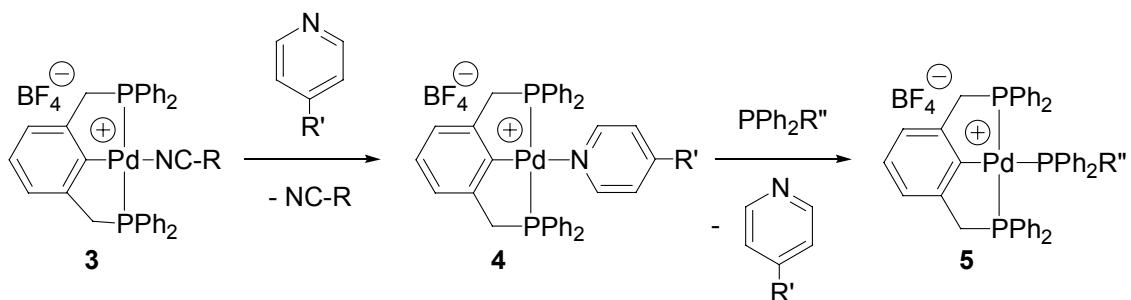
The fourth coordination site of pincer complexes containing Ni(II), Pd(II), or Pt(II) may be occupied by halide or acetate ions to form overall neutral complexes.^{7,9,11} The conversion between neutral and ionic pincer complexes can be readily accomplished by halide abstraction.^{13,21} Treatment of PCP Pd-Cl with AgBF₄ results in formation of an ionic palladium species, where a weakly coordinated solvent molecule occupies the fourth coordination site.²¹ In fact, low temperature ³¹P NMR studies have proven the coordination of halogenated solvents such as CDCl₃ and CD₂Cl₂ in the absence of other ligands, with no evidence of BF₄⁻ coordination (Scheme 3.1).²¹

Scheme 3.1 Dechlorination of Pd-Cl PCP pincer complexes.



The ease to which the fourth coordination site can be modified makes pincer complexes exceptionally good candidates for use in molecular recognition. In particular, palladium and platinum pincer complexes have found tremendous utility as non-covalent building blocks in self-assembly.⁷ This is mainly because of their high stabilities and unique structural attributes which allow for easy access to a single noncoordinate cationic palladium species (**2**) that can subsequently undergo substitution with a variety of ligands.^{7,19} Ordered according to strength, nitrile, pyridine, and phosphorous ligands have found tremendous utility in supramolecular science.⁷ Covalent tethering of these functional groups to small molecules gives rise to anchoring units. Furthermore, the ability to tune the strength of pincer-metal-ligand interactions by direct replacement of a weaker ligand for a stronger one has allowed for facile modification of self-assembled structures (Scheme 3.2).^{17,22,23}

Scheme 3.2 Ligand displacement reactions.



From a self-assembly standpoint, ligand displacement *trans* to the carbon-metal bond corresponds to a host-guest interaction, where the $[\text{Pd}(\text{ECE})]$ moiety serves as a host (receptor) for nitrile, pyridine, and phosphorous guests.⁷ The most predominate host-

guest interactions found in the literature are based on palladated SCS pincer complexes.^{13-15,17,20,24,25} Reinhoudt and coworkers have well established this concept for the non-covalent synthesis of metallodendrimers (**6**), where a bimetallic Pd₂-CN synthon and a trimetallic Pd₃ core are combined in a divergent manner via repetitive halide abstraction.^{7,13-15,17} Similar strategies have been reported for the construction of molecular assemblies based on bimetallic SCS Pd-Cl components.^{20,24,25} Here, the geometry of the pyridine-based ligand bound to the fourth coordination site dictates either the formation of molecular macrocycles (**7**)²⁵ or linear polymers (**8**)^{20,24} (Figure 3.3).

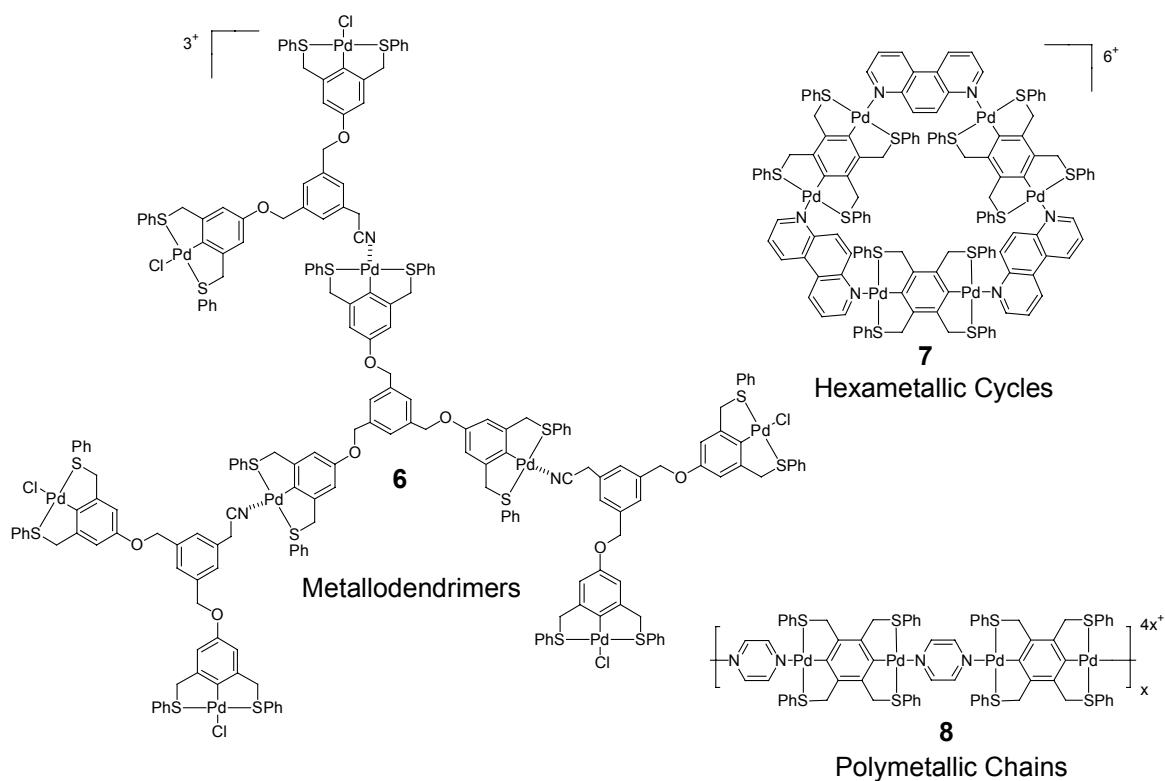


Figure 3.3 Self-assembled palladium SCS pincer complexes in supramolecular science.

Based on the above reports, which establish the use of palladated SCS pincer complexes as strong, quantitative, and thermally stable self-assembly motifs, it was rationalized that pincer ligands could play a critical role in the development of the UPB concept. Furthermore, the ability of such complexes to accommodate a variety of simple ligands would aid in the preparation of a versatile arsenal of “anchored” mesogens that could be easily characterized. However, the synthesis, polymerization, and self-assembly behavior of palladated SCS pincer complexes located along a polymer backbone had not yet been investigated.

To enable the study of these parameters, a polymerization technique, inextricably related to monomer structure, had to be selected prior to monomer design. Specifically, the polymerization strategy must: i) operate highly efficiently in the presence of palladated SCS pincer complexes, ii) form well-defined homopolymers, and iii) offer the potential to access random and block copolymers. With these considerations in mind, ROMP was chosen as the polymerizable method to provide an efficient, well-defined route to homopolymers and copolymers with low polydispersities.

3.2.2 *Ring-Opening Metathesis Polymerization*

ROMP is a transition-metal catalyzed polymerization method that employs the olefin-metathesis reaction shown in Figure 3.4.²⁶⁻²⁹ The mechanism for this reaction, proposed by Chauvin in 1971, involves the formation and subsequent cleavage of a mettalocyclobutane intermediate and results in the transpositioning of carbon-carbon double bonds.³⁰

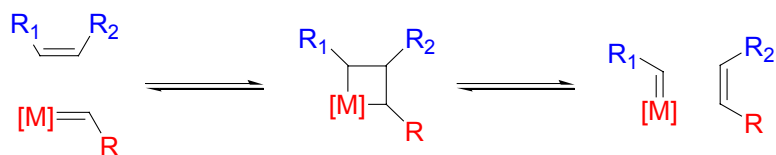


Figure 3.4 Chauvin's mechanism for the olefin metathesis reaction.

In principle, ROMP operates by the same mechanism developed by Chauvin, but with the exception that it utilizes strained cyclic olefins as monomers to give polyolefins (Figure 3.5).²⁷⁻²⁹ It is enthalpically driven by the removal of ring strain, making highly strained olefins such as norbornenes, cyclobutenes, barrelenes, and cyclooctadienes excellent monomer candidates.²⁷

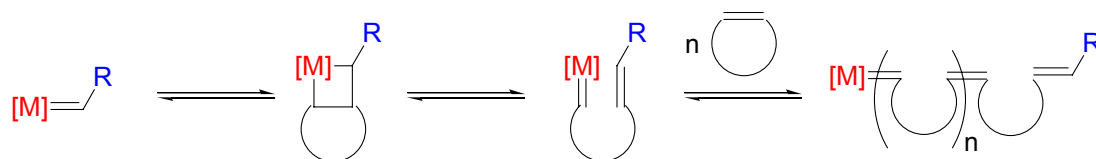


Figure 3.5 Mechanism for ROMP.

Modern catalysts commonly employed in ROMP are based on molybdenum- and ruthenium- alkylidene transition metal complexes that were developed by Schrock^{28,31} and Grubbs^{26,28} respectively. In particular, Grubbs' catalysts (**9-11**)^{26,32,33} have enjoyed much utility due to their high functional group tolerance and the ability to withstand the presence of air and water (Figure 3.6).²⁷⁻²⁹

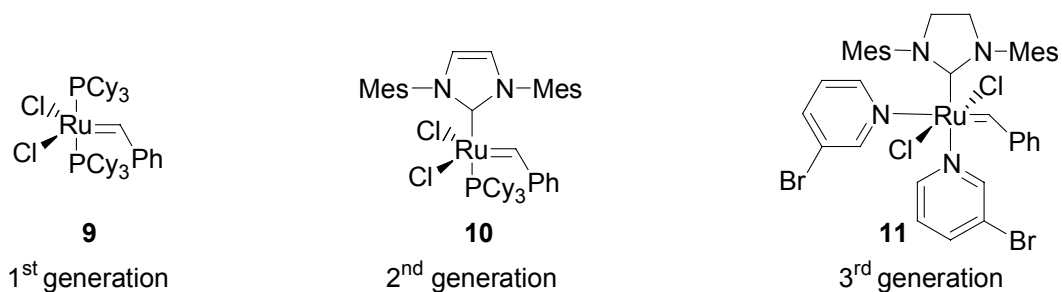


Figure 3.6 Grubbs' ruthenium alkylidene olefin metathesis catalysts.

Unlike other polymerization techniques, such as free radical polymerization, ROMP usually proceeds in a living manner.²⁷⁻²⁹ Living polymerizations give maximum control over molecular weight, composition, and polydispersity allowing for the formation of well-defined structures.³⁴ Furthermore, living polymerizations enable block copolymer formation, which is otherwise difficult or impossible to achieve otherwise.^{34,35}

3.2.3 Monomer Design

The basic structural features of the monomers used herein are comprised of three essential components: i) a polymerizable unit, ii) an aliphatic tether, and iii) the recognition unit. As shown in Figure 3.7, the monomers chosen for this project are preprogrammed for facile modification and tuning of the polymer structures. First, norbornene was chosen as the polymerizable unit to provide a well-controlled route to polymers via ring-opening metathesis polymerization.²⁶⁻²⁹ In particular, norbornene acid chlorides, a class of highly strained norbornene derivatives that readily undergo condensation reactions with a variety of nucleophiles, were selected to facilitate ease of synthesis. Second, a flexible C₁₁ alkyl chain was situated between the metal coordination motif and the polymeric backbone to decouple the recognition motif from the backbone.

This feature, which can be easily modified, has the potential to enhance solubility and provide flexibility to the self-assembly.^{36,37} The final design element, the incorporation of the metal coordinating unit, required the preparation a functionalized pincer ligand that would allow for facile attachment to the spacer group. Therefore, *para*-hydroxy functionalized pincer ligands were chosen because they easily undergo substitution and condensation relations to form ethers and esters respectively.¹⁶

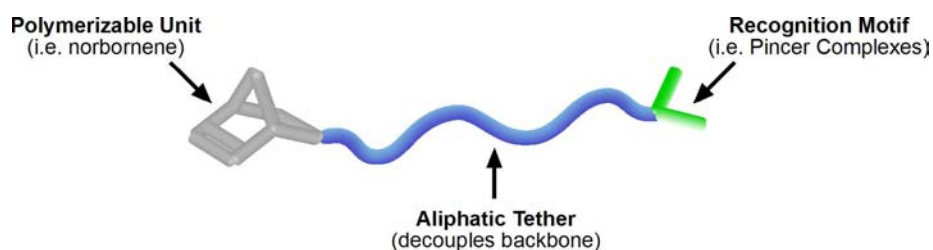
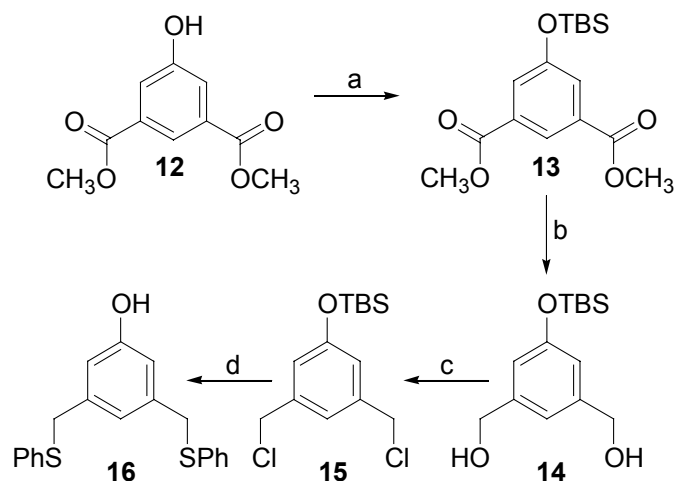


Figure 3.7 The structural components of monomer design.

3.3 Monomer and Polymer Synthesis

The synthesis of polymer **21** began with the preparation of the hydroxy functionalized SCS ligand **16**.¹⁶ This was accomplished by derivatization of 5-hydroxy isophthalic acid dimethyl ester **12**. Protection of the hydroxyl functionality of **12** with *tert*-butyldimethylsilyl chloride provided silyl ether **13** in quantitative yields. Reduction to the corresponding diol **14**, followed by chlorination using mesityl chloride gave dichloride **15**.³⁸ The remainder of the synthesis proceeded by substitution of **15** with sodium thiophenolate salt to form the protected dithioether intermediate, which was subsequently deprotected using tetrabutylammonium fluoride to prepare hydroxy functionalized SCS pincer ligand **16** in four steps (Scheme 3.3).

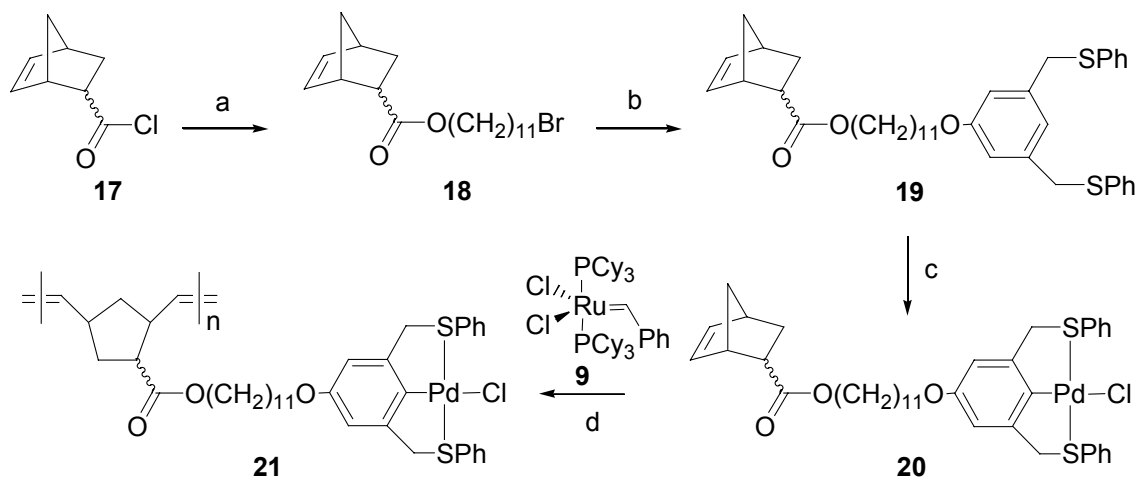
Scheme 3.3 Synthesis of *para*-hydroxy SCS pincer ligand.



Reagents and Conditions: a) TBDMSCl, Et₃N, DMAP, CH₂Cl₂, 25 °C, 16 h, 99%; b) LiAlH₄, THF, 25 °C, 14 h, 73%; c) MsCl, Et₃N, CHCl₃, 38 °C, 12 h, 68%; d) i) NaSPh, THF, 50 °C, 12 h; ii) TBAF, THF, 38 °C, 16 h, 72%.

Synthesis of monomer **20** commenced by condensation of acid chloride **17**³⁹ with 11-bromoundecan-1-ol to provide bromoester **18**, followed by coupling of **18** to **19** under basic conditions to form **19**. A simple two step procedure beginning with ligand exchange of [Pd (CH₃CN)₄](BF₄)₂⁴⁰ and **19** to form the corresponding cationic Pd-BF₄ intermediate followed by chlorination with aqueous sodium chloride provided the desired neutral Pd-Cl complex **20** in high yield. Monomer **20** was polymerized via ROMP by employment of catalyst **9**. At low temperatures propagation was sluggish, resulting in incomplete conversion due to catalyst decomposition over time (>24 h). However, moderate heating (45 °C) in CDCl₃ afforded polymer **21** in 12 h with low polydispersities (PDI = 1.10-1.25) and in quantitative yield (Scheme 3.4).

Scheme 3.4 Monomer synthesis and ROMP.

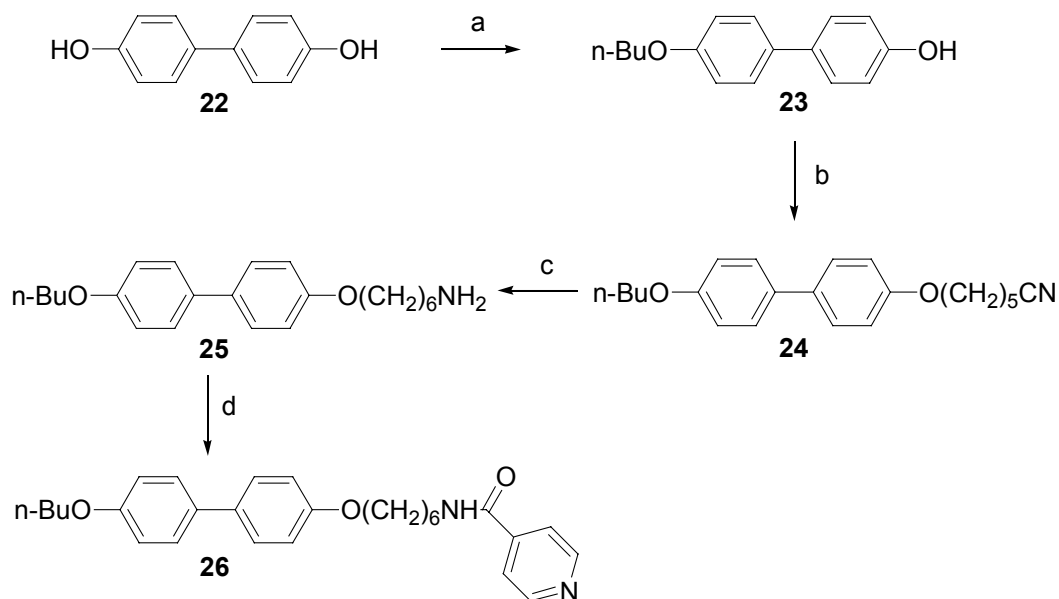


Reagents and Conditions: a) 11-bromo-1-undecanol, Et₃N, THF, reflux, 16 h, 91%; b) 16, K₂CO₃, DMF, 90 °C, 16 h, 59 %; c) i) Pd[CH₃CN]₄(BF₄)₂, CH₃CN, 15 min; ii) NaCl_(aq), 3:1 CH₂Cl₂/CH₃CN, 1 h, 77 %, d) CHCl₃, 45 °C, 12 h, 95 %.

3.4 Synthesis of Nitrile and Pyridine Anchored Mesogenic Units

In order to investigate the structure-property relationships governing both the self-assembly of small molecules to the polymeric backbone as well as the mesogenic behavior of the non-covalent entities, biphenyl based mesogens possessing either a nitrile (24 and 28) or pyridine (26 and 27) recognition unit were synthesized. To examine the possibility that steric factors in the vicinity of the metal coordination site might effect the self-assembly, both nitrile and pyridine functionalized mesogens were prepared with (24 and 26) and without (27 and 28) an alkyl spacer group situated between the biphenyl and the recognition unit.

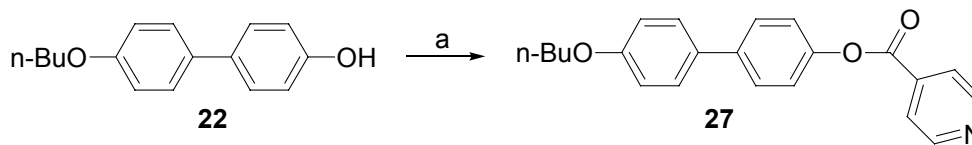
Scheme 3.5 Synthesis of spaced nitrile and pyridine based mesogens.



Reagents and Conditions: a) 1-bromo-butane, K₂CO₃, DMF, reflux, 5 h, 46 %; b) 6-bromo-hexanenitrile, K₂CO₃, DMF, 110 °C, 16 h, 74 %; c) LiAlH₄, THF, reflux, 12 h, 83%; d) isonicotinoyl chloride hydrochloride, Et₃N, CH₂Cl₂, 25 °C, 24 h, 84%.

Spaced biphenyl ligands **24** and **26** were synthesized by alkylation of 4'-butoxybiphenyl-4-ol **22** with one equivalent of 1-bromobutane resulting in a statistical mixture of dialkylated and monoalkylated products. The desired monoalkylated phenol **23** could be isolated by crystallization from ethanol. Reaction of **23** with commercially available 6-bromohexanenitrile under basic conditions yielded the C₅ spaced nitrile **24** in two steps. Reduction of **24** with LiAlH₄ to the corresponding amine (**25**) followed by condensation with isonicotinoyl chloride hydrochloride provided the desired C₆ spaced pyridine **26** in 83% yield (Scheme 3.5).

Scheme 3.6 Synthesis of non-spaced pyridine functionalized mesogen.



Reagents and Conditions: a) Isonicotinoyl chloride hydrochloride, Et₃N, CH₂Cl₂, 25 °C, 24 h, 86%.

In a similar manner, the non-spaced pyridine functionalized mesogen (27) was prepared directly from phenol 22 in 86% yield (Scheme 3.6). The non-spaced nitrile based mesogen, 4'-(Pentyloxy)-4-biphenylcarbonitrile (28), was commercially available and therefore did not require synthesis (Figure 3.8).

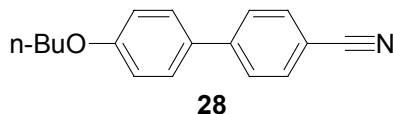


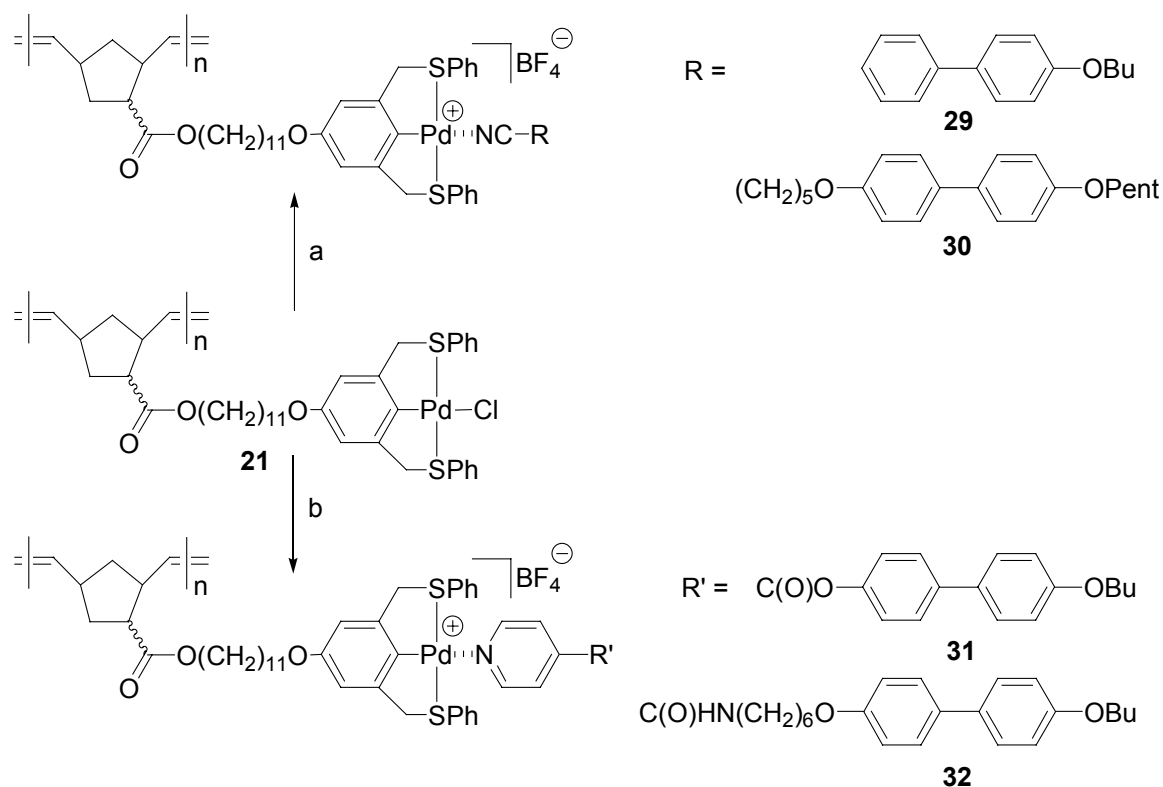
Figure 3.8 Non-spaced nitrile functionalized mesogen 28.

3.5 Polymer Functionalization

Self-assembly of the four mesogenic ligands 24, 26, 27, and 28, onto the polymeric scaffold (21) was carried out by addition of one equivalent of AgBF_{4(aq)} to a 1:1 mixture of polymer to mesogen in methylene chloride. Instantaneously, the chloride located on the palladated pincer moiety precipitated as AgCl and a non-coordinate Pd-BF₄ intermediate was formed. Subsequent ligation of the resultant non-coordinate intermediate by either nitrile or pyridine containing ligands 24, 26, 27, or 28 was

quantitative (as indicated by ^1H NMR spectroscopy) thereby providing polymers **29**, **30**, **31**, or **32** in one simple step (Scheme 3.7).

Scheme 3.7 Synthesis of side-chain functionalized polymers via metal coordination.



Reagents and Conditions: a) **24** or **28**, AgBF_4 , CH_2Cl_2 , 10 min, 100 %. b) **26** or **27**, AgBF_4 , CH_2Cl_2 , 10 min, 100 %.

3.6 Characterization of Self-Assembly

The self-assembly of pyridine-based mesogens can be easily characterized by ^1H NMR spectroscopy due to dramatic changes in the electronics of the free ligands (**26** and **27**) when compared to their coordinated counterparts (**31** and **32**), respectively. Specifically, a diagnostic downfield shift in the ^1H NMR spectrum of the α -pyridyl

protons from ca. 8.9 ppm to ca. 8.3 ppm provides direct evidence that self-assembly has taken place.^{41,42} On the other hand, characterization of the self-assembly of nitrile containing mesogens via ¹H NMR spectroscopy is somewhat hampered by the lack of protons in the vicinity of coordination. Furthermore, the complexity of ¹³C NMR spectra make it difficult to formulate conclusions regarding the nature of self-assembly despite the large number of observed spectral shifts. Thus, FT-IR becomes an essential tool in evaluating the self-assembly by way of the nitriles (CN stretch). Diagnostic shifts from ca. 2250 cm⁻¹ (before complexation) to ca. 2290 cm⁻¹ (after complexation) are well known, and can therefore be used to characterize the self-assembly process.⁴³

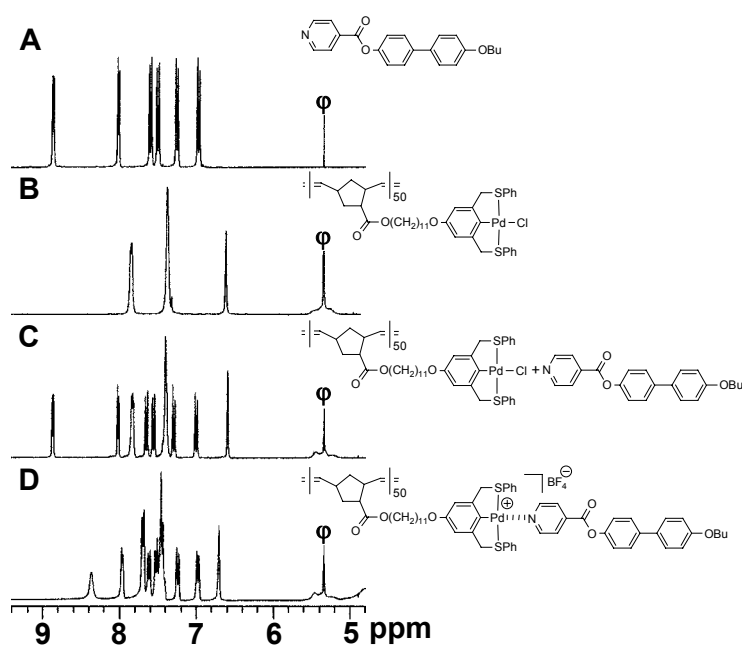
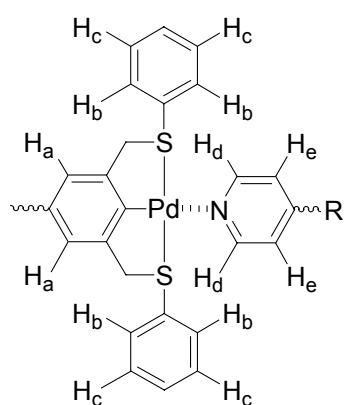


Figure 3.9 The aromatic and olefin region of the ¹H NMR spectra depicting the metal coordination of mesogen **27** onto **21** ($\phi = \text{CD}_2\text{Cl}_2$). A) Mesogen **27**, B) polymer **21**. C) a 1:1 mixture of **27** and **21**, and D) the 1:1 mixture after addition of 1 equiv. of AgBF_{4(aq)} (polymer **31**).

Figure 3.9 shows the ^1H NMR spectra of A) pure **27**, B) pure **21**, C) a 1:1 mixture of **27** and **21**, and D) the 1:1 mixture following addition of one equivalent of $\text{AgBF}_4(\text{aq})$ (polymer **31**). Comparison of Figure 3.9-C and Figure 3.9-D shows characteristic changes in the ^1H NMR spectra. In particular, the α -pyridine proton at 8.85 ppm and the β -pyridine proton at 8.00 ppm in Figure 3.9-C are shifted to 8.35 ppm and 7.95 ppm respectively. Furthermore, the complete disappearance of the non-coordinated pyridyl protons in Figure 3.9-D indicates that the self-assembly is quantitative. A downfield shift of the protons *meta* to the palladated pincer complex from 6.57 ppm to 6.69 ppm and an up-field shift of the *ortho*-thioether protons from 7.81 to 7.68 ppm provide further evidence that self-assembly had taken place. Polymer **32** was also characterized by ^1H NMR spectroscopy and showed similar spectral changes to those described for polymer **31**. These results are summarized in Table 3.1.

Table 3.1 Comparison of ^1H NMR chemical shifts of the 1:1 mixture (polymer **21** and mesogen **26** or **27**) and the pyridine functionalized polymers **31** and **32** respectively.



	Polymer 31		Polymer 32	
	1:1 mix (ppm)	Assembled (ppm)	1:1 mix (ppm)	Assembled (ppm)
H _a	6.57	6.69	6.57	6.67
H _b	7.81	7.68	7.81	7.66
H _c	7.39	7.44	7.38	7.39
H _d	8.85	8.35	8.69	8.05
H _e	8.00	7.95	7.58	7.56

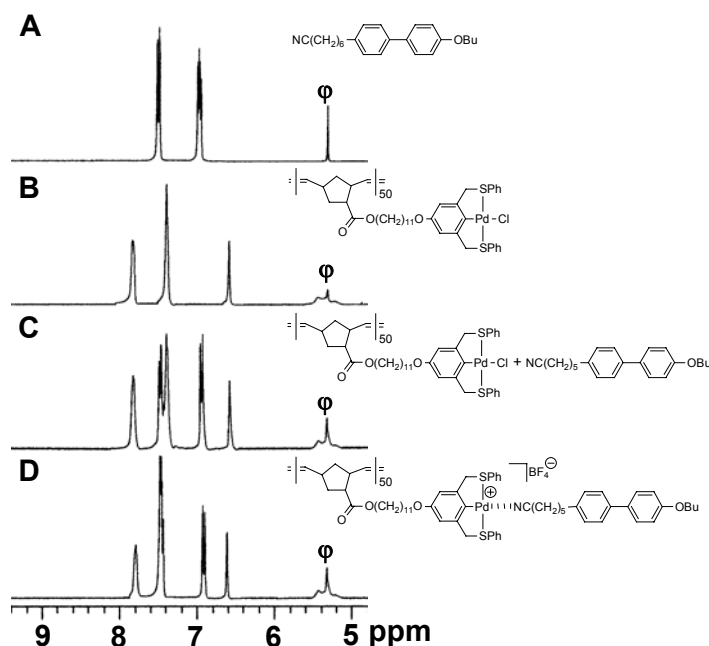
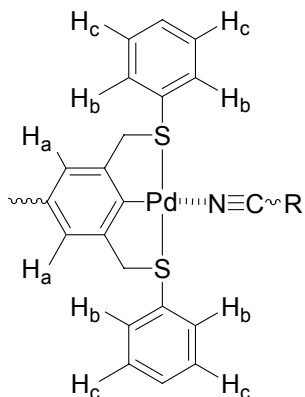


Figure 3.10 The aromatic and olefin region of the ^1H NMR spectra depicting the metal coordination of mesogen **14** onto **11** ($\phi = \text{CD}_2\text{Cl}_2$). A) Mesogen **14**, B) polymer **11**, C) a 1:1 mixture of **14** and **11**, and D) the 1:1 mixture after addition of 1 equiv. of $\text{AgBF}_4(\text{aq})$ (polymer **20**).

Unlike the pyridine-based mesogens, the nitrile moieties of **24** and **28** do not possess protons that allow for facile identification of the coordination step using ^1H NMR spectroscopy. Nonetheless, the self-assembly of nitrile based mesogens was also examined using ^1H NMR spectroscopy to explore whether minor shifts about the pincer complex could indicate whether coordination had taken place. Figure 3.10 shows the ^1H NMR spectra of A) pure **24**, B) pure **21**, C) a 1:1 mixture of **24** and **21**, and D) the 1:1 mixture following addition of 1 equivalent of $\text{AgBF}_4(\text{aq})$ (polymer **30**). Consistent with observations made for **31**, a downfield shift of the *meta* protons of the Pd center from 6.59 ppm to 6.60 ppm and an up-field shift of the *ortho*-thioether protons from 7.83 to

7.79 ppm provided preliminary evidence for the self-assembly. Similar spectral observations were made for polymer **29** and are summarized in Table 3.2.

Table 3.2 Comparison of ^1H NMR chemical shifts of the 1:1 mixture (polymer **21** and mesogens **24** or **28**) and the self-assembled nitrile-based polymers **29** and **30**.



	Polymer 29		Polymer 30	
	1:1 mix (ppm)	Assembled (ppm)	1:1 mix (ppm)	Assembled (ppm)
H _a	6.57	6.69	6.59	6.60
H _b	7.81	7.89	7.83	7.79
H _c	7.38	7.53	7.40	7.45

However, to unequivocally conclude that nitrile based mesogens had coordinated to the metal center, FT-IR studies comparing the frequency of the CN stretch before and after self-assembly were performed. Complete disappearance of the non-coordinated stretches at 2229 cm^{-1} (compound **24**) and 2244 cm^{-1} (compound **28**) followed by the appearance of new stretches at 2254 cm^{-1} (polymer **29**) and 2283 cm^{-1} (polymer **30**) confirmed that the coordination of nitrile containing mesogens had taken place quantitatively.

These results clearly show, that in all cases, self-assembly is fast and quantitative. Furthermore, there are no differences in the self-assembly behavior of small molecules with or without an alkyl spacer illustrating the potential versatility of the synthetic strategy.

Thermal analysis of the self-assembled polymers provides important information regarding the stability of these systems. Thermal gravimetric analysis showed that the onset of decomposition occurred in the range of 214-230 °C and 262-269 °C for the nitrile-based polymers (**29** and **30**), and pyridine-based polymers (**30** and **31**) respectively (Table 3.3). The thermal stability of the pyridines compared to the nitriles suggests that the coordination to the metal center is significantly stronger for the pyridines. Differential scanning calorimetry (DSC) shows glass transition endotherms at 59 °C, 42 °C, 80 °C and 72 °C for polymers **29**, **30**, **31**, and **32** respectively. For polymers **29**, **30**, and **31**, no other transitions were visible prior to decomposition. However, polymer **32** showed two first order transitions at 160.0 °C and 197.0 °C, which could indicate a possible liquid crystalline mesophase.⁴⁴⁻⁴⁶

Table 3.3 Thermal characterization data.

Polymer	Decomposition Onset (°C)	Glass Transition Temperature (°C)
29	231	59
30	215	42
31	268	80
32	263	72

3.7 Conclusion

In this chapter, non-covalent routes to side-chain self-assembled homopolymers that incorporate design elements and characterization techniques that enable the larger goal of realizing the UPB concept were described. Poly(norbornene)s bearing palladated SCS

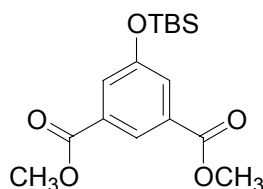
pincer complexes at every repeat unit have been synthesized via ROMP. Subsequent coordination of pyridine and nitrile anchored biphenyls to these well-defined polymeric scaffolds takes place instantaneously, quantitatively, and with full solubility. The self-assembly behavior of both pyridine-palladium and nitrile-palladium interactions was easily characterized using ^1H NMR and FT-IR spectroscopy. Thermal characterization of these polymers has shown that pyridine-based anchoring units are significantly more thermally stable when compared to the nitriles. These results demonstrate the ability of poly(norbornene)s bearing Pd^{II} pincer complexes to be utilized as metal-containing polymeric scaffolds and suggest their future use in developing the UPB concept.

3.8 Experimental

All reagents were purchased either from Acros Organic or Aldrich. All chemicals were reagent grade and used without further purification. Triethylamine and DMF were distilled from calcium hydride. THF and CH_2Cl_2 were dried via passage through copper oxide and alumina columns.⁴⁷ NMR spectra were taken on a 300 MHz Varian Mercury spectrometer. All spectra were referenced to residual proton solvent. Mass spectral analysis was kindly provided by the Georgia Tech Mass Spectrometry Facility using a VG-70se spectrometer. The IR spectra were obtained in an evacuated chamber using a Bruker IFS 66v/S spectrometer. DSC was performed under nitrogen using a Perkin-Elmer DSC 7 equipped with an Intracooler II cooling device. The temperature program provided heating and cooling cycles between 5 and 200 °C at 30 °C/min. TGA was performed using a Perkin-Elmer TGA 7 and all samples were heated from 25-800 °C. GPC analyses were carried out using a Waters 1525 binary pump coupled to a Waters 2414 refractive index detector. The GPC was calibrated using polystyrene standards on a

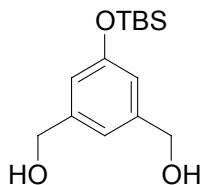
Styragel® HR 4 and HR 5E column set with methylene chloride as an eluant. Elemental analyses were performed by Atlantic Microlab, Norcross GA.

Synthesis of 5-(tert-butyl-dimethyl-silanyloxy)-isophthalic acid dimethyl ester (**13**)



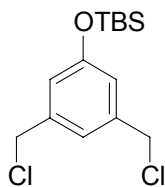
5-Hydroxyisophthalic acid dimethyl ester **12** (9.9 g, 0.047 mol), Et₃N (7.3g, 0.072 mol), and DMAP (cat. amount) were dissolved in CH₂Cl₂ (150 mL) and cooled to 0 °C. A solution of *tert*-butyldimethylsilyl chloride (12.4 g, 0.082 mol) in CH₂Cl₂ (50 mL) was slowly added to the stirred mixture and the temperature was allowed to rise to 25 °C. After stirring for 16 h, the mixture was washed with 1N HCl (100 mL), a saturated solution of NaHCO₃ (100 mL), and brine (100 mL). The combined organic layers were dried (MgSO₄) and the solvent was removed *in vacuo* to provide **13** (15.2 g, 99%) as a white solid. ¹H NMR (CDCl₃): δ = 8.28 (s, 1H, ArH), 7.67 (s, 2H, ArH), 3.93 (s, 6H, OCH₃), 1.00 (s, 9H, *t*-Bu), 0.23 (s, 6H, SiCH₃). ¹³C NMR (CDCl₃): δ = 166.3, 156.1, 132.0, 125.6, 123.9, 52.6, 25.8, 18.4, -4.2. MS (EI): *m/z* = 324.2 (M⁺, calcd 324.1). Anal. Calcd. for C₁₆H₂₄O₅Si: C, 59.23; H, 7.46; Found: C, 59.10; H, 7.31

Synthesis of 5-bis(hydroxymethyl)phenol *tert*-butyldimethylsilyl ether (**14**)



Diester **13** (15.0 g, 0.046 mol) was dissolved in anhydrous THF (100 mL) and slowly added to a stirred suspension of LiAlH_4 (100 mL of a 1M solution in THF, 0.10 mol) at 0 °C. After stirring for 14 h at 25 °C the THF was removed. The resulting white paste was redissolved in CH_2Cl_2 (200 mL), cooled to 0 °C, and 2N HCl was added until the milky solution turned clear. Extraction of the aqueous layer with CH_2Cl_2 (3 x 100 mL), drying of the combined organic layers (MgSO_4), and removal of the solvent provided pure **14** (9.1 g, 73%) as a white solid. ^1H NMR (CDCl_3): δ = 6.94 (s, 1H, ArH), 6.77 (s, 2H, ArH), 4.63 (s, 4H, CH_2O), 0.98 (s, 9H, *t*-Bu), 0.20 (s, 6H, SiCH_3). ^{13}C NMR (CDCl_3): δ = 156.1, 143.0, 118.5, 117.8, 64.9, 25.9, 18.4, -4.2. MS (EI): m/z = 268.1 (M^+ , calcd 268.1). Anal. Calcd. for $\text{C}_{14}\text{H}_{24}\text{O}_3\text{Si}$: C, 62.64; H, 9.01; Found: C, 62.48; H, 9.09

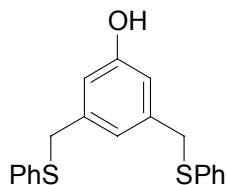
Synthesis of 3,5-bis(chloromethyl)phenol *tert*-butyl-dimethylsilylether (**15**)



Diol **14** (8.9 g, 0.033 mol) and Et_3N (9.1 g, 0.090 mol) were dissolved in anhydrous CHCl_3 (170 mL) and cooled to 0 °C. To the stirred solution, methanesulfonyl chloride (10.4 g, 0.09 mol) was added drop wise over the course of 1h. The reaction mixture was

then slowly heated to 38 °C for 12 h. Subsequent washing with 1M NaOH (80 mL), 1N HCl (80 mL), drying (MgSO₄), and evaporation of the solvent afforded the crude product. Further purification via column chromatography (SiO₂, eluant: hexane/EtOAc 70:30) gave **15** (6.8 g, 68%) as a colorless oil. ¹H NMR (CDCl₃): δ = 7.00 (s, 1H, ArH), 6.82 (s, 2H, ArH), 4.52 (s, 4H, CH₂Cl), 0.99 (s, 9H, *t*-Bu), 0.21 (s, 6H, SiCH₃). ¹³C NMR (CDCl₃): δ = 156.4, 139.5, 121.7, 120.4, 45.9, 64.9, 25.9, 18.4, -4.2. MS (EI): *m/z* = 304.082 (M⁺, calcd. 304.081). Anal. Calcd. for C₁₄H₂₂Cl₂OSi: C, 55.07; H, 7.26; Found: C, 55.13; H, 7.31

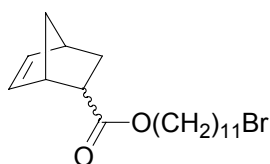
Synthesis of 3,5-bis(phenylthiomethyl)phenol (**16**)



Sodium thiophenolate salt (12.5 g, 0.095 mol) was dissolved in dry THF (100 mL) and dichloride **15** (6.9 g, 0.024 mol) was slowly added to the reaction mixture at room temperature. The reaction was then stirred for 12 h at 50 °C, the THF was removed, and the crude mixture was redissolved in CH₂Cl₂ (100 mL). The organic phase was washed with brine (50 mL), 2N NaOH (50 mL), H₂O (50 mL), dried (MgSO₄), and concentrated under reduced pressure to afford a yellow oil. The TBS group was then cleaved by dissolving the thioether in THF (100 mL) and adding an excess of tetrabutylammonium fluoride trihydrate (13.6 g, 0.043 mol). After stirring overnight at 38 °C, the THF was removed by evaporation and the crude oil was dissolved in CH₂Cl₂ (100 mL), washed with brine (50 mL), H₂O (50 mL), and dried with MgSO₄. The solvent was removed,

revealing a highly viscous oil. Further purification by column chromatography (SiO₂, eluant: CH₂Cl₂) gave the pincer ligand **16** (5.7 g, 72%) as a colorless oil. ¹H NMR (CDCl₃): δ = 7.30-7.15 (m, 10H, SPH), 6.81 (s, 1H, ArH), 6.65 (s, 2H, ArH), 4.88 (bs, 1H, OH), 4.01 (s, 4H, CH₂S). ¹³C NMR (CDCl₃): δ = 155.4, 139.2, 135.9, 129.5, 128.8, 126.3, 121.8, 121.7, 114.6, 114.5, 38.5. MS (EI): *m/z* (%) = 338.077 (M⁺, calcd. 338.080). Anal. Calcd. for C₂₀H₁₈OS₂: C, 70.97; H, 5.36; Found: C, 71.07; H, 5.45

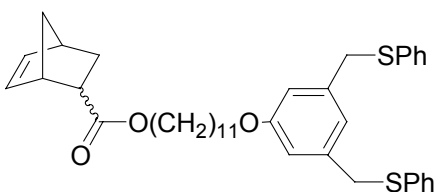
Synthesis of bicyclo[2.2.1]hept-5-ene-2-carboxylic acid 11-bromo-undecyl ester (**18**)



Norbornene acid chloride **17** (2.3 g, 0.015 mol) was added drop-wise to a stirred solution of 11-bromo-1-undecanol (3.1 g, 0.012 mol) and Et₃N (1.9 g, 0.018 mol) in THF (25 mL). Upon complete addition, the reaction was heated to reflux for a period of 16 h. The salts generated during the course of the reaction were filtered, and the THF was evaporated. The crude product was redissolved in CH₂Cl₂ (100 mL), washed with brine (50 mL), H₂O (50 mL), dried (MgSO₄), and the solvent was removed *in vacuo*. Further purification by column chromatography (SiO₂, eluant: CH₂Cl₂) provided pure bromo ester **18** (4.1 g, 91%, 80:20 *endo/exo*) as a colorless oil. ¹H NMR (CDCl₃): δ = 6.18 (d of d, 1H, *J* = 3.3 Hz, *endo*), 6.12 (m, 2H, *exo*), 5.92 (d of d, 1H, *J* = 3.3 Hz, *endo*), 4.09-3.95 (m, 4H, *endo* + *exo*), 3.53 (t, 2H, *J* = 7.1 Hz, *endo*), 3.40 (t, 2H, *J* = 7.1 Hz, *exo*), 3.22-3.18 (m, 1H, *endo*), 3.05-3.01 (m, 1H, *exo*), 2.97-2.87 (m, 4H, *endo* + *exo*), 2.24-2.19 (m, 1H, *exo*), 1.95-1.84 (m, 2H, *endo* + *exo*), 1.80-1.71 (m, 4H, *endo* + *exo*), 1.65-1.56 (m, 4H,

endo + exo), 1.45-1.38 (m, 5H, *endo + exo*), 1.34-1.25 (m, 28H, *endo + exo*). ¹³C NMR (CDCl₃): δ = 176.5, 175.0, 138.2, 138.0, 136.0, 132.6, 64.8, 64.5, 49.8, 46.6, 46.0, 45.9, 45.4, 43.6, 43.4, 42.8, 42.7, 41.9, 41.8, 33.0, 32.9, 30.5, 29.6, 29.4, 29.1, 29.0, 28.9, 28.4, 27.1, 26.1. MS (EI): *m/z* (%) = 371.157 (M⁺, calcd. 371.159)

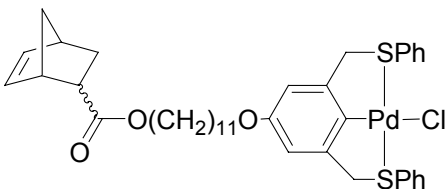
Synthesis of bicyclo[2.2.1]hept-5-ene-2-carboxylic acid 11-(3,5-bis(phenylthiomethyl)phenoxy)-undecyl ester (19)



11-bromo-undecyl ester **18** (1.6 g, 0.0042 mol) was slowly added to a stirred suspension of **16** (1.4 g, 0.0042 mol) with K₂CO₃ (1.2 g, 0.0084 mol) in dry DMF (40 mL) at 25 °C. Once heated to 90 °C, the reaction was stirred overnight, at which point the DMF was distilled under reduced pressure. The crude product was then redissolved in CH₂Cl₂ (150 mL), washed with 1N HCl (50 mL), a saturated solution of NaHCO₃ (50 mL), and brine (50 mL). The organic layer was dried (MgSO₄), the solvent evaporated, and the crude product was further purified by column chromatography (A. SiO₂, eluant: CH₂Cl₂, B. SiO₂, eluant: 70:30 hexanes/ CH₂Cl₂) to afford pure **19** (1.6 g, 59%) as a colorless oil. ¹H NMR (CDCl₃): δ = 7.30-7.15 (m, 20H, SPh, *endo + exo*), 6.81 (s, 2H, ArH, *endo + exo*), 6.69 (s, 4H, ArH, *endo + exo*), 6.19 (d of d, 1H, *J*=3.3 Hz, *endo*), 6.12 (m, 2H, *exo*), 5.92 (d of d, 1H, *J*=3.3 Hz, *endo*), 4.094-3.96 (12 H, *endo + exo*), 3.84 (t, 2H, *J*=6.6 Hz, OCH₂, *endo*), 3.53 (t, 2H, *J*=7.1 Hz, OCH₂, *endo*), 3.22-3.17 (m, 1H, *endo*), 3.05-3.01 (m, 1H, *exo*), 2.97-2.90 (m, 4H, *endo + exo*), 2.24-2.18 (m, 1H, *exo*), 1.95-1.84 (m, 2H,

endo + exo), 1.80-1.71 (m, 4H, *endo + exo*), 1.65-1.56 (m, 4H, *endo + exo*), 1.45-1.38 (m, 5H, *endo + exo*), 1.37-1.25 (m, 28H, *endo + exo*). ^{13}C NMR (CDCl_3): $\delta = 176.1, 174.7, 159.2, 138.9, 137.9, 137.6, 136.2, 135.6, 132.2, 129.7, 128.7, 126.2, 121.4, 121.3, 113.7, 113.6, 67.8, 64.4, 64.2, 49.5, 46.5, 46.4, 45.6, 45.0, 43.3, 43.1, 42.5, 42.4, 41.6, 41.5, 38.8, 32.7, 32.5, 30.2, 29.4, 29.3, 29.1, 28.8, 28.6, 26.8, 25.9, 25.8$. MS (EI): m/z (%) = 628.0 (M^+ , calcd. 628.3). Anal. Calcd. for $\text{C}_{39}\text{H}_{48}\text{O}_3\text{S}_2$: C, 74.48; H, 7.69; Found: C, 74.20; H, 7.74.

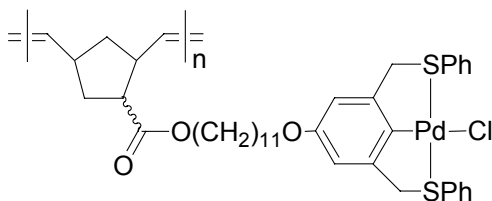
Synthesis of Pd-Cl bicyclo[2.2.1]hept-5-ene-2-carboxylic acid 11-(3,5-bis(phenylthiomethyl)phenoxy)-undecyl ester (20)



Ligand **19** (100 mg, 0.159 mmol) was dissolved in CH_2Cl_2 (6 mL) and placed under an Argon atmosphere. $\text{Pd} [\text{CH}_3\text{CN}]_4(\text{BF}_4)_2$ (69.3 mg, 0.16 mmol) in dry CH_3CN (2 mL) was added in one portion at 25 °C. The orange solution was stirred for 15 min at which time the color changed to pale yellow. The 3:1 $\text{CH}_3\text{CN}/\text{CH}_2\text{Cl}_2$ mixture was immediately poured into a saturated solution of NaCl (25 mL) and was stirred vigorously for 1 h. The Pd-Cl complex was then extracted from the brine with CH_2Cl_2 (3 x 25 mL). The organic layer was washed with water (50 mL), dried (MgSO_4), and the solvent was removed under reduced pressure. Purification by column chromatography (SiO_2 , eluant: $\text{CH}_2\text{Cl}_2/\text{MeOH}$ 99:1) provided Pd-Cl complex **20** (94.2 mg, 77%) as an amorphous yellow solid. ^1H NMR (CDCl_3): $\delta = 7.80\text{-}7.77$ (m, 8H, SPh, *endo + exo*), 7.34-7.29 (m,

12H, SPh, *endo + exo*), 6.55 (s, 4H, ArH, *endo + exo*), 6.15 (d of d, 1H, $J=2.7$ Hz, *endo*), 6.09 (m, 2H, *exo*), 5.88 (d of d, 1H, $J=2.7$ Hz, *endo*), 4.51 (bs, 8H, CH₂S, *endo + exo*), 3.83 (t, 2H, $J=6.6$ Hz, *endo*), 3.20-3.14 (m, 1H, *endo*), 3.02-2.98 (m, 1H, *exo*), 2.94-2.84 (m, 4H, *endo + exo*), 2.22-2.16 (m, 1H, *exo*), 1.93-1.82 (m, 2H, *endo + exo*), 1.75-1.65 (m, 4H, *endo + exo*), 1.63-1.51 (m, 4H, *endo + exo*), 1.42-1.33 (m, 5H, *endo + exo*), 1.32-1.23 (m, 28H, *endo + exo*). ¹³C NMR (CDCl₃): δ = 176.1, 174.6, 156.8, 151.2, 149.9, 137.8, 137.5, 135.5, 132.2, 131.1, 129.5, 129.4, 108.7, 108.6, 67.9, 64.3, 64.1, 51.4, 49.4, 46.1, 45.5, 45.4, 43.1, 43.0, 42.3, 42.2, 30.1, 29.3, 29.1, 29.0, 28.9, 28.4, 25.8, 25.7. MS (FAB): m/z (%) = 732.9 (M⁺-Cl, calcd. 733.20). Anal. Calcd. for C₃₉H₄₇ClO₃PdS₂: C, 60.85; H, 6.15; Found: C, 61.05; H, 6.38

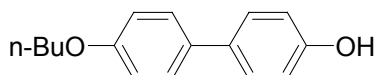
Synthesis of poly (Pd-Cl Bicyclo[2.2.1]hept-5-ene-2-carboxylic acid 11-(3,5-bis(phenylthiamethyl)phenoxy)-undecyl ester) (21)



Pd-Cl SCS monomer **20** (175 mg, 0.227 mmol) was weighed into a 20 mL vial, dissolved in CDCl₃ (1 mL), and stirred under an Argon atmosphere. Catalyst **9** (3.74 mg, 0.005 mmol) was dissolved in CDCl₃ (0.5 mL), and added to the stirred solution of monomer. Upon addition of the catalyst, the solution changed color from deep yellow to light brown indicating that initiation had occurred. The reaction mixture was then heated to 45°C for 12 h. Upon complete conversion, the polymerization was terminated by adding 2 drops of ethyl vinyl ether into the reaction vessel. The product was obtained by precipitation from

cold hexanes, filtration through Celite[®], followed by extraction with CH₂Cl₂ to provide pure polymer **21** (167 mg, 95%, 100% by ¹H NMR) as a slightly green solid. ¹H NMR (CDCl₃): δ = 7.78 (m, 4H, SPh), 7.32 (m, 6H, SPh), 6.55 (s, 2H, ArH), 5.50-5.17 (bm, 2H, CH=C), 4.58 (bs, 4H, CH₂S), 4.00-3.85 (m, 2H, OCH₂), 3.84-3.80 (m, 2H, OCH₂), 3.24-2.30 (bm, 3H), 2.03-1.50 (bm, 8H), 1.98-1.07 (m, 14H). ¹³C NMR (CDCl₃): δ = 174.4, 156.8, 151.3, 149.9, 132.3, 131.2, 129.6, 129.5, 108.7, 108.6, 67.9, 64.2, 51.5, 48.0, 45.4, 40.4, 37.3, 36.0, 29.3, 29.2, 28.9, 28.6, 26.0, 25.8.

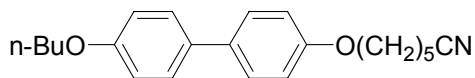
Synthesis of 4'-butoxy-biphenyl-4-ol (**23**)



A solution of 1-bromo-butane (12.3 g, 0.089 mol) in DMF (200 mL) was added dropwise to a hot solution (100 °C) of 4,4'-biphenol (16.7 g, 0.089 mol) and K₂CO₃ (12.4 g, 0.089 mol) in DMF (90 mL) over the course of 1 h. The mixture was then heated to reflux for an additional 5 h, cooled to room temperature and the crude product was isolated by precipitation into cold water (500 mL). The white precipitate was crystallized from ethanol. Further purification by column chromatography (SiO₂, eluant: CH₂Cl₂) provided pure **23** (10.0 g, 46%) as a flaky white solid. ¹H NMR (DMSO-*d*₆): δ = 9.47 (s, 1H, OH), 7.45 (d, 2H, *J*=8.2 Hz, ArH), 7.41 (d, 2H, *J*=8.8 Hz, ArH), 6.92 (d, 2H, *J*=8.8 Hz, ArH), 6.84 (d, 2H, *J*=8.8 Hz, ArH), 3.93 (t, 2H, *J*=6.6 Hz, CH₂O), 1.68 (m, 2H, CH₂), 1.42 (m, 2H, CH₂), 0.92 (t, 3H, *J*=7.6 Hz CH₃). ¹³C NMR (DMSO-*d*₆): δ = 157.5, 156.5, 132.6, 130.7, 127.1, 126.9, 115.6, 114.7, 67.1, 30.8, 18.8, 13.7. MS (EI): *m/z* (%) = 242.130

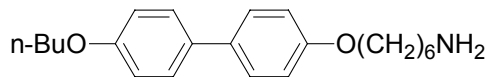
(M⁺, calcd. 242.131). Anal. Calcd. for C₁₆H₁₈O₂: C, 79.31; H, 7.49; Found: C, 79.26; H, 7.37

Synthesis of 6-(4'-butoxy-biphenyl-4-yloxy)-hexanenitrile (**24**)



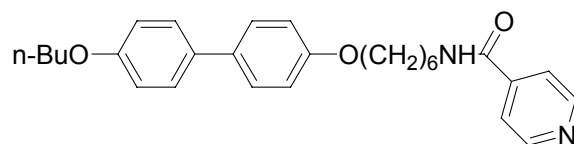
4'-Butoxy-biphenyl-4-ol **23** (1.0 g, 4.13 mmol) was dissolved in DMF (10 mL) and K₂CO₃ (0.86 g, 6.2 mmol) was added in one portion. The mixture was heated to 90 °C and 6-bromo-1-hexanenitrile (0.726 g, 4.13 mmol) was slowly added via syringe. Upon complete addition, the reaction temperature was raised to 110 °C and stirred for an additional 16 h. The reaction vessel was then allowed to cool to r.t. and the reaction mixture was precipitated into cold water (150 mL). The crude product was filtered, dried *in vacuo*, and further purified by column chromatography (SiO₂, eluant: CH₂Cl₂) to afford pure **24** (1.03g, 74%) as a crystalline white powder. ¹H NMR (CDCl₃): δ = 7.50-7.47 (m, 4H, ArH), 6.98-6.93 (m, 4H, ArH), 4.00 (t, 4H, *J*=6.3 Hz, CH₂O), 2.38 (t, 2H, *J*=6.9 Hz, CH₂CN), 1.87-1.63 (m, 8H, CH₂), 1.56-1.49 (m, 2H, CH₂), 1.01 (t, 3H, *J*=7.6 Hz, CH₃). ¹³C NMR (CDCl₃): δ = 158.1, 157.8, 133.4, 133.0, 127.5, 119.5, 114.6, 114.5, 67.6, 67.3, 31.2, 28.4, 25.3, 25.1, 19.2, 17.0, 13.8. MS (EI): *m/z* (%) = 337.204 (M⁺, calcd. 337.200). Anal. Calcd. for C₂₂H₂₇NO₂: C, 78.30; H, 8.06; N, 4.15; Found: C, 78.13; H, 8.04; N, 4.05.

Synthesis of 6-(4'-butoxy-biphenyl-4-yloxy)-hexylamine (**25**)



A solution of 6-(4'-butoxy-biphenyl-4-yloxy)-hexanenitrile **24** (3.0 g, 0.0090 mol) in THF (50 mL) was added drop wise at 0 °C to a suspension of lithium aluminum hydride (0.95 g, 0.025 mol) in dry THF (50 mL). Upon complete addition, the reaction was heated to reflux for 12 h. The mixture was then cooled to 0 °C and quenched by addition of 0.5 M KOH (100 mL). The resultant aluminum hydroxide salts were filtered and washed with hot CHCl₃ (2 x 100 mL). The aqueous layer was extracted with CHCl₃ (3 x 50 mL), the combined organic layers were dried (MgSO₄), and the solvent was removed under reduced pressure. Further drying on high vacuum yielded pure **25** (2.5g, 83%) as a waxy white solid. ¹H NMR (CDCl₃): δ = 7.48-7.45 (m, 4H, ArH), 6.96-6.93 (m, 4H, ArH), 4.00-3.97 (m, 4H, CH₂O), 2.71 (m, 2H, CH₂N), 1.81-1.77 (m, 4H, CH₂), 1.55-1.41 (m, 10H, CH₂, NH₂), 0.99 (t, 3H, *J*=7.1 Hz, CH₃). ¹³C NMR (CDCl₃): δ = 158.1, 158.0, 133.3, 133.2, 127.5, 114.7, 114.6, 67.8, 67.6, 42.1, 33.7, 31.3, 29.2, 26.6, 25.9, 19.2, 13.8. MS (EI): *m/z* (%) = 341.234 (M⁺, calcd. 341.236)

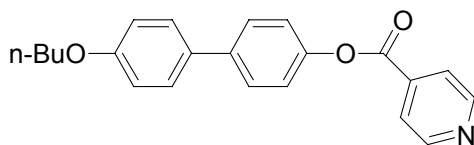
Synthesis of isonicotinic acid-6-(4'-butoxy-biphenyl-4ylaminon)-hexyl ester (**26**)



Isonicotinoyl chloride hydrochloride (324 mg, 1.82 mmol) was added to a solution of **25** (295 mg, 0.864 mmol) and Et₃N (368 mg, 3.64 mmol) in dry CH₂Cl₂ (50 mL). The

mixture was stirred for 24 h at ambient temperature and subsequently was washed with 2 N NaOH (50 mL), brine (50 mL) and dried over Na₂SO₄. The solvent was filtered, evaporated, and the final product was purified by column chromatography (neutral alumina, eluent: CH₂Cl₂/MeOH 99:1) to provide **26** (325 mg, 84%) as a white solid upon drying. ¹H NMR (CDCl₃): δ = 8.70 (d, 2H, *J*=5.5 Hz, Pyr_αH), 7.60 (d, 2H, *J*=5.5 Hz, Pyr_βH), 7.47-7.44 (m, 4H, ArH), 6.95-6.91 (m, 4H, ArH), 6.53 (bs, 1H, NH), 4.00-3.96 (m, 4H, CH₂O), 3.45 (m, 2H, CH₂N), 1.85-1.73 (m, 4H, CH₂), 1.70-1.60 (m, 2H, CH₂), 1.56-1.41 (m, 6H, CH₂), 0.98 (t, 3H, *J*=7.1 Hz, CH₃). ¹³C NMR (CDCl₃): δ = 165.5, 158.2, 158.0, 150.3, 141.8, 133.3, 127.5, 120.8, 114.6, 67.7, 40.1, 31.3, 29.4, 29.1, 26.6, 25.7, 19.2, 13.8. MS (EI): *m/z* (%) = 446.257 (M⁺, calcd. 446.257). Anal. Calcd. for C₂₈H₃₄N₂O₂: C, 75.31; H, 7.67; N, 6.27; Found: C, 75.38; H, 7.71; N, 6.31

Synthesis of isonicotinic acid 4'-butoxy-biphenyl-4-yl ester (**17**)



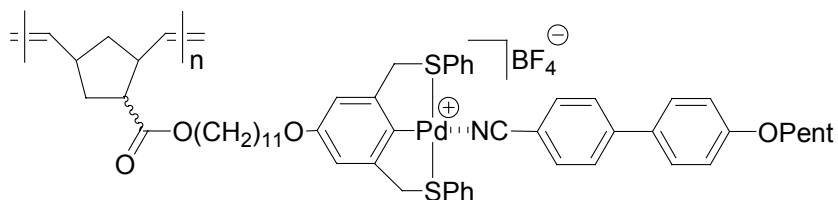
To a stirred solution of **23** (524 mg, 2.16 mmol) and Et₃N (460 mg, 4.54 mmol) in CH₂Cl₂ (50 mL) was added isonicotinoyl chloride hydrochloride (385 mg, 2.16 mmol) in one portion. The mixture was then allowed to stir at r.t. for 24 h. Following dilution with CH₂Cl₂ (50 mL), work up proceeded by washing with 1 N HCl (100 mL), 2N NaOH (100 mL), and brine (100 mL). Drying with Na₂SO₄ followed by recrystallization from ethanol provided pure **27** (647 mg, 86%) as a white crystalline solid. ¹H NMR (CDCl₃): δ = 8.84 (d, 2H, *J*=5.5 Hz, Pyr_αH), 8.02 (d, 2H, *J*=5.5 Hz, Pyr_βH), 7.61 (d, 2H, *J*=8.2 Hz, ArH),

7.51(d, 2H, $J=8.2$ Hz, ArH), 7.27 (d, 2H, $J=8.2$ Hz, ArH), 6.98 (d, 2H, $J=8.2$ Hz, ArH), 4.01 (t, 2H, $J=6.6$ Hz, CH₂O), 1.85-1.75 (m, 2H, CH₂), 1.58-1.46 (m, 2H, CH₂), 1.00 (t, 3H, $J=7.6$ Hz, CH₃). ¹³C NMR (CDCl₃): δ = 163.8, 158.9, 150.8, 149.3, 139.2, 136.7, 132.4, 128.1, 127.8, 123.2, 121.5, 114.8, 67.7, 31.3, 19.2, 13.8. MS (EI): m/z (%) = 347.156 (M⁺, calcd. 347.152). Anal. Calcd. for C₂₂H₂₁NO₃: C, 76.06; H, 6.09; N, 4.03; Found: C, 75.92; H, 6.07; N, 3.93

General procedure for polymer functionalization (29-32)

One equivalent of the desired mesogen **24**, **26**, **27** or commercially available 4'-(pentyloxy)-4-biphenylcarbonitrile (**28**) (0.100 mmol) was added to a solution of polymer **21** (0.100 mmol) in CH₂Cl₂ (10 mL) and stirred at room temperature. One equivalent of AgBF_{4(aq)} (19.49 μ L of a 5.13 M stock solution, 0.100 mmol) was added to the 1:1 mixture at which point AgCl precipitated from solution. The mixture was stirred for an additional 10 min, filtered over Celite, and the solvent was removed *in vacuo* to provide self-assembled polymers **29-32** in quantitative yield.

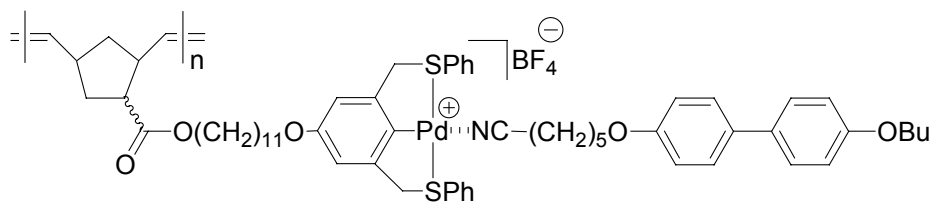
Polymer (29)



¹H NMR (CD₂Cl₂): δ = 7.89 (m, 4H, SPh), 7.64 (d, 4H, $J=8.2$ Hz, ArH), 7.54 (d, 2H, $J=8.8$ Hz, ArH), 7.53 (m, 6H, SPh), 6.98 (d, 2H, $J=8.8$ Hz, ArH), 6.69 (s, 2H, ArH), 5.50-5.20 (bm, 2H, CH=C), 4.71 (bs, 4H, CH₂S), 3.99 (t, 2H, $J=6.6$ Hz, OCH₂), 3.98-

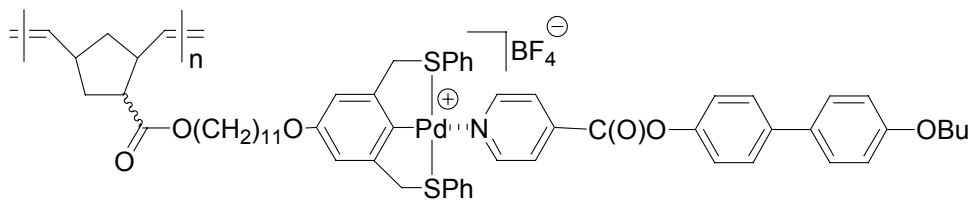
3.85 (m, 4H, OCH₂), 3.24-2.30 (bm, 3H), 2.03-1.00 (m, 28H), 0.93 (t, 3H, *J*=6.6 Hz, 7.1 Hz, CH₃). ¹³C NMR (CD₂Cl₂): δ = 175.1, 160.8, 158.6, 150.9, 133.6, 132.6, 132.8, 131.8, 131.3, 130.9, 128.9, 127.6, 115.6, 110.4, 110.3, 68.9, 68.7, 64.7, 51.8, 48.6, 46.1, 43.0, 36.5, 36.1, 30.2, 30.0, 29.8, 29.4, 29.3, 28.6, 26.6, 23.0, 14.4.

Polymer (30)



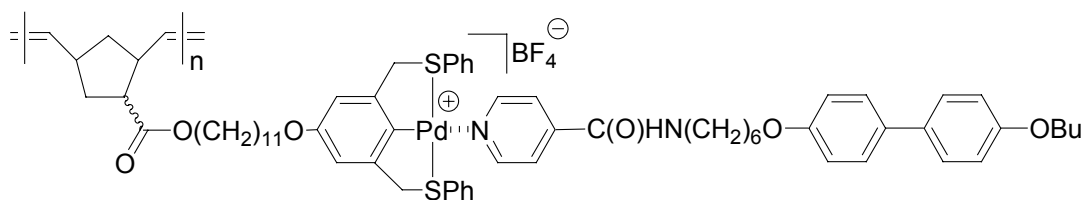
¹H NMR (CD₂Cl₂): δ = 7.79 (m, 4H, SPh), 7.48-7.43 (m, 10H, SPh + ArH), 6.92 (d, 4H, *J*=7.1 Hz, ArH), 6.60 (s, 2H, ArH), 5.50-5.15 (bm, 2H, CH=C), 4.57 (bs, 4H, CH₂S), 3.97 (t, 2H, *J*=6.6 Hz, OCH₂), 3.96-3.83 (m, 4H, OCH₂), 3.24-2.30 (bm, 3H), 2.37 (t, 2H, *J*=7.1 Hz, CH₂CN), 2.03-1.12 (m, 32H), 0.97 (t, 3H, *J*=7.1 Hz, CH₃). ¹³C NMR (CD₂Cl₂): δ = 174.7, 160.3, 158.9, 158.5, 151.1, 133.8, 133.3, 131.7, 131.2, 130.8, 130.6, 127.9, 115.2, 110.3, 110.2, 68.3, 67.7, 65.0, 51.5, 48.6, 46.1, 43.0, 36.5, 36.1, 31.9, 30.1, 29.9, 29.7, 29.2, 28.7, 26.5, 25.6, 24.7, 19.8, 18.0, 14.2.

Polymer (31)



^1H NMR (CD_2Cl_2): $\delta = 8.35$ (s, 2H, $\text{Pyr}_\alpha\text{H}$), 7.95 (d, 2H, $J=5.5$ Hz, Pyr_βH), 7.68 (d, 4H, $J=7.1$, SPh), 7.60 (d, 2H, $J=7.7$ Hz, ArH), 7.51 (d, 2H, $J=8.2$ Hz, ArH), 7.44-7.40 (m, 6H, SPh), 7.23 (d, 2H, $J=7.7$ Hz, ArH), 6.96 (d, 2H, $J=8.2$ Hz, ArH), 6.69 (s, 2H, ArH), 5.50-5.13 (bm, 2H, CH=C), 4.78 (bs, 4H, CH_2S), 3.99 (t, 2H, $J=6.6$ Hz, OCH_2), 3.95-3.88 (m, 4H, OCH_2), 3.24-2.30 (bm, 3H), 2.03-1.10 (m, 26H), 0.98 (t, 3H, $J=7.1$ Hz, CH_3). ^{13}C NMR (CD_2Cl_2): $\delta = 175.0$, 162.7, 159.6, 158.5, 152.1, 151.6, 149.6, 147.2, 139.9, 132.6, 131.7, 131.0, 130.9, 128.6, 128.2, 126.1, 121.9, 115.4, 110.2, 110.1, 68.8, 68.4, 64.7, 52.0, 48.6, 46.1, 43.0, 36.5, 36.1, 31.8, 30.2, 29.8, 29.3, 26.6, 19.8, 14.2.

Polymer (32)



^1H NMR (CD_2Cl_2): $\delta = 8.05$ (s, 2H, $\text{Pyr}_\alpha\text{H}$), 7.66 (m, 4H, SPh), 7.56 (d, 2H, $J=6.6$ Hz, Pyr_βH), 7.43 (d, 4H, $J=7.1$ Hz, ArH), 7.39 (m, 6H, SPh), 6.90 (d, 4H, $J=8.8$ Hz, ArH), 6.67 (s, 2H, ArH), 5.50-5.13 (bm, 2H, CH=C), 4.68 (bs, 4H, CH_2S), 3.96-3.86 (m, 4H, OCH_2), 3.33 (m, 2H, CH_2NH), 3.24-2.30 (bm, 3H), 2.03-1.10 (m, 34H), 0.96 (t, 3H, $J=7.1$ Hz, CH_3). ^{13}C NMR (CD_2Cl_2): $\delta = 174.8$, 160.4, 158.8, 158.4, 151.7, 151.2, 137.7, 133.5, 131.8, 131.6, 130.9, 130.7, 127.9, 124.4, 120.1, 115.2, 110.1, 110.0, 68.8, 68.5, 68.3, 64.9, 51.7, 48.6, 46.1, 43.0, 36.5, 36.1, 31.9, 30.2, 30.0, 29.8, 29.7, 29.5, 29.2, 27.1, 26.6, 26.2, 19.8, 14.2.

3.9 References

- (1) The contents of this chapter have been published. See: Pollino, J. M.; Weck, M. *Synthesis* **2002**, 1277.
- (2) Aakeröy, C. B.; Beatty, A. M.; Lorimer, K. R. *J. Chem. Soc., Dalton Trans.* **2000**, 3869.
- (3) Archer, R. D. *Coord. Chem. Rev.* **1993**, 128, 49.
- (4) Holliday, B. J.; Mirkin, C. A. *Angew. Chem. Int. Ed.* **2001**, 40, 2022.
- (5) Swigers, G. F.; Malefetse, T. J. *Chem. Rev.* **2000**, 100, 3483.
- (6) Zaworotko, M. J. *Angew. Chem. Int. Ed.* **1998**, 37, 1211.
- (7) Albrecht, M.; van Koten, G. *Angew. Chem. Int. Ed.* **2001**, 40, 3750.
- (8) Van Koten, G. *Pure Appl. Chem.* **1989**, 61, 1681.
- (9) Moulton, C. J.; Shaw, B. L. *J. Chem. Soc. Dalton Trans.* **1976**, 1020.
- (10) Errington, J.; McDonald, W. S.; Shaw, B. L. *J. Chem. Soc. Dalton Trans.* **1980**, 2312.
- (11) Gorla, F.; Venanzi, L. M.; Albinati, A. *Organometallics* **1994**, 13, 1607.
- (12) Huck, W. T. S.; van Veggel, F. C. J. M.; Kropman, B. L.; Blank, D. H. A.; Keim, E. G.; Smithers, M. M. A.; Reinhoudt, D. N. *J. Am. Chem. Soc.* **1995**, 117, 8293.
- (13) Huck, W. T. S.; van Veggel, F. C. J. M.; Reinhoudt, D. N. *Angew. Chem. Int. Ed. Engl.* **1996**, 35, 1213.
- (14) Huck, W. T. S.; Hulst, R.; Timmerman, P.; van Veggel, F. C. J. M.; Reinhoudt, D. N. *Angew. Chem. Int. Ed. Engl.* **1997**, 36, 1006.
- (15) Huck, W. T. S.; Snellink-Ruel, B.; van Veggel, F. C. J. M.; Reinhoudt, D. N. *Organometallics* **1997**, 16, 4287.
- (16) Huck, W. T. S.; van Veggel, F. C. J. M.; Reinhoudt, D. N. *J. Mater. Chem.* **1997**, 7, 1213.
- (17) Huck, W. T. S.; Prins, L., J.; Fokkens, R. H.; Nibbering, N. M. M.; van Veggel, F. C. J. M.; Reinhoudt, D. N. *J. Am. Chem. Soc.* **1998**, 120, 6240.

- (18) Albrecht, M.; Gossage, R. A.; Lutz, M.; Spek, A. L.; van Koten, G. *Chem. Eur. J.* **2000**, *6*, 1431.
- (19) van Manen, H.-J.; Nakashima, K.; Shinkai, S.; Kooijman, H.; Spek, A. L.; van Veggel, F. C. J. M.; Reinhoudt, D. N. *Eur. J. Inorg. Chem.* **2000**, 2533.
- (20) Loeb, S. J.; Shimizu, G. K. H. *J. Chem. Soc., Chem. Commun.* **1993**, 1395.
- (21) Kraatz, H.-B.; Milstein, D. J. *J. Organomet. Chem.* **1995**, *488*, 223.
- (22) Chuchuryukin, A. V.; Dijkstra, H. P.; Suijkerbuijk, B. M. J. M.; Gebbink, R. J. M.; van Klink, G. P. M.; Mills, A. M.; Spek, A. L.; Van Koten, G. *Angew. Chem. Int. Ed.* **2003**, *42*, 228.
- (23) Pollino, J. M.; Nair, K. P.; Stubbs, L. P.; Adams, J.; Weck, M. *Tetrahedron* **2004**, *60*, 7205.
- (24) Steenwinkel, P.; Kooijman, H.; Smeets, W. J. J.; Spek, A. L.; Grove, D. M.; van Koten, G. *Organometallics* **1998**, *17*, 5411.
- (25) Hall, J. R.; Loeb, S. J.; Shimizu, G. K. H.; Yap, G. P. A. *Angew. Chem. Int. Ed.* **1998**, *37*, 121.
- (26) Trnka, T. M.; Grubbs, R. H. *Acc. Chem. Res.* **2001**, *34*, 18.
- (27) Fürstner, A. *Angew. Chem. Int. Ed. Engl.* **2000**, *39*, 3012.
- (28) Grubbs, R. H. *Tetrahedron* **2004**, *60*, 7118.
- (29) Ivin, K. J.; Mol, J. C. *Olefin Metathesis and Metathesis Polymerization*; Academic Press, Inc.: San Diego, 1997.
- (30) Herrison, J.-L.; Chauvin, Y. *Makromol. Chem.* **1971**, 161.
- (31) Schrock, R. R. *Acc. Chem. Res.* **1990**, *23*, 158.
- (32) Schwab, P.; Grubbs, R. H.; Ziller, J. W. *J. Am. Chem. Soc.* **1996**, *115*, 100.
- (33) Love, J. A.; Morgan, J. P.; Trnka, T. M.; Grubbs, R. H. *Angew. Chem. Int. Ed.* **2002**, *41*, 4035.
- (34) Webster, O. W. *Science* **1991**, *251*, 887.
- (35) Weck, M.; Schwab, P.; Grubbs, R. H. *Macromolecules* **1996**, *29*, 1789.
- (36) Portugall, M.; Ringsdorf, H.; Wendorff, J. H. *Makromol. Chem.* **1978**, *179*, 273.

- (37) Finkelmann, H.; Happ, M.; Portugall, M.; Ringsdorf, H. *Makromol. Chem.* **1978**, *179*, 2541.
- (38) Thermal decomposition of the benzylic dichloride was observed when reaction temperatures exceeded 38 °C.
- (39) Jacobine, A. F.; Glaser, D. M.; Nakos, S. T. *Polym. Mater. Sci. Eng.* **1989**, *60*, 211.
- (40) Sen, A.; Lai, T.-W. *J. Am. Chem. Soc.* **1981**, *103*, 4627.
- (41) Fujita, M.; Ibukuro, F.; Hagihara, H.; Ogura, K. *Nature* **1994**, *367*, 720.
- (42) Kickham, J. E.; Loeb, S. J. *Inorg. Chem.* **1994**, *33*, 4351.
- (43) Storhoff, B. N.; Lewis, H. C. *Coord. Chem. Rev.* **1977**, *23*, 1.
- (44) Kumar, U.; Kato, T.; Frechet, J. M. J. *J. Am. Chem. Soc.* **1992**, *114*, 6630.
- (45) Stewart, D.; Paterson, B. J.; Imrie, C. T. *Eur. Polym. J.* **1997**, *33*, 285.
- (46) Stewart, D.; Imrie, C. T. *Macromolecules* **1997**, *30*, 877.
- (47) Pangborn, A. B.; Giardello, M. A.; Grubbs, R. H.; Rosen, R. K.; Timmers, F. J. *Organometallics* **1996**, *15*, 1518.

CHAPTER 4.

OPTIMIZATION OF NORBORNENE MONOMERS POSSESSING TERMINAL RECOGNITION ELEMENTS

4.1 Abstract

Isomerically pure *exo*-norbornene esters containing either a Pd^{II} SCS pincer complex or a diaminopyridine unit were synthesized, polymerized, and copolymerized by ROMP using a ruthenium initiator. All polymerizations are living under mild reaction conditions. A comparison between the pure *exo*-monomers and the commonly employed 80:20 *endo/exo* mixtures was carried out. The *exo*-norbornene isomers exhibit significantly higher rates of propagation under milder conditions when compared to the *endo/exo* mixtures. Kinetic studies have shown that the k_p values are highly dependent upon the isomeric purity but completely independent of the terminal diaminopyridine or Pd^{II} SCS Pincer functional groups. The living character of the polymerization has allowed for the first block-copolymerization of norbornene metal-containing pincer complexes and diaminopyridine based hydrogen bonding receptors.

4.2 Introduction

An essential prerequisite of the UPB concept is the optimization of polymerization conditions and monomer structure to obtain fully “living” systems where surgical precision over the architecture of the final polymer and copolymer structures is possible.

Herein, the required steps to realize these goals using functionalized norbornene monomers and ROMP¹⁻⁴ are described.⁵

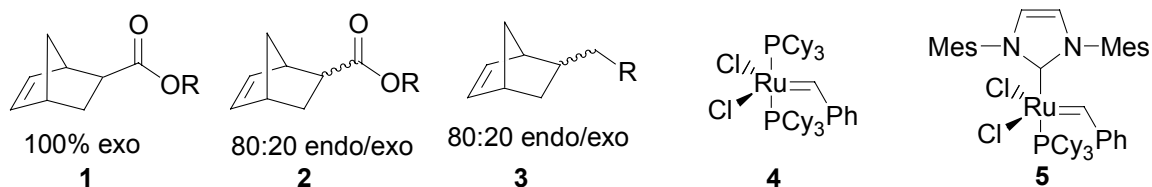


Figure 4.1 Monomers used in ROMP to introduce functionality at the side-chain (**1-3**) and commercially available ruthenium olefin metathesis initiators (**4-5**).

Current norbornene functionalization strategies are based primarily upon elaboration of esters (**2**) synthesized as an 80:20 *endo/exo* isomeric mixture via the Diels-Alder reaction of cyclopentadiene and asymmetric dienophiles.⁶⁻¹⁵ As described earlier, research directed toward the preparation of side-chain polymers possessing hydrogen bonding (Chapter 1) and metal coordination (Chapter 3) recognition motifs via ROMP of functionalized norbornenes has revealed limitations to this methodology. Polymerization of some elaborately functionalized derivatives of monomer **2** where R = a tethered metal complex or a hydrogen bonding unit with catalyst **4** require elevated temperatures and prolonged reaction times at low monomer to initiator stoichiometries ($[M]:[I]$). Although the polymerizations are carried out in a controlled manner, harsh reaction conditions limit molecular weights as well as block-copolymerizations due to partial catalyst decomposition after several hours.

Three possible solutions to these problems can be envisaged. First, a common method used to polymerize functional group intolerant monomers has been the employment of

the more active initiator **5**.² Although **5** is an effective polymerization catalyst, the rate of propagation is much higher than the rate of initiation leaving a high concentration of uninitiated carbene available upon complete monomer consumption, resulting in non-living behavior.² A second approach is the replacement of the carbonyl ester with a pure alkyl spacer (monomer **3**),¹⁶ which dramatically increases the rates of propagation when compared to **2**. However, the rate of initiation for these monomers (**3**) does not increase, resulting in poorly controlled polymerizations for identical reasons as those described for initiator **5**. Therefore, it can be concluded that the carbonyl group plays a critical role in retarding the rate of propagation. It is well known for the ROMP of *endo/exo*-norbornene esters, that the *exo* isomer reacts significantly faster than the *endo* isomer.¹⁷ One detailed mechanistic investigation for the ROMP of *endo* and *exo*-dicyclopentadiene has shown that the rate difference between the two isomers is primarily due to steric interactions between the growing polymer chains and the incoming monomer.¹⁸ Furthermore, a similar preference for the *exo*-isomer has been observed in the palladium catalyzed addition polymerization of norbornene esters.¹⁹⁻²¹ Previously, Kiessling *et al.* have developed a methodology that allows for the functionalization of isomerically pure *exo*-norbornene esters that has been employed extensively for the synthesis of glycopolymers.²²⁻²⁶ Therefore, the utilization of isomerically pure *exo*-monomers could be a potential solution to obtain controllable and efficient polymerizations by providing control over the relative rates of initiation and propagation via the carbonyl ester while simultaneously enhancing the rates of propagation by removal of any steric and/or electronic inhibition caused by the *endo* isomer. This should allow for living behavior under mild reaction conditions. Herein, the use of *exo*-norbornene esters as highly

efficient monomers for living ROMP of densely functionalized norbornenes containing metals and/or aromatic nitrogen containing moieties and the block copolymerization of these monomers is reported. Furthermore, a detailed comparison between the isomerically pure *exo*-monomers and their 80:20 *endo/exo* analogs is presented.

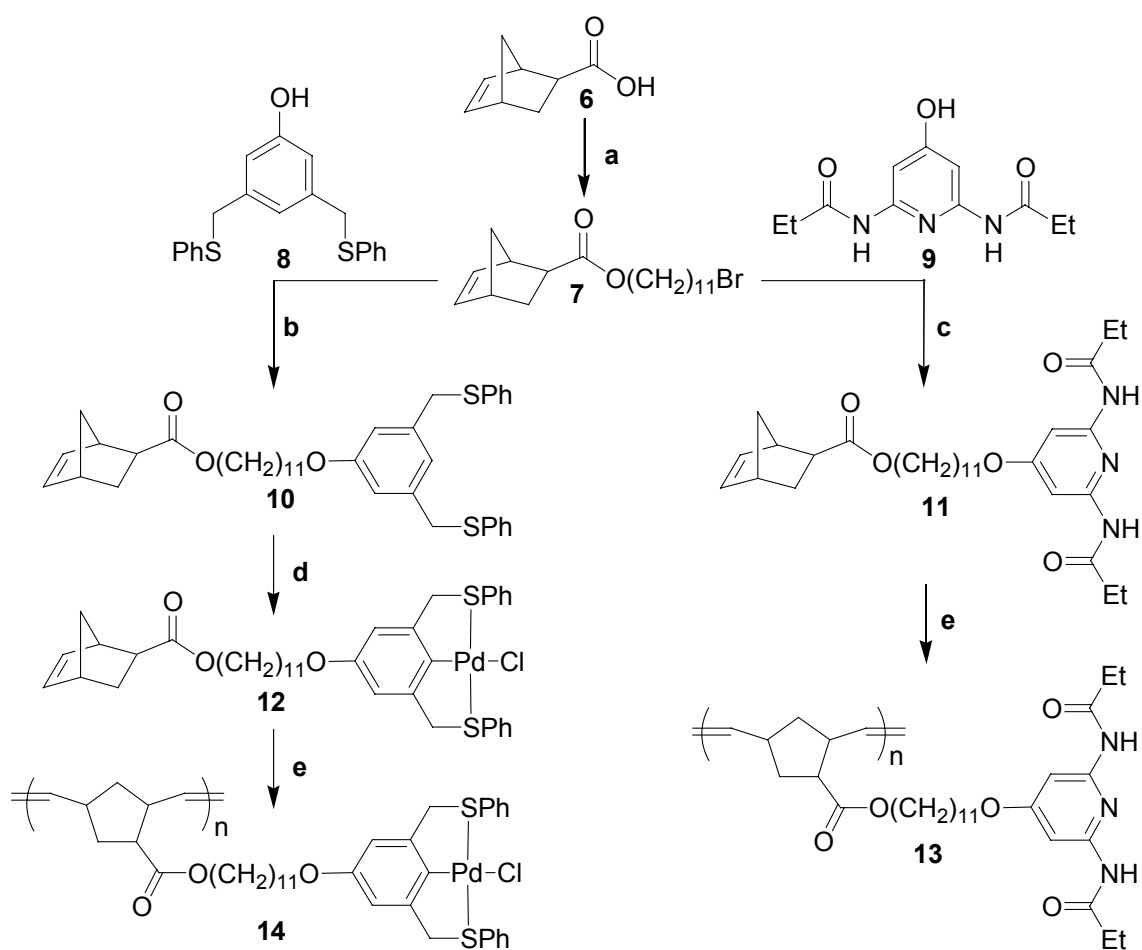
As noted in Chapter 2, the UPB concept requires the use of multiple recognition elements. The monomers studied in this chapter, norbornenes terminally functionalized with recognition motifs for either: i) metal coordination and ii) hydrogen bonding, meet this requirement. The former are based on palladated SCS pincer complexes, which have been previously detailed in Chapter 3.²⁷ The latter employs norbornenes functionalized with DAD diaminopyridine recognition motifs.^{16,28,29} These monomers, developed in our lab (Dr. L. P. Stubbs), have yielded poly(norbornene)s that can be easily functionalized with ADA *N*-butylthymine based anchoring units.¹⁶ Their strong association constants and low dimerization constants make them well suited for use in the UPB concept.

4.3 Monomer Synthesis

Isomerically pure *exo*-norbornene acid **6** was synthesized via isomerization of the corresponding norbornene methyl ester from an 80:20 to a 45:55 *endo/exo* mixture followed by hydrolysis to the norbornene-acid and removal of excess *endo* isomer by selective iodolactonization.^{23,30,31} Functionalization of **6** was carried out via DCC/DMAP assisted esterification with 11-bromoundecan-1-ol to give the corresponding *exo*-undecyl bromide **7**. From **7**, monomer **11** was accessible in one step via a Williamson ether synthesis using compound **9**. Similarly, **10** was synthesized by the coupling of **8** to **7**. To avoid possible palladium catalyzed polyaddition reactions that are known to proceed rapidly for *exo*-norbornenes in the presence of $[\text{Pd}(\text{CH}_3\text{CN})_4](\text{BF}_4)_2$,¹⁹⁻²¹ the previously

reported metallation procedure was modified.^{32,33} Quantitative bis-palladation using 1 equiv. of Pd(PhCN)₂Cl₂ followed by *in-situ* cyclopalladation using 2 equiv. of AgBF₄ provided the cationic Pd-BF₄ intermediate. Subsequent ligand-exchange to the Pd-Cl via prolonged stirring in brine afforded monomer **10** in 87% yield (Scheme 4.1).

Scheme 4.1 Synthesis and ROMP of isomerically pure *exo*-norbornene monomers.



Reagents and Conditions: a) 11-Bromo-undecan-1-ol, DCC/DMAP, CH₂Cl₂, reflux, 16 h, 87%; b) **8**, K₂CO₃, DMF, 40°C, 70 h, 96%; c) **9**, Cs₂CO₃, acetone, 70 °C, 8h, 100%; d) i. Pd (PhCN)₂Cl₂, CH₃CN, r.t., 30 min; ii. AgBF₄, 30 min; iii. NaCl_(aq), 5 h, 87%; e) **4**, CDCl₃, 20-120 min, 100%.

4.4 Polymerization Studies

As described above, previous work involving the polymerizations of 80:20 *endo/exo* mixtures of **11** and **12** was hampered by long reaction times and elevated temperatures. For example, the 80:20 *endo/exo-12* required 12 h at 45 °C for the polymerization of a 50:1 [M]:[I] whereas the 80:20 *endo/exo-11* necessitated 24 h for polymerization under identical conditions.^{32,33} To investigate the behavior of isomerically pure *exo*-monomers, **11** and **12** were polymerized using **4** (Scheme 4.1). At 25 °C in CDCl₃ (20:1 [M]:[I] ratio), *exo-11* and *exo-12* were completely polymerized in less than 30 min. In sharp contrast, under identical conditions the analogous 80:20 *endo/exo-11* and **12** monomers required in excess of 300 min to go to completion (Table 4.1).

Table 4.1 Representative data for polymers initiated by **4**.

Monomer	Isomeric Purity	Time* (min)	[M]:[I]	M _n (10 ⁻³)	M _w (10 ⁻³)	PDI
11	80:20 <i>endo/exo</i>	300	20	13.1	19.8	1.51
12	80:20 <i>endo/exo</i>	300	20	16.0	22.8	1.42
11	100% <i>exo</i>	25	20	6.9	7.5	1.08
11	100% <i>exo</i>	65	60	23.1	24.4	1.05
11	100% <i>exo</i>	120	115	37.6	39.7	1.06
12	100% <i>exo</i>	25	20	49.9	62.6	1.25
12	100% <i>exo</i>	50	44	78.6	98.7	1.26
12	100% <i>exo</i>	120	110	186.3	222.6	1.19

*Time at 100% conversion.

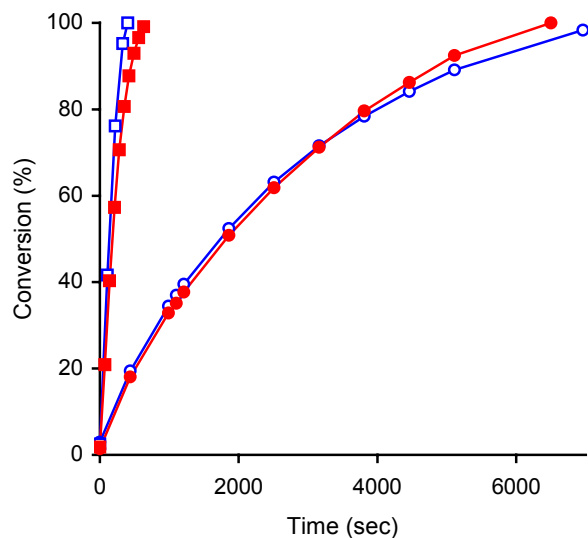


Figure 4.2 Plot of conversion (%) as a function of time (sec) for the polymerization of 80:20 *endo/exo*-**11** (—●—), 80:20 *endo/exo*-**12** (—○—), *exo*-**11** (—■—), and *exo*-**12** (—□—).

Table 4.2 First order rate constants determined for *exo* and 80:20 *endo/exo* **11** and **12**.

Monomer	Isomeric Purity	$k_i^{*\dagger}$ (10^3 sec^{-1})	$k_p^{*\dagger}$ (10^3 sec^{-1})	k_i/k_p
11	80:20 <i>endo/exo</i>	7.18	0.43	16.8
12	80:20 <i>endo/exo</i>	6.91	0.41	16.7
11	100% <i>exo</i>	10.73	6.27	1.7
12	100% <i>exo</i>	9.47	6.51	1.5

*All values were measured using $^1\text{H-NMR}$ spectroscopy.

$\dagger[\text{M}] = 0.222 \text{ M}$ and $[\text{I}] = 0.0111 \text{ M}$.

To gain better control of the ROMP, the kinetics of the polymerization were studied. The rate of initiation was examined *in situ* via $^1\text{H-NMR}$ spectroscopy by monitoring the carbene signal for the propagating species ($\delta = 18.81$ ppm, solvent = CDCl_3) and the non-initiated species **4** ($\delta = 19.95$ ppm, solvent = CDCl_3). For both **11** and **12**, complete disappearance of the non-initiated species for a 20:1 $[\text{M}]:[\text{I}]$ ratio was evident within 5 min at ca. 30% conversion (Figure 4.2, Table 4.2). Since polydispersity is affected by the relative rates of initiation (k_i) and propagation (k_p), PDIs are broader at low $[\text{M}]:[\text{I}]$ ratios due to higher consumption of monomer prior to complete initiation. The k_i and k_p values for monomers **11** and **12** are similar for each respective isomer indicating that the polymerization behavior is independent of the terminal diaminopyridine or Pd^{II} SCS pincer functional groups. Comparison of the k_i values for *endo/exo*-mixtures and the pure *exo*-monomers shows that k_i is only slightly affected by the isomeric purity. In sharp contrast, the k_p values are greatly dependant upon the isomeric purity, with the *exo* isomer propagating 15 times faster than the *endo/exo* mixture.

Controlled molecular weights, high initiator efficiency, and absence of chain-transfer and chain-termination are characteristics of living polymerizations.^{34,35} In accordance with these criteria, the ability to control molecular weight by modification of the reaction stoichiometry was examined. For both monomers (**11** and **12**) a linear relationship between M_n and the corresponding $[\text{M}]:[\text{I}]$ feed ratios was observed suggesting the living character and high control of the polymerization (Figure 4.3).

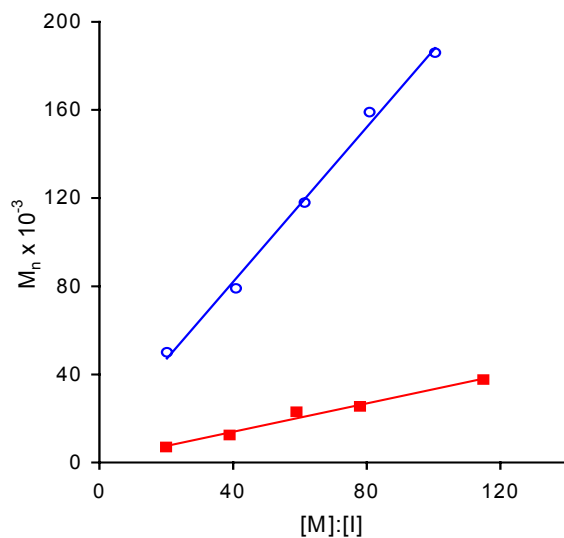


Figure 4.3 Plot of M_n versus monomer-to-catalyst ratios for polymers **13** (—■—, eluant = THF) and **14** (—○—, eluant = CH_2Cl_2).

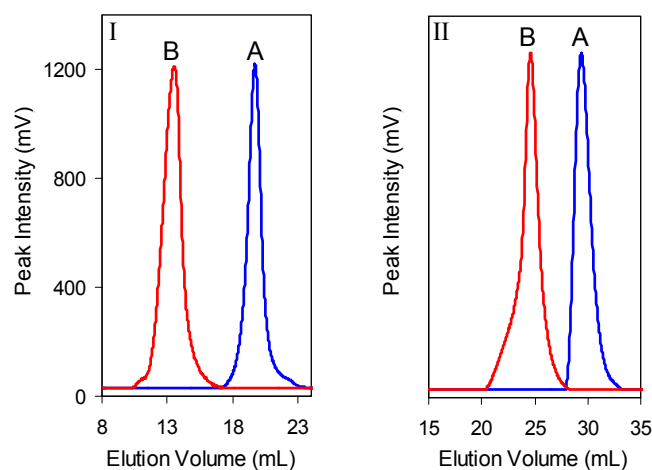


Figure 4.4 I) GPC traces of polymers prepared using monomer **12**. II) GPC traces of polymers prepared using monomer **11**. A) (—) Polymer after complete conversion ($[\text{M}]:[\text{I}] = 20:1$, $M_w(\mathbf{11}) = 8.1 \times 10^3$, $M_n(\mathbf{11}) = 7.2 \times 10^3$, $\text{PDI}(\mathbf{11}) = 1.13$; $M_w(\mathbf{12}) = 6.3 \times 10^4$, $M_n(\mathbf{12}) = 4.9 \times 10^4$, $\text{PDI}(\mathbf{12}) = 1.29$). B) (—) Same polymer after standing for 0.5 h followed by polymerization of 200 equiv ($[\text{M}_2]:[\text{M}_1] = 200:1$, $[\text{M}]:[\text{I}] = 20:1$, $M_w(\mathbf{11}) = 1.0 \times 10^5$, $M_n(\mathbf{11}) = 7.1 \times 10^4$, $\text{PDI}(\mathbf{11}) = 1.41$; $M_w(\mathbf{12}) = 4.5 \times 10^5$, $M_n(\mathbf{12}) = 3.4 \times 10^5$, $\text{PDI}(\mathbf{12}) = 1.32$) of additional monomer.

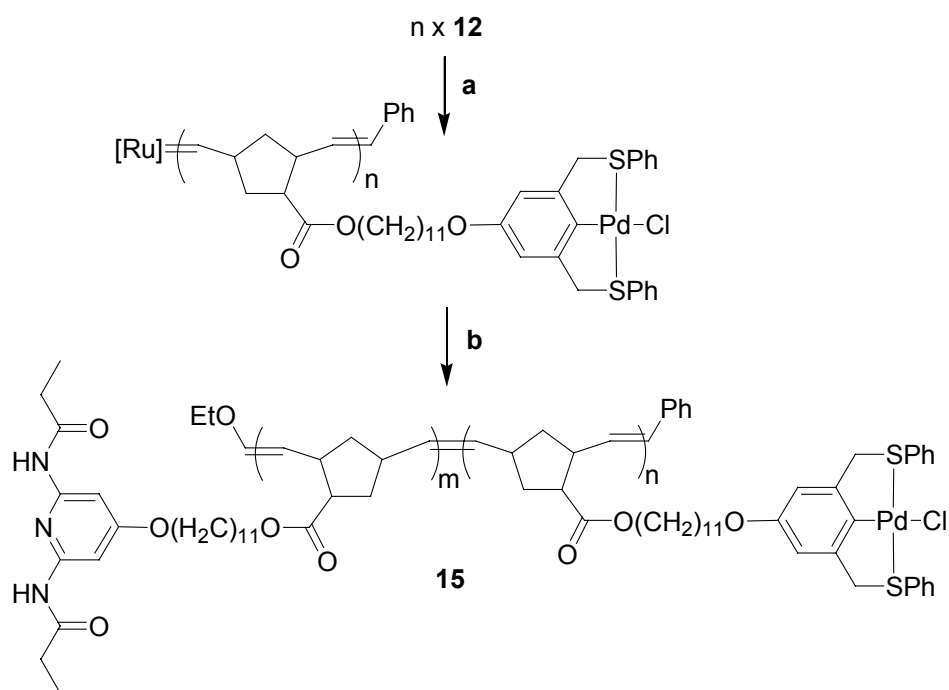
Another decisive factor in characterizing living polymerizations is the synthesis of block copolymers.^{34,35} To show that the polymerizations of *exo*-**11** and *exo*-**12** fulfill this criterion, a two-step polymerization sequence was carried out for both monomers. A 20:1 [M]:[I] ratio of monomer **12** was polymerized to completion and allowed to stir for 30 min, at which time 200 equivalents of additional monomer was added. As shown in Figure 4.4, a dramatic increase in molecular weight was observed for the original polymer (**14**) (I-A) after sequential addition of fresh monomer (**14**) (I-B). Complete absence of chain-termination and chain-transfer is evident by the disappearance of peak A with no residual signal in the baseline. Both chain-termination and chain-transfer would produce non-living polymer chains that would not increase in molecular weight upon further addition of fresh monomer. Identical results were observed for polymer **13** (Figure 4.4-II). These findings, in conjunction with the linear plot of M_n as function of [M]:[I], clearly prove the living character of these systems.

4.5 Copolymerization Studies

Once the living nature of these monomers was established, AB block copolymerizations using both monomers **11** and **12** were possible and carried out (Scheme 4.2). A 75:1 [M]:[I] ratio of monomer **12** was polymerized to completion, at which time 25 equivalents of monomer **11** was added and allowed to stir until all monomer was consumed. The resultant AB block copolymer was isolated by precipitation from hexanes. Identical experiments were carried out for 50:50 and 25:75 compositions of **12** and **11** respectively. GPC analyses of polymers possessing hydrogen bonding recognition units were hampered by interactions with the columns in non-polar eluants. Similar problems were observed for copolymers **15** when subjected to GPC

analysis using CH_2Cl_2 as an eluant. These difficulties were circumvented using DMF as an eluant. For the 25:75 composition of **11** to **12**, molecular weights of $M_w = 1.36 \times 10^5$, $M_n = 7.82 \times 10^4$ were observed with polydispersities of 1.74 and no signs of chain-transfer or chain-termination was evident. However, similar analyses of 75:25 and 50:50 mixtures of **11:12** were unsuccessful due to poor solubility in polar media including DMF and THF.

Scheme 4.2 Synthesis of AB block copolymers containing both diaminopyridine and Pd^{II} pincer receptor units.



Reagents and Conditions: a) **4**, CDCl_3 , 20-120 min, 100%. b) $m \times$ **11**, 20-120 min, 100%.

4.6 Conclusion

In conclusion, isomerically pure *exo*-norbornene esters containing Pd^{II} SCS pincer complexes or diaminopyridine moieties were synthesized and polymerized via ROMP. Using standard characterization techniques, the living character of the polymerizations was proven which allowed for the synthesis of block-copolymers. A comparison between 100% *exo* monomers **11** and **12** and those prepared using the more conventional route as a 80:20 *endo/exo* mixture clearly showed advantageous polymerization behavior for the former with faster reaction times, higher conversions, and more control. Specifically, these studies have shown that i) the carbonyl ester group is central to maintaining k_i/k_p values adequate for living polymerization; ii) the rate of propagation is dependent upon the isomeric purity of the norbornene ester moiety; and iii) the polymerization kinetics are independent of the terminal diaminopyridine or Pd^{II} SCS pincer functional groups. Based on these results, the formation of block copolymers that incorporate both metal coordinating units and hydrogen bonding motifs (block UPBs) have been realized.

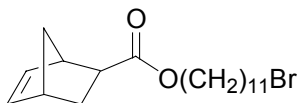
4.7 Experimental

All reagents were purchased either from Acros Organics, Aldrich, or Strem and used without further purification. DMF and CDCl₃ were distilled from calcium hydride and degassed prior to use. THF and CH₂Cl₂ were dried via passage through copper oxide and alumina columns.³⁶ NMR spectra were taken using a 300 MHz Varian Mercury spectrometer. All spectra are referenced to residual proton solvent. Mass spectral analysis was kindly provided by the Georgia Tech Mass Spectrometry Facility using a VG-70se spectrometer. GPC analyses for **14** were carried out using a Waters 1525 binary pump coupled to a Waters 2414 refractive index detector with methylene chloride as an eluant

on American Polymer Standards 10 μ particle size, linear mixed bed packing columns (2x). GPC analysis for **13** were carried out using a waters 510 binary pump coupled to a Waters 410 differential refractometer with THF as an eluant on an American Polymer Standards column set (100 Å, 1000 Å, 100,000 Å, linear mixed bed). All GPCs were calibrated using polystyrene standards. Atlantic Microlab, Norcross GA, performed all elemental analyses.

Exo-bicyclo[2.2.1]hept-5-ene-2-carboxylic acid (**6**) was prepared according to a literature protocol.^{23,30,31} 2,6-Bis-(propionylamino)-4-hydroxypyridine (**9**) was prepared by acylation of 4-benzyloxy-2,6-diaminopyridine^{16,29} with propionyl chloride and subsequent deprotection with H₂/Pd in 88% yield. SCS pincer ligand **8** was prepared according to literature procedure.^{32,37}

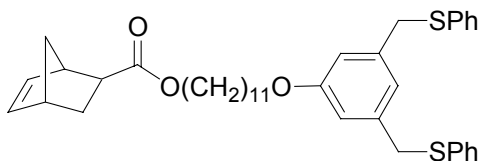
Synthesis of *exo*-bicyclo[2.2.1]hept-5-ene-2-carboxylic acid 11-bromo-undecyl ester (**7**)



Exo-bicyclo[2.2.1]hept-5-ene-2-carboxylic acid **6** (6.1 g, 0.044 mol) and 11-bromo-undecan-1-ol (11.2g, 0.044 mol) were combined, dissolved in anhydrous CH₂Cl₂ (40 mL), and placed under an atmosphere of argon. To the stirred solution, DCC (9.1 g, 0.044 mol) in CH₂Cl₂ (40 mL) and DMAP (cat. amt.) were added at 25 °C. Immediately, the solution became turbid with formation of a white precipitate. Following stirring at reflux for 16 h, the mixture was cooled, diluted with CH₂Cl₂ (200 mL), and the precipitate filtered off. The filtrate was dried (MgSO₄) and the solvent removed to give a solid

residue that was further purified by column chromatography (SiO₂, eluant: 1:1 CH₂Cl₂/hexanes). Drying on high vacuum provided pure **7** as a colorless oil (14.25 g, 87%). ¹H NMR (CDCl₃): δ = 6.09 (m, 2H, CH=CH), 4.04 (t, 2H, *J*=6.9 Hz, CH₂O), 3.37 (t, 2H, *J*=6.9 Hz, CH₂Br), 2.99 (m, 1H), 2.88 (m, 1H), 2.18 (m, 1H), 1.92-1.76 (m, 3H), 1.65-1.55 (m, 3H), 1.55 (m, 1H), 1.53 (m, 1H), 1.41-1.19 (m, 14H). ¹³C NMR (CDCl₃): δ = 176.1, 137.9, 135.6, 64.4, 46.5, 46.2, 43.0, 41.5, 33.8, 32.7, 30.2, 29.3, 29.1, 28.6. HRMS (EI): *m/z* = 370.15432 (M⁺, calcd. 370.1074) Anal. Calcd. for C₁₉H₃₁BrO₂: C, 61.45; H, 8.41; Found: C, 61.64; H, 8.51.

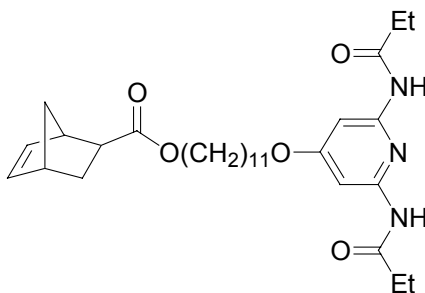
Synthesis of *exo*-bicyclo[2.2.1]hept-5-ene-2-carboxylic acid 11-(3,5-bis-phenylsulfanyl-methyl-phenoxy)-undecyl ester (10**)**



Compound **7** (2.40 g, 0.0065 mol) was slowly added to a stirred suspension of **8** (2.30 g, 0.0068 mol) with K₂CO₃ (2.40 g, 0.017 mol) in dry DMF (20 mL) at 25 °C. Once heated to 60 °C, the reaction was stirred for 60 h at which point the DMF was removed under reduced pressure. The crude product was then redissolved in CH₂Cl₂ (150 mL) and washed with H₂O (100 mL). The organic layer was dried (MgSO₄), the solvent evaporated, and the crude product purified by column chromatography (SiO₂, eluant: 3:2 hexanes/DCM) to afford pure **10** (3.92 g, 96%) as a viscous, colorless oil. ¹H NMR (CDCl₃): δ = 7.28-7.12 (m, 10 H, SPh), 6.80 (s, 1H, ArH), 6.69 (s, 2H, ArH), 6.11(m, 2H, CH=CH), 4.07 (t, *J*=6.6 Hz, 2H, CH₂O), 4.00 (s, 4H, CH₂S), 3.82 (t, *J*=6.6 Hz, 2H,

CH₂O), 3.03 (m, 1 H), 2.90 (m, 1H), 2.21 (m, 1H), 1.91 (m, 1H), 1.75-1.58 (m, 5H), 1.54 (m, 1H), 1.51 (m, 1H), 1.46-1.19 (m, 14H). ¹³C NMR (CDCl₃): δ = 176.1, 159.1, 138.8, 137.9, 136.2, 135.6, 129.6, 128.7, 126.2, 121.4, 113.6, 67.8, 64.4, 46.5, 46.2, 43.1, 41.5, 38.8, 30.2, 29.4, 29.3, 29.1, 28.6, 25.9, 25.8. HRMS (EI): *m/z* = 628.30578 (M⁺, calcd. 628.30449) Anal. Calcd. for C₃₉H₄₈O₃S₂: C, 74.48; H, 7.69; Found: C, 74.41; H, 7.79.

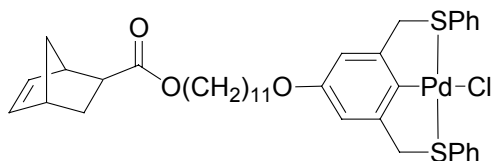
Synthesis of *exo*-bicyclo[2.2.1]hept-5-ene-2-carboxylic acid 11-(2,6-bis-(propionylamino)pyridin-4-yloxy) undecyl ester (11)



11-bromo-undecyl ester **7** (1.6 g, 0.00436 mol), hydroxypyridine **9** (1.057 g, 0.00424 mol) and Cs₂CO₃ (1.6 g, 0.0049 mol) were stirred in 80 mL acetone at reflux for 12 h. The suspension was filtered, the solvent evaporated, and the residue purified by column chromatography (SiO₂, eluant: 1:1 hexanes/ethyl acetate) to afford pure **11** (2.24 g, 100%) as a colorless, viscous oil that crystallized as fine needles after several days. ¹H-NMR (CDCl₃): δ = 7.94 (br s, 2 H, NH), 7.50 (s, 2 H, pyr), 6.08 (m, 2 H, CH=CH), 4.04 (t, *J* = 6.6 Hz, 2 H, CO₂CH₂), 3.97 (t, *J* = 6.6 Hz, 2 H, CH₂O), 3.00 (m, 1 H), 2.87 (m, 1 H), 2.34 (q, *J* = 7.7 Hz, 4 H, CH₂CH₃), 2.18 (m, 2 H), 1.88 (d/tr, *J*₁ = 12.1 Hz, *J*₂ = 3.8 Hz, 1 H), 1.71 (m, 2 H), 1.59 (m, 2 H), 1.48 (m, 1H), 1.40-1.20 (m, 15 H), 1.17 (t, *J* = 7.7 Hz, 6 H, CH₂CH₃). ¹³C-NMR (CDCl₃): δ = 176.2, 172.3, 168.8, 150.5, 137.9, 135.6,

96.0, 68.3, 64.5, 46.5, 46.2, 43.1, 41.5, 30.6, 30.1, 29.3, 29.2, 29.1, 28.7, 28.6, 25.8, 25.7, 9.2. HRMS (EI): $m/z = 527.3367$ (M^+ , calcd. 527.3359). Anal. Calcd. for $C_{30}H_{45}N_3O_5$: C, 68.28; H, 8.60; N, 7.96 Found: C, 67.76; H, 8.70; N, 7.68.

Synthesis of Pd-Cl *exo*-bicyclo[2.2.1]hept-5-ene-2-carboxylic acid 11-(3,5-bis-phenylsulfanylmethyl-phenoxy)-undecyl ester (12)



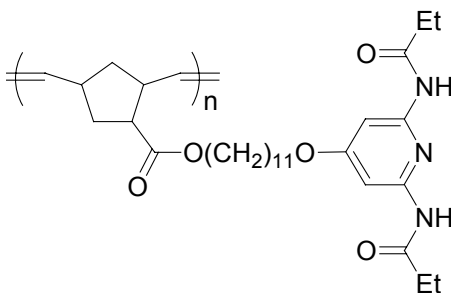
Compound **10** (542 mg, 0.862 mmol) was dissolved in a 1:2 mixture of CH_2Cl_2 (5 mL)/ CH_3CN (10 mL). $Pd(Ph_3CN)_2Cl_2$ (329 mg, 0.862 mmol) was then added in one portion. The dark orange solution was stirred for 30 min under an atmosphere of argon at which point $AgBF_4$ (419 mg, 2.15 mmol) was added and the solution stirred for an additional 30 min. Immediately after addition of the silver salt, the solution became pale yellow in color with formation of a white precipitate. The reaction mixture was then diluted with CH_2Cl_2 (250 mL) and poured into a brine solution (250 mL). Following vigorous stirring for 5 h, the organic layer was separated, dried ($MgSO_4$), and the solvent removed under reduced pressure. Purification by column chromatography (SiO_2 , eluant: $CH_2Cl_2/MeOH$ 99:1) yielded Pd-Cl complex **12** (570 mg, 86%) as an amorphous yellow solid. 1H NMR ($CDCl_3$): $\delta = 7.82-7.79$ (m, 4H, SPh), 7.36-7.32 (m, 6H, SPh), 6.56 (s, 2H, ArH), 6.10 (m, 2H, CH=CH), 4.53 (br s, 4H, CH_2S), 4.06 (t, $J=6.6$ Hz, CH_2O), 3.85 (t, $J=6.6$ Hz, CH_2O), 3.02 (m, 1H), 2.90 (m, 1H), 2.20 (m, 1H), 1.91 (m, 1H), 1.76-1.55 (m, 5H), 1.52 (m, 1H), 1.49 (m, 1H), 1.42-1.23 (m, 14H). ^{13}C NMR ($CDCl_3$): $\delta = 176.2$,

156.9, 151.3, 150.0, 137.9, 135.7, 132.3, 131.3, 129.6, 129.5, 108.7, 68.0, 64.4m 51.6, 46.5, 46.2, 43.1, 41.5, 30.2, 29.4, 29.3, 29.1, 28.6, 25.9, 25.8. HRMS (FAB): $m/z = 733.20142$ ((M-Cl)⁺, calcd. 733.20014). Anal. Calcd. for C₃₉H₄₇ClO₃PdS₂: C, 60.85; H, 6.15; Found: C, 60.40; H, 6.15.

General polymerization procedure

A definitive amount of monomer was weighed into a vial, placed under an atmosphere of argon and dissolved in anhydrous, degassed CDCl₃ (1 mL per 100 mg of monomer). A stock solution of catalyst (in CDCl₃) was prepared and the desired amount was added in one portion to the vigorously stirred monomer solution. Upon complete polymerization, a drop of ethyl vinyl ether was added to terminate the polymerization. The final polymer, was obtained by precipitation from cold hexanes, or by evaporation of volatiles followed by prolonged drying on high vacuum. Polymers **13** and **14** were obtained as gray and pale-yellow solids respectively.

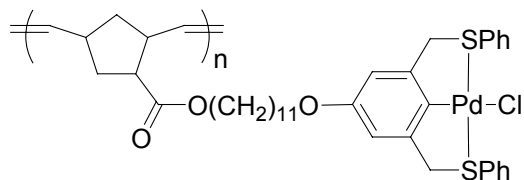
Polymer (13)



¹H NMR (CDCl₃): $\delta = 8.14$ (br s, 2 H, NH), 7.47 (s, 2 H), 5.4-5.1 (br m, 2 H), 3.96 (br m, 4H), 3.2-2.4 (br m, 2 H), 2.33 (br m, $J = 7.1$ Hz, 4 H), 2.2-1.4 (br m, 23 H), 1.15 (br t, $J =$

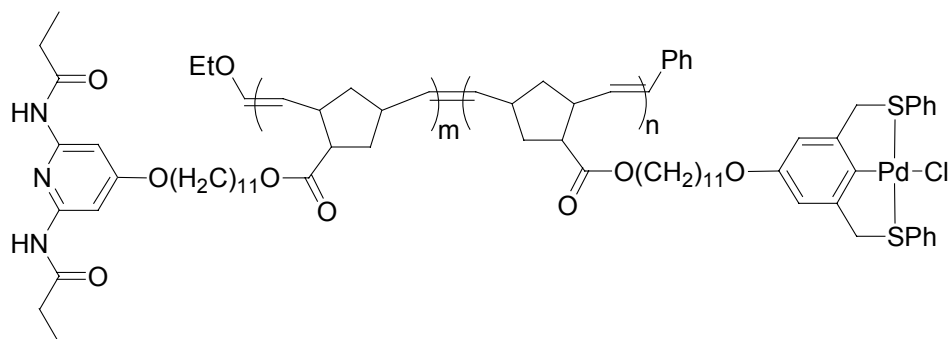
7.1 Hz, 6 H). ^{13}C NMR (CDCl_3): $\delta = 176.1, 172.8, 169.1, 150.8, 134-131, 96.3, 68.6, 64.7, 49.7, 47.8, 42.1, 41.2, 37.1, 36.4, 30.8, 29.7-28.9, 26.0, 9.5$.

Polymer (14)



^1H NMR (CDCl_3): $\delta = 7.78$ (m, 4H, SPh), 7.32 (m, 6H, SPh), 6.55 (s, 2H, ArH), 5.50-5.17 (br m, 2H, CH=C), 4.58 (br s, 4H, CH_2S), 4.00-3.85 (m, 2H, OCH_2), 3.84-3.80 (m, 2H, OCH_2), 3.24-2.30 (br m, 3H), 2.03-1.50 (br m, 8H), 1.98-1.07 (m, 14H). ^{13}C NMR (CDCl_3): $\delta = 174.4, 156.8, 151.3, 149.9, 132.3, 131.2, 129.6, 129.5, 108.7, 108.6, 67.9, 64.2, 51.5, 48.0, 45.4, 40.4, 37.3, 36.0, 29.3, 29.2, 28.9, 28.6, 26.0, 25.8$.

Synthesis of block copolymer (15)



A definitive amount of monomer **12** was weighed into a vial, placed under an atmosphere of argon and dissolved in anhydrous, degassed CDCl_3 (1 mL per 100 mg of monomer). A stock solution of catalyst (in CDCl_3) was prepared and the desired amount was added in one portion to the vigorously stirred monomer solution. Upon complete monomer

consumption, a charge of monomer **11** dissolved in anhydrous, degassed CDCl_3 (1 mL per 100 mg of monomer) was added to the vial and allowed to stir until all monomer was completely consumed. Upon complete polymerization, a drop of ethyl vinyl ether was added to terminate the polymerization. The copolymers, were obtained by precipitation from cold hexanes. Polymers **15** were obtained as light green solids. ^1H NMR (CDCl_3): δ = 8.04 (br s, 2H, NH), 7.79-7.75 (m, 4H, SPh), 7.50 (s, 2H, pyr), 7.34-7.30 (m, 6H, SPh), 6.54 (s, 2H, ArH), 5.42-5.10 (m, 4H, CH=CH), 4.50 (br s, 4H, CH_2S), 4.11-3.92 (br m, 6H, CH_2O), 3.82 (t, $J=6.6$ Hz, CH_2O), 3.2-1.0 (m, 60H).

4.8 References

- (1) Ivin, K. J.; Mol, J. C. *Olefin Metathesis and Metathesis Polymerization*; Academic Press, Inc.: San Diego, 1997.
- (2) Trnka, T. M.; Grubbs, R. H. *Acc. Chem. Res.* **2001**, *34*, 18.
- (3) Grubbs, R. H. *Tetrahedron* **2004**, *60*, 7118.
- (4) Fürstner, A. *Angew. Chem. Int. Ed. Engl.* **2000**, *39*, 3012.
- (5) The contents of this chapter have been published. See: Pollino, J. M.; Stubbs, L. P.; Weck, M. *Macromolecules* **2003**, *36*, 2230.
- (6) Weck, M.; Mohr, B.; Maughon, B. R.; Grubbs, R. H. *Macromolecules* **1997**, *30*, 6430.
- (7) Bolm, C.; Dinter, C. L.; Schiffers, I.; Defrère, L. *Synlett* **2001**, *12*, 1875.
- (8) Maynard, H. D.; Okada, S. Y.; Grubbs, R. H. *Macromolecules* **2000**, *33*, 6239.
- (9) Watson, K. J.; Wolfe, P. S.; Nguyen, S. T.; Zhu, J.; Mirkin, C. *Macromolecules* **2000**, *33*, 4628.
- (10) Schitter, R. M. F.; Jochem, D.; Stelzer, F.; Moszner, N.; Völkel, T. *J. App. Poly. Sci.* **2000**, *78*, 47.
- (11) Seehof, N.; Grutke, S.; Risse, W. *Macromolecules* **1993**, *26*, 695.
- (12) Abd-El-Aziz, A. S.; May, L. J.; Edel, A. L. *Macromol. Rapid Commun.* **2000**, *21*, 598.
- (13) Weck, M.; Schwab, P.; Grubbs, R. H. *Macromolecules* **1996**, *29*, 1789.
- (14) Arehart, S. V.; Pugh, C. *J. Am. Chem. Soc.* **1997**, *119*, 3027.
- (15) Wolfe, P. S.; Wagener, K. B. *Macromolecules* **1999**, *32*, 7961.
- (16) Stubbs, L. P.; Weck, M. *Chem. Eur. J.* **2003**, *9*, 992.
- (17) Fu, Q.; Seery, T. A. P. *Polym. Prepr.* **2001**, *41(1)*, 341.
- (18) Rule, J. D.; Moore, J. S. *Macromolecules* **2002**, *35*, 7878.
- (19) Mathew, J. P.; Reinmuth, A.; Melia, J.; Swords, N.; Risse, W. *Macromolecules* **1996**, *29*, 2755.

- (20) Mehler, C.; Risse, W. *Makromol. Chem., Rapid Commun.* **1991**, *12*, 255.
- (21) Breunig, S.; Risse, W. *Makromol. Chem.* **1992**, *193*, 2915.
- (22) Manning, D. D.; Hu, X.; Beck, P.; Kiessling, L. L. *J. Am. Chem. Soc.* **1997**, *119*, 3161.
- (23) Manning, D. D.; Strong, L. E.; Hu, X.; Beck, P. J.; Kiessling, L. L. *Tetrahedron* **1997**, *53*, 11937.
- (24) Gordon, E. J.; Gestwicki, J. E.; Strong, L. E.; Kiessling, L. L. *Chem. Biol.* **2000**, *7*, 9.
- (25) Strong, L. E.; Kiessling, L. L. *J. Am. Chem. Soc.* **1999**, *121*, 6193.
- (26) Owen, R. M.; Gestwicki, J. E.; Young, T.; Kiessling, L. L. *Org. Lett.* **2002**, *4*, 2293.
- (27) Albrecht, M.; van Koten, G. *Angew. Chem. Int. Ed.* **2001**, *40*, 3750.
- (28) Prins, L. J.; Reinhoudt, D. N.; Timmerman, P. *Angew. Chem. Int. Ed.* **2001**, *40*, 2382.
- (29) Dewey, V. C.; Kidder, G. W. *J. Med. Chem.* **1968**, *11*, 126.
- (30) Ver Nooy, C. D.; Rondestvedt, C. S. *J. Am. Chem. Soc.* **1955**, *77*, 3583.
- (31) Roberts, J. D.; Trumbull, E. R.; Bennett, W.; Armstrong, R. *J. Am. Chem. Soc.* **1950**, *72*, 3116.
- (32) Pollino, J. M.; Weck, M. *Synthesis* **2002**, *9*, 1277.
- (33) Pollino, J. M.; Weck, M. *Org. Lett.* **2002**, *4*, 753.
- (34) Webster, O. W. *Science* **1991**, *251*, 887.
- (35) Quirk, R. P.; Lee, B. *Polym. Inter.* **1992**, *27*, 359.
- (36) Pangborn, A. B.; Giardello, M. A.; Grubbs, R. H.; Rosen, R. K.; Timmers, F. J. *Organometallics* **1996**, *15*, 1518.
- (37) Huck, W. T. S.; van Veggel, F. C. J. M.; Reinhoudt, D. N. *J. Mater. Chem.* **1997**, *7*, 1213.

CHAPTER 5.

MULTI-STEP AND ONE-STEP “UNIVERSAL POLYMER BACKBONE” FUNCTIONALIZATION

5.1 Abstract

A novel methodology for UPB functionalization based on a non-covalent, one-step, multi-functionalization strategy has been developed. Random copolymers possessing both palladated-pincer complexes and diaminopyridine moieties (hydrogen bonding entities) have been synthesized using ring-opening metathesis polymerization. Non-covalent functionalization of the resultant copolymers is accomplished via 1) *directed self-assembly*, 2) *multi-step self-assembly*, and 3) *one-step orthogonal self-assembly*. This system shows complete specificity of each recognition motif for its complementary unit with no observable changes in the association constant regardless of the degree of functionalization.

5.2 Introduction

The UPB concept is based on the premise that multiple recognition units will operate with high fidelity and selectivity in the presence of one another. This concept, known as orthogonality, is required of all natural and unnatural systems where non-covalent multifunctionalization takes place.¹⁻⁶ Until now, all self-assembly experiments involving palladated SCS pincer complexes and diaminopyridine recognition motifs have been

carried out in isolation from one another.^{7,8} In order to realize the primary objective of the UPB concept, the one-step multi-recognition site functionalization of random copolymers via hydrogen bonding and metal coordination, the orthogonal nature of the recognition units must first be elucidated.

To probe this parameter and to explore the versatility of the UPB system, it was rationalized that detailed study of a variety of non-covalent functionalization routes must be carried out. As shown in Figure 5.1, it was envisaged that UPBs could be functionalized using three distinct self-assembly strategies. These routes include: i) directed self-assembly of one terminal recognition motive via either metal coordination or hydrogen bonding, ii) step-wise functionalization starting with either interaction, and ultimately iii) one step self-assembly in which both recognition motifs are spontaneously functionalized in the presence of complimentary recognition units (Figure 5.1).

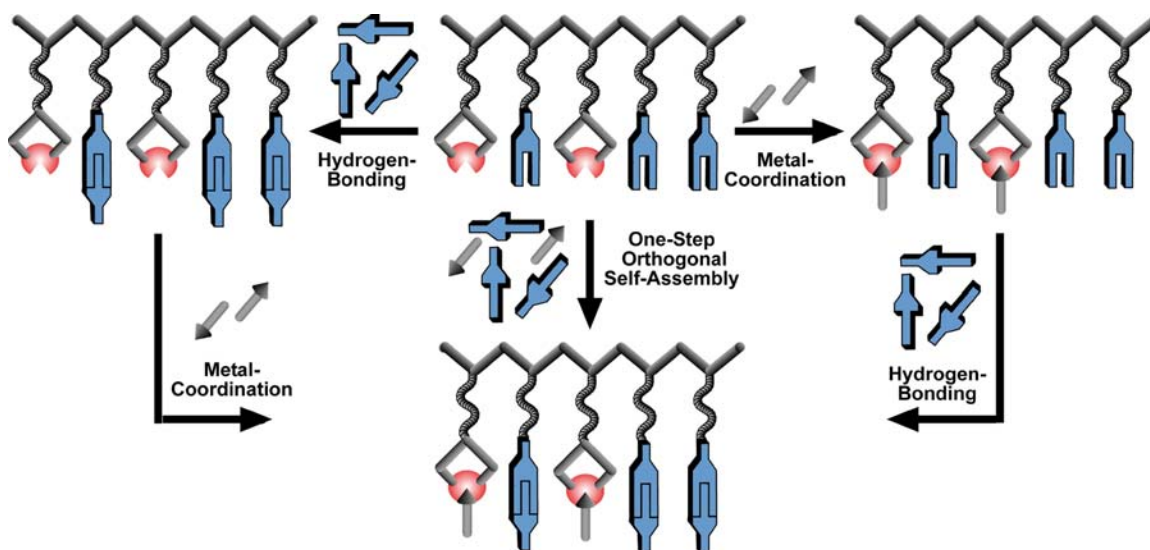


Figure 5.1 A cartoon depicting the formation of complex copolymers using stepwise and one-step, non-covalent multi-functionalization strategies.

5.3 UPB Synthesis and Characterization

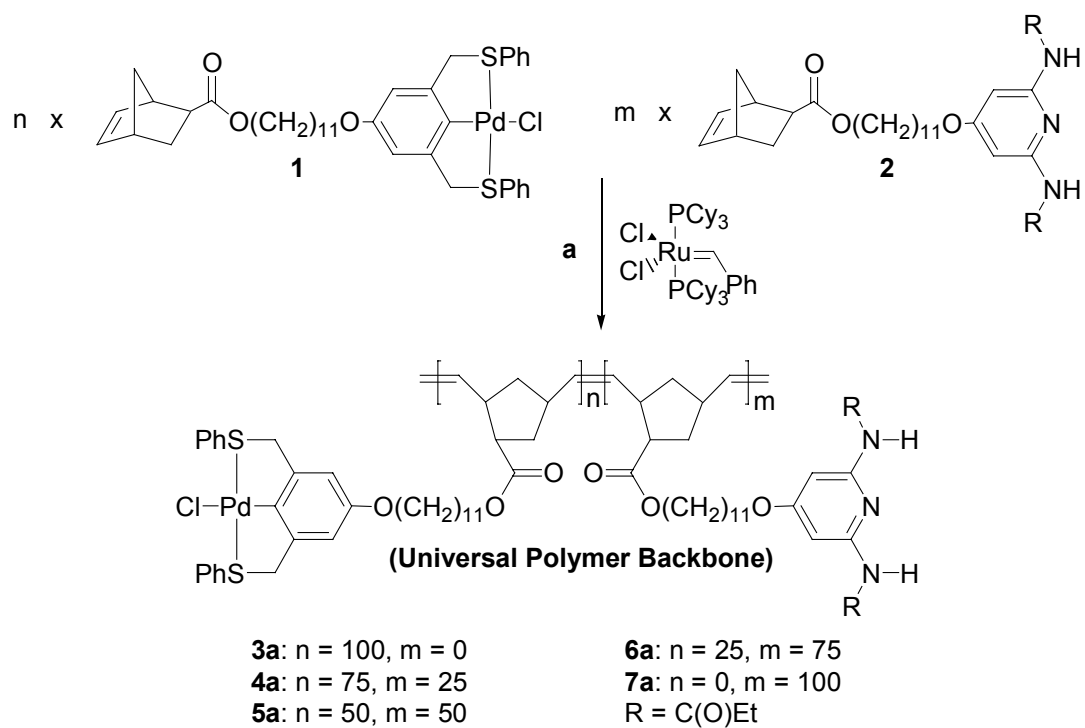
As described in Chapter 4, the synthesis of well defined block copolymers possessing palladated SCS pincer complexes and diaminopyridine residues may be accomplished via living ROMP of isomerically pure *exo*-norbornene monomers **1** and **2**.⁹ Despite this fact, UPBs based on random copolymers were selected as better suited candidates for establishing orthogonality since: i) their composition represents a true mixture of both recognition units that excludes phase segregation and other secondary interactions that might increase the selectivity of the recognition element for its complementary pair, and ii) they are highly soluble, which facilitates the ease of non-covalent functionalization.

In addition, both monomers exhibit polymerization kinetics independent of the terminal recognition motif.⁹ This finding is an important prerequisite that allows for the formation of random copolymers. Furthermore, a linear relationship between molecular weight and monomer to initiator ratios has previously been established for **1** and **2**, allowing for stoichiometric control of copolymer molecular weight.⁹ Thus, by modifying the monomer feed ratios, the copolymer compositions are easily tailored.

To examine the influence of monomer composition on the ability to non-covalently functionalize the resultant copolymers, a series of low polydisperse random copolymers were synthesized (Scheme 5.1, Table 5.1). Furthermore, a series of copolymers composed of fifty percent of each monomer were synthesized with monomer to catalyst ratios of 10:1 (**8a**), 50:1 (**7a**), and 500:1 (**9a**) to study the effect of molecular weight on self-assembly. The resultant copolymers are all soluble in dichloromethane (DCM), however, streaking on the GPC columns was observed for copolymers possessing the diaminopyridine unit in this media. Generally, it was found that the extent of streaking

increases proportionally with an increase in diaminopyridine composition. To circumvent this problem, a more polar solvent, THF, was employed for characterization of **5a-7a**.

Scheme 5.1 UPB synthesis.



Reagents and Conditions: a) CHCl_3 , r.t., 1 h, 100%. Copolymer compositions are expressed as percentages.

Table 5.1 UPB characterization data.

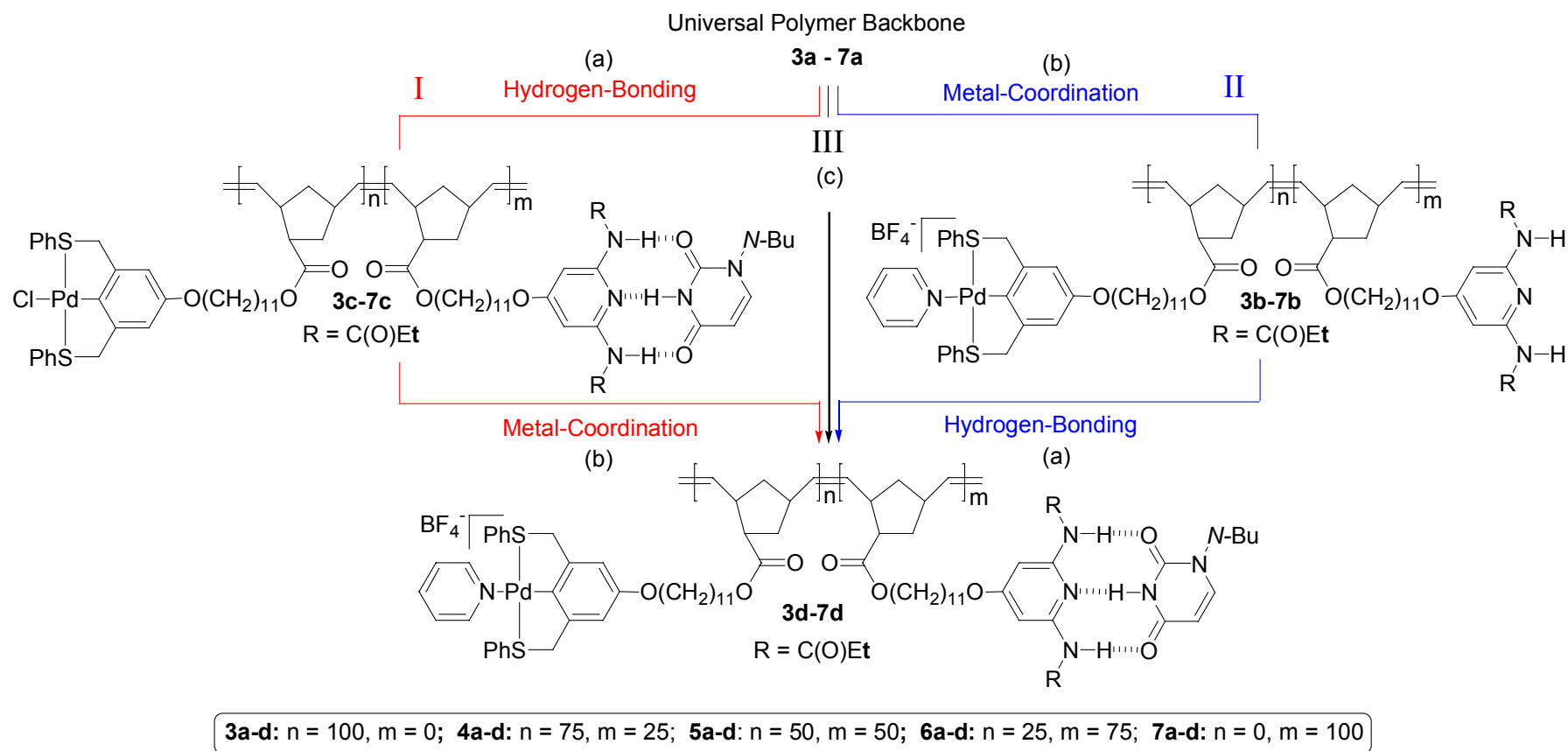
Polymer	Polymer Composition 1:2	[M]/[I]	GPC Eluant	M _n (10 ⁻⁴)	M _w (10 ⁻⁴)	PDI
3a	100:0	50	DCM	7.3	8.0	1.10
4a	75:25	50	DCM	4.5	5.3	1.18
5a	50:50	50	THF	3.0	3.5	1.15
6a	25:75	50	THF	2.7	3.2	1.19
7a	0:100	50	THF	3.6	4.4	1.22
8a	50:50	10	THF	0.56	0.69	1.23
9a*	50:50	500	--	--	--	--

* GPC results are not reported due to insolubility in THF.

5.4 Non-Covalent Functionalization of UPBs

Copolymers **4a-6a** provide the foundation for this chapter's primary goal: the one-step multi-recognition site functionalization of random copolymers via hydrogen bonding and metal coordination. To achieve this objective, several requirements must be realized including strong self-assembly, full solubility of all copolymers, and no interference of the two recognition motifs with each other. To address these concerns, a synthetic scheme was developed and executed that examines the step-wise self-assembly of "functional" anchoring units to each polymer, the effect of functionalization on the solubility, the strength of each self-assembly step, thermal properties of the resultant copolymers, and, ultimately, the one-step orthogonal random copolymer functionalization (Scheme 5.2).

Scheme 5.2 Non-covalent UPB functionalization strategies.



Reagents and Conditions: I.) Step-wise functionalization beginning with hydrogen bonding, II.) step-wise functionalization beginning with metal coordination and III) one-step multi-recognition site self-assembly. (a) *N*-butylthymine, CH_2Cl_2 , (b) pyridine, AgBF_4 , CH_2Cl_2 , (c) *N*-butylthymine, pyridine, AgBF_4 , CH_2Cl_2 .

For ease of characterization, pyridine and *N*-butylthymine have been employed as “functional” complementary recognition units for the Pd^{II} complexes and the diaminopyridine moieties respectively.^{7,8} Copolymers **4a-6a** were functionalized using three distinct methodologies: i) *directed self-assembly* of pyridine to the Pd^{II} complexes or *N*-butylthymine to the diaminopyridine units providing mono-functionalized copolymers **4b-6b** and **4c-6c** respectively, ii) *step-wise functionalization* starting with either hydrogen bonding (Scheme 5.2-I) or metal coordination (Scheme 5.2-II) via two-step sequential addition yielding **4d-6d**, and iii) *orthogonal functionalization* by simple addition of both pyridine and *N*-butylthymine (Scheme 5.2-III) providing the fully functionalized copolymers **4d-6d** in a simple, one-step process. In all cases, the self-assembly of the pyridine is quantitative with strong binding interactions between the diaminopyridine units and *N*-butylthymine. All copolymers are fully soluble in CH₂Cl₂ with the exception of **6b**, which is solubilized by a 75:25 CH₂Cl₂/nitromethane mixture. Addition of *N*-butylthymine to **6b** restores the CH₂Cl₂ solubility of the fully functionalized copolymer **6d**. No diffusion or solubility limitations to this methodology were observed for high or low molecular weight polymers **9a-d** and **8a-d** respectively.

The self-assembly behavior of the step-wise functionalization route beginning with metal coordination can be characterized by monitoring characteristic changes in chemical shifts using ¹H NMR spectroscopy.^{7,8,10,11} Figure 5.2A-C demonstrates the selectivity of the pyridine anchoring unit for the palladated pincer ligand. As depicted, only the α -pyridyl signal at 8.58 ppm shows a characteristic up-field shift to the coordinated species at 8.00 ppm.^{8,10} Notably, the amide signals of the diaminopyridine moiety at 7.93 ppm (Figure 5.2-B) remain unaffected (Figure 5.2-C) by the transformation from **5a** to **5b**.

However, following addition of 1.5 equivalents of *N*-butylthymine a dramatic downfield shift of the amide signal to 9.66 ppm (Figure 5.2-E) is observed in addition to a weaker downfield shift of the imide signal of the *N*-butylthymine from 10.04 ppm (Figure 5.2-D) to 10.53 ppm (Figure 5.2-E).⁷ These results confirm the selectivity of each anchoring unit for its respective recognition motif.

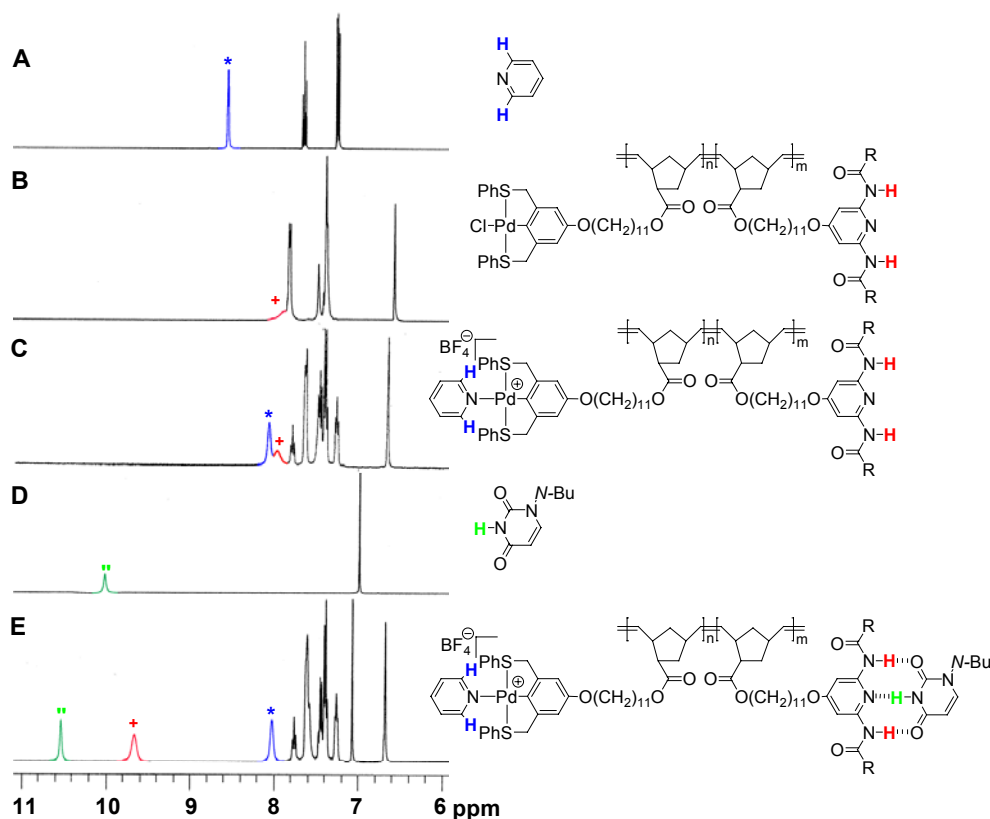


Figure 5.2 The aromatic region of the ^1H NMR spectra depicting the stepwise functionalization (metal coordination followed by hydrogen bonding) of **5a**. A) Pyridine (* = α -pyridyl protons), B) copolymer **5a** (+ = amide protons), C) copolymer following directed metal coordination (**5b**), D) *N*-butylthymine (" = imide proton), and E) fully functionalized copolymer **5d**.

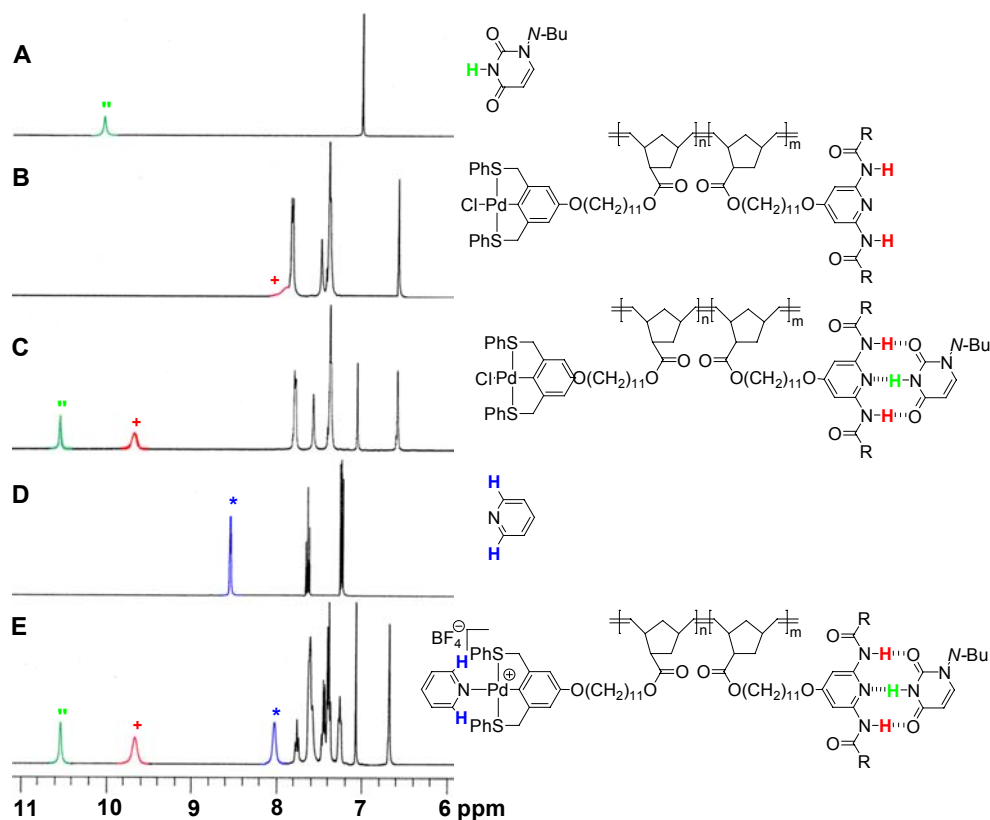


Figure 5.3 The aromatic region of the ^1H NMR spectra depicting the stepwise functionalization (hydrogen bonding followed by metal coordination) of **5a**. A) *N*-butylthymine (“ = imide proton), B) copolymer **5a** (+ = amide protons), C) copolymer following directed hydrogen bonding (**5c**), D) Pyridine (* = α -pyridyl protons), and E) fully functionalized copolymer **5d**.

Similarly, Figure 5.3A-E illustrates the step-wise functionalization of **5a** beginning with hydrogen bonding and ending with metal coordination. Beginning with addition of 1.5 equivalents of *N*-butylthymine, we observe by comparison of Figure 5.3A-C only the diagnostic shifts of the hydrogen bonding amide (7.93 ppm to 9.66 ppm) and imide protons (10.04 ppm to 10.53 ppm) with no observed change of the signals for the aromatic pincer complexes. Once functionalized with *N*-butylthymine, the addition of one

equivalent of pyridine and AgBF_4 resulted in the fully functionalized copolymer **5d** (Figure 5.3-E) whose spectrum is identical to Figure 5.2-E.

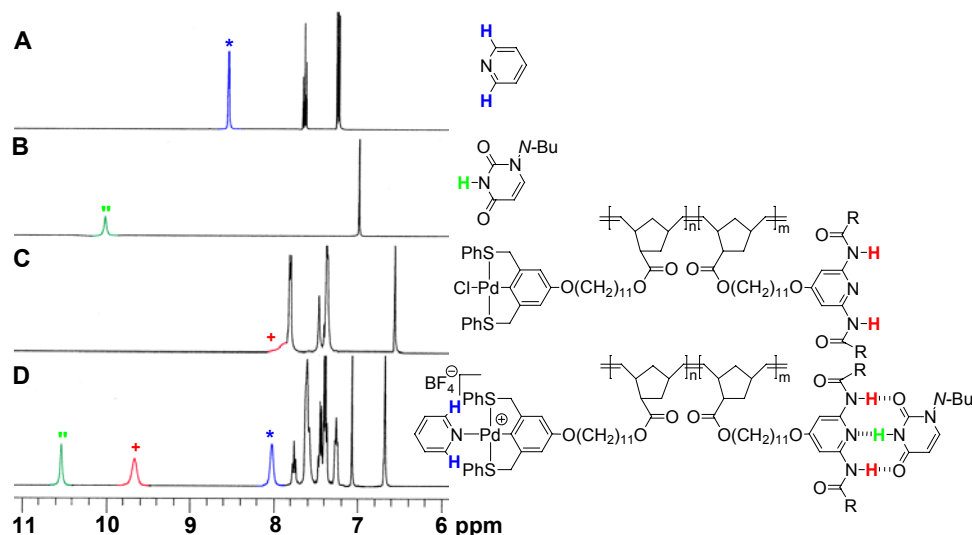


Figure 5.4 The aromatic region of the ^1H NMR spectra depicting the one-step multi-functionalization of **5a**. A) Pyridine (* = α -pyridyl protons) B) *N*-butylthymine (" = imide proton) C) copolymer **5a** (+ = amide protons), and D) fully functionalized copolymer **5d**.

Finally, the one-step multi-functionalization of **5a** was evaluated via ^1H NMR spectroscopy. A large number of significant chemical shifts are visible for the orthogonal transformation of **5a** to **5d**. Most notably, three major shifts occur when comparing Figure 5.4-A, B, and C to Figure 5.4-D: 1) the α -pyridyl signals at 8.58 ppm (Figure 5.4-A) show the characteristic up-field shift to 8.00 ppm (Figure 5.4-D) following coordination, 2) the amide signals of the diaminopyridine moiety at 7.93 ppm (Figure 5.4-C) give a down-field shift to 9.66 ppm (Figure 5.4-D) upon hydrogen bonding, and 3) a significant down-field shift from 10.04 ppm (3-B) to 10.53 ppm (Figure 5.4-D) is

observed for the imide signal for *N*-butylthymine upon association. Again, the final spectra for this one-step process is identical to those obtained via the step-wise routes. Thus, ^1H NMR spectroscopy provides strong evidence for strong and selective binding of the complimentary recognition units and shows that the final, fully functionalized materials are identical, independent of chosen functionalization route.

In addition to selectivity, it is essential that the strength of the non-covalent interactions remain unaltered throughout the course of all functionalization steps. To probe this parameter, ^1H NMR spectroscopy was employed to measure the hydrogen bonding association constants (K_a).^{7,12} In all cases, K_a remains constant within the error ranges with values of $474 \pm 45 \text{ M}^{-1}$, $447 \pm 80 \text{ M}^{-1}$, $537 \pm 97 \text{ M}^{-1}$, $501 \pm 98 \text{ M}^{-1}$ for **2**, **7a**, **5a**, and **5b** respectively. This implies that the hydrogen bonds are unaffected by the polymer backbone and the presence of the functionalized metal-centers.

5.5 Thermal Characterization Studies

To examine the effect of functionalization on the thermal properties, glass-transition temperatures (T_g) and decomposition onsets (T_{dec}) were determined for all polymers (Table 5.2). These parameters were found to be dependent both upon changes in composition as well as functionalization. In general, non-functionalized copolymers showed a decrease in T_g with added thermal integrity as the concentration of diaminopyridine was increased (Table 5.2, row a). In contrast to pyridine coordinated polymers (**3b-6b**), which showed only minor changes in T_g or T_{dec} upon coordination, *N*-butylthymine hydrogen bonded polymers (**3c-6c**) always gave large decreases in T_g and lower decomposition temperatures (Table 5.2, rows a vs. c or d). It is interesting to note that the thermal properties are independent of molecular weight. Polymers possessing 500

(**8a-d**), 50 (**5a-d**) or 10 (**9a-d**) repeat units have identical thermal properties within +/-5 °C of one another (T_g/T_{dec} (°C): **8a** = 69/275, **8b** = 69/277, **8c** = 46/220, **8d** = 44/215, **9a** = 70/275, **9b** = 70/277, **9c** = 41/218, **9d** = 43/219).

Table 5.2 Thermal data for functionalized copolymers.

Entry*	3 T_g/T_{dec} (°C)	4 T_g/T_{dec} (°C)	5 T_g/T_{dec} (°C)	6 T_g/T_{dec} (°C)	7 T_g/T_{dec} (°C)
a	78 / 269	74 / 271	69 / 275	65 / 307	62 / 367
b	69 / 260	77 / 271	67 / 277	78 / 280	--
c	--	62 / 248	48 / 221	42 / 217	31 / 214
d *	--	59 / 242	47 / 219	35 / 215	--

*Values are independent of chosen functionalization route.

To further probe the plasticizer effect on the thermal properties of these materials, a series of copolymers possessing from 0-2 equiv. of *N*-butylthymine and *N*-methyl *N'*-butylthymine were evaluated (Table 5.3). Structurally, the absence of imide protons in *N*-methyl *N'*-butylthymine eliminates the potential for hydrogen bonding (¹H NMR spectroscopy of **9a** and **9b** with *N*-methyl *N'*-butylthymine showed no evidence of amide-carbonyl hydrogen bonding). Therefore, a comparison between *N*-butylthymine and *N*-methyl *N'*-butylthymine should give insights into the influence of hydrogen bonding on the thermal behavior of our materials. To that end, the addition of *N*-butylthymine and *N*-methyl *N'*-butylthymine to copolymer (**9a**) and pyridine-coordinated copolymer (**9b**) both resulted in a linear decrease in the glass transition temperature and a consistent decrease in thermal integrity. The magnitude of this effect for the two additives was significant with consistently lower T_g and T_{dec} values observed for *N*-methyl *N'*-

butylthymine. Thus, the enhanced thermal integrity of the self-assembled *N*-butylthymine functionalized copolymers must be due to stabilization via hydrogen bonding.

Table 5.3 Thermal data: concentration dependence of the complimentary hydrogen bonding unit.

Copolymer	Plasticizer	T _g /T _{dec}	T _g /T _{dec}	T _g /T _{dec}	T _g /T _{dec}	T _g /T _{dec}
		(°C)	(°C)	(°C)	(°C)	(°C)
		0 equiv	0.5 equiv	1.0 equiv	1.5 equiv	2.0 equiv
9a	NBT	69/275	61/258	52/240	41/221	29/200
9b	NBT	69/277	63/262	50/248	43/219	36/181
9a	NMNBT	69/275	49/250	28/226	20/197	--
9b	NMNBT	69/277	43/255	30/229	23/195	--

*NBT = *N*-Butylthymine

*NMNBT = *N*-Methyl *N'*-Butylthymine

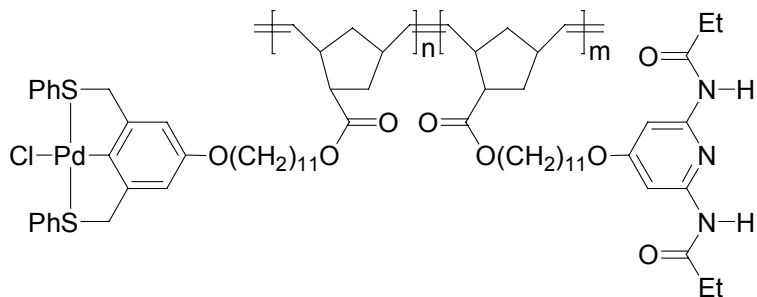
5.6 Conclusion

Herein, a new methodology for random copolymer functionalization based on a non-covalent, one-step, multi-functionalization strategy is introduced.¹³ Copolymers containing both Pd- pincer complexes and diaminopyridine moieties were synthesized using ROMP. Functionalization of the resultant copolymers was accomplished via 1) *directed self-assembly*, 2) *multi-step self-assembly*, and 3) *one-step orthogonal self-assembly*. This system shows complete specificity (orthogonality) of each non-covalent interaction for its complementary recognition unit. This methodology allows for controlled copolymer functionalization in one-simple step and will facilitate rapid development and optimization of random-copolymer based functional materials.

5.7 Experimental

$\text{Ru(=Ph)Cl}_2(\text{PCy}_3)_2$ was purchased from Strem. All monomers and homo-polymers were prepared as previously reported. CDCl_3 was distilled from calcium hydride and degassed prior to use. NMR spectra were taken using a 400 MHz Bruker AMX 400 spectrometer. All spectra are referenced to residual proton solvent. FT-IR data was obtained using a Shimadzu FTIR-8400S infrared spectrophotometer with samples prepared via flash evaporation of polymer solutions (CH_2Cl_2) onto salt plates. UV-VIS data was collected using a Shimadzu UV-2401PC UV-VIS recording spectrophotometer. Gel permeation chromatography (GPC) analyses for **3a** and **4a** were carried out using a Waters 1525 binary pump coupled to a Waters 2414 refractive index detector with CH_2Cl_2 as an eluant on American Polymer Standards 10 μ particle size, linear mixed bed packing columns (2x). GPC analysis for **5a**, **6a**, **7a**, were carried out using a waters 510 binary pump coupled to a Waters 410 differential refractometer with THF as an eluant on an American Polymer Standards column set (100 Å, 1000 Å, 100,000 Å, linear mixed bed). All GPCs were calibrated using polystyrene standards. DSC was performed under nitrogen using a Perkin-Elmer DSC 7 equipped with an Intracooler II cooling device. The temperature program provided heating and cooling cycles between 5 and 200 °C at 40 °C/min. TGA was performed under nitrogen using a Perkin-Elmer TGA 7 and all samples were heated from 50-500 °C.

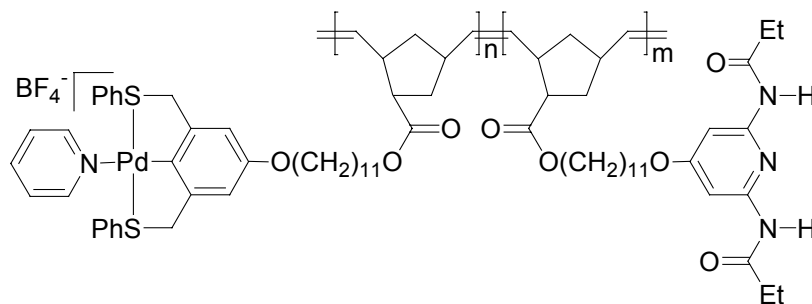
General procedure for the synthesis of UPBs (4a-6a)



Monomers **1** and **2** were weighed, dissolved in degassed, anhydrous CDCl_3 (1 mL per 100 mg), and stirred under an atmosphere of argon. A stock solution of $\text{Ru}(=\text{Ph})\text{Cl}_2(\text{PCy}_3)_2$ was prepared and the desired amount added to the monomer feedstock in one portion. Upon complete polymerization (determined *in situ* via ^1H NMR spectroscopy), a drop of ethyl vinyl ether was added to terminate the polymerization. The final polymers were isolated as dark green solids by precipitation from hexanes followed by prolonged drying on high vacuum (isolated yields: 90-95 %). ^1H NMR (CD_2Cl_2): δ = 7.93 (br s, 2H, CONH), 7.83-7.81 (m, 4H, SPh), 7.48 (m, 2H, Pyr $_{\beta}$), 7.38-7.36 (m, 6H, SPh), 6.57 (s, 2H, ArH), 5.42- 5.17 (br m, 4H, CH=CH), 4.55 (s, 4H, CH_2S), 4.07-3.94 (br m, 6H, CH_2O), 3.84 (br t, J = 6.4 Hz, 2H, CH_2O), 3.16-2.40 (br m, 6H), 2.32 (br m, 4H, CH_2CH_3), 2.12-1.50 (br m, 16H), 1.46-1.07 (br m, 28H), 1.14 (br t, J = 7.4 Hz, 6H, CH_2CH_3). ^{13}C NMR (CD_2Cl_2): δ = 176.2, 173.0, 169.3, 157.7, 152.0, 151.4, 150.7, 134.2, 133.1, 131.9, 130.3, 130.1, 109.4, 96.1, 69.0, 68.6, 64.9, 52.2, 50.8, 48.3, 42.6, 41.6, 36.8, 35.2, 35.1, 32.2, 30.1, 29.9-29.7, 29.5, 29.3, 26.5, 26.4, 25.8, 21.0, 9.6. FT-IR (NaCl): cm^{-1} = 3277, 3054, 2927, 2853, 1727, 1698, 1615, 1582, 1537, 1505, 1438, 1392, 1354,

1316, 1266, 1210, 1162, 1043, 1024, 967, 890, 847, 742, 687. UV-VIS (CH₂Cl₂): λ_{\max} (nm) = 278 (sh), 304(sh), 335.

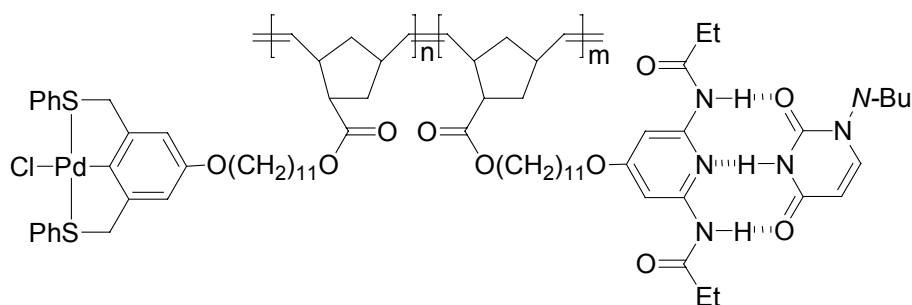
Synthesis of pyridine functionalized UPBs via directed self-assembly (**4b-6b**)



Copolymers **4a-6a** were dissolved in CD₂Cl₂ (0.7 mL per 50 mg). To these solutions, one stoichiometric equivalent (based on the number of pincer complexes) of a pyridine stock solution (in CD₂Cl₂) was added. Subsequently, one equivalent of AgBF₄ (stock solution in nitromethane) was introduced to the mixture and the color changed from dark to pale green. Upon complete coordination, crude polymers **4b-6b** were obtained by filtration over Celite®, removal of the solvent, and drying on high vacuum. To remove excess AgCl salts, the polymers were subjected to repeated (3 times) redissolution in CH₂Cl₂ followed by filtration over Celite®, removal of the solvent, and extensive drying on high vacuum to provide pure **4b-6b**. ¹H NMR (CD₂Cl₂): δ = 8.04 (s, 2H, Pyr _{α} H), 7.93 (br s, 2H, CONH), 7.76 (m, 1H, Pyr _{γ} H), 7.63 (m, 4H, SPh), 7.49-7.37 (br m, 8H, SPh & Pyr _{β}), 7.27 (m, 2H, Pyr _{β}), 6.68 (s, 2H, ArH), 5.42- 5.17 (br m, 4H, CH=CH), 4.74 (br s, 4H, CH₂S), 4.07-3.94 (br m, 6H, CH₂O), 3.84 (br t, J = 6.4 Hz, 2H, CH₂O), 3.16-2.40 (br m, 6H), 2.32 (br m, 4H, CH₂CH₃), 2.12-1.50 (br m, 16H), 1.46-1.07 (br m, 28H), 1.14 (br t, J = 7.4 Hz, 6H, CH₂CH₃). ¹³C NMR (CD₂Cl₂): δ = 176.2, 173.0, 169.3, 158.4, 151.5,

150.7, 147.3, 139.7, 134.2, 132.0, 131.5, 131.1, 130.8, 126.7, 110.1, 96.1, 69.0, 68.6, 64.9, 52.0, 50.8, 48.3, 42.6, 41.6, 36.8, 35.2, 35.1, 32.2, 30.1, 29.9-29.8, 29.5, 29.3, 26.5, 26.4, 25.8, 21.0, 9.6. FT-IR (NaCl): cm^{-1} = 3277, 3054, 2927, 2854, 1725, 1694, 1615, 1580, 1547, 1512, 1437, 1397, 1316, 1267, 1208, 1161, 1062, 1029, 970, 893, 844, 749, 693. UV-VIS (CH_2Cl_2): λ_{max} (nm) = 278 (sh), 315 (sh).

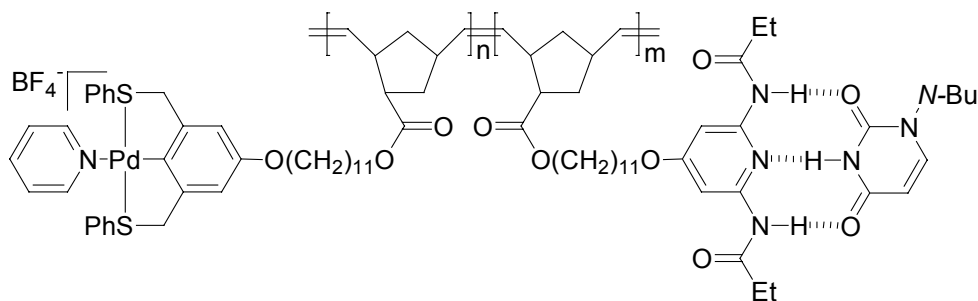
Synthesis of *N*-butylthymine functionalized UPBs via directed self-assembly (4c-6c)



Copolymers **4a-6a** were dissolved in CD_2Cl_2 (0.7 mL per 50 mg). To these solutions, 1.5 stoichiometric equivalents of *N*-butylthymine (based on the number of diaminopyridine moieties: this is the point where the chemical shift of the amide protons no longer changes) were added to the solution and stirred for 5 min. The final polymers were obtained by rota-evaporation of the solvent followed by drying on high vacuum. ^1H NMR (CD_2Cl_2): δ = 10.53 (br s, 1H, NH), 9.66 (br s, 2H, CONH), 7.83-7.81 (m, 4H, SPh), 7.61 (m, 2H, Pyr $_{\beta}$), 7.38-7.36 (m, 6H, SPh), 7.06 (m, 1H, CH=CCH $_3$), 6.57 (s, 2H, ArH), 5.42-5.17 (br m, 4H, CH=CH), 4.55 (br s, 4H, CH $_2$ S), 4.07-3.94 (br m, 6H, CH $_2$ O), 3.84 (br t, J = 6.4 Hz, 2H, CH $_2$ O), 3.70 (t, J = 7.2 Hz, 2H, CH $_2$ N), 3.16-2.40 (br m, 10H), 2.12-1.50 (br m, 21H), 1.46-1.07 (br m, 30H), 1.14 (br t, J = 7.4 Hz, 6H, CH $_2$ CH $_3$), 0.95 (t, J = 7.4 Hz, 3H, CH $_2$ CH $_3$). ^{13}C NMR (CD_2Cl_2): δ = 176.2, 174.2, 169.3, 165.9, 157.7, 152.6,

152.4, 150.7, 141.5, 133.1, 131.9, 130.3, 130.1, 111.0, 109.4, 96.1, 96.8, 69.0, 68.6, 64.9, 52.4, 50.8, 50.1, 48.7, 48.3, 42.6, 41.6, 36.8, 35.2, 35.1, 32.2, 31.6, 30.5, 30.2-29.8, 29.7, 29.5, 29.3, 26.5, 26.4, 20.2, 14.0, 12.5, 9.08. FT-IR (NaCl): cm^{-1} = 3269, 3214, 3162, 3053, 2930, 2857, 1683, 1578, 1546, 1436, 1355, 1315, 1274, 1217, 1165, 1052, 1012, 965, 933, 895, 846, 747, 690. UV-VIS (CH_2Cl_2): λ_{max} (nm) = 271 (sh), 304 (sh), 335.

Synthesis of fully functionalized UPBs via multi-site self-assembly (4d-6d)



A. Multi-step self-assembly starting with metal coordination (4d- 6d)

Copolymers **4b-6b** were dissolved in CD_2Cl_2 (0.7 mL per 50 mg). To these solutions, 1.5 stoichiometric equivalents of N-butylthymine (based on the number of diaminopyridine moieties) was added to the solution and stirred for 5 min. The final polymers were obtained by rota-evaporation of the solvent followed by drying on high vacuum. ^1H NMR (CD_2Cl_2): δ = 10.53 (br s, 1H, NH), 9.66 (br s, 2H, CONH), 8.04 (s, 2H, $\text{Pyr}_\alpha\text{H}$), 7.76 (m, 1H, $\text{Pyr}_\gamma\text{H}$), 7.63 (m, 6H, SPh & Pyr_β), 7.49-7.37 (br m, 6H, SPh), 7.27 (m, 2H, Pyr_β), 7.06 (m, 1H, $\text{CH}=\text{CCH}_3$), 6.68 (s, 2H, ArH), 5.42- 5.17 (br m, 4H, $\text{CH}=\text{CH}$), 4.74 (br s, 4H, CH_2S), 4.07-3.94 (br m, 6H, CH_2O), 3.84 (br t, J = 6.4 Hz, 2H, CH_2O), 3.70 (t, J = 7.2 Hz, 2H, CH_2N), 3.16-2.40 (br m, 10H), 2.12-1.50 (br m, 21H), 1.46-1.07 (br m, 30H), 1.14 (br t, J = 7.4 Hz, 6H, CH_2CH_3) 0.95 (t, J = 7.4 Hz, 3H, CH_2CH_3). ^{13}C NMR

(CD₂Cl₂): δ = 176.2, 174.2, 169.3, 165.9, 158.4, 152.6, 152.4, 151.5, 150.8, 147.3, 141.5, 139.7, 134.2, 131.9, 131.6, 131.0, 126.7, 110.9, 110.0, 96.8, 69.0, 68.6, 64.9, 52.0, 50.8, 50.1, 48.7, 48.3, 42.6, 41.6, 36.8, 35.2, 35.1, 32.2, 31.6, 30.5, 30.2-29.8, 29.7, 29.5, 29.3, 26.5, 26.4, 20.2, 14.0, 12.5, 9.8. FT-IR (NaCl): cm⁻¹ = 3269, 3215, 3162, 3058, 2929, 2856, 1683, 1631, 1580, 1547, 1439, 1435, 1356, 1317, 1281, 1216, 1164, 1060, 968, 933, 895, 847, 804, 751, 692, 682. UV-VIS (CH₂Cl₂): λ_{max} (nm) = 271 (sh), 315(sh).

B. Multi-step self-assembly: starting with hydrogen bonding (4d- 6d)

Copolymers **4c-6c** were dissolved in CD₂Cl₂ (0.7 mL per 50 mg). To these solutions, one stoichiometric equivalent (based on the number of pincer complexes) of a pyridine stock solution (in CD₂Cl₂) was added. Subsequently, one equivalent of AgBF₄ (stock solution in nitromethane) was introduced to the mixture and the color changed from dark to pale green. Upon complete coordination, crude polymers **4d-6d** were obtained by filtration over Celite®, removal of the solvent, and drying on high vacuum. To remove excess AgCl salts, the polymers were subjected to repeated (3 times) redissolution in CH₂Cl₂ followed by filtration over Celite®, removal of the solvent, and extensive drying on high vacuum to provide pure **4d-6d**. ¹H NMR (CD₂Cl₂): δ = 10.53 (br s, 1H, NH), 9.66 (br s, 2H, CONH), 8.04 (s, 2H, Pyr _{α} H), 7.76 (m, 1H, Pyr _{γ} H), 7.63 (m, 6H, SPh & Pyr _{β}), 7.49-7.37 (br m, 6H, SPh), 7.27 (m, 2H, Pyr _{β}), 7.06 (m, 1H, CH=CCH₃), 6.68 (s, 2H, ArH), 5.42- 5.17 (br m, 4H, CH=CH), 4.74 (br s, 4H, CH₂S), 4.07-3.94 (br m, 6H, CH₂O), 3.84 (br t, J = 6.4 Hz, 2H, CH₂O), 3.70 (t, J = 7.2 Hz, 2H, CH₂N), 3.16-2.40 (br m, 10H), 2.12-1.50 (br m, 21H), 1.46-1.07 (br m, 30H), 1.14 (br t, J = 7.4 Hz, 6H, CH₂CH₃) 0.95 (t, J = 7.4 Hz, 3H, CH₂CH₃). ¹³C NMR (CD₂Cl₂): δ = 176.2, 174.2, 169.3, 165.9, 158.4,

152.6, 152.4, 151.5, 150.8, 147.3, 141.5, 139.7, 134.2, 131.9, 131.6, 131.0, 126.7, 110.9, 110.0, 96.8, 69.0, 68.6, 64.9, 52.0, 50.8, 50.1, 48.7, 48.3, 42.6, 41.6, 36.8, 35.2, 35.1, 32.2, 31.6, 30.5, 30.2-29.8, 29.7, 29.5, 29.3, 26.5, 26.4, 20.2, 14.0, 12.5, 9.8. FT-IR (NaCl): cm^{-1} = 3269, 3215, 3162, 3058, 2929, 2856, 1683, 1631, 1580, 1547, 1439, 1435, 1356, 1317, 1281, 1216, 1164, 1060, 968, 933, 895, 847, 804, 751, 692, 682. UV-VIS (CH_2Cl_2): λ_{max} (nm) = 271 (sh), 315(sh).

C. One-step orthogonal self-assembly (4d- 6d)

Copolymers **4a-6a** were dissolved in CD_2Cl_2 (0.7 mL per 50 mg). To these solutions, a stock solution comprised of 1.5 stoichiometric equivalents of N-butylthymine (based on the number of diaminopyridine moieties), 1 equivalent of pyridine, and 1 equivalent of AgBF_4 was added to the solution and stirred for 5 min. Crude polymers **4d-6d** were obtained by filtration over Celite®, removal of the solvent, and drying on high vacuum. To remove excess AgCl salts, the polymers were subjected to repeated (3 times) redissolution in CH_2Cl_2 followed by filtration over Celite®, removal of the solvent, and extensive drying on high vacuum to provide pure **4d-6d**. ^1H NMR (CD_2Cl_2): δ = 10.53 (br s, 1H, NH), 9.66 (br s, 2H, CONH), 8.04 (s, 2H, $\text{Pyr}_\alpha\text{H}$), 7.76 (m, 1H, $\text{Pyr}_\gamma\text{H}$), 7.63 (m, 6H, SPh & Pyr_β), 7.49-7.37 (br m, 6H, SPh), 7.27 (m, 2H, Pyr_β), 7.06 (m, 1H, $\text{CH}=\text{CCH}_3$), 6.68 (s, 2H, ArH), 5.42- 5.17 (br m, 4H, $\text{CH}=\text{CH}$), 4.74 (br s, 4H, CH_2S), 4.07-3.94 (br m, 6H, CH_2O), 3.84 (br t, J = 6.4 Hz, 2H, CH_2O), 3.70 (t, J = 7.2 Hz, 2H, CH_2N), 3.16-2.40 (br m, 10H), 2.12-1.50 (br m, 21H), 1.46-1.07 (br m, 30H), 1.14 (br t, J = 7.4 Hz, 6H, CH_2CH_3) 0.95 (t, J = 7.4 Hz, 3H, CH_2CH_3). ^{13}C NMR (CD_2Cl_2): δ = 176.2, 174.2, 169.3, 165.9, 158.4, 152.6, 152.4, 151.5, 150.8, 147.3, 141.5, 139.7, 134.2, 131.9,

131.6, 131.0, 126.7, 110.9, 110.0, 96.8, 69.0, 68.6, 64.9, 52.0, 50.8, 50.1, 48.7, 48.3, 42.6, 41.6, 36.8, 35.2, 35.1, 32.2, 31.6, 30.5, 30.2-29.8, 29.7, 29.5, 29.3, 26.5, 26.4, 20.2, 14.0, 12.5, 9.8. FT-IR (NaCl): cm^{-1} = 3269, 3215, 3162, 3058, 2929, 2856, 1683, 1631, 1580, 1547, 1439, 1435, 1356, 1317, 1281, 1216, 1164, 1060, 968, 933, 895, 847, 804, 751, 692, 682. UV-VIS (CH_2Cl_2): λ_{max} (nm) = 271 (sh), 315(sh).

Determination of Association Constants

Association constants were measured by titration of a 0.010 M solution of polymers **7a**, **5a**, and **5b** with a 0.005 M solution of *N*-butylthymine, and monitoring of the chemical shift of the amide protons. The molarities of the polymer solutions are based on the number of recognition units. The computer program ChemEquili was used for evaluation of the data.^{7,12}

5.8 References

- (1) Philp, D.; Stoddard, J. F. *Angew. Chem., Int. Ed. Engl.* **1996**, *35*, 1154.
- (2) Lindsey, J. S. *New. J. Chem* **1991**, *15*, 153.
- (3) Wu, A.; Isaacs, L. *J. Am. Chem. Soc.* **2003**, *125*, 4831.
- (4) Lehn, J.-M. *Polym. Int.* **2002**, *51*, 825.
- (5) Lehn, J.-M. *Supramolecular Chemistry*; Wiley-VCH: Weinheim, 1995.
- (6) For an up to date review of single- and multi-site polymer functionalization via self-assembly see Chapter 1 and references therein.
- (7) Stubbs, L. P.; Weck, M. *Chem. Eur. J.* **2003**, *9*, 992.
- (8) Pollino, J. M.; Weck, M. *Synthesis* **2002**, 1277.
- (9) Pollino, J. M.; Stubbs, L. P.; Weck, M. *Macromolecules* **2003**, *36*, 2230.
- (10) Albrecht, M.; Van Koten, G. *Angew. Chem. Int. Ed.* **2001**, *40*, 3750.
- (11) Albrecht, M.; Lutz, M.; Antoine, M. M.; Lutz, E. T. H.; Spek, A. L.; van Koten, G. *J. Chem Soc., Dalton Trans.* **2000**, 3797.
- (12) Solov'ev, V. *ChemEquili 6.1* **1996-1998**.
- (13) The contents of this chapter have been published. See: Pollino, J. M.; Stubbs, L. P.; Weck, M. *J. Am. Chem. Soc.* **2004**, *126*, 563.

CHAPTER 3.

APPLICATIONS OF THE UPB CONCEPT: CROSS LINKED MATERIALS

6.1 Abstract

This chapter explores novel routes to crosslinked and functionalized UPBs. Random UPB terpolymers possessing high concentrations of pendant alkyl chains and small amounts of hydrogen bonding and metal coordinating recognition motifs have been synthesized via ROMP. Non-covalent crosslinking of the resultant copolymers using a directed functionalization strategy leads to dramatic increases in solution viscosities for metal crosslinked polymers while only minor changes in viscosity were observed when hydrogen bonding motifs were employed for crosslinking. The crosslinked materials could be further functionalized via self-assembly by employing the second recognition motif, giving rise to highly functionalized materials with tailored crosslinks. This novel non-covalent polymer crosslinking/functionalization strategy allows for rapid and tunable materials synthesis by overcoming many difficulties inherent to the preparation of covalently crosslinked polymers.

6.2 Introduction

In this chapter, UPB functionalization strategies are extended to the fabrication of non-covalently crosslinked polymers prepared via directional self-assembly processes using both metal coordinating and hydrogen bonding recognition motifs.¹ Furthermore, a

novel crosslinking/functionalization strategy based on one-step orthogonal multisite self-assembly is introduced where the polymeric scaffold is non-covalently crosslinked using one recognition motif, while the other operates simultaneously and selectively to functionalize the backbone (Figure 6.1). These strategies move the focus of this thesis from development of methodology to applications and offers new possibilities for simple and rapid formation of a variety of functionalized and crosslinked polymeric materials.

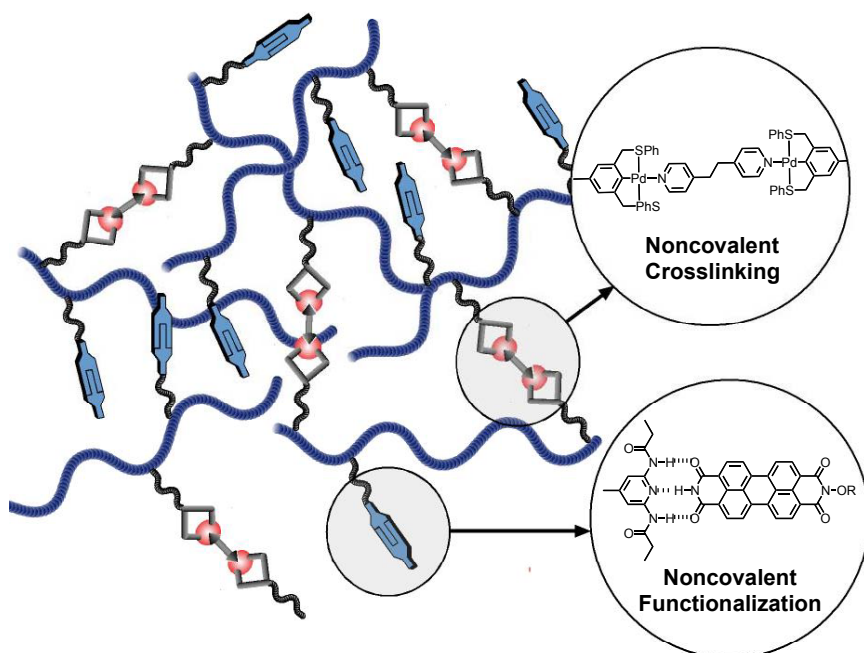


Figure 6.1 A cartoon depicting multi-step self-assembly via metal coordination based crosslinking and polymer functionalization via hydrogen bonding.

In polymer chemistry, the term “crosslinking” usually implies covalent chemical crosslinking, which often provides enhanced mechanical properties and higher thermal stability. Well established routes to crosslinked materials include vulcanization, radiation methods, and photochemical methods, as well as by introducing labile functional groups

into the side-chains.^{2,3} Unfortunately, many disadvantages arise as a consequence of covalent crosslinking. Crosslinking gives rise to poor polymer solubility and an inability to mold materials. The use of crosslinked polymers in industrial processes also has environmental consequences, as these materials are not recyclable due to their inherently poor processability.² Many solutions to these problems have been previously investigated including the incorporation of crosslinkers that undergo rapid thermal or oxidative degradation pathways.^{3,4} These methodologies, however, require covalent bond breakage and are considered unidirectionally reversible. Others have employed strong secondary interactions between polymer chains so that the final material exhibits physical attributes of thermoset materials while remaining thermoplastic.²

More recently, well-designed, strong, and fully reversible non-covalent recognition motifs have been used to prepare crosslinked materials.⁵⁻¹¹ In all cases, side-chain functionalized polymers based on a single recognition unit (usually hydrogen bonding) are employed.^{7,9-11} For example, Coates and coworkers synthesized thermoplastic elastomers from polyolefins possessing pendant self-dimerizing ureidopyrimidinone hydrogen bonding units.¹¹ Furthermore, fully reversible macromolecular architectures such as liquid crystalline materials, smart gels, and microscale molecular objects can be accessed using non-covalent crosslinking methodologies.^{7,9} For example, Kato employed imidazolyl-benzoic acid complexes to create a variety of thermally reversible liquid crystalline networks⁷ and Rotello and coworkers exploited diaminopyridine-thymine complex formation in order to prepare thermally reversible microspheres.⁹

Aside from hydrogen bonding, only a limited number of reports include non-covalent interactions, such as metal coordination, for reversible crosslinked materials formation.¹²

Compared to hydrogen bonding interactions, metal coordination recognition motifs are exceptionally strong.¹³⁻¹⁷ The reversibility of coordination complexes is possible using chemical methodologies such as ligand displacement reactions.^{18,19} Thus, non-covalently crosslinked materials based on coordination motifs may possess distinct advantages for the preparation of crosslinked materials due to their inherent strength and reversibility. Herein, the use of both metal coordination and hydrogen bonding interactions are employed to prepare crosslinked materials that stem from a single UPB and a detailed study of how each recognition unit and their inherent strength effects solution viscosity and materials properties is carried out.

6.3 Research Design

The random copolymer structures (UPBs) previously described (Chapter 5), are derived from only two monomer units containing hydrogen bonding or metal coordination recognition motifs for self-assembly.²⁰ Here, a third, non-functionalized monomer, which dilutes and spaces-out the molecular recognition containing monomers, is incorporated into the copolymer design. Terpolymers for the present study were designed to possess high concentrations of non-functionalized monomer and low concentrations of both recognition motifs in order to study crosslinking and functionalization while simultaneously maintaining good polymer properties including solubility. Norbornene monomers terminally functionalized with palladated sulfur-carbon-sulfur (SCS) pincer complexes¹⁵ and diaminopyridines^{21,22} are structurally identical to those used in Chapters 4 and 5.^{20,23} However, a third monomer based on cyanuric wedges²⁴⁻²⁶ was also introduced so that two unique UPBs, each possessing a different hydrogen bonding motif, could be accessed. This facilitates exploration of how

hydrogen bond strength affects crosslinking since weaker diaminopyridine-thymine complexes undergo only acceptor-donor-acceptor (ADA) to donor-acceptor-donor (DAD) triple hydrogen bonds ($K_a = \text{approx. } 500\text{-}600 \text{ M}^{-1}$), whereas stronger cyanuric wedges (ADA-ADA arrays) can bind to isophthalamide receptors (DAD-DAD arrays) via six hydrogen bonds ($K_a = \text{approx. } 10^6 \text{ M}^{-1}$) (Figure 6.2).^{9,21,22,24-26}

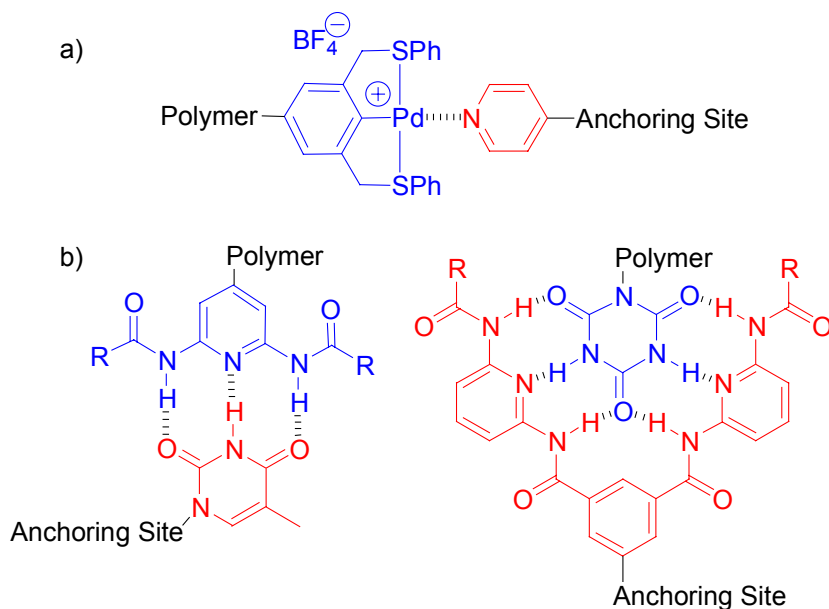


Figure 6.2 Recognition motifs for self-assembly and crosslinking studies: a) metal coordination, b) hydrogen bonding.

Non-covalent crosslinkers were made from alkyl chains containing pyridine, uracil derivatives,^{9,27} or isophthalamide derivatives^{24,25} at each terminus. These recognition units bind palladated pincer complexes,¹⁵ diaminopyridine moieties,^{21,22} or cyanuric wedges,^{24,25} respectively. Structurally simple non-covalent crosslinkers were employed to facilitate ease in crosslinker synthesis and polymer characterization. Soluble perylene moieties bisfunctionalized with ADA recognition counterparts were also prepared.²⁸⁻³⁰ It

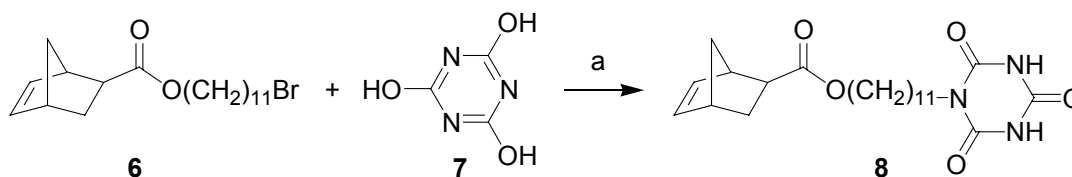
was rationalized that this unique class of functional compounds, commonly employed in the design of electro-optical materials, could serve two purposes: i) as hydrogen bonding crosslinking agents and ii) as photoluminescent chromophores.²⁸⁻³⁰

For small molecule functionalization studies, pyridine, *N*-butyl thymine,²² and isophthalamides^{24,25} were employed. These compounds possess so-called anchoring sites^{16,31,32} where advanced functional entities may be attached using an alkyl tether (Figure 6.2). Furthermore, they are structurally simple to facilitate ease in characterization while simultaneously allowing for one-step, non-covalent approaches to functionalized and crosslinked polymeric materials to be fully demonstrated.

6.4 Monomer and Terpolymer (UPB) Synthesis

All monomers were derived from isomerically pure *exo*-norbornene-2-carboxylic acid.^{23,33,34} Monomers **1** and **2** were synthesized as previously described in Chapter 4.²³ Cyanuric acid monomer **8** was prepared from bromoester **6** in one step (Scheme 6.2).

Scheme 6.1 Cyanuric acid functionalized monomer synthesis.

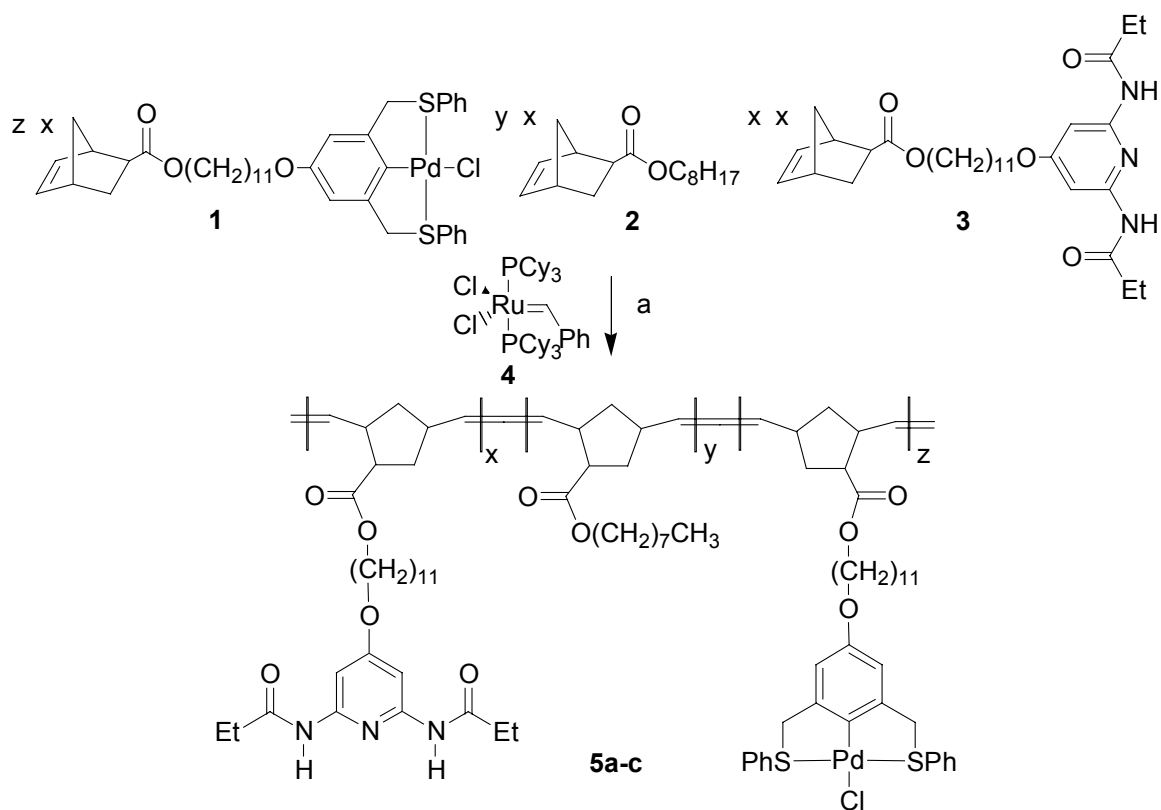


Reagents and Conditions: a) K₂CO₃, DMSO, 25 °C, 48 h, 58%.

ROMP was carried out in chloroform using Grubbs' first generation initiator **4**.³⁵⁻³⁸ Monomers **1**, **2**, and **3** or **1**, **2**, and **8** yielded random terpolymers **5a-c** and **9**, respectively

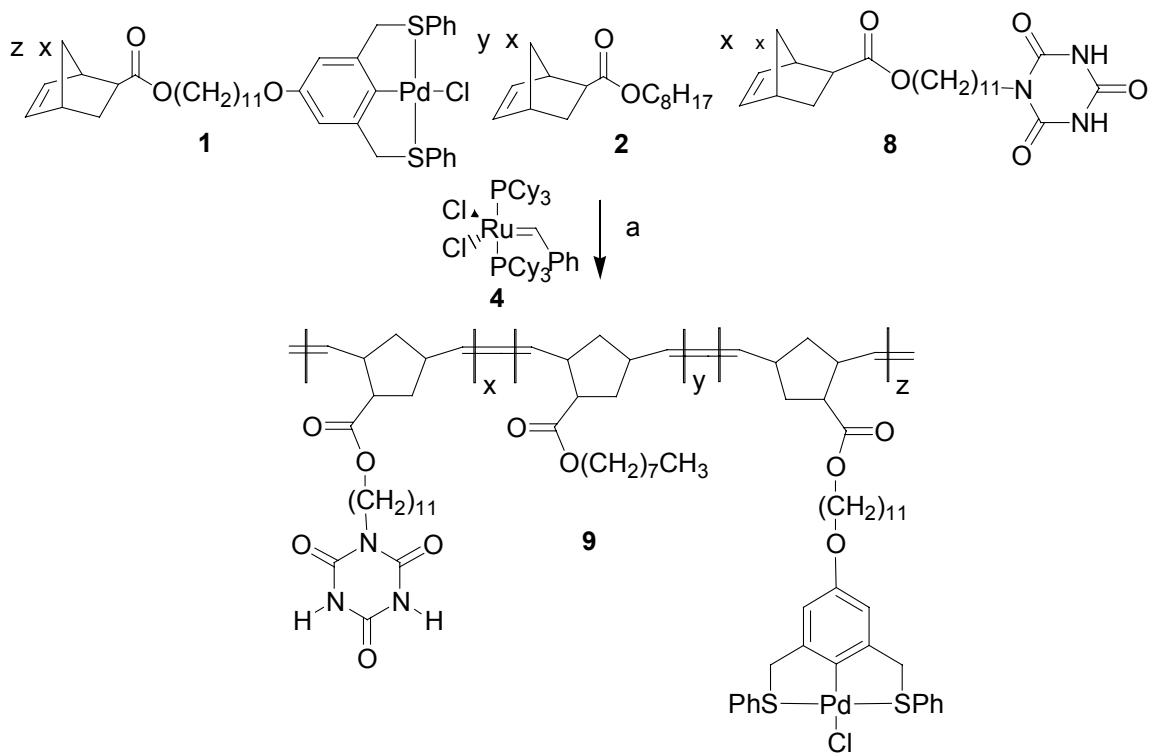
(Scheme 6.2 and Scheme 6.3). In all cases, monomer to catalyst ratios of 200:1 were employed and complete conversion was observed within six hours at ambient temperatures. The resultant copolymers possessed low polydispersities and molecular weights independent of monomer composition (Table 6.1) as determined by GPC analysis. Crosslinking agent **10** was commercially available and **12a-b**²⁷⁻³⁰ and **14**²⁴ were synthesized according to literature protocols.

Scheme 6.2 Synthesis of random terpolymer **5**.



Reagents and Conditions: a) CHCl_3 , r.t., 1 h, 100%.

Scheme 6.3 Synthesis of random terpolymer **9**.



Reagents and Conditions: a) CHCl_3 , r.t., 1 h, 100%.

Table 6.1 UPB characterization data.

Entry*	Composition (%)			M_n (10^{-3})	M_w (10^{-3})	PDI
	x	y	z			
5a	97	1.5	1.5	40	52	1.28
5b	95	2.5	2.5	41	50	1.22
5c	90	5.0	5.0	44	55	1.26
9	95	2.5	2.5	41	52	1.25

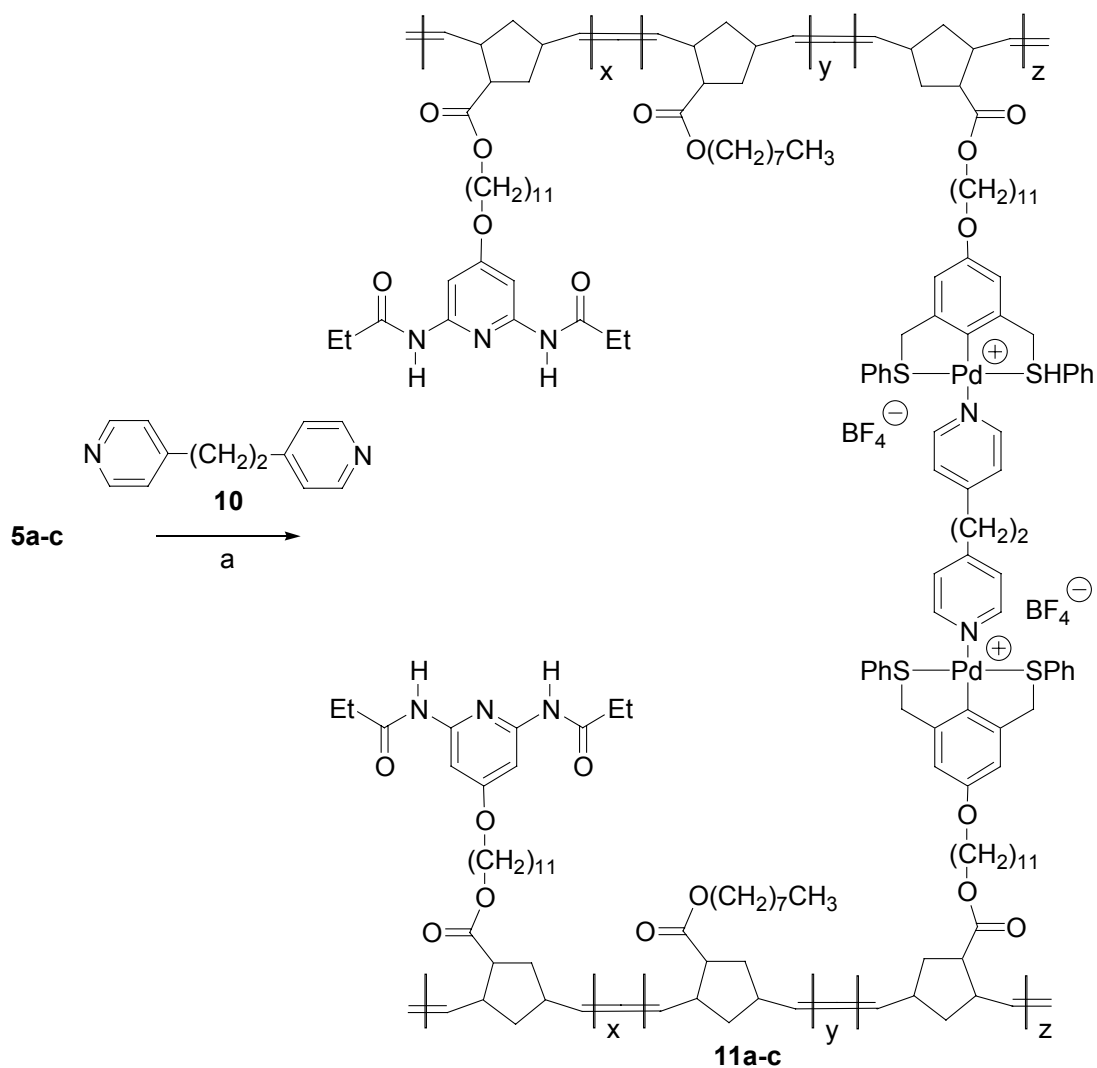
* $[\text{M}] / [\text{I}] = 200:1$

6.5 Directed Self-Assembly: Non-Covalent Crosslinking

After synthesis, copolymers **5a-c** and **9** were non-covalently crosslinked using a directed self-assembly strategy. This methodology allows for a single interaction, metal coordination or hydrogen bonding to be individually and selectively addressed.²⁰ The objective of these preliminary studies was to explore the versatility and limitations of the UPB concept by rapidly and quantitatively creating crosslinked materials via self-assembly. Crosslinking copolymers **5a-c** and **9** with **10**, **12**, and **14** allowed for a variety of variables to be probed including: i) the density of recognition motifs located in the UPB, ii) the different types of interactions: metal coordination versus hydrogen bonding, and iii) the strength of various hydrogen bonding motifs and the crosslinkers effect on solution viscosity.

Initially, metal coordination based crosslinking was explored through the study of palladium-pyridine metal-ligand interactions.^{14-16,19} Copolymers **5a-c** were functionalized using one equivalent of **10** to yield polymeric networks **11a-c** containing 1.5%, 2.5%, and 5% crosslinks, respectively. In each case, crosslinking was selective, quantitative, and instantaneous as determined by NMR (Scheme 6.4).^{20,23}

Scheme 6.4 Directed crosslinking via metal coordination.



Reagents and Conditions: a) $\text{AgBF}_4(\text{aq})$, CHCl_3 , r.t., 100%.

Viscosity is an excellent indicator for the degree of crosslinking and is highly dependent upon the solution concentration.^{2-4,11} At constant polymer concentrations, crosslinking leads to dramatic increases in solution viscosities when compared to non-crosslinked polymer solutions.¹¹ In order to carry out comparisons between metal coordinated and hydrogen bonded polymers, a concentration region for each polymeric

network (**11a-c**) that falls between gel formation and non-viscous flow had to be identified. To accomplish this goal, copolymers **11a-c** were dissolved in chloroform at variable concentrations and “time of flows” were measured relative to pure chloroform using a Cannon–Fenske viscometer.³ Relative viscosities, presented in Figure 6.3, show a strong dependence on both the amount of crosslinker contained within the UPB backbone and the solution concentration. As depicted, the concentration curve for **11a**, possessing 1.5% crosslinks gradually rose to high viscosities reaching gelation at approximately 45 g/L whereas **11c**, containing 5.0% crosslinks, sharply increased in viscosity becoming a gel at a lower concentration of 20 g/L. Compound **11b**, containing 2.5% crosslinks, fell between these two extremes, gelling at approximately 27 g/L (Figure 6.3).

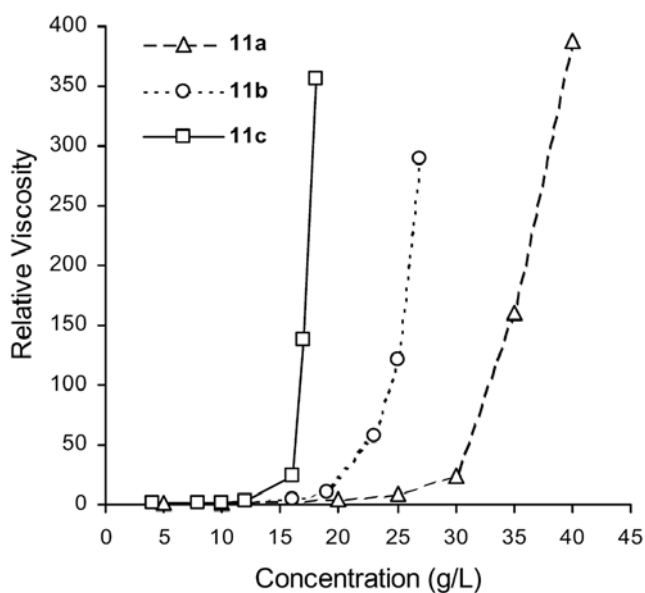
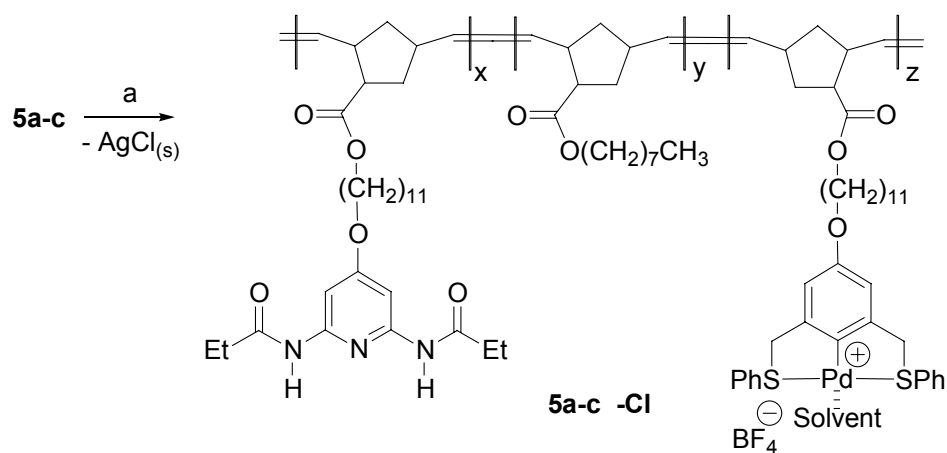


Figure 6.3 Plot of relative viscosity as a function of solution concentration for metal crosslinked copolymers with varying concentrations (**11a** = 1.5%, **11b** = 2.5%, **11c** = 5.0%) of recognition units in the backbone.

All polymers were activated prior to coordination by removal of the chloride from the palladium metal center using AgBF_4 , resulting in the formation of highly charged polymeric species containing BF_4^- counter ions (**5a-c -Cl**) (Scheme 6.5). Upon removal of the chloride, noticeable increases in viscosity were visually observed for chloroform solutions of **5a-c -Cl**.^{15,16,19,39} One explanation for this phenomenon could be competitive intra/intermolecular coordination of the diaminopyridine moieties to the palladated metal centers.^{2,40}

Scheme 6.5 Polymer activation at the metal center.



Reagents and Conditions: a) $\text{AgBF}_4(\text{aq})$, CHCl_3 , r.t., 100%.

To probe this theory, a series of viscosities at variant solution concentrations were measured for neutral polymer **5b**, activated polymer **5b -Cl**, and bispyridine crosslinked polymeric network **11b** (Figure 6.4). While slight increases in solution viscosities were observed when comparing **5b -Cl** to **5b**, these changes were negligible when compared to the viscosity changes measured for **11b**. Thus, increases in viscosity upon activation of

5b are most likely not due to intra/intermolecular palladium-diaminopyridine crosslinking, but probably arise as a consequence of ionic aggregate formation in non-polar solvents.^{2,40}

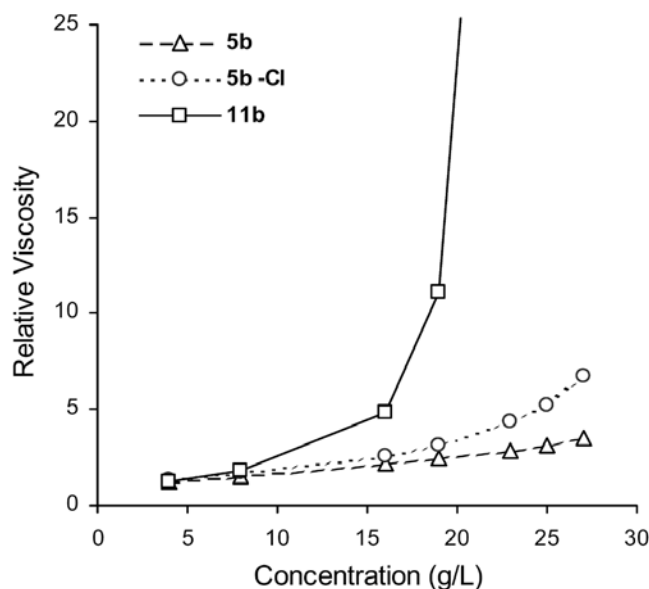


Figure 6.4 Plot of relative viscosity as a function of solution concentration indicating large differences in solution viscosity between metal crosslinked (**11b**) and non-crosslinked copolymers (**5b** and **5b-Cl**).

Solution viscosities can also be easily tuned through alteration of the amount of crosslinker added.^{2,3,11} Indeed, titration of **5b** with **10** at a concentration of 30 g/L resulted in exponential growth of viscosity as a function of added equivalents of crosslinker leading to gelation at less than one equivalent (Figure 6.5). Addition of more than one equivalent of crosslinker led to decreases in viscosity due to the formation of palladium-pyridine complexes possessing a terminal uncoordinated pyridine as excess pyridine complexes became available.

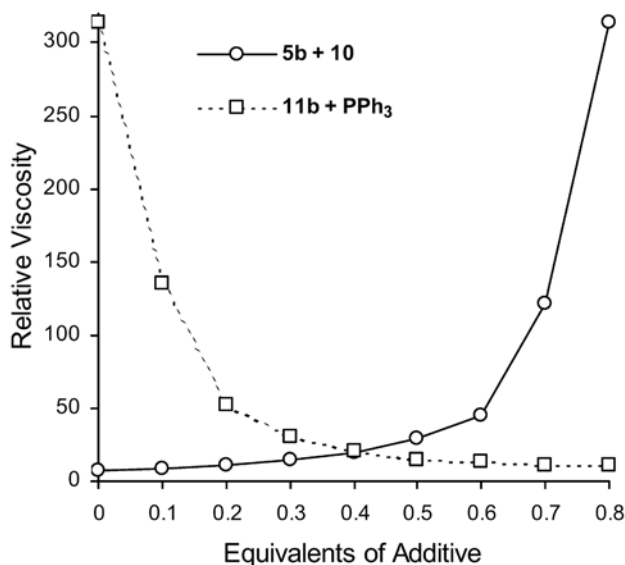


Figure 6.5 Plot of relative viscosity as a function of added mole equivalents of metal crosslinker **10** and the same polymer solution following titration with PPh₃.

Another possibility to tailor the degree of crosslinking of **11a-c** is by the addition of compounds such as PPh₃ that compete for the coordination onto the metal center. It is known that some ligands on functionalized palladated SCS pincer complexes such as nitriles and pyridines can be quantitatively displaced by stronger ones.^{15,19} Thus, it was reasoned that subjecting crosslinked polymers **11a-c** to PPh₃ would provide a simple method to deconstruct non-covalently crosslinked polymers and to tailor viscosities. To investigate this approach, crosslinked polymer **11b** was titrated with PPh₃. The resulting titration curve depicts an exponential decrease in viscosity, giving merit to the concept of chemo-reversible crosslinking (Figure 6.5).

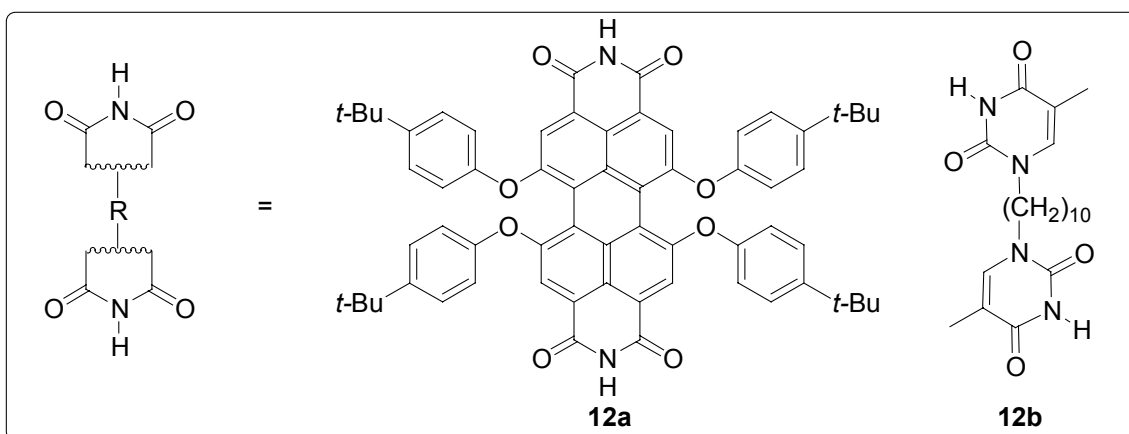
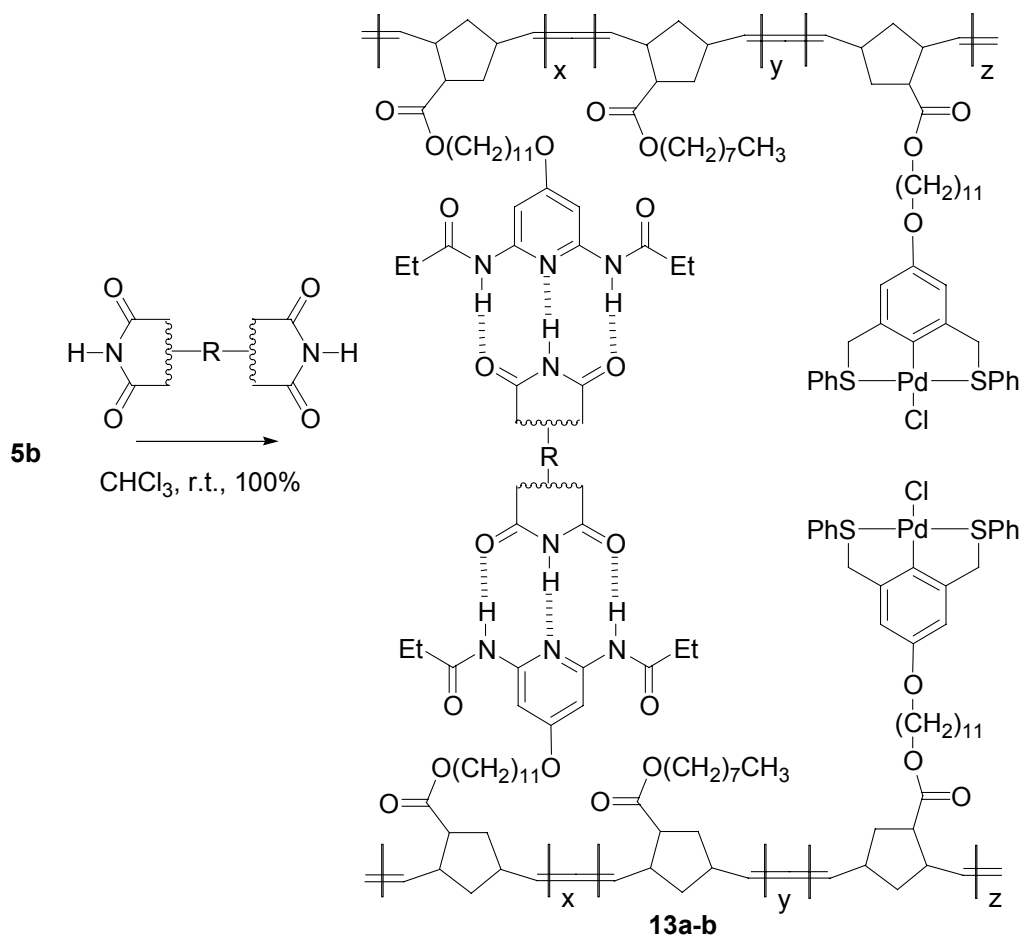
After establishing basic crosslinking conditions for metal coordination, the use of hydrogen bonding motifs for crosslinking was investigated. UPB **5b**, containing 2.5% crosslinks was employed for these studies. Scheme 6.6 presents the use of

thymine/diaminopyridine complementary pairs used in crosslinking. Copolymer **5b** was functionalized with either bisperylene **12a** or bisthymine derivative **12b** by simple 1:1 mixing of the two components (based on the number of recognition motifs) in anhydrous chloroform to form hydrogen bonded polymers **13a** and **13b** respectively (Scheme 6.6).

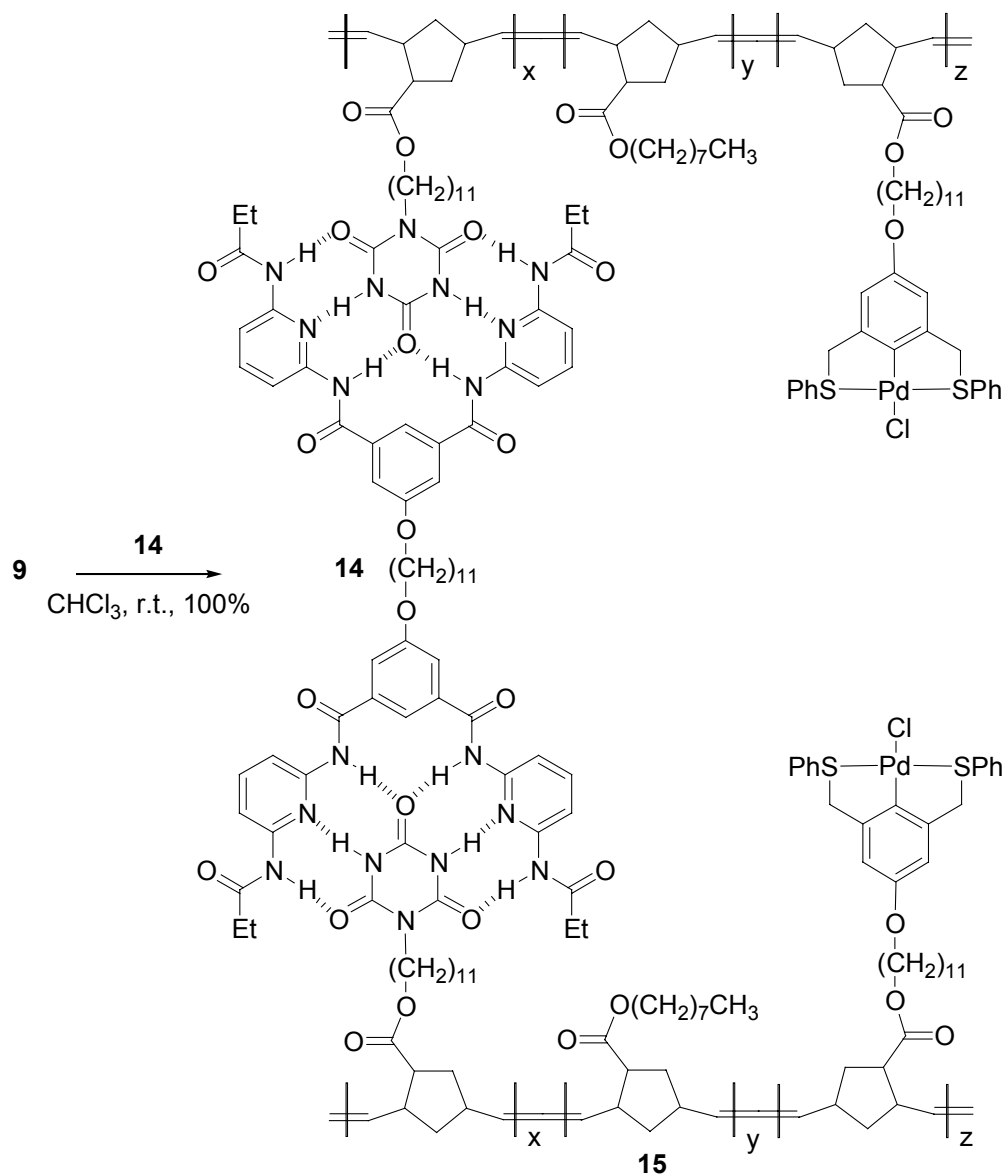
The strength of the hydrogen bonding based crosslinking was examined using solution viscosity titration experiments, identical to those described for **11b**. In contrast to **11b**, upon titration of **5b** with **12a** or **12b** at a concentration of 30 g/L only minor increases in viscosity were observed (Figure 6.6). In comparison to their metal coordinated analog **11b**, hydrogen bonded complexes **13a-b** showed almost a 100 times less change in relative viscosities upon crosslinking. Albeit, it is well known that hydrogen bonds are significantly weaker than metal coordination bonds.^{13,41} However, such a dramatic difference in solution viscosities was unexpected and may be due, in part, to shear forces acting upon the relatively weak hydrogen bonding interactions.²⁻⁴

In an effort to implement stronger hydrogen bonding motifs, terpolymer **9** was prepared possessing palladated pincer ligands and cyanuric wedges. The latter are known to form six hydrogen bonds when complexed with tetra diaminopyridine moieties (**14**) giving rise to association constants as high as 10^6 M^{-1} .^{24,25} Terpolymer **9** was crosslinked with **14** via simple 1:1 mixing of the two components in chloroform (Scheme 6.7). Titration of **9** with **14** at a concentration of 30 g/L led to a large increase in viscosity when compared with **13a** and **13b** (Figure 6.6). However, this system remains inferior when compared to its metal coordinated analog **11b**, showing 33 times lower viscosities upon crosslinking.

Scheme 6.6 Directed crosslinking via triple hydrogen bonded diaminopyridine-thymine interactions.



Scheme 6.7 Directed crosslinking via cyanuric wedges (ADA-ADA arrays) that bind to isophthalamide receptors (DAD-DAD arrays).



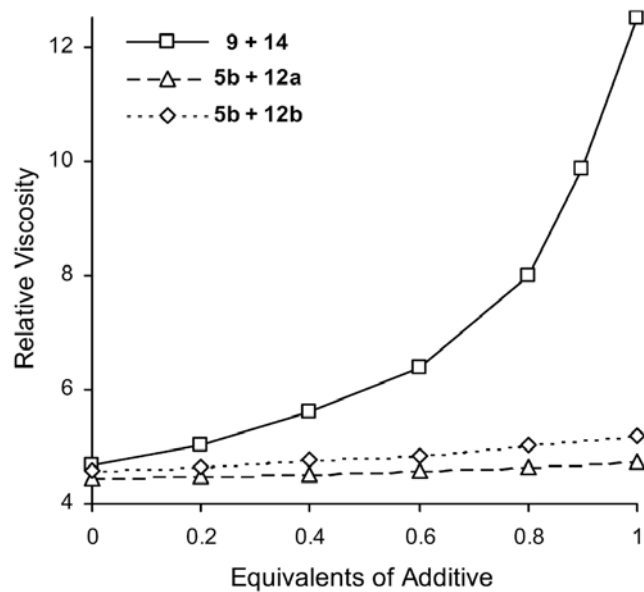


Figure 6.6 Plot of relative viscosity as a function of added mole equivalents of hydrogen bonding crosslinkers **12a**, **12b**, and **14**.

In addition to studying solution viscosities, all copolymers were characterized using DSC and TGA to determine glass-transition temperatures (T_g) and decomposition onsets (T_{dec}), respectively. Table 6.2 summarizes this data. In general, polymeric networks synthesized by the crosslinking via metal coordination displayed higher glass-transition temperatures than their hydrogen bonding analogs. However, all crosslinked polymers show higher decomposition temperatures when compared to their non-crosslinked counterparts.

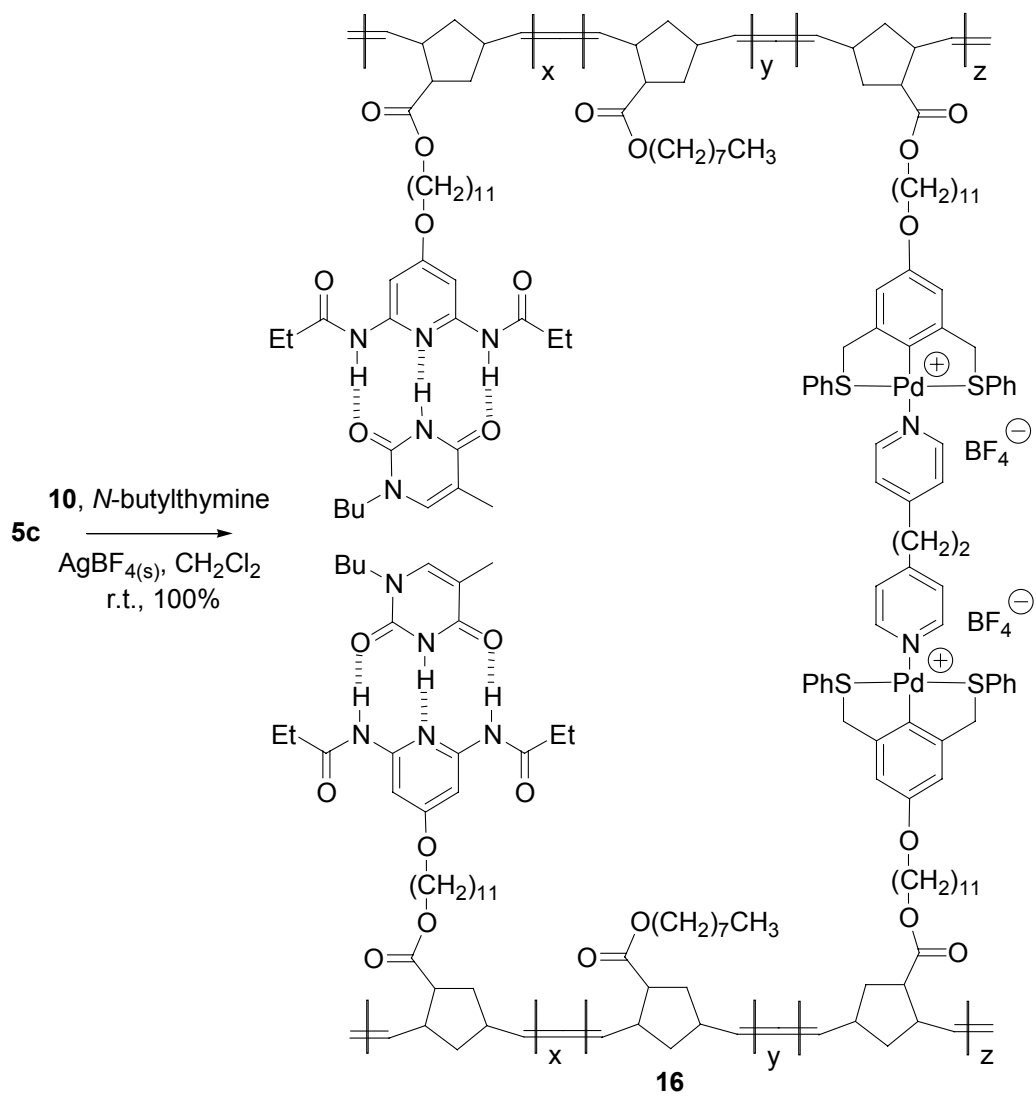
Table 6.2 Thermal characterization data for crosslinked UPBs.

Entry	Composition (%)			T _g (°C)	T _{dec} (°C)
	x	y	z		
5a	97	1.5	1.5	-42	393
5b	95	2.5	2.5	-38	395
5c	90	5	5	-32	381
9	95	2.5	2.5	-37	388
11a	97	1.5	1.5	-42	418
11b	95	2.5	2.5	-26	415
13a	95	2.5	2.5	-40	394
13b	95	2.5	2.5	-74	405
15	95	2.5	2.5	-43	433

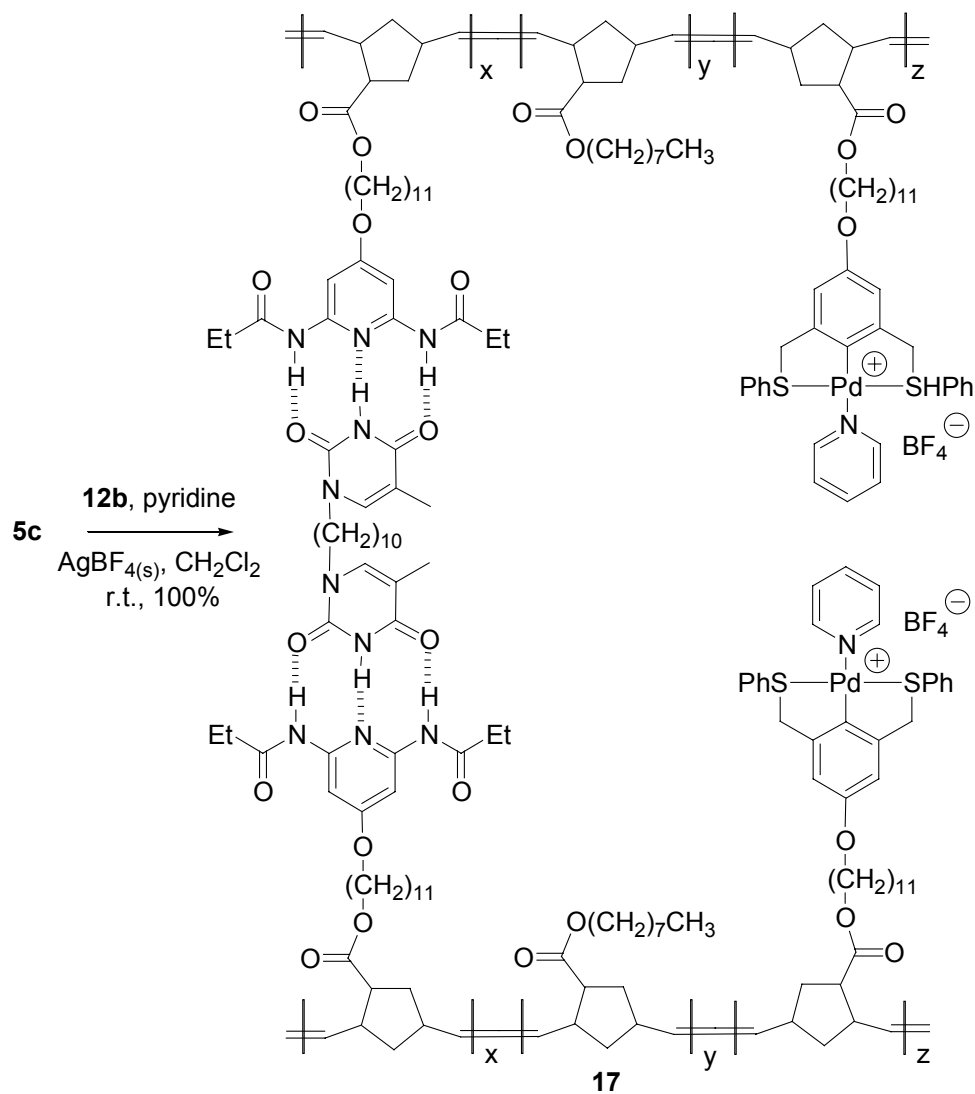
6.6 One-Step Orthogonal Self-assembly: Crosslinking and Small Molecule Functionalization

The ultimate goal of this study, the design and rapid synthesis of functionalized and crosslinked polymeric materials using selective, non-covalent interactions, was accomplished by combining the crosslinking strategies described above with small molecule self-assembly. Polymer **5c** was functionalized in one-step by mixing metal crosslinker **10** with *N*-butylthymine in CH₂Cl₂, which instantaneously yielded **16** (Scheme 6.8). Likewise, combining hydrogen bonding crosslinker **12b**, polymer **5c** and pyridine in CH₂Cl₂ quantitatively provided **17** (Scheme 6.9).

Scheme 6.8 One-step orthogonal self-assembly with metal coordination based crosslinking and hydrogen bonding small molecule functionalization.



Scheme 6.9 One-step orthogonal self-assembly with hydrogen bonding based crosslinking and metal coordination small molecule functionalization.



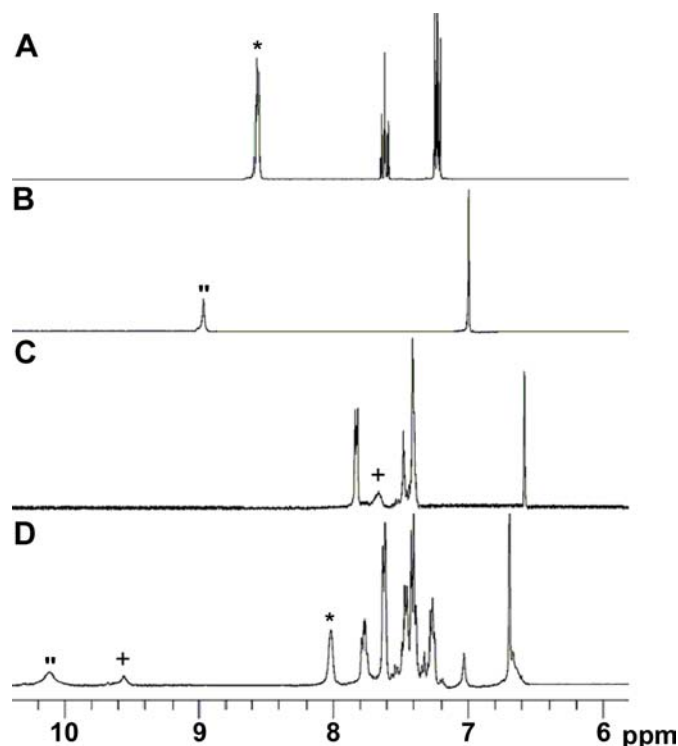


Figure 6.7 The aromatic region of the ^1H NMR spectra showing one-step multifunctionalization of **5c** with hydrogen bonding crosslinker **12b** and pyridine. A) Pyridine (* = α -pyridyl protons), B) Crosslinker **12b** (" = imide proton), C) Terpolymer **5c** (+ = amide protons); and D) Crosslinked and functionalized copolymer **17**.

The one-step functionalization/crosslinking of **5c** was evaluated by ^1H NMR spectroscopy. For example, a large number of significant chemical shifts are visible for the orthogonal transformation of **5c** to **17**. Three diagnostic shifts take place when comparing Figure 6.7-A, B, and C to Figure 6.7-D: i) the α -pyridyl signals of pyridine at 8.58 ppm (Figure 6.7-A) show a characteristic up-field shift to 8.01 ppm (Figure 6.7-D) upon coordination, ii) the amide signals of the diaminopyridine moiety at 7.68 ppm (Figure 6.7-C) give a down-field shift to 9.56 ppm (Figure 6.7-D) upon hydrogen bonding, and iii) a large down-field shift from 8.75 ppm (Figure 6.7-B) to 10.10 ppm (Figure 6.7-D) is observed for the imide signal for bis-thymine **12b** upon association.

Similar diagnostic shifts were observed when following the ^1H NMR signals arising from bis-pyridine **10** (from 8.47 ppm to 8.02 ppm) and *N*-butylthymine (from 10.04 ppm to 10.43 ppm) during the preparation of **16**. Thus, ^1H NMR spectroscopy provides strong evidence for selective, non-covalent polymer crosslinking and small molecule self-assembly clearly demonstrating the proposed orthogonal crosslinking/functionalization scheme is a viable option for fast and easy functionalized polymeric network formation.

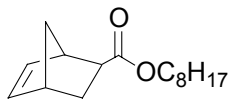
6.7 Conclusion

In this chapter, the orthogonal crosslinking and functionalization of UPBs based on substituted norbornene monomers containing hydrogen bonding and metal coordination motifs are described. Crosslinking or functionalization can be carried out via a modular approach using either metal coordination or hydrogen bonding. Furthermore, through choice of the crosslinking motif and agent and its concentration, the strength of the crosslinked polymeric network can be tailored toward potential applications. This strategy allows for: i) functionalization directed by self-assembly of one recognition unit via hydrogen bonding or metal coordination, ii) non-covalent crosslinking by metal coordination or hydrogen bonding, and ultimately iii) one-step functionalization and crosslinking in which both recognition motifs are spontaneously self-assembled in the presence of complementary recognition units. This novel non-covalent polymer crosslinking/functionalization strategy allows for rapid and tunable materials synthesis thereby overcoming many problems inherent to covalently crosslinked polymers.

6.8 Experimental

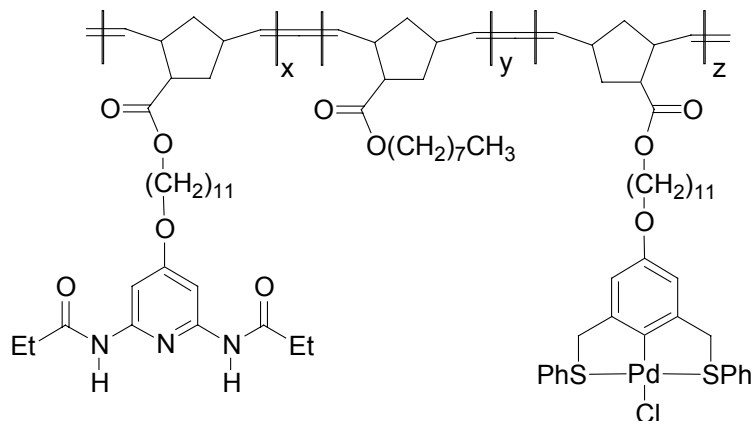
All chemicals were reagent grade and used without further purification unless otherwise indicated. CDCl_3 was distilled from calcium hydride and degassed prior to use. CH_2Cl_2 was dried via passage through copper oxide and alumina columns.⁴² Cyanuric acid **7** and bispyridine **10** were purchased from Acros Organics and Aldrich, respectively. $\text{Ru}(=\text{Ph})\text{Cl}_2(\text{PCy}_3)_2$ **4** was purchased from Strem. Monomers **1** and **3**,²³ crosslinkers **12a**,²⁸⁻³⁰ **12b**,²⁷ and **14**,²⁴ bromoester **6**,²³ and *N*-butylthymine,²² were prepared as previously reported. NMR spectra were taken using either a 300 MHz Varian Mercury spectrometer or a 400 MHz Bruker AMX 400 spectrometer. All spectra were referenced to residual proton solvent. Mass spectral analysis was kindly provided by the Georgia Tech Mass Spectrometry Facility using a VG-70se spectrometer. Elemental analyses were performed by Atlantic Microlabs, Norcross GA. Solution viscosity was measured using a size 100 Cannon–Fenske viscometer (Cannon Instrument Co., State College, PA, USA). The time of fall was recorded with a stopwatch reading to 0.1 s. GPC analyses were carried out using a waters 510 binary pump coupled to a Waters 410 differential refractometer with THF as an eluant on an American Polymer Standards column set (100 Å, 1000 Å, 100,000 Å, linear mixed bed). All GPCs were calibrated using polystyrene standards. DSC was performed under nitrogen using a Mettler Toledo DSC 822e. The temperature program provided heating and cooling cycles between -100 and 200 °C at 10 °C/min. TGA was performed under nitrogen using a Shimadzu TGA-50 and all samples were heated from 25-450 °C at a rate of 10 °C/min.

Synthesis of *exo*-bicyclo[2.2.1] hept-5-ene-2-carboxylic acid octyl ester (**2**)



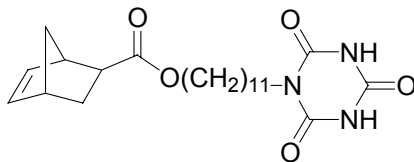
Exo-bicyclo[2.2.1] hept-5-ene-2-carboxylic acid^{33,34} (2.1 g, 0.015 mol) and octan-1-ol (2.0 g, 0.015 mol) were combined, dissolved in anhydrous CH₂Cl₂ (20 mL), and placed under an atmosphere of argon. To the stirred solution, dicyclohexyl-carbodiimide (3.2 g, 0.015 mol) and dimethyl-pyridin-4-yl-amine (cat. amt.) in CH₂Cl₂ (20 mL) were added at 25 °C. Immediately, the solution became turbid with formation of a white precipitate. Following stirring at reflux for 16 h, the mixture was cooled, diluted with CH₂Cl₂ (200 mL), and the precipitate filtered off. The filtrate was dried (MgSO₄) and the solvent removed to give a solid residue that was further purified by column chromatography (SiO₂, eluant: 1:1 CH₂Cl₂/hexanes). Drying provided pure **2** (3.5g, 92%) as a colorless oil. ¹H NMR (300 MHz CDCl₃): δ = 6.12 (m, 2H, CH=CH), 4.07 (t, 2H, *J* = 6.6 Hz, CH₂O), 3.03 (m, 1H), 2.92 (m, 1H), 2.21 (m, 1H), 1.92 (m, 1H), 1.68-1.49 (m, 3H), 1.41-1.24 (m, 12H), 0.88 (t, 3H, *J* = 7.1 Hz, CH₂CH₃). ¹³C NMR (300 MHz CDCl₃): δ = 176.1, 137.8, 135.6, 64.6, 46.6, 46.3, 43.2, 41.6, 31.8, 30.4, 29.3, 28.7, 25.9, 22.7, 14.2. Anal. Calcd. for C₁₆H₂₆O₂: C, 76.75; H, 10.47; Found: C, 76.69; H, 10.51.

Synthesis of palladated SCS pincer/diaminopyridine/alkyl terpolymers (**5a-c**)



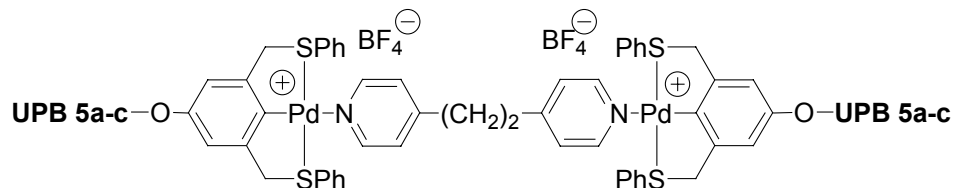
Monomers **1** (171 mg, 0.22 mmol, 5%), **2** (1.0 g, 4.0 mmol, 90%), and **3** (117 mg, 0.22 mol, 5%) were weighed, placed under an atmosphere of argon and dissolved in anhydrous, degassed CDCl₃ (10 mL). A stock solution of catalyst **4** (36.6 mg/mL) in CDCl₃ was prepared and 0.5 mL (18.3 mg, 0.022 mmol) was added in one portion to the vigorously stirred monomer solution. Upon complete polymerization (ca. 6h), 10 drops of ethyl vinyl ether were added to terminate the polymerization. Subsequent precipitation from cold methanol and prolonged drying on high vacuum gave polymers **5a-c** (isolated yield = 1.2 g, 93%). ¹H NMR (300 MHz CD₂Cl₂): δ = 7.84 (m, 4H, SPh), 7.68 (br s, 2H, CONH), 7.49 (m, 2H, Py_βH), 7.42 (m, 6H, SPh), 6.58 (s, 2H, ArH), 5.48- 5.15 (m, 6H, CH=CH), 4.58 (br s, 4H, CH₂S), 4.01 (m, 8H, CH₂O), 3.85 (br t, 2H, *J* = 6.7 Hz, CH₂O), 3.2-1.0 (m, 73H), 1.14 (br t, *J* = 7.4 Hz, 6H, CH₂CH₃), 0.86 (t, 3H, *J* = 7.1 Hz, CH₂CH₃). ¹³C NMR (300 MHz CD₂Cl₂): δ = 175.4, 172.1, 168.6, 156.9, 151.2, 150.6, 149.9, 134.2, 132.4, 132.0, 131.2, 129.7, 129.4, 108.7, 95.4, 68.5, 68.1, 64.3, 51.8, 50.2, 49.8, 49.6, 47.7, 47.4, 43.1, 42.5, 42.1, 41.8, 41.1, 37.2, 36.9, 36.2, 31.9, 30.6, 29.6-28.7, 27.0, 26.9, 26.4, 26.0, 22.7, 14.0, 9.2.

Synthesis of *exo*-bicyclo[2.2.1] hept-5-ene-2-carboxylic acid 11-(2,4,6-trioxo-[1,3,5] triazinan-1-yl)-undecyl ester (8)



Anhydrous K_2CO_3 (1.5 g, 11 mmol) was added to a stirred solution of bromoester **7** (2.0 g, 5.4 mmol) and cyanuric acid **6** (6.9 g, 54 mmol) in DMSO (60 mL). The reaction mixture was allowed to stir at ambient temperature for 48 h, and was subsequently poured into a saturated solution of $NaHSO_3$ (aq) (500 mL), extracted with a 1:1 mixture of CH_2Cl_2 /diethyl ether (3 x 200 mL), dried ($MgSO_4$), and the solvent removed *in vacuo*. The residue was purified by column chromatography (SiO_2 , eluant: 1:1 EtOAc/hexanes) and dried on high vacuum to yield **8** (1.3 g, 58 %) as a white solid. 1H NMR (300 MHz $CDCl_3$): δ = 9.55 (br s, 2H, NH), 6.11 (m, 2H, CH=CH), 4.07 (t, 2H, J = 6.6 Hz, CH_2O), 3.88 (t, 2H, J = 7.7 Hz, CH_2N), 3.03 (m, 1H), 2.91 (m, 1H), 2.22 (m, 1H), 1.91 (m, 1H), 1.69-1.49 (m, 5H), 1.41-1.24 (m, 18H). ^{13}C NMR (300 MHz $CDCl_3$): δ = 176.2, 149.1, 148.3, 137.8, 135.6, 64.6, 46.6, 46.4, 43.2, 42.0, 41.6, 30.3, 29.4, 29.3, 29.2, 29.1, 28.7, 27.7, 26.6, 25.9. MS (EI): m/z (%) = 419.24100 (M^+ , 419.24202 calcd.) Anal. Calcd. for $C_{22}H_{33}N_3O_5$: C, 62.99; H, 7.93; N, 10.02 Found: C, 63.07; H, 7.98; N, 10.00.

Synthesis of metal coordination crosslinked polymers (**11a-c**)

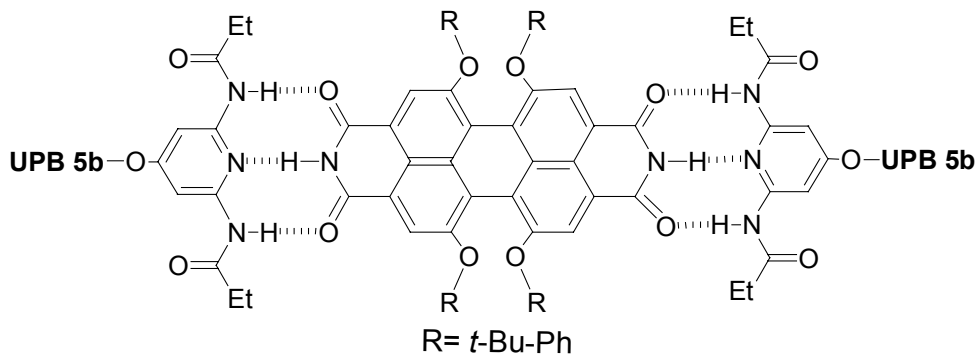


Polymers **5a-c** (300 mg) were dissolved in CHCl_3 (10mL) and one equivalent of $\text{AgBF}_4(\text{aq})$ (based on Pd-Cl content) was added. Immediately, the solution changed color from green to yellow and an increase in viscosity was observed. Following removal of the precipitated silver salts via filtration over cotton, one equivalent of bispyridine (**10**) was slowly added to the vigorously stirred solutions. Subsequent removal of the solvent and prolonged drying on high vacuum provided **11a-c** as a green solid in quantitative yield. $^1\text{H NMR}$ (400 MHz CD_2Cl_2): δ = 8.08 (s, 2H, $\text{Pyr}_\alpha\text{H}$), 7.75 (m, 4H, SPh), 7.68 (br s, 2H, CONH), 7.51-7.41 (br m, 8H, SPh & Pyr_βH), 7.23 (m, 2H, Pyr_βH), 6.68 (s, 2H, ArH), 5.48- 5.15 (m, 6H, CH=CH), 4.72 (br s, 4H, CH_2S), 4.04 (m, 8H, CH_2O), 3.87 (br t, 2H, $J = 6.7$ Hz, CH_2O), 3.2-1.0 (m, 75H), 1.14 (br t, $J = 7.4$ Hz, 6H, CH_2CH_3), 0.86 (t, 3H, $J = 7.1$ Hz, CH_2CH_3).

Synthesis of hydrogen bonding crosslinked polymers (**13a-b** and **14**)

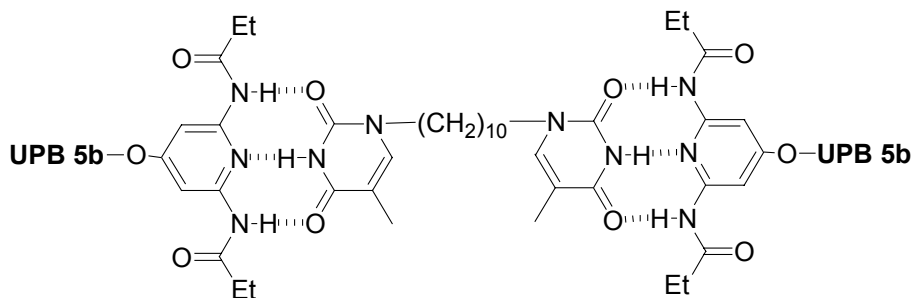
To a stirred solution of Polymer **5b** or **9** (300 mg) in anhydrous CHCl_3 (10mL), one equivalent of **12a-b** or **14** (based on hydrogen bonding motif content) was added respectively. The mixtures were then allowed to stir for 5 min, followed by removal of the solvent. Subsequent drying on high vacuum afforded polymers **13a-b** and **15** in quantitative yields.

Crosslinked polymer (13a)



$^1\text{H NMR}$ (400 MHz CD_2Cl_2): $\delta = 9.27$ (br s, 1H, CONHCO), 8.14 (s, 2H, $\text{ArH}_{\text{peryl}}$), 7.83 (m, 4H, SPh), 7.52 (m, 2H, $\text{Pyr}_{\beta}\text{H}$), 7.42 (m, 6H, SPh), 7.29 (d, 4H, $J = 8.9$ Hz, $t\text{-BuArH}$), 6.86 (d, 4H, $J = 8.9$ Hz, OArH), 6.58 (s, 2H, ArH), 5.50- 5.18 (m, 6H, $\text{CH}=\text{CH}$), 4.61 (br s, 4H, CH_2S), 4.03 (m, 8H, CH_2O), 3.87 (br t, 2H, $J = 6.7$ Hz, CH_2O), 3.4-1.2 (m, 91H), 1.16 (br t, $J = 7.4$ Hz, 6H, CH_2CH_3), 0.88 (t, 3H, $J = 7.1$ Hz, CH_2CH_3).

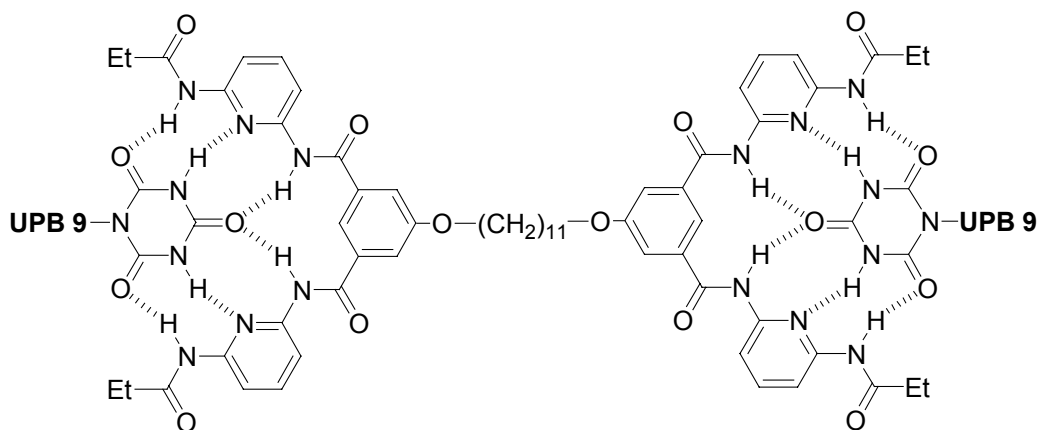
Crosslinked polymer (13b)



$^1\text{H NMR}$ (400 MHz CD_2Cl_2): $\delta = 10.10$ (br s, 1H, CONHCO), 9.56 (brs, 2H, CONH), 7.84 (m, 4H, SPh), 7.57 (m, 2H, $\text{Pyr}_{\beta}\text{H}$), 7.42 (m, 6H, SPh), 7.05 (s, 1H, $\text{CH}=\text{CCH}_3$), 6.58 (s, 2H, ArH), 5.48-5.15 (m, 6H, $\text{CH}=\text{CH}$), 4.58 (br s, 4H, CH_2S), 4.01 (m, 8H, CH_2O),

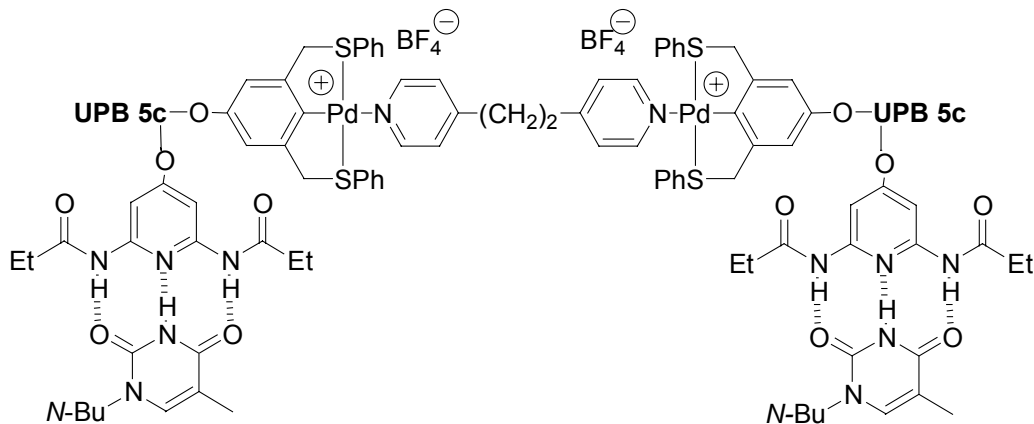
3.85 (br t, 2H, $J = 6.7$ Hz, CH₂O), 3.70 (br t, 2H, $J = 7.4$ Hz, CH₂N), 3.2-1.0 (m, 84H),
 1.14 (br t, $J = 7.4$ Hz, 6H, CH₂CH₃), 0.88 (t, 3H, $J = 7.1$ Hz, CH₂CH₃).

Crosslinked polymer (15)



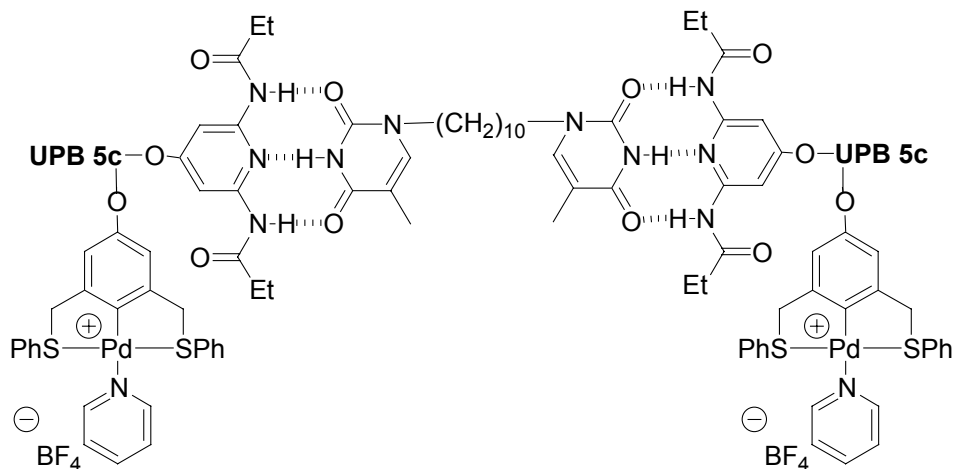
¹H NMR (400 MHz CD₂Cl₂): $\delta = 9.87$ (br s, 2H, CONH), 9.51 (br s, 2H, CONH), 8.11-
 7.93 (br m, 7H, PyrH, ArH), 7.84 (m, 4H, SPh), 7.67 (s, 2H, ArH), 7.42 (m, 6H, SPh),
 6.58 (s, 2H, ArH), 5.50-5.07 (m, 6H, CH=CH), 4.55 (br s, 4H, CH₂S), 4.09-3.9 (m, 8H,
 CH₂O), 3.8-3.7 (m, 4H, CH₂O, CH₂N), 3.2-1.0 (m, 81H), 1.18 (t, 6H, 0.86 $J = 7.5$ Hz,
 CH₂CH₃) (t, 3H, $J = 7.1$ Hz, CH₂CH₃).

Synthesis of metal crosslinked and *N*-butylthymine hydrogen bonded Polymer (16).



One equivalent of **10**, $\text{AgBF}_4(\text{s})$, and *N*-butylthymine were added to a stirred solution of Polymer **5c** (100 mg) in anhydrous CH_2Cl_2 (10 mL), which instantaneously and quantitatively yielded polymer **16**. ^1H NMR (400 MHz CD_2Cl_2): δ = 10.43 (br s, 1H, CONHCO), 9.43 (br s, 2H, CONH), 8.02 (s, 2H, $\text{Pyr}_\alpha\text{H}$), 7.75 (m, 4H, SPh), 7.53-7.37 (br m, 8H, SPh & Pyr_βH), 7.23 (m, 2H, Pyr_βH), 7.05 (s, 1H, $\text{CH}=\text{CCH}_3$), 6.68 (s, 2H, ArH), 5.48- 5.15 (m, 6H, $\text{CH}=\text{CH}$), 4.70 (br s, 4H, CH_2S), 4.04 (m, 8H, CH_2O), 3.87 (br t, 2H, J = 6.7 Hz, CH_2O), 3.68 (br t, 2H, J = 7.4Hz, CH_2N), 3.2-1.0 (m, 82H), 1.14 (br t, J = 7.4 Hz, 6H, CH_2CH_3), 0.95 (t, J = 7.4 Hz, 3H, CH_2CH_3), 0.86 (t, 3H, J = 7.1 Hz, CH_2CH_3).

Synthesis of hydrogen bonding crosslinked and pyridine metal coordinated polymer (17).



One equivalent of **12b**, pyridine, and $\text{AgBF}_4(\text{s})$, were added to a stirred solution of Polymer **5c** (100 mg) in anhydrous CH_2Cl_2 (10 mL) to instantaneously yield polymer **17** in quantitative yield. ^1H NMR (400 MHz CD_2Cl_2): δ = 10.10 (br s, 1H, CONHCO), 9.56 (brs, 2H, CONH), 8.01 (s, 2H, $\text{Pyr}_\alpha\text{H}$), 7.77 (m, 1H, $\text{Pyr}_\gamma\text{H}$), 7.62 (m, 6H, SPh and Pyr_β), 7.49-7.37 (br m, 6H, SPh), 7.27 (m, 2H, Pyr_β), 7.03 (m, 1H, $\text{CH}=\text{CCH}_3$), 6.69 (s, 2H, ArH), 5.48-5.15 (m, 6H, $\text{CH}=\text{CH}$), 4.58 (br s, 4H, CH_2S), 4.01 (m, 8H, CH_2O), 3.85 (br t, 2H, $J = 6.7$ Hz, CH_2O), 3.70 (br t, 2H, $J = 7.4$ Hz, CH_2N), 3.2-1.0 (m, 84H), 1.14 (br t, $J = 7.4$ Hz, 6H, CH_2CH_3), 0.88 (t, 3H, $J = 7.1$ Hz, CH_2CH_3).

6.9 References

- (1) The contents of this chapter have been published. See: Pollino, J. M.; Weck, M. *Tetrahedron* **2004**, *60*, 7205.
- (2) Stevens, M. P. *Polymer Chemistry: An Introduction*; Oxford University Press: New York, 1999.
- (3) Rosen, S. L. *Fundamental Principles of Polymeric Materials*; 2 ed.; Wiley: New York, 1993.
- (4) Odian, G. *Principles of Polymerization*; 3rd ed.; Wiley: New York, 1991.
- (5) Hilger, C.; Dräger, M.; Stadler, R. *Macromolecules* **1992**, *25*, 2498.
- (6) Müller, M.; Dardin, A.; Seidel, U.; Balsamo, V.; Iván, B.; Spiess, H. W.; Stadler, R. *Macromolecules* **1996**, *29*, 2577.
- (7) Kato, T.; Kihara, H.; Kumar, U.; Uryu, T.; Fréchet, J. M. J. *Angew. Chem. Int. Ed. Engl.* **1994**, *33*, 1644.
- (8) Thibault, R. J.; Galow, T. H.; Turnberg, E. J.; Gray, M.; Hotchkiss, P. J.; Rotello, V. M. *J. Am. Chem. Soc.* **2002**, *124*, 15249.
- (9) Thibault, R. J.; Hotchkiss, P. J.; Gray, M.; Rotello, V. M. *J. Am. Chem. Soc.* **2003**, *125*, 11249.
- (10) Zhao, Y.; Yuan, G.; Roche, P. *Polymer* **1999**, *40*, 3025.
- (11) Rieth, L. R.; Eaton, R. F.; Coates, G. W. *Angew. Chem. Int. Ed.* **2001**, *40*, 2153.
- (12) Lehn, J.-M. *Polym. Int.* **2002**, *51*, 825.
- (13) Lehn, J.-M. *Supramolecular Chemistry*; Wiley-VCH: Weinheim, 1995.
- (14) Huck, W. T. S.; Hulst, R.; Timmerman, P.; van Veggel, F. C. J. M.; Reinhoudt, D. N. *Angew. Chem. Int. Ed. Engl.* **1997**, *36*, 1006.
- (15) Albrecht, M.; van Koten, G. *Angew. Chem. Int. Ed. Engl.* **2001**, *40*, 3750.
- (16) Pollino, J. M.; Weck, M. *Synthesis* **2002**, 1277.
- (17) Schmatloch, S.; Schubert, U. S. *Macromol. Symp.* **2003**, *199*, 483.
- (18) Cotton, F. A.; Wilkinson, G.; Murillo, C. A.; Bochmann, M. *Advanced Inorganic Chemistry*; 6th ed.; John Wiley Sons, Inc.: New York, NY, 1999.

- (19) Albrecht, M.; Lutz, M.; Antoine, M. M.; Lutz, E. T. H.; Spek, A. L.; van Koten, G. *J. Chem. Soc., Dalton Trans.* **2000**, 3797.
- (20) Pollino, J. M.; Stubbs, L. P.; Weck, M. *J. Am. Chem. Soc.* **2004**, *126*, 563.
- (21) Dewey, V. C.; Kidder, G. W. *J. Med. Chem.* **1968**, *11*, 126.
- (22) Stubbs, L. P.; Weck, M. *Chem. Eur. J.* **2003**, *9*, 992.
- (23) Pollino, J. M.; Stubbs, L. P.; Weck, M. *Macromolecules* **2003**, *36*, 2230.
- (24) Berl, V.; Schmutz, M.; Krische, M. J.; Khoury, R. G.; Lehn, J.-M. *Chem. Eur. J.* **2002**, *8*, 1227.
- (25) Binder, W. H.; Kunz, M. J.; Kluger, C.; Hayn, G.; Saf, R. *Macromolecules* **2004**, *37*, 1749.
- (26) Tecilla, P.; Jubian, V.; Hamilton, A. D. *Tetrahedron* **1995**, *51*, 435.
- (27) Itahara, T. *Bull. Chem. Soc. Jpn.* **1997**, *70*, 2239.
- (28) Dobrawa, R.; Würthner, F. *Chem. Commun.* **2002**, 1878.
- (29) Würthner, F.; Sautter, A.; Thalacker, C. *Angew. Chem. Int. Ed.* **2000**, *39*, 1243.
- (30) Würthner, F.; Thalacker, C.; Sautter, A.; Schaertl, W.; Ibach, W.; Hollricher, O. *Chem. Eur. J.* **2000**, *6*, 3871.
- (31) Finkelmann, H.; Happ, M.; Portugall, M.; Ringsdorf, H. *Makromol. Chem.* **1978**, *179*, 2541.
- (32) Portugall, M.; Ringsdorf, H.; Wendorf, J. H. *Makromol. Chem.* **1978**, *179*, 273.
- (33) Roberts, J. D.; Trumbull, E. R.; Bennett, W.; Armstrong, R. *J. Am. Chem. Soc.* **1950**, *72*, 3116.
- (34) Ver Nooy, C. D.; Rondestvedt, C. S. *J. Am. Chem. Soc.* **1955**, *77*, 3583.
- (35) Grubbs, R. H. *Tetrahedron* **2004**, *60*, 7118.
- (36) Schwab, P.; Grubbs, R. H.; Ziller, J. W. *J. Am. Chem. Soc.* **1996**, *115*, 100.
- (37) Fürstner, A. *Angew. Chem. Int. Ed.* **2000**, *39*, 3012.
- (38) Trnka, T. M.; Grubbs, R. H. *Acc. Chem. Res.* **2001**, *34*, 18.

- (39) Kraatz, H.-B.; Milstein, D. J. *J. Organomet. Chem.* **1995**, *488*, 223.
- (40) Carlise, J. R.; Weck, M. J. *Poly. Science A, Poly. Chem.* **2004**, *42*, 2973.
- (41) Brunsveld, L.; Folmer, B. J. B.; Meijer, E. W.; Sijbesma, R. P. *Chem. Rev.* **2001**, *101*, 4071.
- (42) Pangborn, A. B.; Giardello, M. A.; Grubbs, R. H.; Rosen, R. K.; Timmers, F. J. *Organometallics* **1996**, *15*, 1518.

CHAPTER 7.

THE UPB CONCEPT: TODAY'S SYSTEM AND POTENTIAL APPLICATIONS OF TOMORROW

7.1 Abstract

The concept of the UPB has been brought to reality. However, many of the exciting applications and potential impact of these systems have yet to be realized. This chapter critically reviews the current status of the UPB concept and the important achievements made during its development, and suggests logical methodological extensions of the concept. Furthermore, evaluation of how UPBs may be used to optimize materials and its potential use in fabricating unique electro-optical materials, thermoplastic elastomers, sensors, and drug delivery vesicles are explored. A broad look at the potential deficiencies of the current system (when applied to specific applications) have been acknowledged and methods for resolving these problems are suggested.

7.2 The Current Status of the UPB Concept: Summary and Perspective

At the commencement of this thesis, synthetic polymers possessing multiple recognition elements on the side-chain were unknown. Over the past four years, this so-called UPB concept has been taken from drawing board to the development of a working model. Throughout the course of development, this concept has not only spawned a new area of polymer science concerned with orthogonal side-chain multifunctionalization, but

has also improved upon previous reported side-chain self-assembled polymers possessing a single recognition motif.

Prior to the earlier work in this dissertation, the field of side-chain self-assembly suffered from three major deficiencies: i) inefficient routes to polymers containing recognition units where poorly defined post-polymerization functionalization strategies were prevalent, ii) exhausted use of hydrogen bonding based molecular recognition, which limited the scope of materials preparation, and iii) the lack of truly orthogonal and modular multifunctionalization strategies.¹ With the introduction of side-chain metal containing polymer scaffolds (a class of homopolymers that was previously unknown), many of these problems have been overcome.²⁻⁴ These homopolymers have not only prefaced the realization of the orthogonal multifunctionalization strategies, but have provided alternative synthetic routes for covalent attachment of side-chain recognition units that makes use of pre-polymerization strategies, thereby providing well-defined homopolymeric backbones that contain recognition motifs at every repeat unit. The unique properties of metal-based SCS pincer systems have given rise to self-assembly strategies that are highly versatile, allowing for pyridines or nitrile based complementary pairs to be quantitatively and instantaneously coordinated to the backbone.⁴

Another area of polymer chemistry affected by this thesis is ROMP. For decades, the polymerization of simple norbornene esters has enjoyed tremendous success for the synthesis of various well-defined polymer architectures.⁵⁻¹⁰ However, when translated to elaborate monomer structures, such as those used in molecular recognition, the technique has suffered from extended catalysts decomposition over time.^{3,4,11,12} To overcome these difficulties, researchers have previously turned to more active initiators, but at the cost of

creating poorly defined structures.¹² To overcome this barrier for our monomers, the effect of implementing isomerically pure *exo*-norbornene monomers containing Pd^{II} SCS pincer complexes or diaminopyridine moieties was studied in detail and compared with the polymerization behavior of their respective *endo/exo* mixtures.^{13,12,14,15} These investigations have proven successful as a method to obtain fully “living” UPB systems where surgical precision over the architecture of the final polymer scaffold and copolymer structures is possible.^{5,16} This work has been foundational to the preparation of both block and random copolymer UPBs, and offers an alternative method for evading difficulties associated with polymerizing complex monomer structures using ROMP.

The most important achievement of my thesis work has undoubtedly been the realization of the UPB concept, which has potential implications for the fields of supramolecular chemistry and materials science.¹ Novel methodologies for UPB functionalization based on a non-covalent, one-step, multi-functionalization strategy were developed using non-covalent functionalization strategies. Backbone multifunctionalization was accomplished using 1) directed self-assembly, 2) multi-step self-assembly, and 3) one-step orthogonal self-assembly. This system shows complete specificity of each recognition motif, thereby establishing the concept of side-chain orthogonality.²

Additionally, some applications of the UPB have been explored with materials science in mind including the fabrication of well-controlled cross-linked materials.¹⁷ These systems are unique in that the strength of a crosslinked polymeric network can be tailored toward potential applications. The strategy described in this thesis allows for: i) functionalization directed by self-assembly of one recognition unit via hydrogen bonding

or metal coordination, ii) non-covalent crosslinking by metal coordination or hydrogen bonding, and ultimately iii) one-step functionalization and crosslinking in which both recognition motifs are spontaneously self-assembled in the presence of complementary recognition units.¹⁷ This crosslinking/functionalization methodology could eventually give rise to rapid and tunable elastomeric materials.

Although a reality, today's UPB system represents only the first generation of the UPB concept, which widely remains in its infancy. The future of the UPB is promising and has thus far matured to a point where immediate entry to advanced applications is possible. Prior to its implementation some system improvements might prove valuable. In the following two sections, some of the deficiencies of the current system are expanded upon and suggested methods for overcoming them are outlined. Furthermore, recommended methods of preparing higher generation UPBs and ways in which the concept may be directly applied to UPB based devices and materials synthesis are outlined.

7.3 Future Development of UPB Methodologies

The potential utility of the UPB concept is highly dependent upon the development of new methodologies that are able to incorporate new design elements, which eliminate current and future system limitations while simultaneously retaining the original objectives of the UPB concept. Thus, this section aims to suggest potential modifications to the current UPB system that, in some cases, will give rise to entirely new classes of UPBs that may be able to either: i) improve UPB synthesis and functionalization, ii) expand the versatility of the UPB concept, or iii) circumvent specific limitations of today's UPB system.

7.3.1 UPBs Based on One Type of Recognition Unit

Perhaps the most important modification of the UPB system should involve the alteration of the recognition elements since they dictate the thermal strength of the system as well as which solvents must be employed during self-assembly.¹⁸⁻²⁰ The UPBs previously described in this thesis employ two unique classes of recognition elements; namely hydrogen bonding¹⁸ and metal coordination,^{21,22} which give rise to a versatile system possessing both dynamic character as well as moderate thermal integrity.

Future multicomponent systems should be extended to UPBs based on a single type of interaction, either weak or strong. As depicted in Figure 7.1, UPBs based exclusively on metal coordination or hydrogen bonding may be envisaged.²³ For example, metal-based systems could be prepared by employment of terpyridine ligands and palladated pincer complexes, which can bind to a variety of metal-ligand complexes (such as Ru, Cu, Co, Ni, Fe) and are metal specific for palladium respectively (Figure 7.1-A). These systems could be classified as strong. Weaker hydrogen bonding based UPBs could be prepared using diaminopyridine and cyanuric acid wedges, each possessing distinct association constants for their respective complimentary pairs; thymine and isophthalamide receptors, respectively (Figure 7.1-B).

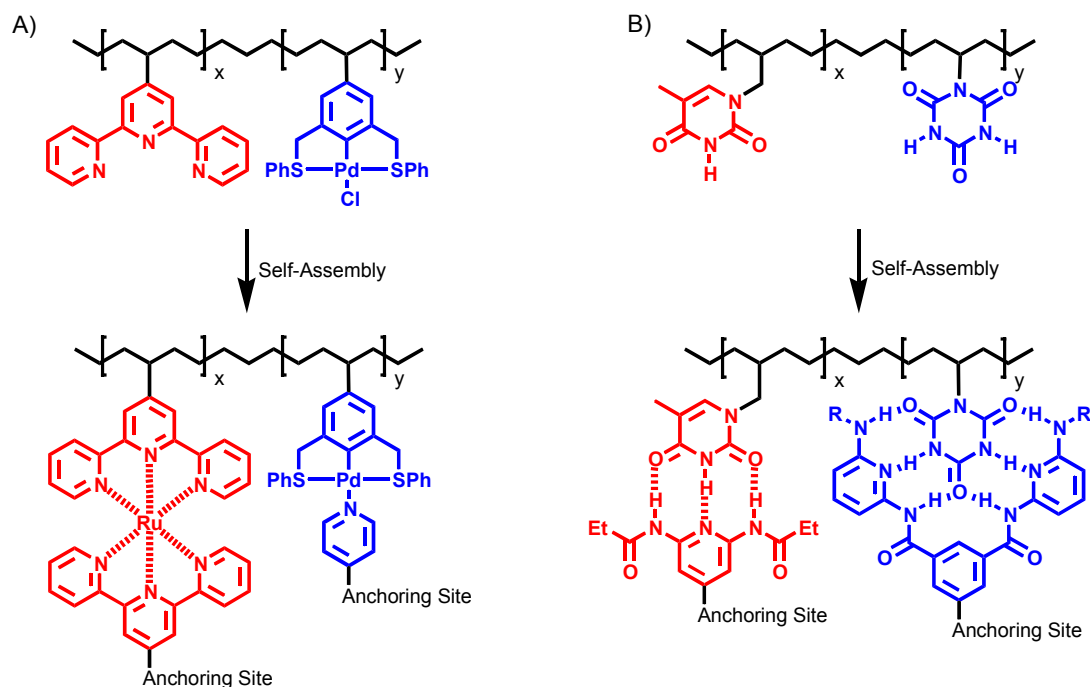


Figure 7.1 Proposed UPB structures based on a single type of interaction: A) multisite functionalization of metal coordination UPBs, and B) multisite self-assembly onto hydrogen bonding UPBs.

This methodology is advantageous for several reasons. First, systems possessing stronger bonds tend to be thermally robust, whereas those possessing weak interactions have a propensity to be dynamic. A particular UPB category may be selected according to the intended application. For example, an electronic device requiring several working hours must be thermally stable for prolonged periods of time and would benefit from the use of metal-only interactions (Figure 7.1-A). Whereas a system used in biomaterials applications may require the ability to come apart when subjected to heat, perform a specific function, and return upon cooling thereby requiring the use of weaker, dynamic hydrogen bonding only interactions (Figure 7.1-B). Second, the solubility of current UPBs is somewhat hampered by this fundamental mix matching of hydrogen bonding

and metal coordinating interactions, which often limits the choice of media to meet the requirements of both recognition units. In the case of UPBs based on a single type of recognition motif, system incompatibilities may be alleviated since the solvent conditions would be similar for a particular recognition motif. For example, metal-centers tend to be ionic in nature and therefore usually require polar solvents, whereas hydrogen bonding complexes are often destroyed in the presence of polar media.²² Albeit, the use of multiple identical or multiple different types of interactions may both be useful depending on the application. Moreover, development of this methodology would enhance both the applicability and versatility of the UPB concept.

7.3.2 *Metal Connected Di-Block UPBs*

Today's UPB system has incorporated design features that allow facile access to block copolymer structures via living ROMP. Although viable, the current approach is somewhat limited since it does not easily allow for the synthesis of a large variety of backbones. Furthermore, the olefin rich backbone of the poly(norbornene) structures have limited shelf life since they easily undergo oxidative decomposition pathways.^{7,24-26} Even though alternate polymerization techniques such as radical, condensation, or cationic methods will eventually allow for the synthesis of a variety of random backbones with, the ability to form block-UPB copolymers will always be limited in scope to the implementation of living polymerization methods such as ROMP or ATRP.

Recently, reports describing the synthesis of block copolymer structures via a convergent self-assembly approach have emerged.²⁷⁻³⁰ These systems utilize terpyridine initiators, where an assortment of backbone structures including poly(oxazoline)s²⁹ and poly(ethylene oxide)s³⁰ can propagate from the initiator, thereby creating homopolymers

possessing a single terminal terpyridine recognition motif. Subsequent self-assembly of these end-functionalized homopolymers gives rise to di-block copolymer structures, thereby eliminating the need for living polymerization techniques. Merging this approach with the UPB concept could simplify polymer synthesis and provide routes to a variety of block copolymer UPB structures that are not living and therefore cannot be accessed otherwise.

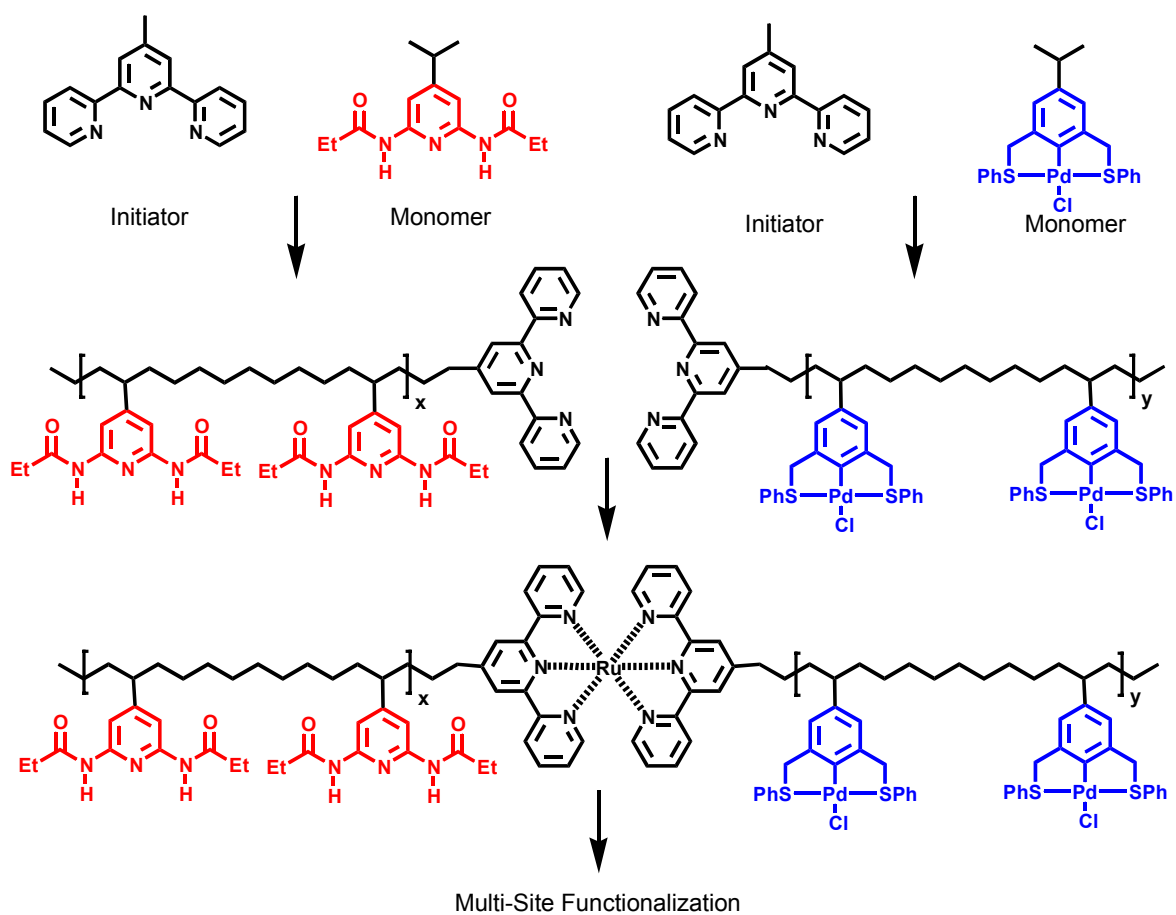


Figure 7.2 Di-block UPB synthesis using metal-centered trpy-Ru-trpy bridges.

As outlined in Figure 7.2, terpyridine end-functionalized homopolymers containing side-chain recognition units at every repeat unit could be prepared using a variety of polymerization techniques that do not require living character. Subsequent self-assembly via the well-known and thermally robust trpy-Ru-trpy metal-bond would give rise to di-block UPB copolymers possessing varying degrees of polymerization or even entirely different backbones (Figure 7.2). One unique feature of these systems is the fact that combinatorial libraries of UPBs could be rapidly prepared allowing for facile optimization of di-block UPB solubility and backbone character prior to the implementation of orthogonal multifunctionalization strategies. Furthermore, this approach could give access to highly conjugated and fully conducting diblock UPB backbones since Heck or Stille coupling polymerization reactions may be employed and the redox active metal-centered terpyridine complexes may serve as electronic junctions for conductivity across both segments.

7.3.3 *Grafted UPBs*

Another potential extension of the UPB concept that fundamentally expands the versatility of multisite orthogonal functionalization involves the grafting of recognition units onto the side-chain. Here, a functional group, asymmetrically difunctionalized with two different recognition units, could be sequentially added to the side-chains of a UPB to grow functional polymeric brushes with unique structure attributes (Figure 7.3). If the UPB system were synthesized via methods that allow for perfectly alternating backbone sequences (i.e. poly styrene co- maleic anhydride)²⁶ of recognition units, then grafting of this type could result in the formation of perfectly alternating 2D grids of functional entities (Figure 7.3-A).

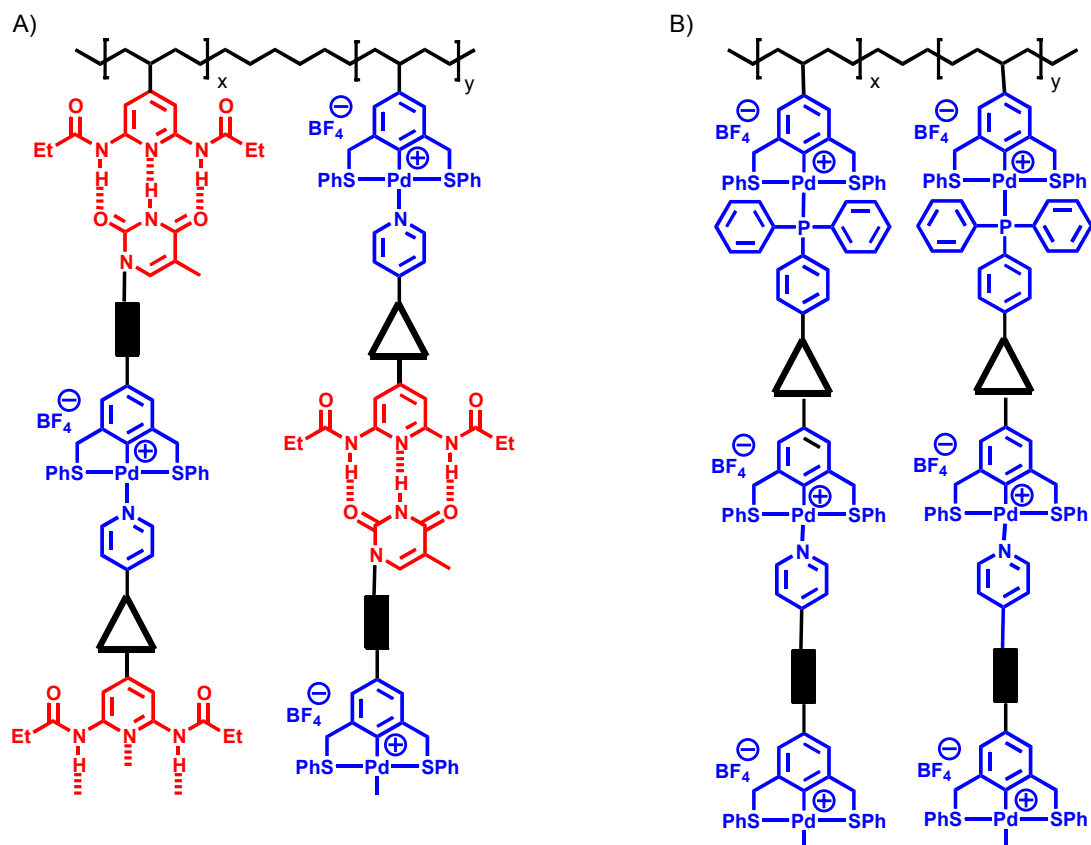


Figure 7.3 Multicomponent polymer brushes based on the UPB concept. A) alternating grid structures formed using perfectly alternating UPB copolymers. B) perfectly alternating layers formed from pincer homopolymer grafting.

Alternatively, this approach could also eliminate the need for copolymer synthesis all together since palladated pincer complexes could be iteratively functionalized by several sequential dechlorination/complexation events to form perfectly alternating layered grafts (Figure 7.3-B). By definition, this system does not constitute a UPB. However, it deserves mentioning since it offers a unique approach to rapid and simple formation of elaborate multifunctionalized polymeric brushes with exact control over structure properties.

7.3.4 *Main-chain UPBs*

In the future, one could imagine eliminating backbone synthesis all together in order to prepare well-defined UPBs. Systems based exclusively on self-assembly could provide the ultimate in UPB methodology where all information for both backbone structure and side-chain functionalization are contained within the individual self-assembling parts. To a large extent, UPBs of this type will more closely mimic Natural self-assembling biomaterials like the tobacco mosaic virus and could therefore give entry to the preparation of materials that are both highly functionalized and exceptionally functional.^{31,32} Furthermore, the synthesis of these UPBs would no longer require any traditional polymerization strategies, but synthesis would be reduced to the preparation of only the individual self-assembling parts.

One method to creating this class of UPBs could involve the augmentation of Meijer's well-known ureidopyrimidinone main-chain self-assembled polymers whose physical properties mimic the behavior of covalent linear polymers, but with the exception that they possess thermal reversibility (Figure 7.4-A).³³⁻³⁶ The examples proposed in Figure 7.4 are based on this system and could be prepared from either: i) mixtures of two different telechelic pentane units, each end functionalized with ureidopyrimidinone hydrogen bonding units that contain centrally located recognition units for self-assembly such as bipyridines and pincer complexes (Figure 7.4-B), or ii) systems where only one telechelic hydrogen bonding unit possessing several central recognition units is prepared (Figure 7.4-C). The latter case would result in the formation of perfectly alternating copolymers, whereas the former could provide statistical UPBs. This concept could easily be translated to the preparation of variety of backbones, or use

of metal coordinating main-chain systems, and therefore, could be tuned to meet the requirements of a specific applications.

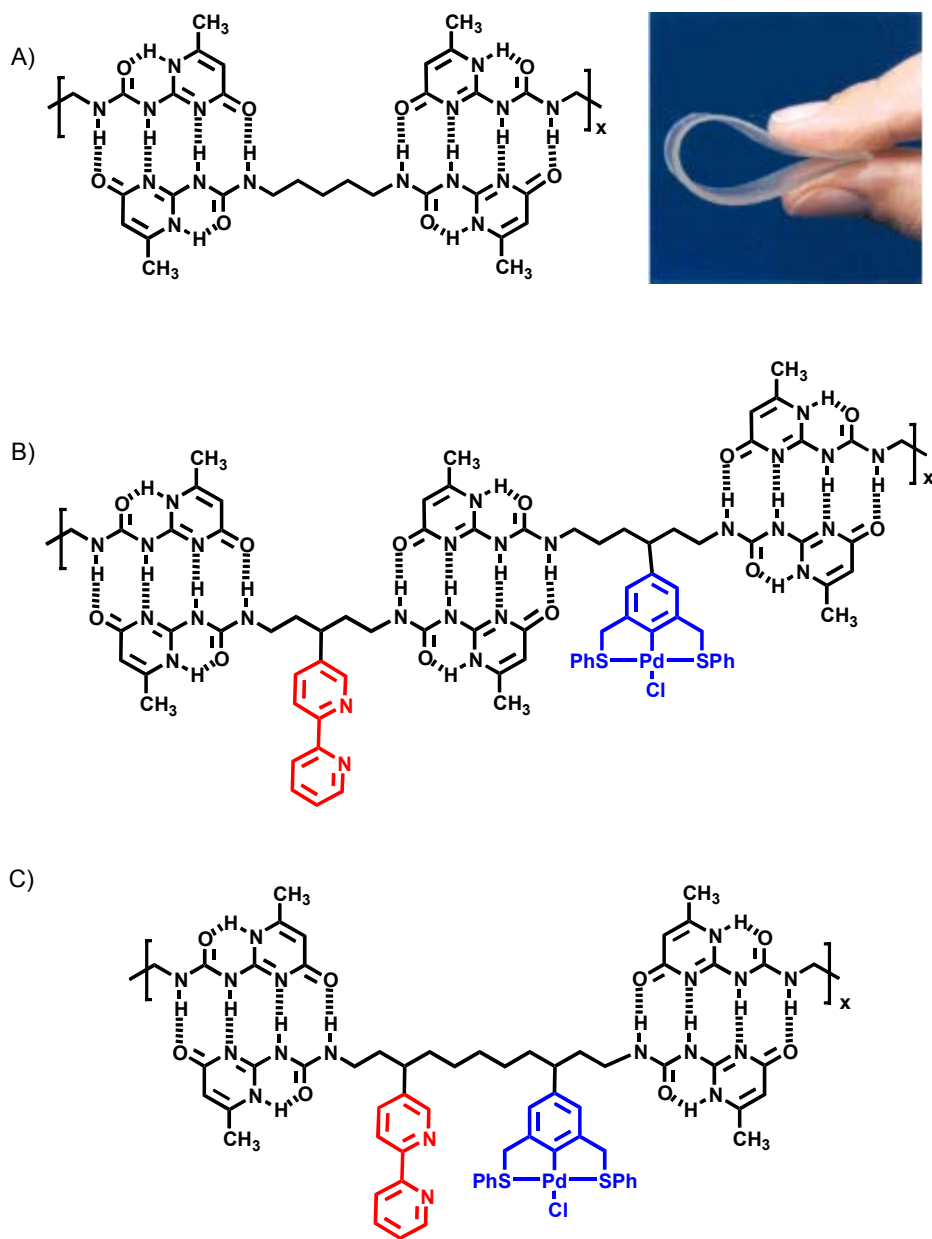


Figure 7.4 Main-chain self-assembled polymers. A) Meijer's famous telechelic ureidopyrimidinone main-chain self-assembled polymer,³⁴ B) proposed statistical UPBs formed from monomer mixtures, and C) proposed perfectly alternating UPBs derived from a single self-assembling monomer unit.

Overall, the systems described above constitute some interesting changes that may expand both the versatility and synthetic utility of creating complex polymers via orthogonal multi functionalization strategies. However, the above-mentioned variations are not all-inclusive, but rather focus upon the less obvious fundamental changes that may prove useful to the future growth of concepts in the field. Obvious augmentations to today's UPBs may also be needed. For example, every UPB scenario explored thus far is based upon only two recognition elements. An oblate expansion of this concept would involve the use of even larger numbers and types of recognition units. Furthermore, simple backbone modification may also be required, which may be possible by employment of any number of polymerization strategies.²⁶

In the future, thousands of novel and elaborate UPB methodologies may come to fruition. However, the development of new UPB concepts should be motivated by a variety of factors including synthetic utility, extension of concept, or to tailor a UPB for a particular application. Care should be exercised in these endeavors to reduce all new UPB systems to essential components. The full realization the UPB concept will require a marked trend toward simpler systems. Thus, cognition of the original goals of UPB concept, built upon the premise that synthesis and polymer functionalization be streamlined, must always remain at the forefront of design when exploring new UPB methodologies.

7.4 Potential Applications

Since its first conception, the UPB concept has always been intended for use as a synthetic tool that allows facile access to complex materials and elaborate, functional devices that are otherwise difficult or impossible to manufacture and optimize.³⁷ The

UPBs described so far in this thesis have evolved to a level that will allow for immediate device fabrication and applications oriented implementation. When appropriately applied, the utility of the UPB concept will most likely span numerous of scientific disciplines including materials science, biotechnology, nanotechnology and catalysis. Placement of UPBs into these exciting and growing areas of technology will inevitably reveal the dual nature and unique characteristics of the concept. First, the fact that UPBs can be rapidly and quantitatively multifunctionalized will give rise to entirely new classes of functional devices. Second, all novel materials accessed by applying the UPB concept will enjoy rapid device optimization times and parallel functionalization routes where manufacturing processes are streamlined and system modifications are remarkably efficient.

This section will outline some of the many new and exciting areas of science where the UPB concept may assist in technological advancement. In each case, suggested UPB modifications that will be necessary to bridge the gap between today's system and the applications of tomorrow will be pointed out. An example of each device or technology will be mentioned and extrapolation to other areas of a particular field will be made when necessary.

7.4.1 Photorefractive Polymers

The ability to manipulate the fundamental characteristics of light including the frequency, path, phase, or polarization has profound technological ramifications for the production of tunable laser light and optical data storage.^{32,38-41} Today, a tremendous amount of research in materials focuses on the development of polymeric devices that exhibit non-linear optical effects, particularly second harmonic generation (SHG), which

put simply causes a doubling in the frequency of incident light.³⁸ Present designs for photorefractive polymer materials require three principal components: i) a charge generator (CG), ii) a charge transport agent (CTA) or photoconductor, and iii) a non-linear optical chromophore (NLO). Typically, these systems are synthesized by doping photoconducting polymers with small molecule NLO and CG components.^{40,41} Designer systems with all three components built into a single covalent network have shown superior materials properties, but suffer from extensive synthesis for each structural change.⁴¹ As elaborated upon in detail (Chapter 2) the UPB concept is specifically designed to give ready access to a variety of photorefractive materials that are amenable to combinatorial methods and iterative optimization strategies.

In order to tailor the UPB concept to photorefractive materials applications, several adjustments to the present day system should be made. These modifications include: i) minimization of insulating aliphatic material to allow for enhanced photoconductivity, ii) preparation of a three component UPB to accommodate all components inherent to photorefractive materials, and iii) synthesis of anchored photorefractive mesogens that will self-assemble onto the polymer scaffold. As outlined in Figure 7.5, UPB modification may be carried out by: i) inclusion of a third (ionic) recognition motif, ii) reduction in the aliphatic chain length situated between the polymer backbone and the recognition motif, and iii) synthesis of functional groups anchored to pyridines, thymines, and sulfonates that may include stilbene based NLO chromophores, a carbazole photoconductor, and perylene or C-60 charge generators.³⁹⁻⁴¹ Other augmentations that may prove beneficial include use of conducting backbone, inclusion of specific metal-NLO chromophore interactions that are known in some cases to enhance NLO

properties,³⁸ and use of recognition motifs based exclusively on metal coordination to prepare thermally robust devices. Moreover, the UPB grafting strategies described in the previous section (pg. 190) may also allow for the preparation of NLO materials. This concept could also be carried out using electroluminescent components to fabricate polymeric OLEDs.⁴²⁻⁴⁵

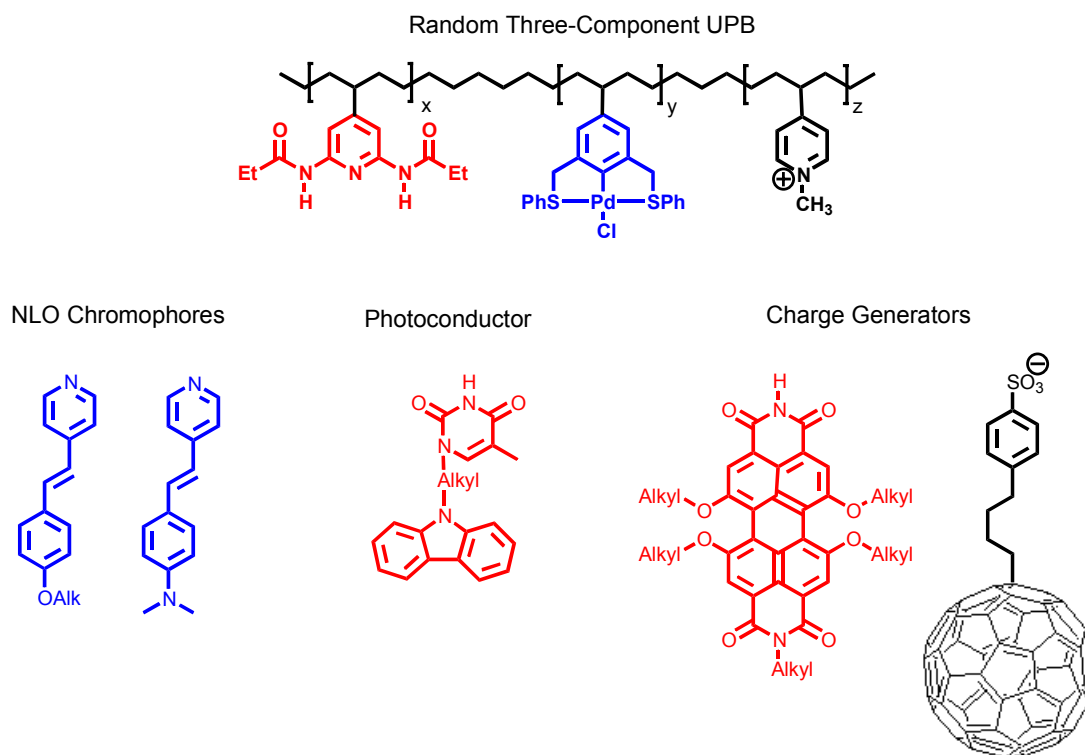


Figure 7.5 A random three-component UPB amenable to one-step orthogonal functionalization and tethered functional groups that constitute the components required for photorefractivity.

7.4.2 *Drug Delivery Devices*

Diversification of the UPB concept will eventually lead to its implementation in biologically relevant devices. One could envision several uses for multi-component non-covalent bioUPBs for use in biomineralization, tissue engineering, and drug delivery.⁴⁶⁻⁴⁸

In particular, the unique character of the UPB concept could bring about revolutionary drug delivery technologies. For example, a UPB system could be deployed where multiple therapeutic agents are non-covalently attached to a polymer backbone (Figure 7.6). By careful design, these systems could provide a multi-stage drug delivery mechanism where several drugs may: i) be released at different rates depending upon the nature of non-covalent linkage, ii) allow for sequential release of drugs with varying potency, where perhaps the first drug weakens a cancer cell, while the second delivers the lethal punch (in lower concentrations) to induce cell death, or iii) give the ability for drug cocktails to be delivered simultaneously.

Conversion of the current system to a biocompatible drug delivery device could be carried out in a number of ways. Most likely, the side-chains would be composed of water-soluble poly(ethylene oxide)s, and the system should incorporate a biodegradable backbone such as poly(lactic acid)s.⁴⁶ Random or block copolymers may be employed depending upon the desired effect. Preparation of micelle delivery vesicles may be accomplished using segregated block copolymers,³⁰ whereas non-covalent crosslinking of random copolymers could assist in device fabrication by allowing for microsphere formation.⁴⁹ Moreover, immunoglobulins and carbohydrates, which are frequently utilized as disease targeting moieties, could be incorporated onto the side-chains to assure delivery to the infected area.⁴⁷ One limitation of UPBs in drug delivery would be potential bioincompatibility of the recognition units. This problem could be circumvented

by implementation of non-covalent interactions that have previously been well established for use in biological systems.

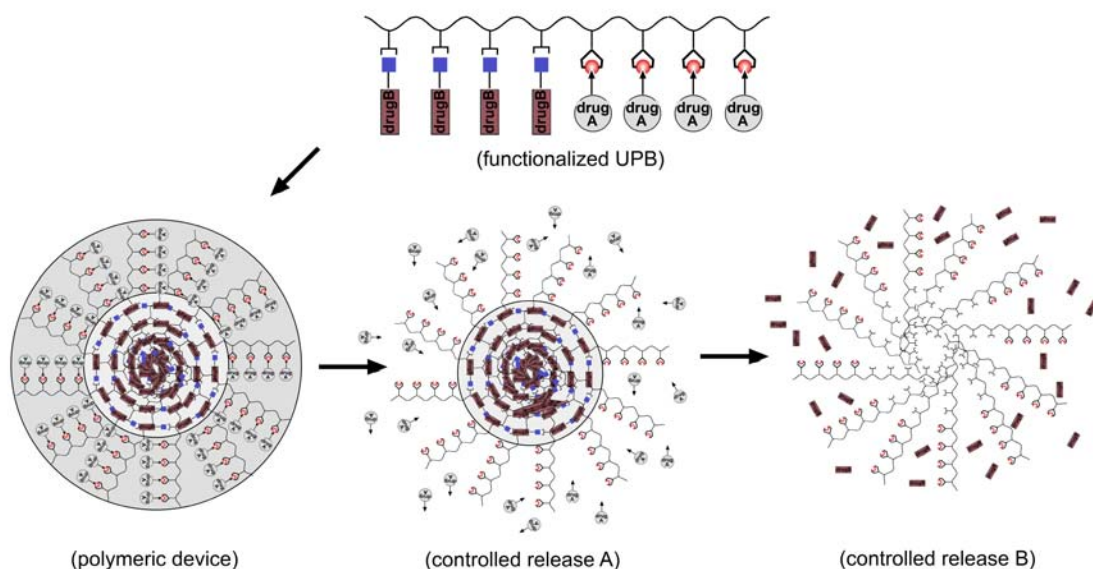


Figure 7.6 A proposed multi-stage drug delivery vessel that could be prepared from biocompatible UPBs.

7.4.3 Sensor Technologies

Numerous applications of the UPB concept may be envisaged for the field of semiochemistry⁵⁰ where multi-functionalization of the scaffold could lead to multicomponent sensors. The system could allow for specialized sensing technologies to be developed where quantitative analyte analysis may be performed using a single “universal” sensor. The most straightforward modification of today’s UPBs to meet these technologies would involve simple non-covalent attachment of well known photochemical, electrochemical, and fluorophore sensors to the backbone.³² However, more advanced modification of the UPB could allow for the backbone itself to receive,

process, and transfer a chemical signal to a second component thereby inducing a mechanical response such as the release of one of the functionalized components from the backbone. One could imagine that advanced technologies such as these would have potential ramifications for the field of drug delivery.

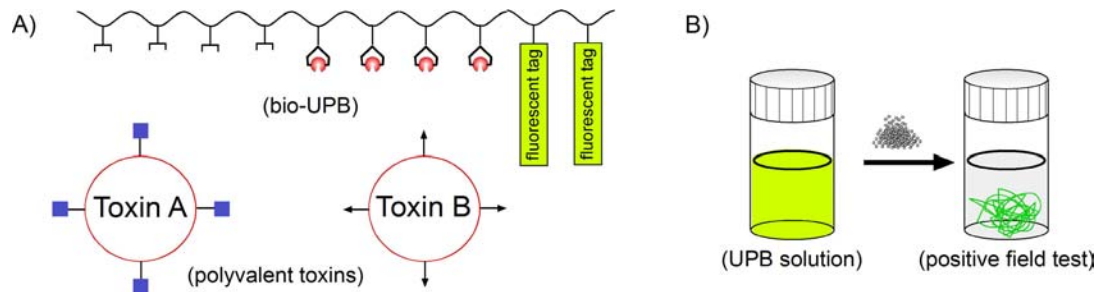


Figure 7.7 One example of UPBs applied to sensor technology. A) a fluorescent UPB containing binding units for polyvalent toxins, B) a “universal” field-test kit that could potentially detect the presence of large numbers of biological threats.

A more immediate extension of today’s UPB could involve qualitative detection of bioterror related toxins such as ricin, anthrax, and sarin. Here, a UPB scaffold would be modified so that several toxin specific sugars or protein recognition units are located along the backbone (Figure 7.7–A). The polyvalent character of most toxins would allow for immediate crosslinking of the UPB, forcing the polymer out of solution.⁵¹ A simple “universal” field test kit could be imagined, where the presence of a large number of potential threats could be determined in one simple assay. Such a system would likely incorporate a fluorescent moiety so that the addition of a suspected toxin would result in distinct color changes and the presence of a fluorescent clump of polymer at the bottom of the vial (Figure 7.7-B).

7.4.4 Thermoplastic Elastomers

As introduced in Chapter 6, non-covalent crosslinking of UPBs can potentially lead to thermoplastic elastomeric materials.^{24,25,52} Non-covalent methods of achieving elastomeric behavior are particularly attractive because the resulting materials are highly processable.^{17,24-26} An interesting extension of this concept would be the employment of multiple non-covalent crosslinkers with varying bond strengths to produce materials with unique elastomeric materials properties that are yet unknown. It could be speculated that the incorporation of two unique bifunctional crosslinkers, one based on a strong interaction such as metal coordination and the other based on a weak interaction such as hydrogen bonding, could give rise to coiled polymers capable of undergoing two discrete elongation periods (Figure 7.8-A).⁵³

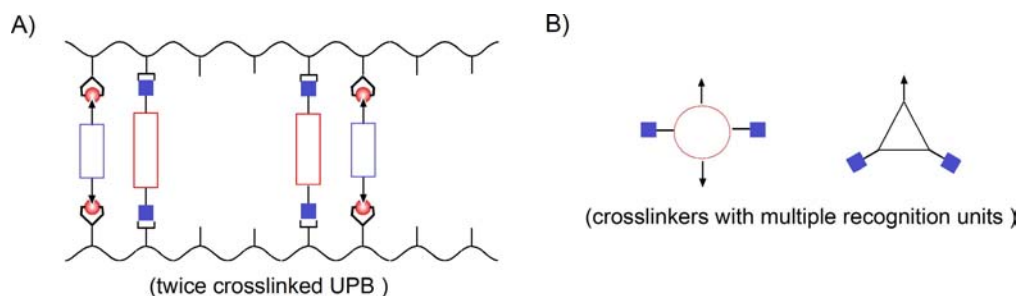


Figure 7.8 UPB crosslinking methods that could potentially result in interesting “elastomers contained within elastomers” type materials. A) a UPB crosslinked with bifunctional crosslinkers, and B) tri- and tetra- heterofunctionalized crosslinkers.

Additionally, a similar effect would most likely be achieved by the incorporation of tri- and tetra- functionalized crosslinkers anchored to more than one type of complimentary pair (Figure 7.8-B). To successfully prepare these unique thermoplastic elastomeric materials, some minor modifications of the current UPB should be

considered. Particularly, the backbone should be made more flexible and the molecular weights of the polymers should be dramatically increased to maximize the differences between amorphous and crystalline states.²⁴⁻²⁶ These polymers could be thought of as “elastomers contained within elastomers” and their properties may prove useful for the rubber, fabric, and building materials industries.

7.4.5 UPB Assisted Formation of Nano-Devices via Hierarchical Self-Assembly

UPBs may also be used as a powerful tool for producing functional materials by induction of hierarchical self-assembly processes via well-designed side-chain functionalization strategies.⁵⁴ Block copolymers containing largely different interfaces are known to undergo self-assembly into lamellar and higher order structural phases.^{25,26} These mesophases have been particularly useful in preparing nanoscale devices and objects.⁵⁴ Marrying this concept with the UPB strategies described in this thesis may allow easy access to a variety of interesting and dynamic hierarchical devices that are created by simple adjustments made to the functional groups attached to the backbone.

As outlined in Figure 7.9, block copolymer UPBs with varying chain lengths could be prepared. One-step orthogonal multi-functionalization of the backbone with two or more different complementary units, each possessing unique physical properties, such as long flexible aliphatic tails or short charged rigid groups could bring about repulsive immiscibility of block segments. Depending upon the side-chain group employed, hierarchical structures such as hexagonally packed cylindrical mesophases could be made.²⁴⁻²⁶ The reversible nature of the side-chain non-covalent interaction could then allow for selective removal of one of the recognition units resulting in the formation of cylindrical nano-objects and nano-porous materials. One could imagine that nano-

filtration devices or even molecular wires could be rapidly prepared and optimized by these routes (Figure 7.9).

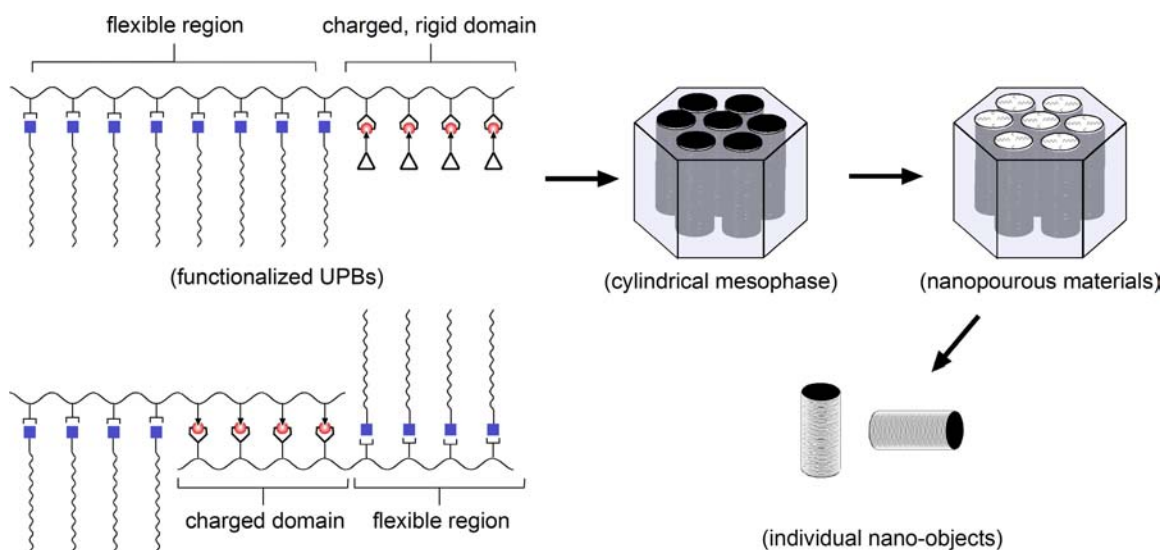


Figure 7.9 Schematic showing the rapid formation of hierarchical architectures and nano-scale devices, which may be possible via implementation of the UPB concept.

In conclusion, the UPB concept has the potential to overcome some of the drawbacks of covalent copolymer synthesis including reagent incompatibility and lengthy synthesis. Modifications of the current system will yield tremendous capabilities for the rapid production of a variety of materials. This technology will undoubtedly see continuing advances that will further establish the methodology. However, realization of its full potential will be dependent on its use and acceptance in materials applications. Based on the creative leaps and advances made in this thesis, the future will most certainly see interesting usage of the concept and development of new devices that have not yet been made possible using covalent synthesis.

7.5 References

- (1) Pollino, J. M.; Weck, M. *Chem. Soc. Rev.* **2004**, In Press.
- (2) Pollino, J. M.; Stubbs, L. P.; Weck, M. *J. Am. Chem. Soc.* **2004**, *126*, 563.
- (3) Pollino, J. M.; Weck, M. *Org. Lett.* **2002**, *4*, 753.
- (4) Pollino, J. M.; Weck, M. *Synthesis* **2002**, 1277.
- (5) Webster, O. W. *Science* **1991**, *251*, 887.
- (6) Trnka, T. M.; Grubbs, R. H. *Acc. Chem. Res.* **2001**, *34*, 18.
- (7) Grubbs, R. H. *Tetrahedron* **2004**, *60*, 7118.
- (8) Fürstner, A. *Angew. Chem. Int. Ed. Engl.* **2000**, *39*, 3012.
- (9) Weck, M.; Schwab, P.; Grubbs, R. H. *Macromolecules* **1996**, *29*, 1789.
- (10) Ivin, K. J.; Mol, J. C. *Olefin Metathesis and Metathesis Polymerization*; Academic Press, Inc.: San Diego, 1997.
- (11) Stubbs, L. P.; Weck, M. *Chem. Eur. J.* **2003**, *9*, 992.
- (12) Pollino, J. M.; Stubbs, L. P.; Weck, M. *Macromolecules* **2003**, *36*, 2230.
- (13) This approach has been employed previously, but with out detailed studies of the kinetics or living behavior. For more information see the Kiessling references below.
- (14) Manning, D. D.; Strong, L. E.; Hu, X.; Beck, P. J.; Kiessling, L. L. *Tetrahedron* **1997**, *53*, 11937.
- (15) Manning, D. D.; Hu, X.; Beck, P.; Kiessling, L. L. *J. Am. Chem. Soc.* **1997**, *119*, 3161.
- (16) Quirk, R. P.; Lee, B. *Polym. Inter.* **1992**, *27*, 359.
- (17) Pollino, J. M.; Weck, M. *Tetrahedron* **2004**, *60*, 7205.
- (18) Prins, L. J.; Reinhoudt, D. N.; Timmerman, P. *Angew. Chem. Int. Ed.* **2001**, *40*, 2382.

- (19) Brunsveld, L.; Folmer, B. J. B.; Meijer, E. W.; Sijbesma, R. P. *Chem. Rev.* **2001**, *101*, 4071.
- (20) Lehn, J.-M. *Polym. Int.* **2002**, *51*, 825.
- (21) Albrecht, M.; van Koten, G. *Angew. Chem. Int. Ed.* **2001**, *40*, 3750.
- (22) Lehn, J.-M. *Supramolecular Chemistry*; Wiley-VCH: Weinheim, 1995.
- (23) This concept is currently being investigated for hydrogen bonding base UPBs (Caroline Burd).
- (24) Stevens, M. P. *Polymer Chemistry: An Introduction*; Oxford University Press: New York, 1999.
- (25) Rosen, S. L. *Fundamental Principles of Polymeric Materials*; 2 ed.; Wiley: New York, 1993.
- (26) Odian, G. *Principles of Polymerization*; 3rd ed.; Wiley: New York, 1991.
- (27) Schubert, U. S.; Heller, M. *Chem. Eur. J.* **2001**, *7*, 5252.
- (28) Schubert, U. S.; Eschbaumer, C. *Angew. Chem. Int. Ed.* **2002**, *41*, 2892.
- (29) Heller, M.; Schubert, U. S. *Macromol. Symp.* **2002**, 87.
- (30) Gohy, J.-F.; Lohmeijer, B. G. G.; Schubert, U. S. *Macromolecules* **2002**, *35*, 4560.
- (31) Philp, D.; Stoddart, J. F. *Angew. Chem. Int. Ed. Eng.* **1996**, *35*, 1154.
- (32) Steed, J. W.; Atwood, J. L. *Supramolecular Chemistry*; John Wiley & Sons, Ltd: Chichester, West Sussex, 2000.
- (33) Folmer, B. J. B.; Cavini, E.; Sijbesma, R. P.; Meijer, E. W. *Chem. Commun.* **1998**, 1847.
- (34) Folmer, B. J. B.; Sijbesma, R. P.; Versteegen, R. M.; van der Rijt, J. A. J.; Meijer, E. W. *Adv. Mater.* **2000**, *12*, 874.
- (35) Folmer, B. J. B.; Sijbesma, R. P.; Meijer, E. W. *Polym. Mater. Sci. Eng.* **1999**, *217*, 39.
- (36) Sijbesma, R. P.; Beijer, F. H.; Brunsveld, L.; Folmer, B. J. B.; Hirschberg, J. H. K. K.; Lange, R. F. M.; Lowe, J. K. L.; Meijer, E. W. *Science* **1997**, *278*, 1601.

- (37) For more details on rapid optimization of materials via the UPB concept see Chapter 2.
- (38) Marder, S. R. In *Inorganic Materials*; 2nd ed.; Bruce, D. W., O'Hare, D., Eds.; Wiley: Chichester, 1996, p 121.
- (39) Moerner, W. E.; Silence, S. M. *Chem. Rev.* **1994**, *94*, 127.
- (40) Yu, L.; Chan, W. K.; Peng, Z.; Gharavi, A. *Acc. Chem. Res.* **1996**, *29*, 13.
- (41) Bratcher, M. J.; DeClue, M. S.; Grunnet-Jepsen, A.; Wright, D.; Smith, B. R.; Moerner, W. E.; Siegel, J. S. *J. Am. Chem. Soc.* **1998**, *120*, 9680.
- (42) Davidov, D.; Neumann, R. *Acta Polym.* **1998**, *49*, 642.
- (43) Sheats, J. R. *Science* **1997**, *277*, 191.
- (44) Sheats, J. R.; Antoniadis, H.; Hueschen, M.; Leonard, W.; Miller, J.; Moon, R.; Roitman, D.; Stocking, A. *Science* **1996**, *273*, 884.
- (45) Friend, R. H.; Gymer, A. B.; Holmes, J. H.; Burroughes, J. H.; Marks, R. N.; Taliani, C.; Bradley, D. D. C.; Dos Santos, D. A.; Brédas, J. L. *Nature* **1999**, *397*, 121.
- (46) Uhrich, K. E.; Cannizzaro, S. M.; Langer, R.; Shakesheff, K. M. *Chem. Rev.* **1999**, *99*, 3181.
- (47) Langer, R. *Science* **1990**, *249*, 1527.
- (48) Langer, R. *Acc. Chem. Res.* **2000**, *33*, 94.
- (49) Thibault, R. J.; Hotchkiss, P. J.; Gray, M.; Rotello, V. M. *J. Am. Chem. Soc.* **2003**, *125*, 11249.
- (50) Fabbrizzi, L.; Poggi, A. *Chem. Soc. Rev.* **1995**, *24*, 197.
- (51) Mammen, M.; Choi, S.-K.; Whitesides, G. M. *Angew. Chem. Int. Ed.* **1998**, *37*, 2754.
- (52) Rieth, L. R.; Eaton, R. F.; Coates, G. W. *Angew. Chem. Int. Ed.* **2001**, *40*, 2153.
- (53) Work on a variety of crosslinked UPB structures is currently in progress in our laboratory (Kamlesh P. Nair).
- (54) Ikkala, O.; ten Brinke, G. *Science* **2002**, *295*, 2407.

APPENDIX A.

TANDEM CATALYSIS AND SELF-ASSEMBLY

A.1 Abstract

In this chapter, the catalytic behavior of poly(norbornene)s containing palladium(II)-SCS pincer precatalysts for the Heck reaction were studied. It was determined that these catalyst precursors give rise to quantitative transformations of small molecules to form mesogens with limited decomposition of the metal center. Exploitation of both the catalytic and self-assembly properties has led to the development of a controlled, one-pot tandem catalysis/self-assembly sequence for the synthesis of densely functionalized polymers.

A.2 Introduction

As described in this thesis and elsewhere, palladated SCS pincer complexes are able to serve as recognition motifs for the rapid and quantitative formation of a variety of supramolecular entities via self-assembly.¹⁻¹³ However, most published accounts concerning pincer ligands are centered upon their use in catalysis.¹⁴⁻³⁴ In fact, the metal-based molecular scaffolds employed throughout this thesis are known to promote a variety of organic transformations including carbon-carbon coupling reactions,^{23-31,34} transfer hydrogenation,³³ and alkane dehydrogenation.¹⁴⁻¹⁹

Of these reactions, the palladium-catalyzed Heck reaction, developed independently by Mizoroki³⁵ and Heck³⁶ in the 1970's, has become an indispensable tool in modern organic synthesis, especially for the fine chemical and pharmaceutical industries. Mechanistically, the Heck reaction is well understood.³⁷⁻³⁹ The generally accepted mechanism assumes that, regardless of the palladium precursor, the active catalytic species is always a coordinatively unsaturated, 14 electron species (PdL_2). Typically, the Pd^0 catalyst is generated *in situ* by reduction of Pd^{II} salts [e.g. $\text{Pd}(\text{OAc})_2$, PdCl_2] with an excess of PPh_3 ligand and the catalytic transformation takes place via $\text{Pd}^0/\text{Pd}^{\text{II}}$ cycle.

Despite this, the nature of the active species has been poorly understood for most palladacycles, including pincer complexes.^{20,21,34,37-49} This more modern class of catalysts has exhibited a number of distinctive characteristics when compared to traditional palladium complexes including unusually high thermal stability and activity onsets only at elevated temperatures in polar media.^{24,44,46} Their purported stability to air and moisture at elevated temperatures (>180 °C) for prolonged periods of time has been unprecedented. Therefore, for years, it has been speculated that this particular class of Heck catalysts operate via an “unlikely” $\text{Pd}^{\text{II}}/\text{Pd}^{\text{IV}}$ catalytic pathway.^{20,21,28,40,44,45,48} These claims have spawned much debate.^{23,40,49} In response, several reports have attempted to elucidate the catalytic cycle and active species responsible in these systems.^{21,47,48}

Recently, it has been unequivocally shown through kinetic experiments and poisoning studies that palladacycle decomposition is responsible for the high activity of these systems under such harsh reaction conditions.^{22,34} Apparently, rupture of the palladium-ligand bonds liberates low concentrations of soluble Pd^0 , which carries out the transformation. This occurrence has, until now, remained largely undetected since the

extent of decomposition is not large enough to be visually identified using standard techniques such as filtration, elemental analysis, and ^1H NMR spectroscopy.^{22,34} Thus, palladacycles, such as the palladated SCS pincer complexes described in this thesis, can serve as precatalysts for the Heck reaction without large decomposition of the metal-center.

This chapter describes one potential use for these unique precatalysts that exploits the dual nature of palladated SCS pincer complexes to i) serve as sources of low concentrations of Pd^0 for Heck catalysis, ii) act as host-guest receptors in molecular recognition, and iii) to do both sequentially, thereby providing a novel strategy for the synthesis of highly functionalized side-chain polymers via a controlled tandem catalysis and self-assembly sequence (Figure A.1).⁵⁰

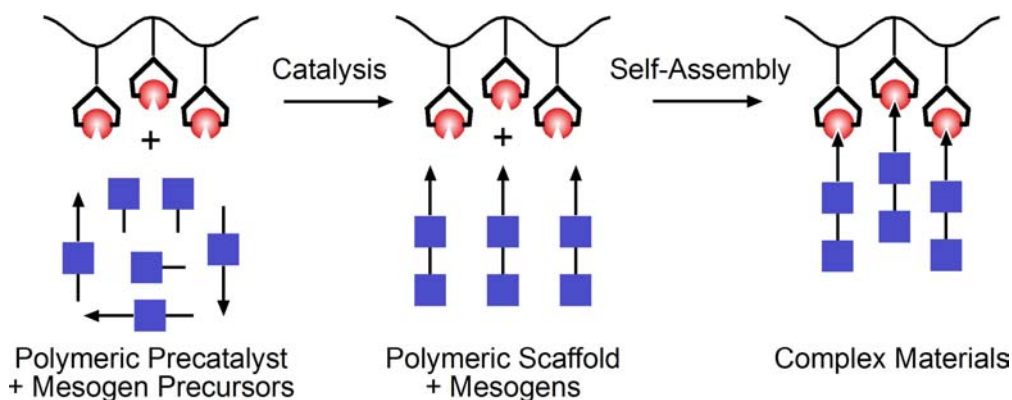


Figure A.1 Cartoon depicting a one-pot tandem catalysis and self-assembly sequence.

A.3 Design, Prerequisites, and Objectives

The polymeric precatalyst/scaffold used for the experiments described herein is polymer **1**, which was synthesized as outlined in Chapter 3.⁹ A unique feature of this

backbone is the fact that terminal palladated SCS pincer complexes are located at every repeat unit, which makes it: i) the highest loaded of all polymeric pincer-ligand based Heck precatalysts, and ii) a scaffold that can form densely functionalized materials upon self-assembly. These factors are critical to the implementation of one-pot tandem catalysis and self-assembly approaches to materials.

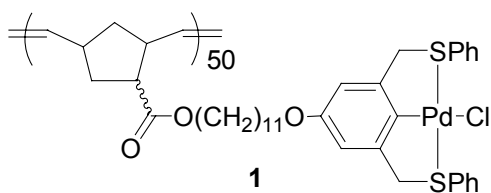


Figure A.2 Structure of polymer **1**, a supported Heck catalyst precursor and polymeric scaffold for self-assembly.

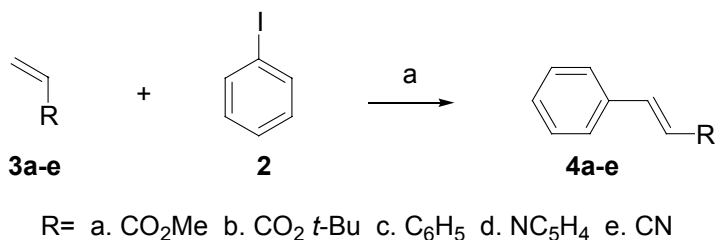
The aim of this chapter is to prove this concept of tandem catalysis and self-assembly in polymer science. However, prior to the successful implementation of this methodology, detailed studies directed toward the elucidation of the catalytic properties and the self-assembly behavior of polymer **1** must be carried out. In particular, catalysis must: i) allow for clean, quantitative transformations of small molecule precursors to form mesogens, and ii) not result in extensive decomposition of the catalyst precursor, since the recognition motif must remain intact for self-assembly. Self-assembly must take place quantitatively and in media containing the components used for catalysis. Furthermore, the self-assembly behavior of the mesogenic unit to be used for tandem catalysis/self-assembly must be independently characterized using materials synthesized

by alternate methods so that direct comparison between tandem catalysis/self-assembly and traditional routes may be carried out.

A.3 Catalytic Properties of Polymer Supported SCS Pincer Ligands

With these requirements in mind, experiments directed toward understanding the catalytic activity of polymer **1** commenced. Specifically, Heck coupling experiments between **2** and various alkene acceptors **3a-e** were examined (Scheme A.1).⁵¹ In general, all reactions proceeded with high fidelity of the recognition motif, in quantitative yields, and with high turnover numbers (Table A.1). Furthermore, it was determined that compounds possessing electron-withdrawing substituents (**3a** and **3b**) accelerate the reaction when compared to those with electron donating substituents (**3c** and **3d**). However, an overall decrease in the reactivity (based on time required for completion) of nitrogen containing olefins (**3d** and **3e**) was observed. In addition to electronic effects, this may also be attributed to partial deactivation of the precatalyst through competitive metal coordination.³⁹ Albeit, these results clearly demonstrate the efficiency and versatility of **1** as a Heck precatalyst.

Scheme A.1 The Heck reaction.⁵¹



Reagents and Conditions: a) **1**, DMF, 120 °C, NEt₃.

Table A.1 Heck reaction data using **1** as a precatalyst.

Entry	Product	Yield ^a (%)	Time (h)	TON ^b	TOF ^c
1	4a	>99	2.5	1000	400
2	4b	>99	3.5	1000	286
3	4c	97	11	1000	91
4	4d	92	16	1000	63
5	4e	95	10.5	1000	95

^a Yield of isolated product.

^b Turnover numbers are expressed as mol **4** / mol **1** [Pd].

^c Turnover frequencies are expressed as TON / h.

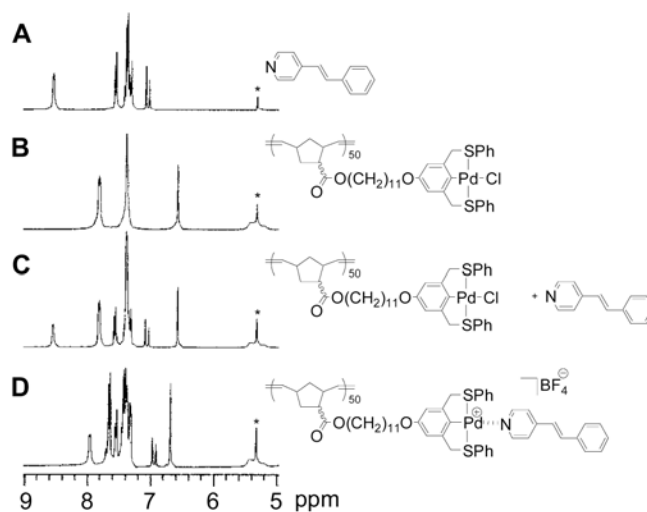


Figure A.3 The aromatic and olefin region of the ¹H NMR spectra depicting the metal coordination of stilbene **4d** onto **1** (*CD₂Cl₂). A) Stilbene **4d**. B) Polymer **1**. C) A 1:1 mixture of **4d** and **1**. D) The 1:1 mixture after addition of 1 equiv. of AgBF₄(aq).

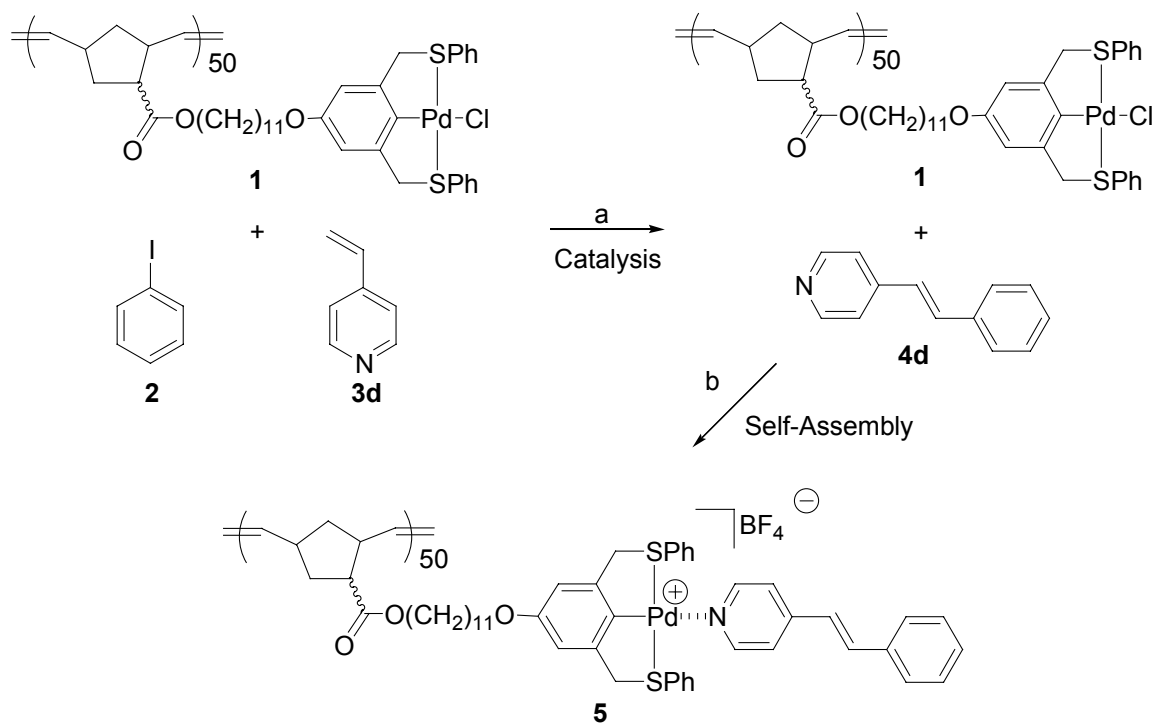
A.4 Self-Assembly of a Mesogenic Component Onto the Polymer Backbone

To investigate the self-assembly behavior of the polymer backbone (**1**), pure **4d** was independently synthesized and purified via column chromatography. Stilbene **4d** was employed as a model compound for several reasons. First, stilbenes provide an efficient route to liquid crystalline materials.⁵² Second, stilbene **4d** is easily synthesized by the Heck reaction of vinyl pyridine and iodobenzene using precatalyst **1** (Scheme A.1). Moreover, pyridyl recognition units have previously been employed as donor ligands to palladated SCS pincer complexes in supramolecular chemistry (Chapter 3, Chapter 5, and Chapter 6).^{1-13,32}

The coordination of **4d** to **1** was carried out and followed *in situ* by ¹H NMR spectroscopy in order to identify exact characteristic spectral changes that could be easily and directly compared to those observed for the future tandem catalysis/self-assembly sequence (Figure A.3). To that end, self-assembly experiments were performed by adding 1 equivalent of AgBF_{4(aq)} to a dichloromethane solution of a 1:1 mixture of **1** and **4d**. Instantaneously, AgCl precipitated, opening a free coordination site, which was subsequently ligated by the pyridyl moiety of the stilbene. Figure A.3-A and Figure A.3-B show the spectra of pure **4d** and **1** respectively. Figure A.3-C depicts a 1:1 mixture of **4d** and **1**, which clearly shows all signals characteristic of the individual components. Figure A.3-D displays the 1:1 mixture after self-assembly. Of particular interest are the chemical shifts for the α -protons of the pyridyl moiety at 8.56 ppm and the singlet at 6.58 ppm assigned as the protons in the *meta* position of the palladated phenyl ring. In Figure A.3-D, an up-field shift of the pyridyl α -protons from 8.56 ppm to 7.97 ppm with complete disappearance of the signal at 8.56 ppm as well as a slight downfield shift of the

meta pincer protons from 6.58 ppm to 6.68 ppm were observed. This shows that the α -pyridyl groups have coordinated to the Pd center.^{9,13,53} Also, shifts of the alkene protons of the stilbene from 7.09 ppm and 7.03 ppm to 6.97 ppm and 6.91 ppm, respectively, and other minor shifts throughout Figure 1D provide additional support for the self-assembly process. The products could be isolated by precipitation from hexanes to afford polymer **5** (Scheme A.2).

Scheme A.2 Tandem catalysis and self-assembly.



Reagents and Conditions: a) Na_2CO_3 , DMF, 120 °C, 10 h, 100%, b) $\text{AgBF}_4(\text{aq})$, CH_2Cl_2 , r.t., 100%.

A.5 One-Pot Tandem Catalysis and Self-Assembly

After establishing that precatalyst **1** gives rise to excellent catalytic activity and capability to serve as a recognition unit for self-assembly, the use of both properties in a one-pot Heck coupling/self-assembly sequence was examined. Polymer **1** was employed in tandem experiments as both precatalyst for the synthesis of **4d** and recognition unit for the self-assembly of **4d** (Scheme A.2). Analogous to the method used above, the progress of the reaction was followed *in situ* by ^1H NMR (Figure A.4).

Quantitative Heck coupling of **2** and **3d** (spectrum of a mixture of the pure compounds is shown in Figure A.4-A) was carried out at 120 °C for 10 h in the presence of **1** (Figure A.4-B) to provide exactly 1 equivalent of stilbene **4d** (Figure A.4-D). The disappearance of the olefin signals at 6.85-6.75 ppm, 6.20-6.14 ppm, and 5.56-5.52 ppm in Figure A.4-C (a 1:1:1 mixture of **1**, **2**, **3d**) and the appearance of new signals at 7.70 ppm (Figure A.4-D) are direct evidence for this transformation. Prior to self-assembly, one volumetric equivalent of CD_2Cl_2 was added to the DMF solution to solubilize the non-coordinated intermediate. Addition of $\text{AgBF}_4(\text{aq})$ resulted in instantaneous and quantitative self-assembly (Figure A.4-E). Comparison of Figure A.4-E and Figure A.4-D provides evidence for the coordination of the *in situ* prepared **4d** to the Pd center with the diagnostic up-field shift and broadening of the α -pyridine protons from 8.61 ppm to 8.28 ppm.^{9,13,53} A change in chemical shifts of the signals arising from protons on the phenyl group of the thioether of the pincer ligand were also evident with shifts from 7.88 ppm and 7.43 ppm to 7.84 ppm and 7.52 ppm, respectively. The final polymer could be isolated by precipitation from hexanes. The NMR spectra of isolated polymer **5** (in CD_2Cl_2) synthesized by both the tandem and step-wise routes were identical (with the

exception that it was taken in different solvents), indicating that the tandem catalysis/self-assembly route is a viable strategy towards the synthesis of functionalized polymers.

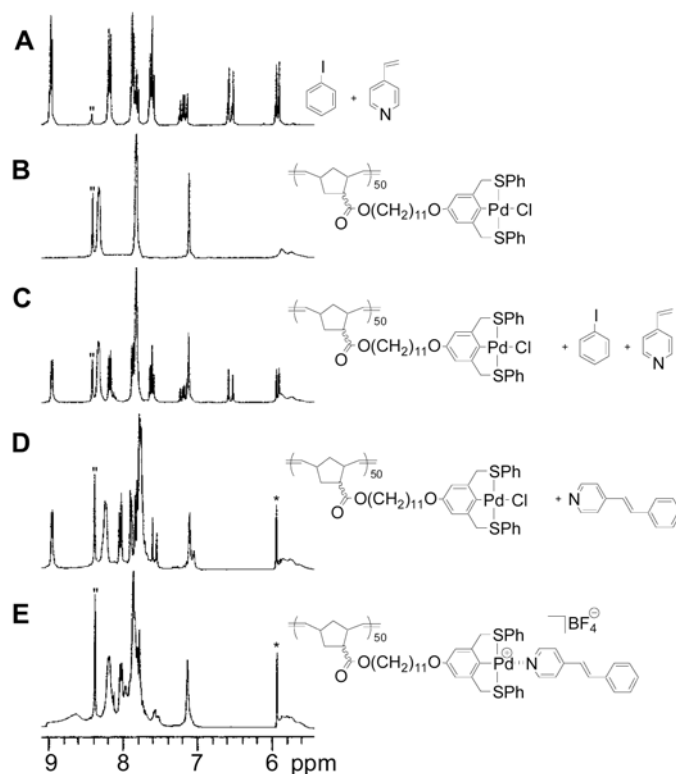


Figure A.4 The aromatic and olefin region of the ^1H NMR spectra depicting the tandem catalysis/self-assembly sequence ($^2\text{H}_2\text{O}$, $^2\text{H}_2\text{O}$). A) 1:1 mixture of **2** and **3**. B) Polymer **1**. C) A 1:1:1 mixture of **1**, **2**, and **3d**. D) The 1:1 mixture of **4d** and **1** following catalytic Heck coupling. E) The 1:1 mixture following the addition of 1 equiv. of $\text{AgBF}_4(\text{aq})$.

A.6 Conclusion

In conclusion, a bifunctional polymer system was synthesized that can be used: i) as a Heck catalyst precursor, ii) as a recognition motif in self-assembly, or iii) in a tandem catalysis/self-assembly sequence to provide a simple and efficient route to the synthesis of self-assembled polymers. Polymer **1** possesses the highest palladium loading of all

pincer ligand-based polymeric Heck precatalysts reported to date. Furthermore, this strategy facilitates ease of synthesis when compared to step-wise functionalization strategies because separation of small molecules is not required when prepared *in situ*.

A.8 References

- (1) Chuchuryukin, A. V.; Dijkstra, H. P.; Suijkerbuijk, B. M. J. M.; Gebbink, R. J. M.; van Klink, G. P. M.; Mills, A. M.; Spek, A. L.; Van Koten, G. *Angew. Chem. Int. Ed.* **2003**, *42*, 228.
- (2) Hall, J. R.; Loeb, S. J.; Shimizu, G. K. H.; Yap, G. P. A. *Angew. Chem. Int. Ed.* **1998**, *37*, 121.
- (3) Huck, W. T. S.; van Veggel, F. C. J. M.; Kropman, B. L.; Blank, D. H. A.; Keim, E. G.; Smithers, M. M. A.; Reinhoudt, D. N. *J. Am. Chem. Soc.* **1995**, *117*, 8293.
- (4) Huck, W. T. S.; van Veggel, F. C. J. M.; Reinhoudt, D. N. *Angew. Chem. Int. Ed. Eng.* **1996**, *35*, 1213.
- (5) Huck, W. T. S.; Hulst, R.; Timmerman, P.; van Veggel, F. C. J. M.; Reinhoudt, D. N. *Angew. Chem. Int. Ed. Eng.* **1997**, *36*, 1006.
- (6) Huck, W. T. S.; Snellink-Ruel, B.; van Veggel, F. C. J. M.; Reinhoudt, D. N. *Organometallics* **1997**, *16*, 4287.
- (7) Huck, W. T. S.; Prins, L., J.; Fokkens, R. H.; Nibbering, N. M. M.; van Veggel, F. C. J. M.; Reinhoudt, D. N. *J. Am. Chem. Soc.* **1998**, *120*, 6240.
- (8) Pollino, J. M.; Stubbs, L. P.; Weck, M. *J. Am. Chem. Soc.* **2004**, *126*, 563.
- (9) Pollino, J. M.; Weck, M. *Synthesis* **2002**, 1277.
- (10) Pollino, J. M.; Nair, K. P.; Stubbs, L. P.; Adams, J. A.; Weck, M. *Tetrahedron* **2004**, *60*, 7205.
- (11) Albrecht, M.; Gossage, R. A.; Lutz, M.; Spek, A. L.; van Koten, G. *Chem. Eur. J.* **2000**, *6*, 1431.
- (12) Steenwinkel, P.; Kooijman, H.; Smeets, W. J. J.; Spek, A. L.; Grove, D. M.; van Koten, G. *Organometallics* **1998**, *17*, 5411.
- (13) Loeb, S. J.; Shimizu, G. K. H. *J. Chem. Soc., Chem Commun.* **1993**, 1395.
- (14) Gupta, M.; Hagen, C.; Flesher, R. J.; Kaska, W. C.; Jensen, C. M. *Chem. Commun.* **1996**, 2083.
- (15) Gupta, M.; Hagen, C.; Kaska, W. C.; Cramer, R. E.; Jensen, C. M. *J. Am. Chem. Soc.* **1997**, *119*, 840.

- (16) Gupta, M.; Kaska, W. C.; Jensen, C. M. *Chem. Commun.* **1997**, 461.
- (17) Jensen, C. M. *Chem. Commun.* **2000**, 2443.
- (18) Liu, F.; Pak, E. B.; Singh, B.; Jensen, C. M.; Goldman, A. S. *J. Am. Chem. Soc.* **1999**, *121*, 4086.
- (19) Morales-Morales, D.; Lee, D. W.; Wang, Z.; Jensen, C. *Organometallics* **2001**, *20*, 1144.
- (20) Shaw, B. L.; Perera, S. D.; Staley, E. A. *Chem. Commun.* **1998**, 1361.
- (21) Shaw, B. L. *New J. Chem.* **1998**, 77.
- (22) Yu, K.; Sommer, W.; Weck, M.; Jones, C. W. *J. Catal.* **2004**, *226*, 101.
- (23) Beletskaya, I. P.; Kashin, A., N; Karlstedt, N., B.; Mitin, A. V.; Cheprakov, A., V.; Kazankov, G. M. *J. Organomet. Chem.* **2001**, *622*, 89.
- (24) Bergbreiter, D. E.; Osburn, P. L.; Yun-Shan, L. *J. Am. Chem. Soc.* **1999**, *121*, 9531.
- (25) Bergbreiter, D. E.; Osburn, P. L.; Frels, J. D. *J. Am. Chem. Soc.* **2001**, *123*, 11105.
- (26) Kiewel, K.; Liu, Y.; Bergbreiter, D. E.; Sulikowski, G. A. *Tetrahedron Lett.* **1999**, *40*, 8945.
- (27) Miyazaki, F.; Yamaguchi, K.; Shibasaki, M. *Tetrahedron Lett.* **1999**, *40*, 7379.
- (28) Morales-Morales, D.; Redon, R.; Yung, C.; Jensen, C. *Chem. Commun.* **2000**, 1619.
- (29) Morales-Morales, D.; Grause, C.; Kasoka, K.; Redon, R.; Cramer, R. E.; Jensen, C. M. *Inorg. Chim. Acta.* **2000**, 958.
- (30) Ohff, M.; Ohff, A.; van der Boom, M. E.; Milstein, D. *J. Am. Chem. Soc.* **1997**, *119*, 11687.
- (31) Peris, E.; Loch, J. A.; Mata, J.; Crabtree, R. H. *Chem. Commun.* **2001**, 201.
- (32) Albrecht, M.; van Koten, G. *Angew. Chem. Int. Ed.* **2001**, *40*, 3750.
- (33) Dani, P.; Karlen, T.; Gossage, R. A.; Gladiali, S.; van Koten, G. *Angew. Chem. Int. Ed.* **2000**, *39*, 743.
- (34) Yu, K.; Sommer, W.; Weck, M.; Jones, C. W. *Adv. Synth. Catal.* **2004**, in press.

- (35) Mizoroki, T.; Mori, K.; Ozaki, A. *Bull. Chem. Soc. Jpn.* **1971**, *44*, 581.
- (36) Heck, R. F.; Nolley, J. P. *J. Org. Chem.* **1972**, *14*, 2320.
- (37) Crisp, G. T. *Chem. Soc. Rev.* **1998**, *27*, 427.
- (38) Whitcomb, N. J.; Hii, K. K.; Gibson, S. E., *Tetrahedron* **2001**, 7449.
- (39) Cotton, F. A.; Wilkinson, G.; Murillo, C. A.; Bochmann, M. *Advanced Inorganic Chemistry*; 6th ed.; John Wiley Sons, Inc.: New York, NY, 1999.
- (40) Dupont, J.; Pfeffer, J.; Spencer, J. *Chem. J. Inorg. Chem.* **2001**, 1917.
- (41) Beletskaya, I. P.; Cheprakov, A. V. *Chem. Rev.* **2000**, *100*, 3009.
- (42) Beller, M.; Riermeier, T. H. *Eur. J. Inorg. Chem.* **1998**, 29.
- (43) Hermann, W. A.; Brossmer, C.; Reisinger, C. P.; Riermeier, T. H.; Öfele, K.; Beller, M. *Chem. Eur. J.* **1997**, *3*, 1357.
- (44) Herrmann, W. A.; Brossmer, C.; Öfele, K.; Reisinger, C. P.; Riermeier, T.; Beller, M.; Fisher, H. *Angew. Chem. Int. Ed. Engl.* **1995**, *34*, 1844.
- (45) Herrmann, W. A. B., V.P.W.; Reisinger, C.P. , 576, 23. *J. Organomet. Chem.* **1999**, *576*, 23.
- (46) Morales-Morales, D.; Redon, R. Y., C.; Jensen, C. M. *J. Am. Chem. Soc.* **1997**, *119*, 11687.
- (47) Morales-Morales, D.; Redon, R.; Yung, C.; Jensen, C. M. *Chem. Commun.* **2000**, 1619.
- (48) Ohff, M.; Ohff, A.; Milstein, D. *Chem. Commun.* **1999**, 357.
- (49) Whitcombe, N. J.; Hii, K. K.; Gibson, S. E. *Tetrahedron* **2001**, 7449.
- (50) Some contents of this chapter have been published. See: Pollino, J. M.; Weck, M. *Org. Lett.* **2002**, *4*, 753.
- (51) Heck reactions were carried out at 120 °C in DMF. To a vessel charged with 0.002 mmol of **1**, 2mmol of vinyl pyridine, 3 mmol of olefin, and 3 mmol of NEt₃ were added. The reaction was monitored by GC-MS. The products were isolated by precipitation in water followed by extraction with dichloromethane.
- (52) Kumar, U.; Kato, T.; Fréchet, J. M. J. *J. Am. Chem. Soc.* **1992**, *114*, 6630.

(53) Fujita, M.; Ibukuro, F.; Hagihara, H.; Ogura, K. *Nature* **1994**, 720.